ESCUELA DE DOCTORADO
INTERNACIONAL DE LA USC

Chester Andrew
Sellers Walden

Tesis doctoral

Remote sensing applied to landslide risk management and governance

Lugo, 2023

Programa de doctorado en Gestión Sostenible de la Tierra y del Territorio

DOCTORAL THESIS

REMOTE SENSING APPLIED TO LANDSLIDE RISK MANAGEMENT AND GOVERNANCE

Chester Andrew Sellers Walden

INTERNATIONAL DOCTORAL SCHOOL OF THE UNIVERSITY OF SANTIAGO DE COMPOSTELA
DOCTORAL PROGRAMME IN SUSTAINABLE SOIL AND LAND MANAGEMENT

LUGO - SPAIN
2022

DECLARACIÓN DEL AUTOR/A DE LA TESIS

D./Dña. **Chester Andrew Sellers Walden**

Título da tese: **Remote Sensing Applied to Landslide Risk Management and Governance.**

Presento mi tesis, siguiendo el procedimiento adecuado al Reglamento y declaro que:

1) La tesis abarca los resultados de la elaboración de mi trabajo.
2) De ser el caso, en la tesis se hace referencia a las colaboraciones que tuvo este trabajo.
3) Confirmo que la tesis no incurre en ningún tipo de plagio de otros autores ni de trabajos presentados por mí para la obtención de otros títulos.
4) La tesis es la versión definitiva presentada para su defensa y coincide la versión impresa con la presentada en formato electrónico.

Y me comprometo a presentar el Compromiso Documental de Supervisión en el caso que el original no esté depositado en la Escuela.

En **Lugo España**, **09 de diciembre de 2022**.

Firma electrónica

AUTORIZACIÓN DEL DIRECTOR / TUTOR DE LA TESIS

[Remote Sensing Applied to Landslide Risk Management and Governance.]

D./Dª. David Miranda Barros
D./Dª. Sandra Buján Seoane

INFORMA/N:

Que la presente tesis, se corresponde con el trabajo realizado por D/Dª. Chester Andrew Sellers Walden, bajo mi dirección/tutorización, y autorizo su presentación, considerando que reúne los requisitos exigidos en el Reglamento de Estudios de Doctorado de la USC, y que como director de esta no incurre en las causas de abstención establecidas en la Ley 40/2015.

De acuerdo con lo indicado en el Reglamento de Estudios de Doctorado, declara también que la presente tesis doctoral es idónea para ser defendida en base a la modalidad Monográfica con reproducción de publicaciones en los que la participación del doctorando/a fue decisiva para su elaboración y las publicaciones se ajustan al Plan de Investigación.

En Ponferrada, 13 de Diciembre de 2022

To my family of blood or not, the people that where always there, to with enchanting words, provided the positive energy to conquer this phase.

Labor omnia vincit improbus

Science literacy is the artery through which the solutions of tomorrow's problems flow.
We live on this speck called Earth - think about what you might do, today or tomorrow - and make the most of it.
Elshahed y Tyson (2020)
Everything is theoretically impossible, until it is done..

Acknowledgements

Firstly, I would like to express my sincere gratitude to my advisors PhD. Sandra Bujan Seoane and PhD David Miranda Barros, for the continuous support of my Ph.D study and related research, for their patience, motivation, and immense knowledge. Your guidance helped me in all the time of research and writing of this thesis. I could not have imagined having better advisors and mentors for my Ph.D study.

With a very special mention to, Rafael Crecente, mentor and guide, person who believed at first glance in this humble man. He saw with interest and passion the opportunities and potentials of the people and groups that work with him. It was fantastic to have the opportunity to work the majority of my research in your facilities. It was a honor and a pleasure to know you Rafael, farewell where ever you are!

A very, very special mention to Sandra Bujan, a great person and friend who gave more than what was expected as a director, as friend, as a mentor. Totally enthusiastic person of who I respect and admire, never change SAN.

Special mention to Diego DiMartire a great professional, even a greater person, for you guide and kindness. Also to the University Federico II of Naples and to DiSTAR (Dipartimento di Scienze della Terra, dell Ambiente e delle Risorte), to Professor Domenico Calcaterra and professor Massimo Ramondini for the opportunity to work with you and all the knowledge acquired.

And finally, last but by no means least, also to everyone Majo, Bea,

Miguel, Zeus, Lucy, Pablo, Marcos, Quico, Nieves, Urbano, Francisco, it was great sharing laboratory with all of you during this years.

A very special gratitude goes to the University of Santiago de Compostela at the LaboraTE, also to the University of Azuay in the name of PhD Francisco Salgado (Thanks Paquito for your trust and friendship) for helping and providing the funding for this work.

Thanks for all your encouragement!

Abstract

Since the last decade of the 20th century, the main challenge for reducing the risk of disasters has been assumed; the change in focus that has been seen, moving from a view linked to the unpredictability and inescapability of their occurrence to considering them as a problem linked to the processes of development of countries, regions, and options to use in planning of the territory.

With the growing concern at an international level for the increase in the frequency and severity of natural disasters and threats, and in the current context in which we live, with an epidemic on a planetary scale, in the midst of increasingly frequent natural events and of increasingly extreme magnitudes, many of them as a consequence of climate change, the different dimensions in which a disaster can affect people's well-being are evident.

Among the main causes of the occurrence of a catastrophe is the inadequate way of implementing disaster risk management in the territory, as well as the lack of awareness and responsibility on the subject on the part of political decision-makers and the community itself. This risk management involves, among other aspects, the reduction of risk in the face of the occurrence of disasters. Through this approach, the reduction of social, economic, and environmental vulnerabilities is pursued, increasing the resilience and general well-being of the population through a rights-based perspective. When a country integrates policy instruments for disaster risk management with national policy frameworks, it facilitates the allocation of human, technical and financial resources to achieve these goals.

These issues were debated and raised for public scrutiny and formalized during the World Conference on Disaster Reduction (WCDR) in Kobe, Hyogo, Japan (January 2005), with the Sendai Framework being the instrument that succeeds it in the update. In accordance with the Sendai Framework and the 2030 Agenda, comprehensive risk reduction strategies must go beyond civil protection systems and also include elements of an intersectoral nature, such as urban risk management, spatial planning, watershed management resources, financial protection, public investment resilience, or preparedness and early warning, all issues that cannot be addressed globally by any single sector strategy or plan. Ecuador, a signatory since 2015 of the Sendai Framework Convention for Disaster Risk Reduction, is focused on the adoption of measures on the three dimensions of risk disaster, that is, exposure to hazards, vulnerability and capacity, and characteristics of threats; with the purpose of preventing new risks from occurring, reducing existing ones and increasing resilience.

This shows the need to carry out more scientific studies that clarify the vulnerabilities that affect the territory. This problem can be addressed through today's technological advances, such as GPS technology, satellite systems, remote sensors, or increasingly robust computer systems with never-before-seen capabilities. Remote sensors emerge as a fundamental tool for managing and governance risks because they allow the generation of information in a fast, reliable, and multi-temporal way, aspects of great importance when planning the territory, even more so when it comes to risks. In this sense, the generation of digital models and indices from this type of data allows detecting, controlling, and evaluating the risk associated with landslides. The establishment of a methodology for the management and use of the information from these sensors, applied to the management of the risk of landslides, represents a very important contribution to the management, development, and planning of the territory. This doctoral thesis develops some of these methods from the construction and materialization for the generation of information and knowledge explicitly applied to the risks of landslides.

On the other hand, landslide assessment remains a crucial task in land management and hazard/risk management. This task has been

undertaken successfully and unsuccessfully by all types of stakeholders (governments, non-governmental organizations, the private sector, and research institutes) in a broad spectrum of locations and magnitudes. A decade ago, Guzzetti et al. (2012) mentioned in his research the need to provide quality indicators of inventory maps (integrity, geographic and thematic accuracy). However, despite the technological advances described, this practice remains anecdotal and is not free of problems. Furthermore, despite the tools and methodologies developed to develop, update and validate landslide inventories at the regional or national level using personal electronic devices, these initiatives are anecdotal in regions such as Latin America.

Natural and anthropic landslides are common in the Ecuadorian Andes, causing severe and ongoing damage. Unfortunately, only a few studies have been carried out in the country (Basabe et al., 1996), and no databases record these phenomena or updated inventory maps. Landslides are the most common type of geohazard worldwide and play an important role in the evolution of landforms. Collecting qualitative and quantitative data on landslide occurrences is a difficult task. Based on the location, type, and impact of the phenomena, this is a challenge in itself to record the data correctly. It is clear that the accuracy, the correct description of the phenomena, and their magnitude are crucial data to include in a collapse inventor.

Chapter 1. With this in mind, we developed a mobile application to locate, characterize and typify landslides using the Open Data Kit (ODK) system to undertake the task of collecting that data. This development fulfills three purposes: 1) increase the number of studies carried out with landslides to reduce the negative impact of these events on infrastructure, properties, and people; 2) make available to the scientific community, municipal technicians, and civilians a low-cost and easy-to-use tool for the massive collection of data from collapses; and 3) obtain current and detailed information to develop and update inventory maps at the regional level; train and validate automatic methodologies to obtain these maps at smaller scales, and enrich existing databases (at regional, national and global level).

Employing this tool makes reporting quick, easy, and cost-effective,

with the added benefit that no specialist knowledge is required to use it. MARLI offers two forms: one open to all citizens (without prior knowledge), a group that can provide very useful and up-to-date information, and a second form for specialized users. MARLI's user interface, designed according to the needs and capabilities of different users, allows information to be easily entered into the database.

Analysis of data recorded by MARLI showed that the area affected by landslides has increased over the past two decades. This circumstance may be a consequence of the processes of informality in the occupation of land that takes place in Ecuador, either due to the advance of the agricultural frontier or due to the existence of informal settlements on the outskirts of the cities. In addition, the analyzes carried out revealed that a significant number of landslides registered with the MARLI threaten populations and infrastructures, exposing the community to personal and material damage. This information can be taken as indicative of the increase in regional instability, showing the need to monitor these phenomena linked to territorial dynamics and factors derived from climate change.

The impact of this development can be seen when comparing, at a regional level, the inventory carried out with MARLI and the one achieved within the framework of the PRECUPA project in 1996. The number of landslides recorded in PRECUPA (130) is multiplied by 5 in the inventory carried out from MARLI (668), which causes the landslide density to increase from 3.6 to 45.8 per km^2. However, in the inventory drawn up from the MARLI, the area occupied by said phenomena is three times smaller than that recorded in the PRECUPA inventory (3.83% and 9.55%, respectively). Thus, it follows that the mere existence of a local database (updated, standardized and complete) of landslides, together with its availability to the public, facilitates the mapping of susceptibility to landslides. Maintaining this milestone over time involves creating, maintaining, and updating landslide databases as a well-established practice and encouraging their use in the design of land use planning policies.

Chapter 2. This part of the thesis addresses the intrinsic vulnerability of population settlements in the face of disasters due to

poverty, poor governance, and little or no management of the territory, as well as the lack of mitigation protocols and the absence of tools for planning of urban occupation, all leading to such impacts being particularly serious. Cuenca (Ecuador) is a significant example of a city that experienced considerable demographic growth in recent decades linked to increased losses due to landslides. Despite such effects, urban planning tools are absent. This circumstance requires a multi-temporal landslide risk assessment. To address this challenge, it is proposed here to analyze the population's exposure to the occurrence of landslides and the evolution of this risk in the last decade (2010 - 2020). For this purpose, it was necessary to calculate the updated spatial distribution of landslides and the distribution of the population in the period 2010 - 2020.

In the absence of data on the location of the population, the data from the electricity supply contracts were used as an approximation of the distribution of the population in the territory. The results indicate that the current relative risk is found in the municipalities in the study area's southern sector (ie Turi, Valle, Santa Ana, Tarqui, and Paccha). In addition, the multitemporal analysis indicates that most of the city's municipalities located in the mountainous areas that delimit the center (that is, Sayausi, San Joaquín, Tarqui, Valle, Sidcay, Baños, Sidcay, Ricaurte, Paccha, and Chiquintad), experience growth in sustained population, exposed to greater risk with a constant growth trend.

Based on the distribution of landslides, the relative landslide risk in the city of Cuenca, i.e. landslide susceptibility, was estimated using a machine learning algorithm, MaxEnt. In this perspective, a set of environmental variables was selected as potential predisposing factors for landslide initiation, and their multicollinearity was analyzed. In the context of the proposed analysis, the data from the susceptibility analysis and the electricity supply contracts were used as a basis for the multitemporal assessment of the landslide risk over the study area considering only the risk to people. The most susceptible areas of the city of Cuenca resulting from the analysis are located on the slopes that flank the city. In these areas, slopes are steep and concave, where roads create local discontinuities. In contrast, peri-urban and rural areas are in areas of medium to very high susceptibility with gentler slopes.

The availability of a landslide inventory map made it possible to evaluate the model, taking field data into account. By crossing the landslide points and the final susceptibility map, information was obtained on the landslide distribution together with the surface extent of the susceptibility classes. The results highlight that almost 75% of the real landslides were located in the high and very high susceptibility classes. Thus, this study provided information on important issues such as i) the effect of the sustained expansion of urban areas due to population growth on the relative variation of collapse risk and ii) the risk assessment method of reduced complexity in the presence of data only partial (ie susceptibility to landslides), instead of danger, and electricity supply contracts instead of population distribution).

The relative risk maps obtained are useful to guide the planning of the territory, the restriction of occupation, and the adoption of early warning strategies. Also, the methodological approach used, which takes into account landslide susceptibility and population variation through the analysis of indirect data, has the potential to be applied to cities in low-income countries where you have a minimal data set.

Chapter 3. This thesis chapter addresses a specific vulnerability in the region, rock falls. These phenomena are considered the main danger in mountain areas around the world, partly because of their direct consequences on the territory and the population. The mapping of rock fall susceptibility is fundamental both the prior assessment of the impact of the implementation of infrastructure and for establishing, subsequently, restrictions in relation to the use of the soil around these areas, with the main objective of avoiding the loss of human life and material goods. The vast majority of the methods developed to identify areas susceptible to rockfalls require previously identifying the so-called source points. These points are considered the origin of the rockfall and, therefore, the location from which the most exposed areas are identified in the event of said phenomenon.

Thus, in this research, a novel hybrid approach is developed based on counting trajectories per pixel obtained using the QPROTO tool, which allows calculating the susceptibility to rockfall. So, these results are used for several purposes: 1) to identify points of origin of rock fall;

2) to evaluate the susceptibility to rockfall, 3) to classify the physical consequences of rockfall events on the Molleturo road, the city's main connection with the rest of the country, and 4) analyze the influence of the resolution of the Digital Elevation Models on the accuracy of the results.

The analyzes carried out in this study are considered to be of particular relevance both for the prior assessment of the impact of the implementation of infrastructures, the particular case of communication routes in environments prone to the occurrence of rock fall events, which would allow to modify the constructive conditions and/or implement the most appropriate prevention measures for the identified risk circumstances; as well as establishing restrictions later in relation to the use of land in the surroundings of these areas, with the main purpose of avoiding the loss of human lives and material goods, as well as the consequent disconnection that the beneficiary cities of said infrastructures entail. In addition, these results also help researchers to consider the effects of the resolution of Digital Elevation Models in the identification of rockfall origin points, the mapping of rockfall susceptibility, or the identification of road sections through the use of automatic prediction tools, which may be affected by rockfall or subsidence phenomena.

Chapter 4. Chapter four revolves around the prevention and mitigation of slope instability, which requires effective technologies to reduce the vulnerability of existing structures. Landslides are global phenomena caused by natural geological phenomena or induced by anthropogenic sources. Slow and intermittent landslides result in a significant number of physical damages and significant economic losses on private and public property. The vulnerability of buildings to landslides is a term used to describe their potential for physical loss when affected by movements induced by unstable ground. Therefore, monitoring plays a key role in natural hazard management and provides cost-effective solutions to mitigate physical and economic losses.

Monitoring structures plays an increasingly important role in the context of life and the management of these natural hazards. Therefore, it is necessary to study the evolution of this type of event and consider its

consequences. In reality, these phenomena' prevention, forecasting, and monitoring are the most appropriate tools to minimize their secondary effects. The development of unstable areas in urban contexts has sparked a growing interest in innovative approaches to provide information on the temporal and spatial evolution of their interaction with existing buildings.

Remote sensing techniques have proven to be powerful research tools due to their high spatial and temporal coverage, rapid data acquisition, and generally reasonable costs. Differential Interferometry SAR (DinSAR) meets these needs very well among the different types of remote sensing techniques. Thus, the main objective of the present study was to provide a general methodology that can be used to predict the spatial and temporal evolution of a slow landslide. In particular, this work analyzes a slow phenomenon that affects the University of Azuay (Cuenca, Ecuador). For this purpose, an integrated system of monitoring and analysis was implemented both on a local and detailed scale, highlighting the importance of the DInSAR technique as an additional monitoring technique and as an alternative method, at least in the preliminary evaluations of the phenomena, in the traditional surveillance systems of the land Cite that thanks to the inter-institutional collaboration agreement between the Federico II University of Naples and the University of Azuay, it was possible to obtain SAR images of the Cosmo-SkyMed satellite constellation, in the period March 2016 - January 2018. We must mention that this collaboration and Image analysis continues today.

This research provided an integrated monitoring methodology that can be used to predict the spatial and temporal evolution of a slow landslide affecting buildings within the University of Azuay campus. A multilevel analysis integrated with innovative monitoring techniques along with traditional and detailed methods such as geophysical surveys has also been established, presenting a valid strategy for continuous risk updates. This is the first step to prevent and mitigate the risk of natural disasters such as landslides that affect the city of Cuenca, a UNESCO World Heritage Site.

Chapter 5. This chapter presents a study carried out in Zaruma,

a well-known mining district in the province of *El Oro* in Ecuador, which suffers from subsidence phenomena related to illegal underground mining. The city of Zaruma is among the most dangerous places of subsidence in the world. This danger is related to a dense network of unknown legal and illegal tunnels, which increases the fragility of the municipal territory. Mining in this area dates back to pre-Hispanic times. Recorded history shows the first settlements of the Cañari culture and through the Inca culture, from the Spanish, American, and Canadian presence in the area to modern times. Mining in this district has steadily shifted from legal to illegal, technical, and non-technical mining. Currently, the predominant activities are illegal and non-technical in an area declared as a no-exploitation zone under the city of Zaruma. This brings a series of problems, such as land subsidence, that affect the aforementioned city. Subsidence and collapses have accumulated sporadically in the past, but in recent years (since 2017), this phenomenon has become a relatively constant occurrence.

In fact, on December 15, 2021, a subsidence event occurred that caused the evacuation of more than 300 people and the prohibition of access to more than ten blocks. For this reason, it is essential to find a fast and economical technique that can generate information on the spatial and temporal development of uncontrolled underground activities to improve risk management. In this work, the Differential Interferometry Synthetic Aperture Radar (DInSAR) technique, developed in the SUBSIDENCE software, was used to study the deformation of the ground linked to illegal artisanal mining in the city of Zaruma as part of a collaboration project between local and international universities.

This study presents the primary displacement rates recorded throughout the analyzed time interval. It was observed that in the area affected by the collapse of December 15, 2021, the identified PSs show significant deformation rates higher than 0.5 cm/year.
An even more significant element is the time series of these points, which shows an acceleration from June 2021, six months before the collapse. Likewise, to verify the interferometric results, a field survey was carried out using the MARLI application.

With this study, the need to implement a continuous monitoring system using remote sensing techniques was put on the table to prevent phenomena like what happened in 2021 by identifying those areas of the city that need a more complete knowledge of the underground, probably affected by unknown excavation activities.

The Sendai Framework for Disaster Risk Reduction (2015 - 2030), is considered the first milestone of the paradigm shift in natural disaster management because prevention and risk management are prioritized instead of crisis management, with the main purpose of avoiding the loss of life and the effects on the economy of material losses. Thus, the Framework urges countries, before 2030, to deploy national and local strategies whose main objectives are 1) to improve the resilience of communities, 2) to increase scientific knowledge and early warning, and 3) to increase the preparedness of the population in the face of disasters. In this way, prevention and governance are the main pillars on which efforts to deal with natural disasters are based. Ecuador has been associated with the Framework since 2015.

In this context, the need for multi-purpose training in risk management is highlighted; the development of efficient data capture tools and the application of methods and procedures for the generation of information that allow the organization of priority actions with the purpose of making an appropriate and efficient disaster risk management at a cantonal, regional and local level. Undoubtedly, the success of this chain of actions requires, in an essential way, to strengthen the relations between institutions and between this and society, establishing dynamics of cooperation and dialogue.

Taking into account the background described, this thesis is born from the imperative need to develop new methodologies applicable to the management and governance of risk through the use of remote sensors as the main element for the location of threats. This chapter describes how real demands and events, not always foreseen, shaped my research work until it was transformed into tools, developments, methodologies, and information that made it possible, in various ways, to contribute to risk governance in areas both close and distant, such as the university, the scientific, and the political-institutional. Implicitly addressed

several margins on the employment and management of disaster risk at the national, cantonal, and local level. A socialization process was also carried out of the achievements achieved through participation in congresses, symposium, consultancies, and work meetings with competent authorities both in the area of risks and in the area of territorial management and with the sectional government.

Resumen

Desde la última década del siglo XX se ha asumido el principal reto para la reducción del riesgo de desastres; el cambio de enfoque que se ha visto, pasando de una mirada ligada a la imprevisibilidad e ineludibilidad de su ocurrencia a considerarlos como un problema vinculado a los procesos de desarrollo de los países, regiones y opciones de uso y ordenamiento del territorio.

Con la creciente preocupación a nivel internacional por el aumento en la frecuencia y severidad de los desastres naturales y amenazas, y en el contexto actual que vivimos, con una epidemia a escala planetaria, en medio de eventos naturales cada vez más frecuentes y de en magnitudes cada vez más extremas, muchas de ellas como consecuencia del cambio climático, se evidencian las diferentes dimensiones en que un desastre puede afectar el bienestar de las personas.

Entre las principales causas para la ocurrencia de una catástrofe se encuentra la forma inadecuada de implementar la gestión del riesgo de desastres en el territorio, así como la falta de conciencia y responsabilidad sobre el tema por parte de los decisores políticos y de la propia comunidad. Esta gestión del riesgo implica, entre otros aspectos, la reducción del riesgo ante la ocurrencia de desastres. A través de este enfoque se persigue la reducción de las vulnerabilidades sociales, económicas y ambientales, aumentando la resiliencia y el bienestar general de la población desde una perspectiva de derechos. Cuando un país integra los instrumentos de políticas para la gestión del riesgo de desastres con los marcos de políticas nacionales, facilita la asignación de recursos humanos, técnicos y financieros para lograr estos objetivos.

Estos temas fueron debatidos y planteados para el escrutinio público y formalizados durante la Conferencia Mundial sobre Reducción de Desastres (WCDR) en Kobe, Hyogo, Japón (enero de 2005), siendo el Marco de Sendai el instrumento que lo sucede en la actualización. De acuerdo con el Marco de Sendai y la Agenda 2030, las estrategias integrales de reducción de riesgos deben ir más allá de los sistemas de protección civil e incluir también elementos de carácter intersectorial, como la gestión del riesgo urbano, la ordenación del territorio, la gestión de recursos de cuencas hidrográficas, la protección financiera, la resiliencia de la inversión pública, o preparación y alerta temprana, todos los problemas que no pueden ser abordados globalmente por ninguna estrategia o plan de un solo sector. Ecuador, signatario desde 2015 del Convenio Marco de Sendai para la Reducción del Riesgo de Desastres, está enfocado en la adopción de medidas sobre las tres dimensiones del riesgo de desastres, es decir, exposición a las amenazas, vulnerabilidad y capacidad, y características de las amenazas; con el fin de prevenir la ocurrencia de nuevos riesgos, reducir los existentes y aumentar la resiliencia.

Esto muestra la necesidad de realizar más estudios científicos que esclarezcan las vulnerabilidades que afectan al territorio. Este problema se puede abordar a través de los avances tecnológicos actuales, como la tecnología GPS, los sistemas satelitales, los sensores remotos o los sistemas informáticos, cada vez más robustos con capacidades nunca antes vistas. Los sensores remotos emergen como una herramienta fundamental para la gestión y gobernanza de riesgos porque permiten generar información de forma rápida, confiable y multitemporal, aspectos de gran importancia a la hora de planificar el territorio, más aún cuando se trata de riesgos. En este sentido, la generación de modelos e índices digitales a partir de este tipo de datos permite detectar, controlar y evaluar el riesgo asociado a deslizamientos. El establecimiento de una metodología para la gestión y uso de la información de estos sensores, aplicada a la gestión del riesgo de deslizamientos, representa una contribución muy importante a la gestión, desarrollo y planificación del territorio. Esta tesis doctoral desarrolla algunos de estos métodos a partir de la construcción y materialización para la generación de información y conocimiento aplicado explícitamente a los riesgos de deslizamientos.

Por otro lado, la evaluación de deslizamientos sigue siendo una tarea crucial en la gestión de la tierra y la gestión de peligros/riesgos. Esta tarea ha sido emprendida con éxito y sin éxito por todo tipo de partes interesadas (gobiernos, organizaciones no gubernamentales, el sector privado e institutos de investigación) en un amplio espectro de ubicaciones y magnitudes. Hace una década, Guzzetti et al. (2012) mencionó en su investigación la necesidad de proporcionar indicadores de calidad de los mapas de inventario (integridad, precisión geográfica y temática). Sin embargo, a pesar de los avances tecnológicos descritos, esta práctica sigue siendo anecdótica y no está exenta de problemas. Además, a pesar de las herramientas y metodologías desarrolladas para desarrollar, actualizar y validar inventarios de deslizamientos a nivel regional o nacional utilizando dispositivos electrónicos personales, estas iniciativas son anecdóticas en regiones como América Latina.

Los deslizamientos de tierra naturales y antrópicos son comunes en los Andes ecuatorianos, causando daños severos y continuos. Lamentablemente, en el país se han realizado pocos estudios (Basabe et al., 1996), y no existen bases de datos que registren estos fenómenos ni mapas de inventarios actualizados. Los deslizamientos de tierra son el tipo de geoamenaza más común en todo el mundo y juegan un papel importante en la evolución de los accidentes geográficos. La recopilación de datos cualitativos y cuantitativos sobre los deslizamientos de tierra es una tarea difícil. Basado en la ubicación, el tipo y el impacto de los fenómenos, este es un desafío en sí mismo para registrar los datos correctamente. Está claro que la precisión, la correcta descripción de los fenómenos y su magnitud son datos cruciales a incluir en un inventario de deslizamientos.

Capítulo 1. Con esto en mente, desarrollamos una aplicación móvil para localizar, caracterizar y tipificar deslizamientos utilizando el sistema Open Data Kit (ODK) para llevar a cabo la tarea de recolectar esos datos. Este desarrollo cumple con tres propósitos: 1) aumentar el número de estudios realizados con deslizamientos para reducir el impacto negativo de estos eventos en la infraestructura, las propiedades y las personas; 2) poner a disposición de la comunidad científica, técnicos municipales y civiles una herramienta de bajo costo y fácil manejo para la recolección masiva de datos de derrumbes;

y 3) obtener información actualizada y detallada para desarrollar y actualizar mapas de inventario a nivel regional; entrenar y validar metodologías automáticas para obtener estos mapas a escalas más pequeñas, y enriquecer las bases de datos existentes (a nivel regional, nacional y global). El uso de esta herramienta hace que los informes sean rápidos, fáciles y rentables, con el beneficio adicional de que no se requieren conocimientos especializados para usarlos. MARLI ofrece dos formularios: uno abierto a todos los ciudadanos (sin conocimientos previos), un grupo que puede proporcionar información muy útil y actualizada, y un segundo formulario para usuarios especializados. La interfaz de usuario de MARLI, diseñada de acuerdo con las necesidades y capacidades de los diferentes usuarios, permite ingresar fácilmente la información en la base de datos.

El análisis de los datos registrados por MARLI mostró que el área afectada por deslizamientos de tierra ha aumentado en las últimas dos décadas. Esta circunstancia puede ser consecuencia de los procesos de informalidad en la ocupación del suelo que se dan en el Ecuador, ya sea por el avance de la frontera agrícola o por la existencia de asentamientos informales en las afueras de las ciudades. Además, los análisis realizados revelaron que un número importante de deslizamientos registrados en el MARLI amenazan a las poblaciones e infraestructuras, exponiendo a la comunidad a daños personales y materiales. Esta información puede tomarse como indicativa del aumento de la inestabilidad regional, mostrando la necesidad de monitorear estos fenómenos vinculados a dinámicas territoriales y factores derivados del cambio climático.

El impacto de este desarrollo se puede apreciar al comparar, a nivel regional, el inventario realizado con MARLI y el realizado en el marco del proyecto PRECUPA en 1996. El número de deslizamientos registrados en PRECUPA (130) se multiplica por 5 en el inventario realizado desde MARLI (668), lo que hace que la densidad de deslizamientos aumente de 3.6 a 45.8 por km^2. Sin embargo, en el inventario elaborado a partir del MARLI, el área ocupada por dichos fenómenos es tres veces menor que la registrada en el inventario de PRECUPA (3,83% y 9,55%, respectivamente). Por lo tanto, se deduce que la mera existencia de una base de datos local (actualizada, estandarizada y completa) de deslizamientos, junto con su disponibilidad al público, facilita el

mapeo de la susceptibilidad a los deslizamientos. Mantener este hito en el tiempo implica crear, mantener y actualizar bases de datos de deslizamientos como una práctica bien establecida y fomentar su uso en el diseño de políticas de ordenamiento territorial.

Capítulo 2. Esta parte de la tesis aborda la vulnerabilidad intrínseca de los asentamientos de población frente a desastres por pobreza, mala gobernabilidad y poca o nula gestión del territorio, así como la falta de protocolos de mitigación y la ausencia de herramientas para la planificación urbana. ocupación, todo lo cual lleva a que dichos impactos sean particularmente graves. Cuenca (Ecuador) es un ejemplo significativo de una ciudad que experimentó un crecimiento demográfico considerable en las últimas décadas vinculado al aumento de las pérdidas por deslizamientos. A pesar de tales efectos, las herramientas de planificación urbana están ausentes. Esta circunstancia requiere una evaluación de riesgo de deslizamientos multitemporal. Para abordar este desafío, aquí se propone analizar la exposición de la población a la ocurrencia de deslizamientos y la evolución de este riesgo en la última década (2010 - 2020). Para ello fue necesario calcular la distribución espacial actualizada de los deslizamientos y la distribución de la población en el periodo 2010 - 2020.

En ausencia de datos sobre la ubicación de la población, se utilizaron los datos de los contratos de suministro eléctrico como una aproximación a la distribución de la población en el territorio. Los resultados indican que el riesgo relativo actual se encuentra en los municipios del sector sur del área de estudio (ie Turi, Valle, Santa Ana, Tarqui y Paccha). Además, el análisis multitemporal indica que la mayoría de los municipios de la ciudad ubicados en las zonas montañosas que delimitan el centro (es decir, Sayausi, San Joaquín, Tarqui, Valle, Sidcay, Baños, Sidcay, Ricaurte, Paccha y Chiquintad), experimentan crecimiento sostenido de la población, expuesta a mayor riesgo con una tendencia de crecimiento constante.

Con base en la distribución de deslizamientos, se estimó el riesgo relativo de deslizamientos en la ciudad de Cuenca, es decir, la susceptibilidad a deslizamientos, utilizando un algoritmo de aprendizaje automático, MaxEnt. En esta perspectiva, se seleccionó un conjunto

de variables ambientales como posibles factores predisponentes para la iniciación de deslizamientos y se analizó su multicolinealidad. En el contexto del análisis propuesto, los datos del análisis de susceptibilidad y los contratos de suministro de energía eléctrica se utilizaron como base para la evaluación multitemporal del riesgo de deslizamiento sobre el área de estudio considerando solo el riesgo para las personas. Las zonas más susceptibles de la ciudad de Cuenca resultantes del análisis se ubican en las laderas que flanquean la ciudad. En estas áreas, las pendientes son empinadas y cóncavas, donde los caminos crean discontinuidades locales. En cambio, las áreas periurbanas y rurales se encuentran en áreas de susceptibilidad media a muy alta con pendientes más suaves.

La disponibilidad de un mapa de inventario de deslizamientos permitió evaluar el modelo teniendo en cuenta los datos de campo. Al cruzar los puntos de deslizamiento y el mapa de susceptibilidad final, se obtuvo información sobre la distribución de deslizamiento junto con la extensión superficial de las clases de susceptibilidad. Los resultados destacan que casi el 75% de los deslizamientos reales se ubicaron en las clases de susceptibilidad alta y muy alta. Así, este estudio proporcionó información sobre temas importantes como i) el efecto de la expansión sostenida de las áreas urbanas debido al crecimiento de la población sobre la variación relativa del riesgo de colapso y ii) el método de evaluación de riesgo de complejidad reducida en presencia de datos solo parciales. (es decir, susceptibilidad a deslizamientos de tierra). En lugar de peligro, y contratos de suministro eléctrico en lugar de distribución de población).

Los mapas de riesgo relativo obtenidos son útiles para orientar la planificación del territorio, la restricción de la ocupación y la adopción de estrategias de alerta temprana. Además, el enfoque metodológico utilizado, que tiene en cuenta la susceptibilidad a los deslizamientos de tierra y la variación de la población a través del análisis de datos indirectos, tiene el potencial de aplicarse a ciudades en países de bajos ingresos donde se tiene un conjunto de datos mínimo.

Capítulo 3. Este capítulo de tesis aborda una vulnerabilidad específica en la región, los desprendimientos de rocas. Estos fenómenos son considerados el principal peligro en las zonas montañosas de todo

el mundo, en parte por sus consecuencias directas sobre el territorio y la población. El mapeo de susceptibilidad al desprendimiento de rocas es fundamental tanto para la evaluación previa del impacto de la ejecución de infraestructuras como para establecer, posteriormente, restricciones en relación al uso del suelo alrededor de estas áreas, con el objetivo principal de evitar la pérdida de la vida humana y los bienes materiales. La gran mayoría de los métodos desarrollados para identificar áreas susceptibles de desprendimiento de rocas requieren identificar previamente los denominados puntos fuente. Estos puntos son considerados el origen del desprendimiento de rocas y, por tanto, el lugar desde el que se identifican las zonas más expuestas en caso de producirse dicho fenómeno.

Así, en esta investigación se desarrolla un novedoso enfoque híbrido basado en el conteo de trayectorias por píxel obtenido mediante la herramienta QPROTO, que permite calcular la susceptibilidad al desprendimiento de rocas. Entonces, estos resultados se utilizan para varios propósitos: 1) para identificar los puntos de origen de la caída de rocas; 2) evaluar la susceptibilidad al desprendimiento de rocas, 3) clasificar las consecuencias físicas de los eventos de desprendimiento de rocas en la vía Molleturo, principal conexión de la ciudad con el resto del país, y 4) analizar la influencia de la resolución de los Modelos Digitales de Elevación en la exactitud de los resultados.

Los análisis realizados en este estudio se consideran de especial relevancia tanto para la evaluación previa del impacto de la ejecución de infraestructuras, el caso particular de vías de comunicación en entornos propensos a la ocurrencia de eventos de caída de rocas, que permitiría modificar las condiciones constructivas y/o implementar las medidas de prevención más adecuadas a las circunstancias de riesgo identificadas; así como establecer restricciones posteriores en relación con el uso del suelo en el entorno de estas áreas, con el objetivo principal de evitar la pérdida de vidas humanas y bienes materiales, así como la consiguiente desconexión que conllevan las ciudades beneficiarias de dichas infraestructuras. Además, estos resultados también ayudan a los investigadores a considerar los efectos de la resolución de Modelos Digitales de Elevación en la identificación de puntos de origen de desprendimientos de rocas, el mapeo de la susceptibilidad a

desprendimientos de rocas o la identificación de tramos de carretera mediante el uso de herramientas de predicción automática, que pueden ser afectados por fenómenos de derrumbe o hundimiento.

Capítulo 4. El capítulo cuatro gira en torno a la prevención y mitigación de la inestabilidad de taludes, lo que requiere tecnologías efectivas para reducir la vulnerabilidad de las estructuras existentes. Los deslizamientos de tierra son fenómenos globales causados por fenómenos geológicos naturales o inducidos por fuentes antropogénicas. Los deslizamientos de tierra lentos e intermitentes resultan en un número significativo de daños físicos y pérdidas económicas significativas en la propiedad privada y pública. La vulnerabilidad de los edificios a los deslizamientos de tierra es un término utilizado para describir su potencial de pérdida física cuando se ven afectados por movimientos inducidos por suelos inestables. Por lo tanto, el monitoreo juega un papel clave en la gestión de peligros naturales y proporciona soluciones rentables para mitigar las pérdidas físicas y económicas.

Las estructuras de monitoreo juegan un papel cada vez más importante en el contexto de la vida y la gestión de estos peligros naturales. Por ello, es necesario estudiar la evolución de este tipo de eventos y considerar sus consecuencias. En realidad, la prevención, previsión y seguimiento de estos fenómenos son las herramientas más adecuadas para minimizar sus efectos secundarios. El desarrollo de áreas inestables en contextos urbanos ha despertado un creciente interés en enfoques innovadores para proporcionar información sobre la evolución temporal y espacial de su interacción con los edificios existentes.

Las técnicas de teledetección han demostrado ser poderosas herramientas de investigación debido a su alta cobertura espacial y temporal, rápida adquisición de datos y, en general, costos razonables. La interferometría diferencial SAR (DinSAR) satisface muy bien estas necesidades entre los diferentes tipos de técnicas de teledetección. Por lo tanto, el objetivo principal del presente estudio fue proporcionar una metodología general que pueda usarse para predecir la evolución espacial y temporal de un deslizamiento lento. En particular, este trabajo analiza un fenómeno lento que afecta a la Universidad del Azuay (Cuenca, Ecuador). Para ello se implementó un sistema integrado de

monitoreo y análisis tanto a escala local como de detalle, destacando la importancia de la técnica DINSAR como técnica adicional de monitoreo y como método alternativo, al menos en las evaluaciones preliminares de los fenómenos, en los sistemas de vigilancia terrestre tradicionales. Citar que gracias al convenio de colaboración interinstitucional entre la Universidad Federico II de Nápoles y la Universidad del Azuay, se logró obtener imágenes SAR de la constelación de satélites Cosmo-SkyMed, en el periodo marzo 2016 - Enero 2018. Cabe mencionar que esta colaboración y análisis de imágenes continúa en la actualidad.

Esta investigación proporcionó una metodología de monitoreo integrada que puede ser utilizada para predecir la evolución espacial y temporal de un deslizamiento lento que afecta a edificios dentro del campus de la Universidad del Azuay. También se ha establecido un análisis multinivel integrado con técnicas de monitoreo innovadoras junto con métodos tradicionales y detallados, como estudios geofísicos, que presenta una estrategia válida para actualizaciones continuas de riesgos. Este es el primer paso para prevenir y mitigar el riesgo de desastres naturales como los deslizamientos de tierra que afectan a la ciudad de Cuenca, Patrimonio de la Humanidad por la UNESCO.

Capítulo 5. Este capítulo presenta un estudio realizado en Zaruma, un conocido distrito minero en la provincia de *El Oro* en Ecuador, que sufre fenómenos de hundimiento relacionados con la minería subterránea ilegal. La ciudad de Zaruma se encuentra entre los lugares de hundimiento más peligrosos del mundo. Este peligro está relacionado con una densa red de túneles legales e ilegales desconocidos, lo que aumenta la fragilidad del territorio municipal. La minería en esta zona se remonta a la época prehispánica. La historia registrada muestra los primeros asentamientos de la cultura Cañari ya través de la cultura Inca, desde la presencia española, americana y canadiense en la zona hasta los tiempos modernos. La minería en este distrito ha cambiado constantemente de minería legal a ilegal, técnica y no técnica. Actualmente, las actividades predominantes son ilegales y no tecnificadas en un área declarada como zona de no explotación bajo la ciudad de Zaruma. Esto trae consigo una serie de problemas, como el hundimiento de terrenos, que afectan a la citada ciudad. Los hundimientos y derrumbes se han acumulado esporádicamente en el

pasado, pero en los últimos años (desde 2017), este fenómeno se ha vuelto relativamente constante.

De hecho, el 15 de diciembre de 2021 se produjo un evento de hundimiento que provocó la evacuación de más de 300 personas y la prohibición de acceso a más de diez manzanas. Por esta razón, es fundamental encontrar una técnica rápida y económica que pueda generar información sobre el desarrollo espacial y temporal de las actividades subterráneas no controladas para mejorar la gestión del riesgo. En este trabajo se utilizó la técnica de Radar de Apertura Sintética de Interferometría Diferencial (DInSAR), desarrollada en el software SUBSIDENCE, para estudiar la deformación del suelo vinculado a la minería artesanal ilegal en la ciudad de Zaruma como parte de un proyecto de colaboración entre locales e internacionales. Universidades.

Este estudio presenta las tasas de desplazamiento primario registradas a lo largo del intervalo de tiempo analizado. Se observó que, en el área afectada por el derrumbe del 15 de diciembre de 2021, los PS identificados muestran tasas de deformación significativas superiores a 0,5 cm/año. Un elemento aún más significativo es la serie temporal de estos puntos, que muestra una aceleración a partir de junio de 2021, seis meses antes del colapso. Asimismo, para verificar los resultados interferométricos se realizó un levantamiento de campo utilizando la aplicación MARLI.

Con este estudio se planteaba sobre la mesa la necesidad de implantar un sistema de monitorización continua mediante técnicas de teledetección para prevenir fenómenos como el ocurrido en 2021 identificando aquellas zonas de la ciudad que necesitan un conocimiento más completo del subsuelo, probablemente afectado por desconocidos actividades de excavación.

En el marco de Sendai para la Reducción del Riesgo de Desastres (2015 - 2030), se considera el primer hito del cambio de paradigma en la gestión de desastres naturales porque se prioriza la prevención y la gestión del riesgo frente a la gestión de crisis, con el propósito principal de evitar la pérdida de vidas y los efectos en la economía de las pérdidas materiales. Así, el Marco insta a los países, antes de 2030, a desplegar

estrategias nacionales y locales cuyos principales objetivos son 1) mejorar la resiliencia de las comunidades, 2) aumentar el conocimiento científico y la alerta temprana, y 3) aumentar la preparación de la población frente a desastres De esta forma, la prevención y la gobernanza son los principales pilares sobre los que se asientan los esfuerzos para hacer frente a los desastres naturales. Ecuador está asociado al Marco desde 2015.

En este contexto, se destaca la necesidad de una formación polivalente en gestión de riesgos; el desarrollo de herramientas eficientes de captura de datos y la aplicación de métodos y procedimientos para la generación de información que permitan la organización de acciones prioritarias con el propósito de hacer una adecuada y eficiente gestión del riesgo de desastres a nivel cantonal, regional y local. Sin duda, el éxito de esta cadena de acciones requiere, de manera esencial, fortalecer las relaciones entre las instituciones y entre éstas y la sociedad, estableciendo dinámicas de cooperación y diálogo.

Teniendo en cuenta los antecedentes descritos, esta tesis nace de la imperiosa necesidad de desarrollar nuevas metodologías aplicables a la gestión y gobernanza del riesgo mediante el uso de sensores remotos como elemento principal para la localización de amenazas. Este capítulo describe cómo las demandas y los acontecimientos reales, no siempre previstos, moldearon mi trabajo de investigación hasta transformarlo en herramientas, desarrollos, metodologías e información que permitieron, de diversas formas, contribuir a la gobernanza del riesgo en áreas cercanas y lejanas, como el universitario, el científico y el político-institucional. Implícitamente abordó varios márgenes sobre el empleo y la gestión del riesgo de desastres a nivel nacional, cantonal y local. También se llevó a cabo un proceso de socialización de los logros alcanzados a través de la participación en congresos, simposios, consultorías y reuniones de trabajo con autoridades competentes tanto en el área de riesgos como en el área de gestión territorial y con el gobierno seccional.

Resumo

Dende a última década do século XX asumiuse como o principal reto para a redución do risco de catástrofes, o cambio de foco co que se viu, pasando dunha visión ligada ao imprevisíbel e ineludíbel da súa aparición, a consideralas como unha problemática vencellada aos procesos de desenvolvemento dos países, rexións, e ás opcións de uso e ordenación do territorio.

Coa crecente inquietude a nivel internacional polo aumento da frecuencia e gravidade das catástrofes e ameazas naturais, e no contexto actual no que vivimos, cunha epidemia a escala planetaria, en pleno apoxeo de eventos naturais cada vez máis recorrentes e de magnitudes cada vez máis extremas, moitas delas como consecuencia do cambio climático, manifféstanse de forma evidente as diferentes dimensións nas que un desastre pode repercutir no benestar das persoas.

Entre as causas principais da ocorrencia dunha catástrofe atópase a inadecuada forma de implantar a xestión do risco de catástrofes no territorio, así como a falta de concienciación e responsabilidade sobre o tema por parte dos decisores políticos e da propia comunidade. Dita xestión do risco envolve, entre outros aspectos, a redución do risco ante a ocorrencia de desastres. Por medio de este enfoque, se persegue a redución das vulnerabilidades sociais, económicas e ambientais; o incremento da resiliencia e o benestar xeral da poboación mediante un punto de vista baseado en dereitos. Cando un país integra instrumentos políticos para a xestión do risco de desastres cos marcos políticos nacionais, facilita a asignación de recursos humanos, técnicos e financeiros para acadar estas metas.

Estas cuestións foron debatidas e suscitadas para o seu escrutinio público e oficiadas durante a Conferencia Mundial sobre a Redución dos Desastres (WCDR) en Kobe, Hyogo, Xapón (xaneiro de 2005), sendo o Marco de Sendai o instrumento que o sucede na actualizade. De acordo co Marco de Sendai e a Axenda 2030, as estratexias integrais de redución de riscos deben ir máis alá dos sistemas de protección civil e incluír tamén elementos de carácter intersectorial, como a xestión do risco urbano, a ordenación do territorio, a xestión de concas hidrográficas, a protección financeira, a resiliencia do investimento público, ou a preparación e alerta temperá, cuestións todas elas que non poden ser abordadas globalmente por ningunha estratexia ou plan sectorial único. Ecuador, asinante dende 2015 do Convenio Marco de Sendai para a Redución do Risco de Desastres, atópase centrado na adopción de medidas sobre as tres dimensións do risco de desastres, isto é: exposición a perigos, vulnerabilidade e capacidade, e características das ameazas; co propósito de previr que ocorran novos riscos, diminuír os existentes e incrementar a resiliencia.

Isto amosa a necesidade de levar a cabo máis estudos científicos que aclaren as vulnerabilidades que afectan ó territorio. Este problema pódese abordar a través dos avances tecnolóxicos actuais, como a tecnoloxía GPS, sistemas de satélite, sensores remotos ou sistemas informáticos cada vez máis robustos con capacidades nunca vistas. Os sensores remotos xorden como unha ferramenta fundamental para a xestión e goberno de riscos pois permiten xerar información de forma rápida, fiábel e multi-temporal, aspectos de gran importancia á hora de planificar o territorio, máis aínda no que se refire aos riscos que o afectan. Neste senso, a xeración de modelos e índices dixitais a partir deste tipo de datos permite detectar, controlar e avaliar o risco asociado os desprendementos de terra. O establecemento dunha metodoloxía para a xestión e uso da información destes sensores, aplicada á xestión do risco de desprendementos de terra, supón unha contribución de gran importancia á xestión, desenvolvemento e ordenación do territorio. Esta tese de doutoramento desenvolve algúns destes métodos a partir da construción e materialización para a xeración de información e coñecemento aplicado especificamente os riscos dos desprendementos de terra.

Por outra banda, a avaliación do derrubamento segue sendo unha tarefa crucial na xestión do territorio e na xestión de perigos/riscos. Dita tarefa foi acometida con e sen éxito por todo tipo de partes interesadas (gobernos, organizacións non gobernamentais, sector privado e institutos de investigación), nun amplo espectro de localizacións e magnitudes. Fai xa unha década que Guzzetti et al. (2012) mencionou na súa investigación a necesidade de proporcionar indicadores de calidade dos mapas de inventario (integridade, precisión xeográfica e temática). Porén, a pesar dos avances tecnolóxicos descritos, esta práctica segue sendo anecdótica, e non está libre de problemas. Ademais, a pesar das ferramentas e metodoloxías desenvoltas para elaborar, actualizar e validar inventarios de desprendementos de terra a nivel rexional ou nacional empregando dispositivos electrónicos persoais, estas iniciativas son anecdóticas en rexións como América Latina.

Os derrubamentos naturais e antrópicos son habituais nos Andes do Ecuador, producindo danos graves e continuos. Desafortunadamente, só se realizaron algúns estudos no país (Basabe et al., 1996), e actualmente non existen bases de datos que rexistren estes fenómenos nin mapas de inventario actualizados. Os desprendementos de terra son o tipo de xeo-perigo máis común en todo o mundo e xogan un papel importante na evolución das formas do relevo. A recollida de datos cualitativos e cuantitativos das ocorrencias de desprendementos de terra é unha tarefa difícil. Partindo da localización, do tipo e da afectación dos fenómenos, iso supón un reto en si mesmo para rexistrar os datos correctamente. É evidente que a exactitude, a correcta descrición dos fenómenos e a súa magnitude son datos cruciais para incluír nun inventario de derrubamentos.

Capítulo 1. Tendo en conta o dito, desenvolvemos unha aplicación móbil para localizar, caracterizar e tipificar os desprendementos de terra empregando o sistema Open Data Kit (ODK) para acometer a tarefa de recoller eses datos. Este desenvolvemento cumpre tres finalidades: 1) incrementar o número de estudos realizados con desprendementos de terra para reducir o impacto negativo destes eventos sobre infraestruturas, propiedades e persoas; 2) poñer a disposición da comunidade científica, técnicos municipais e civís unha ferramenta de baixo custo e fácil uso para a recollida masiva de datos

de derrubamentos; e 3) obter información actual e detallada para elaborar e actualizar mapas de inventario a nivel rexional; adestrar e validar metodoloxías automáticas para obter estes mapas a escalas máis pequenas; e enriquecer as bases de datos existentes (a nivel rexional, nacional e mundial).

O emprego desta ferramenta fai que os informes sexan rápidos, sinxelos e rendibles cun beneficio engadido, non se require coñecemento especializado para o seu uso. MARLI ofrece dous formularios: un aberto a toda a cidadanía (sen coñecementos previos), colectivo que pode achegar información moi útil e actualizada; e un segundo formulario para usuarios especializados. A interface de usuario de MARLI, deseñada de acordo coas necesidades e capacidades dos diferentes usuarios, permite introducir de forma sinxela a información na base de datos.

A análise dos datos rexistrados por MARLI amosou que a superficie afectada polos desprendementos de terra aumentou durante as últimas dúas décadas. Esta circunstancia pode ser consecuencia dos procesos de informalidade na ocupación do solo que acontece no Ecuador, ben polo avance da fronteira agraria ben pola existencia de asentamentos informais nos arredores das cidades. Ademais, as análises realizadas desvelaron que un importante número de derrubes rexistrados co MARLI ameazan poboacións e infraestruturas, expoñendo á comunidade a danos persoais e materiais. Esta información pódese tomar como indicativo do aumento da inestabilidade rexional, mostrando a necesidade de facer un seguimento destes fenómenos vencellados á dinámica territorial e aos factores derivados do cambio climático.

O impacto deste desenvolvemento apreciase ó comparar, a nivel autonómico, o inventario realizado con MARLI e o acadado no marco do proxecto PRECUPA no ano 1996. O número de desprendementos de terra rexistrados en PRECUPA (130) multiplícase por 5 no inventario realizado a partir de MARLI (668), o que fai que a densidade de corrementos de terra aumente de 3.6 a 45.8 por km^2. Non obstante, no inventario elaborado a partir do MARLI, a superficie ocupada por ditos fenómenos é tres veces menor que a rexistrada no inventario PRECUPA (3.83% e 9.55%, respectivamente). Así, dedúcese que a mera existencia dunha base de datos local (actualizada, estandarizada

e completa) de derrubamentos, xunto a súa disposición ao público, facilita o cartografado da susceptibilidade aos derrubes. Manter este fito ó longo do tempo pasa por crear, manter e actualizar as bases de datos de desprendementos de terra como unha práctica ben consolidada e fomentar o seu uso no deseño das políticas de ordenación do territorio.

Capítulo 2. Nesta parte da tese abórdase a vulnerabilidade intrínseca, ante a ocorrencia de desastres, dos asentamentos de poboación debido á pobreza, á mala gobernanza e á escasa ou nula xestión do territorio, así como á falta de protocolos de mitigación e inexistencia de ferramentas para a planificación da ocupación urbana, conducindo todos eles a que tales impactos sexan especialmente graves. Cuenca (Ecuador) é un exemplo significativo dunha cidade que experimentou un crecemento demográfico considerable nas últimas décadas vencellado ó aumento das perdas por desprendementos de terra. A pesar de tales efectos, as ferramentas de planificación urbana están ausentes. Esta circunstancia require unha avaliación multitemporal do risco de desprendementos de terra. Para abordar dito desafío, proponse aquí analizar a exposición da poboación á ocorrencia de desprendementos de terra conxuntamente ca evolución de dito risco na última década (2010 - 2020). Para tal fin, foi preciso contar ca distribución espacial actualizada dos desprendementos e a distribución da poboación no período 2010 - 2020.

Ó non dispor de datos sobre a localización da poboación, empregáronse os datos dos contratos de subministración eléctrica como aproximación da distribución da poboación no territorio. Os resultados indican que o risco relativo actual atópase nos municipios situados no sector sur da área de estudo (é dicir, Turi, Valle, Santa Ana, Tarqui e Paccha). Ademais, a análise multitemporal indica que a maioría dos municipios da cidade situados nas zonas montañosas que delimitan o centro (é dicir, Sayausi, San Joaquín, Tarqui, Valle, Sidcay, Baños, Sidcay, Ricaurte, Paccha e Chiquintad), experimentan crecemento da poboación sostido, expostos a un maior risco cunha tendencia de crecemento constante.

A partir da distribución dos desprendementos, estimouse mediante un algoritmo de aprendizaxe automática, MaxEnt, o risco relativo de

derrube na cidade de Cuenca, é dicir, a susceptibilidade ao derrube. Nesta perspectiva, seleccionouse un conxunto de variables ambientais como potenciais factores predispoñentes para o inicio do desprendemento de terra e analizouse a súa multicolinealidade. No contexto da análise proposta, os datos procedentes da análise de susceptibilidade e dos contratos de subministración de enerxía eléctrica utilizáronse como base para a avaliación multitemporal do risco de derrube sobre a zona de estudo considerando só o risco para as persoas. As zonas máis susceptibles da cidade de Cuenca resultantes da análise localízanse nas ladeiras que flanquean a cidade. Nestas zonas, as pendentes son pronunciadas e cóncavas onde as estradas crean descontinuidades locais. Pola contra, as zonas periurbanas e rurais atópanse en áreas de susceptibilidade media a moi alta con ladeiras máis suaves.

A dispoñibilidade dun mapa de inventario de desprendementos de terra fixo posible a avaliación do modelo tendo en conta tamén os datos de campo. Ao cruzar os puntos de derrube e o mapa de susceptibilidade final, obtívose información sobre a distribución do desprendemento conxuntamente ca extensión superficial das clases de susceptibilidade. Os resultados destacan que case o 75% dos desprendementos reais foron localizados nas clases de susceptibilidade alta e moi alta. Así, este estudo proporcionou información sobre cuestións importantes como i) o efecto da expansión sostida das áreas urbanas debido ao crecemento da poboación sobre a variación relativa do risco de derrubamento e ii) o método de avaliación do risco de complexidade reducida só en presenza de datos parciais (é dicir, a susceptibilidade aos derrubamentos de terra), en lugar de perigo, e contratos de subministración eléctrica en lugar de distribución da poboación).

Os mapas de risco relativo obtidos resultan útiles para orientar a planificación do territorio, a restrición da ocupación e a adopción de estratexias de alerta temperá. Así mesmo, o enfoque metodolóxico empregado, que ten en conta a susceptibilidade dos derrubamentos de terra e a variación da poboación mediante a análise de datos indirectos, ten o potencial de aplicarse a cidades de países con ingresos baixos, onde normalmente se dispón dun conxunto de datos mínimo.

Capítulo 3. Neste capítulo da tese abórdase unha vulnerabilidade

específica na rexión, as caídas de rochas. Estes fenómenos considéranse o principal perigo nas zonas de montaña de todo o mundo, en parte polas súas consecuencias directas sobre o territorio e a poboación. A cartografía de susceptibilidade á caída de rochas é fundamental tanto para a avaliación previa do impacto da implantación de infraestruturas como para establecer, con posterioridade, restricións en relación ó uso do solo arredor destas zonas, co obxectivo principal de evitar a perda de vidas humanas e bens materiais. A gran maioría dos métodos desenvolvidos para identificar áreas susceptibles a caídas de rochas, requiren identificar previamente os chamados puntos fonte. Estes puntos considéranse a orixe da caída de rochas e, polo tanto, a localización dende a que se realiza a identificación das zonas máis expostas no caso de producirse o devandito fenómeno.

Así, nesta investigación, desenvólvese un novidoso enfoque híbrido baseado no reconto de traxectorias por píxel, obtidas a partir do uso da ferramenta QPROTO a cal permite calcular a susceptibilidade á caída de rochas. Entón, ditos resultados empréganse con varias finalidades: 1) identificar puntos de orixe de caída de rochas; 2) avaliar a susceptibilidade á caída de rochas, 3) clasificar as consecuencias físicas dos sucesos de caída de rochas na estrada de Molleturo, principal conexión da cidade co resto do país, e 4) analizar a influencia da resolución dos Modelos Dixitais de Elevación na precisión dos resultados.

As análises realizadas neste estudo considéranse de especial relevancia tanto para a avaliación previa do impacto da implantación de infraestruturas, o caso particular das vías de comunicación, en contornas propensas á aparición de eventos de caída de rochas, que permitirían modificar as condicións construtivas e/ou implantar as medidas de prevención máis axeitadas para as circunstancias de risco identificadas; así como establecer restricións con posterioridade en relación ao uso do solo na contorna destas zonas, coa finalidade principal de evitar a perda de vidas humanas e bens materiais, así como a consecuente desconexión a que supoñan as cidades beneficiarias das devanditas infraestruturas. Ademais, estes resultados tamén axudan aos investigadores a considerar os efectos da resolución dos Modelos Dixitais de Elevación na identificación de puntos de orixe de caída de rochas, o cartografado da susceptibilidade á caída de rochas ou a identificación de

tramos de estrada, mediante o emprego de ferramentas automáticas de predición, que poden verse afectados por fenómenos de caída de rochas ou afundimentos.

Capítulo 4. O capítulo catro xira arredor da prevención e mitigación da inestabilidade de ladeiras, que requiren tecnoloxías eficaces para reducir a vulnerabilidade das estruturas existentes. Os desprendementos de terra son fenómenos globais causados por fenómenos xeolóxicos naturais ou inducidos por fontes antrópicas. Os desprendementos lentos e intermitentes dan lugar a un número importante de danos físicos e importantes perdas económicas en propiedade privada e pública. A vulnerabilidade das construcións aos desprendementos de terra é un termo usado para describir o seu potencial de perda física cando se ven afectados por movementos inducidos por terreos inestables. Polo tanto, a vixilancia xoga un papel fundamental na xestión dos riscos naturais e asume a tarefa fundamental de ofrecer solucións rendibles para mitigar as perdas físicas e económicas.

A vixilancia das estruturas xoga un papel cada vez máis importante no contexto da vida e da xestión destes riscos naturais. Polo tanto, é necesario estudar a evolución deste tipo de eventos e considerar as súas consecuencias. En realidade, a prevención, a previsión e o seguimento destes fenómenos son as ferramentas máis adecuadas para minimizar os seus efectos secundarios. O desenvolvemento de áreas inestables en contextos urbanos suscitou un interese crecente por enfoques innovadores para proporcionar información sobre a evolución temporal e espacial da súa interacción cos edificios existentes.

As técnicas de teledetección demostraron ser poderosas ferramentas de investigación pola súa alta cobertura espacial e temporal, a rápida adquisición de datos e aos seus custos razoables en xeral. Entre os diferentes tipos de técnicas de teledetección, a Interferometría Diferencial SAR (DinSAR) cumpre moi ben con estas necesidades. Así, o obxectivo principal do presente estudo foi proporcionar unha metodoloxía xeral que poida ser empregada para predicir a evolución espacial e temporal dun desprendemento lento. En particular, este traballo analiza un fenómeno lento que afecta á Universidade do Azuay (Cuenca, Ecuador). Para tal fin, implantouse un sistema integrado de

seguimento e análise tanto a escala local como de detalle, destacando a importancia da técnica DInSAR como técnica adicional de seguimento e como método alternativo, polo menos nas avaliacións preliminares dos fenómenos, nos sistemas tradicionais de vixilancia do terreo. Citar que grazas ao convenio de colaboración inter-institucional entre a Universidade Federico II de Nápoles e a Universidade de Azuay, foi posible obter imaxes SAR da constelación de satélites Cosmo-SkyMed, no período marzo 2016 - xaneiro 2018. Temos que mencionar que esta colaboración e análise de imaxe continúa ata hoxe.

Esta investigación proporcionou unha metodoloxía de seguimento integrada que se pode empregar para predicir a evolución espacial e temporal dun desprendemento lento que afecta a edificios dentro do campus da Universidade de Azuay. Estableceuse tamén unha análise multinivel integrada con técnicas innovadoras de seguimento xunto con métodos tradicionais e detallados como son os levantamentos xeofísicos, presentando unha estratexia válida para as actualizacións continuas do risco. Este supón o primeiro paso para previr e mitigar o risco de catástrofes naturais como os desprendementos de terra que afectan á cidade de Cuenca, Patrimonio da Humanidade da UNESCO.

Capítulo 5. Neste capítulo preséntase un estudo realizado en Zaruma, un coñecido distrito mineiro da provincia de *El Oro* en Ecuador, que sofre fenómenos de subsidencia relacionados coa explotación mineira ilegal subterránea. A cidade de Zaruma está entre os lugares máis perigosos de sumidoiros do mundo. Esta perigosidade relacionase cunha densa rede de túneles legais e ilegais, moitos deles descoñecidos, o que aumenta a fraxilidade do territorio municipal. A minería nesta zona remóntase á época pre-hispánica. A historia rexistrada mostra os primeiros asentamentos da cultura cañari e a través da cultura inca, pasando da presenza española, americana e canadense na zona ata os tempos modernos. A minería neste distrito pasou constantemente de minería legal a ilegal, técnica e non técnica. Na actualidade, as actividades predominantes son ilegais e non técnicas nunha área declarada como zona de non explotación baixo a cidade de Zaruma. Isto trae unha serie de problemas como o afundimento de terreos que afecta á cidade citada. Os afundimentos e colapsos acumuláronse esporadicamente no pasado, pero nos últimos anos (dende 2017), este

fenómeno converteuse nun feito relativamente constante.

De feito, o 15 de decembro de 2021 aconteceu un evento de sumidoiro que provocou a evacuación de máis de 300 persoas e a prohibición de acceso a máis de dez cuadras. Por este motivo, é fundamental atopar unha técnica rápida e económica que poida xerar información sobre o desenvolvemento espacial e temporal das actividades subterráneas incontroladas para mellorar a xestión do risco. Neste traballo empregouse a técnica de Radar de Apertura Sintética de Interferometría Diferencial (DInSAR), desenvolvida no software SUBSIDENCE, para estudar a deformación do terreo vencellada a minería artesanal ilegal na cidade de Zaruma como parte dun proxecto de colaboración entre universidades locais e internacionais.

Este estudo presenta as taxas de desprazamento primarias rexistradas ao longo do intervalo de tempo analizado. Observouse como na zona afectada polo colapso do 15 de decembro de 2021, os PS identificados mostran taxas de deformación significativas superiores a 0.5 cm/ano. Un elemento aínda máis significativo é a serie temporal destes puntos, que mostra unha aceleración a partir de xuño de 2021, seis meses antes do colapso. Así mesmo, para verificar os resultados interferométricos levouse a cabo un levantamento de campo mediante a aplicación MARLI.

Con este estudo púidose por sobre a mesa a necesidade de implantar un sistema de vixilancia continua mediante técnicas de teledetección, para previr fenómenos como o acontecido no 2021 por medio da identificación daquelas zonas da cidade que precisan dun coñecemento máis completo do subsolo, probablemente afectado por actividades de escavación descoñecidas.

Capítulo 6. O *Marco de Sendai para la Reducción de Riesgo de Desastres (2015 - 2030)*, considérase o primeiro fito do cambio de paradigma da xestión de desastres naturais, pois se prima a prevención e a xestión do risco en lugar da xestión da crisis, co principal propósito de evitar a perda de vidas e os efectos na economía das perdas materiais. Así, o Marco urxe os países, antes de 2030, a despregar estratexias nacionais e locais que teñan como principais obxectivos 1) a mellora da resiliencia das comunidades; 2) aumentar o coñecemento científico e

a alerta temperá e 3) incrementar a preparación da poboación ante os desastres. Deste xeito, a prevención e a gobernanza son os principais piares sobre os que se basean os esforzos para afrontar os desastres naturais. Ecuador encóntrase asociado ó Marco dende 2015.

Neste contexto, ponse de manifesto a necesidade de formación multipropósito en xestión de riscos; o desenvolvemento de ferramentas de captura eficiente de datos e aplicación de métodos e procedementos para a xeración de información que permitan a organización das accións prioritarias co propósito de facer unha axeitada e eficiente xestión do risco de desastres a nivel cantonal, rexional e local. Sen dúbida, o éxito desta cadea de accións precisa de xeito imprescindible fortalecer as relacións entre institucións e de estas ca sociedade, instaurando dinámicas de cooperación e diálogo.

Tendo en conta os antecedentes descritos, esta tese nace da necesidade imperativa do desenrolo de novas metodoloxías aplicables á xestión e gobernanza do risco mediante o emprego de sensores remotos como elemento principal para a localización de ameazas. Neste capítulo relátase como as demandas reais e acontecementos, non sempre previstos, foron moldeando o meu traballo de investigación hasta transformalo en ferramentas, desenvolvementos, metodoloxías e información que posibilitou, de varias formas, aportar á gobernanza do risco en ámbitos, tan próximos como afastados, como o universitario, o científico e o político-institucional. Implicitamente abordáronse varios marxes sobre o emprego e xestión do risco de desastres a nivel nacional, cantonal e local. Tamén levouse a cabo un proceso de socialización dos logros acadados por medio da participación en congresos, simposios, consultorías e reunións de traballo con autoridades competentes tanto na área de riscos como na área xestión do territorio e co goberno seccional.

Contents

List of Publications

Journal Papers

- Sellers, C.A., Buján, S., Miranda, D. MARLI: a mobile application for regional landslide inventories in Ecuador. Landslides 18, 3963-3977 (2021). https://doi.org/10.1007/s10346-021-01764-9.
- Di Napoli, M., Miele, P., Guerriero, L., Annibali Corona, M., Calcaterra, D., Ramondini, M., Sellers, C. and Di Martire, D. Multitemporal relative landslide exposure and risk analysis for the sustainable development of rapidly growing cities. Landslides (*minor revision*) (2023).
- Sellers, C., Di Martire, D., Rodas, R., Ramondini, M., Infante, D., Miranda, D. and Buján, S. An integrated approach for rockfall susceptibility assessment along linear infrastructure in Cuenca (Ecuador). Remote Sensing (*submitted*) (2023).

Book Chapters

- Sellers, C., Rodas, R., Carrasco, N.P., De Stefano, R., Di Martire, D., Ramondini, M. (2021). Ground Deformation Monitoring of a Strategic Building Affected by Slow-Moving Landslide in Cuenca (Ecuador). In: Rizzo, P., Milazzo, A. (eds) European Workshop on Structural Health Monitoring. EWSHM 2020. Lecture Notes

in Civil Engineering, vol 128. Springer, Cham.
https://doi.org/10.1007/978-3-030-64908-114.

- Sellers, C., Ammirati, L., Khalili, M.A., Buján, S., Rodas, R.A., Di Martire, D. (2023). The Use DInSAR Technique for the Study of Land Subsidence Associated with Illegal Mining Activities in Zaruma - Ecuador, a Cultural Heritage Cite. In: Rizzo, P., Milazzo, A. (eds) European Workshop on Structural Health Monitoring. EWSHM 2022. Lecture Notes in Civil Engineering, vol 270. Springer, Cham.
https://doi.org/10.1007/978-3-031-07322-956.

Conferences

- **V Conferencia de la Red de Investigación en Gestión del Territorio y Tecnologías de la Información Geoespacial (RIGTIG):** Conocimiento en Acción para la Gestión Territorial, presentación oral, **"MARLI: App para la actualización de inventarios de deslizamientos en el Ecuador"**, Chester Sellers, Sandra Buján, Ricardo Rodas, David Miranda, 30 de marzo 2022. Guayaquil - Ecuador.
- **10th European Workshop on Structural Health Monitoring**, presentación oral, **"The use DInSAR technique for the study of land subsidence associated with illegal mining activities in Zaruma - Ecuador, a cultural heritage cite."**, Chester Sellers, Lorenzo Ammirati, Mohammad Amin Khalili, Sandra Buján, Ricardo Adolfo Rodas, Diego Di Martire, 4 al 7 de julio 2022, Palermo - Italia..
- **VIII Congreso Internacional De Investigación REDU 2021**, presentación oral, **"Actualización de inventario de deslizamientos a partir de herramientas de bajo coste en el cantón Cuenca"**, Chester Sellers, Sandra Buján, David Miranda, 15 al 18 de noviembre 2021, Ambato - Ecuador.
- **90° Congresso della Società Geologica italiana**, presentación oral, **"Multi-temporal relative landslide risk analysis for sustainable development of rapidly growing city in Latin America: the case of Cuenca, UNESCO site, Ecuador"**, Di Napoli Mariano,

Miele Pietro, Guerriero Luigi, Annibali Corona Mariagiulia, Calcaterra Domenico, Ramondini Massimo, Sellers Chester, Di Martire Diego, 14 al 16 de septiembre 2021. Trieste - Italia.

- **XIII International Symposium on Landslides- XIII ISL**, presentación oral, **"DInSAR data for landslides mapping in UNESCO World Heritage sites: Cuenca (Ecuador) study case"**, Lorenzo Ammirati, Ricardo Rodas, Domenico Calcaterra, Massimo Ramondini, Chester Sellers, Diego Di Martire, 22 al 26 de febrero 2021. Cartagena - Colombia.
- **EWSHM 2020 10th European Workshop on Structural Health Monitoring**, Oral presentation, **"Ground Deformation Monitoring of a Strategic Building Affected by Slow-Moving Landslide in Cuenca (Ecuador)"**, Chester Sellers, Ricardo Rodas, Nadia Paulina Carrasco, Rita De Stefano, Diego Di Martire, Massimo Ramondini, 6 al 9 de Julio 2020, Palermo - Italia.
- **First International Forum: Risk and prevention - Vulnerability and improvement, made up of representatives from the University of Cuenca (Ecuador), the University del Azuay (Ecuador) and the National University of Colombia (Colombia)**, Oral Presentation "**SAR interferometry and low-cost tools for landslide inventories in the Cuenca canton**",MSc. Chester Sellers, PhD. Sandra Buján, PhD David Miranda, PhD Diego Di Martire, Phd Doménico Calcaterra, PhD Mássimo Ramondini, MSc Paúl Bravo1, MSc Diego Pacheco, Ing. Ricardo Rodas, 26 of august 2022, Cuenca - Ecuador
- **International Symposium on Resilience in the Built Environment**, Oral presentation, **"Slow-moving landslide monitoring using remote sensing and In-situ techniques in Cuenca-Ecuador a UNESCO Heritage site."**, Chester Sellers, Ricardo Rodas, Paúl Bravo, Omar Delgado,Diego Di Martire, Massimo Ramondini, Domenico Calcaterra, 7 de June 2022, Cuenca - Ecuador.

Introduction and Motivation

In the last decades, the ongoing climate change, associated with global population growth and organic expansion of urbanized areas, has been responsible for an increase in the frequency and impact of natural disasters due to floods, landslides, and wildfires (Knox, 1993, Xu et al., 2013, Arnell y Gosling, 2016, Gariano y Guzzetti, 2016, Di Napoli et al., 2020a). Developing countries have experienced an even more severe impact because people are often concentrated in high-hazard urban areas where housing is highly vulnerable due to poor building, and early warning systems are commonly absent (Zorn, 2018, Aguirre-Ayerbe et al., 2020).

Natural disasters increased in frequency and intensity on a global scale and have affected a large part of the worlds population, causing human and economic losses and a quality of life that led to the emergence of a number of problems. Countries of Latin America and the Caribbean are territories most affected by natural phenomena such as earthquakes, landslides, volcanic eruptions, tsunamis, and hurricanes (Gariano y Guzzetti, 2016).

Landslides are among the most important and frequent natural disasters: after earthquakes, they cause the highest number of victims and damage to artificial structures. For this reason, the evaluation and prevention of the risk of landslides is the fundamental step for a correct planning and management of the territory, as shown by the growing scientific evidence in this field (Albano et al., 2016, Di Martire et al., 2016, Confuorto et al., 2017, Infante et al., 2019).

As mentioned, landslides are the most common type of geo-hazard worldwide and play a major role in the evolution of landforms (Malamud et al., 2004). These complex natural phenomena can be characterized and classified into many types (Varnes, 1978, Cruden y Varnes, 1996, Reichenbach et al., 2018) and are controlled by several conditioning factors such as soil type, land use, slope, or geology (van Westen et al., 2008, Reichenbach et al., 2018). Also, it is very well known that extreme climatic events, such as precipitation, snow melting, or temperature changes, and their variations, affect the stability of natural and engineered slopes and have consequences on landslides (Gariano y Guzzetti, 2016). Several studies have raised the impact of climate change on landslides (Petley, 2010, Coe y Godt, 2012). In this scenario, an increase in the temperature of the earth's surface is estimated, which influences the intensity and frequency of precipitation, increasing the occurrence of landslides and, therefore, the risk to properties and people.

Although there has been an increase in studies in the last decade in South America, scientific production is still far from countries like Norway or Italy (Sepúlveda y Petley, 2015). Because of the magnitude of landslide impact from both a personal and economic standpoint, it is critical to strengthen the process for assessing landslide susceptibility, hazard, and risk; formulating prevention and mitigation strategies; and conducting appropriate and timely planning responses to the occurrence of such phenomena (Tao et al., 2019). In this context, the role of Landslide Inventories (LI) is unquestionable.

The amplitude of the spectrum of landslide phenomena makes it difficult, if not impossible, to define one single methodology to identify and map landslides, thus evaluate landslide hazards and to characterize the associated risk. The uncertainties in data acquisition and data processing added to the complexity and vulnerability of the population living in territory, landslide inventories, landslide susceptibility zoning, landslide hazard evaluation, and landslide risk determination is a costly effort. Solutions to these challenging problems may come from new scientific advances that can help to cope with these problems: personal smart devices, Differential Interferometry SAR (DInSAR),... (Franceschetti et al., 1992)). In this context, increasing efforts are needed to make methods for landslide mapping, landslide

susceptibility zoning, and hazard assessment and risk determination better documented and more reproducible at local and regional scales.

It is the aim of this thesis to contribute to reduce some of these gaps by providing a scientific, rationale, standardized, and validated tool and methodical approach for the quick, reliable survey of mass movements (landslides) by means of the presentation of study cases applied to territory and validated in the territory.

Objectives and Main Contributions of the Thesis

The main objective of this doctoral thesis is to analyze the use of remote sensors and the information that can be obtained to determine how this data can be used to generate and update geospatial information for risk management and governance. This objective is complemented by the search for technological and methodological developments capable of achieving said purpose.

To achieve this main objective and transversally to all chapters, we carried out a strong and exhaustive bibliographic review of the types and sources of information, current available methodologies, methodologies in development that allow through the use of remote sensors to detect, monitor and manage the risk associated with mass movements. This allows us to identify the current needs and demands in the field of management and risk governance. With this knowledge, it is intended to develop new standardized method that allow the generation, automation of processes for the generation of information associated with the risk management due to mass landslides, an input of vital importance within the territorial planning. These developments have been applied to different territorial scales. Specifically, this thesis is structured in 6 chapters, five of which are research-technical papers/comunications, published or in revision, and a sixth chapter namely "The role of risk management and governance" that states de normativity and impacts derived of this thesis in the local administration, all this in timeline structure.

In **chapter one**, a thorough literature investigation was conducted to stablish the theoretical and practical framework for the development of the application for landslide inventories. Thus, this chapter describes the development of MARLI, a simple but efficient open-access platform to report landslide events using ODK system. Its design makes reporting fast, simple and cost-effective with an added benefit, and a specialized knowledge is not required for its use. The development of MARLI was to achieve three purposes: 1) To increase the number of studies carried out with landslides as a tool to reduce the negative impact of these events in infrastructure, properties and people; 2) To make available to the scientific community, municipal technicians, and civilians a low-cost and easy-to-use tool for the mass collection of landslide data; 3) To obtain current and detailed information (high spatial and temporal resolution) to (a) elaborate and update inventory maps at regional level; (b) train and validate automatic methodologies to obtain these maps at smaller scales; and (c) enrich existing databases (at a regional, national and global level).

In **chapter two**, an analysis of the exposure to landslides, its multitemporal variation between 2010 and 2020, and related relative risk for the city of Cuenca in Ecuador (Latin America) has been presented using an integrated method consisting of 1) machine-learning-based susceptibility assessment by using Maximum Entropy algorithm, 2) energy supply contract analysis for exposure quantification and 3) relative risk estimation. This study provides insights into important issues, such as 1) the effect of the sustained expansion of urban areas due to population growth on landslide exposure variation and 2) the reduced complexity method of risk assessment in the presence of partial data only (i.e., landslide susceptibility rather than hazard, and electricity supply contracts rather than population distribution).

In **chapter three**, considering the lack of a useful and updated products for highway safety management from a rockfall risk perspective, our primary goal was to increase the efficiency and precision of data processing to obtain rockfall susceptibility maps at medium-large scale (wall-to-wall) by combining existing tools. For this, in this research: 1) a novel hybrid approach that integrates the QPROTO tool and various functions of the R software is applied for automatically identifying the

areas which might be affected by rockfall; 2) the factors that characterize the source points are analyzed to increase the efficiency and precision of data processing to obtain rockfall susceptibility maps; 3) a methodology for the differentiation between rockfall and subsidence phenomena in relation to the layout of a communication route is developed; and 4) the influence of Digital-Elevation-Model resolution on the accuracy of the results is analyzed. Thus, the analyzes carried out may be particularly relevant both for the prior evaluation of the impact of the implementation of infrastructures, the particular case of communication routes, as well as to establish a posteriori restrictions in relation to land use around these areas, with the main purpose of preventing the loss of human lives and material goods.

Two specific and local applications for the use of Differential Interferometry Synthetic Aperture Radar (DInSAR) technique, implemented in the SUBSOFT and SUBSIDENCE softwares, were included in **chapters four and five**, respectively, in order 1) (chapter four) to provide an integrated monitoring methodology that can be used to predict the spatial and temporal evolution of a slow landslide which affects buildings inside the campus of Azuay University; and 2) (chapter five) to study terrain deformation related to illegal artisanal mining in Ecuador. In the first case, multi-level analysis integrated with innovative monitoring techniques together with traditional and detailed methods such as geophysical surveys, as a valid strategy for continuous risk update, laying the foundations for greater accuracy for the prevention and prediction of such phenomena. In the second case, an up-to-date study of the monitoring and detection of subsidence phenomena in the city of Zaruma was present. This research allowed to detect and monitor mining-related subsidence phenomena. Thus, it was possible to highlight the need to implement a continuous monitoring system in order to prevent phenomena such as those that occurred in 2016 and 2021 by identifying those areas of the city that need a more comprehensive knowledge of the subsoil that is probably affected by subsidence phenomena that to date are still unknown.

Finally, the **chapter six** describes how the actual demands and different events, not always foreseen, shaped the research work developed within the framework of this thesis until it was transformed into tools,

implementations, methodologies, and information that represented my bit of support to the challenge of prevention and governance of landslide risk in Ecuador. The main objective of this chapter is to continue contributing to the process of socializing the findings achieved with the research presented in this thesis, putting in black on white my experience in management and risk governance.

Main Contributions of the Thesis

The main contributions of this Thesis can be summarized as:

- A standardized methodology to create and update landslide inventories.
- An application in ODK to facilitate ground survey for landslide inventories creation and update.
- First landslide inventory with all the characteristics to describe these phenomena using international standards for the city of Cuenca and the surrounding parishes.
- First update of this inventory using the methodology created in this thesis.
- First spatial data infrastructure (IDE) publishing this data.
- A direct relation with local authorities political and technical regarding the products and experiences obtained was established.
- Close collaborative relationship with international higher education institutions was established.
- A methodology to determine expansion areas of the city by a proxy data of the electrical connections, stating multi- temporally the growth of the city.
- A methodology to determine the exposure of the population, in the expansion areas, prone to mass movements.

- First landslide susceptibility map of expansion areas with their level of exposure to this type of phenomena.
- A novel and integrated approach for rockfall susceptibility assessment along linear infrastructures.
- An integrated monitoring methodology that can be used to predict the spatial and temporal evolution of a slow landslide which affects buildings or infrastructures using remote sensing techniques, specifically Differential SAR Interferometry (DInSAR).
- Studies and proof applied to real cases for monitoring, infrastructures, mass movements and subsidence phenomena using remote sensors like SAR, using free and proprietary data.

CHAPTER 1

MARLI: A Mobile Application for Regional Landslide Inventories in Ecuador

The regions of Central and South America most susceptible to the occurrence of landslides will become even more vulnerable in the context of climate change. *The Josefina disaster*, in 1993, demonstrated both the vulnerability of local infrastructures and communities in the Paute River basin (Ecuador). Since this natural phenomena, several landslide inventories and susceptibility studies were developed, revealing the vulnerability of the Paute River basin to unstable terrain and the need for further studies throughout the basin. Despite this, no studies have been done since then to update the information generated. This paper describes a Mobile Application for Regional Landslide Inventories (MARLI), a simple but efficient open-access platform to report landslide events using the Open Data Kit system. Its design makes reporting fast, simple and cost-effective with an added benefit, and a specialized knowledge is not required for its use. MARLI was tested for the collection of landslides in Cuenca (Ecuador). From the data taken in the field, it was possible to analyze the performance and suitability of collected data and compare the results with regional inventories in the same area. Additionally, these results can be used for the elaboration and update of large-scale inventories or the training of automatic identification systems of landslides and later evaluation of their precision in a small-medium scale. Likewise, this product constitutes a fundamental input for the formulation of mitigation strategies, to formulate the appropriate response and in time, also the elaboration of reconstruction plans before the increase in the occurrence of such phenomena.

Keywords: Citizen science, Mobile tool, Open source, MARLI.

1.1 Introduction

Landslides are the most common type of geo-hazard worldwide and play a major role in the evolution of landforms (Malamud et al., 2004). These complex natural phenomena can be characterized and classified in many types (Varnes, 1978, Cruden y Varnes, 1996, Reichenbach et al., 2018) and are controlled by several conditioning factors such as soil type, land use, slope or geology (van Westen et al., 2008, Reichenbach et al., 2018). Also, it is very well known that extreme climatic events, such as precipitation, snow melting or temperature changes, and its variations, affect the stability of natural and engineered slopes and have consequences on landslides (Gariano y Guzzetti, 2016). Several studies have raised the impact of climate change on landslides (Petley, 2010, Coe y Godt, 2012). In this scenario, an increase in the temperature of the earth's surface is estimated, which influences the intensity and frequency of precipitation, increasing the occurrence of landslides and therefore the risk to properties and people. Latin America will be one of the regions most affected by this chain of phenomena (Gariano y Guzzetti, 2016). Petley (2012b) showed in his study that research can play an important role in reducing the impact of such phenomena, so that those countries with higher levels of research, present a lower number of fatalities. Although in the last decade there has been an increase in studies in this area, in South America, scientific production is still far from countries like Norway or Italy (Sepúlveda y Petley, 2015).

Because of the magnitude of landslide impact from both a personal and economic standpoint, it is critical to strengthen the process for assessing landslide susceptibility, hazard, and risk; formulating prevention and mitigation strategies; and conducting appropriate and timely planning response to the occurrence of such phenomena (Tao et al., 2019). In this context, the role of Landslide Inventories (LI) is unquestionable. As defined by Malamud et al. (2004), an LI map is the representation of the spatial distribution of landslides at a given cartographic scale. Although there are different ways to classify the types of inventories (based on scale, based on the method used to obtain it, based on the purpose of the inventory...), one of the most popular

classifications is the one proposed by Guzzetti et al. (2012). In this way, four types of geomorphological LI are differentiated: (1) historical, where the accumulated effects of many landslides over a long period of time (tens or hundreds of years) are shown; (2) event-driven, where the effects caused by a single trigger are shown; (3) seasonal, where slides occurring during one or several seasons are shown; and (4) multi-temporal inventories, where slides produced by multiple events over years are shown.

Gathering qualitative and quantitative data from landslide occurrences is a hard task. Starting from the location, the type, and the affectation of the phenomena, that poses a challenge in itself to correctly register data. It is evident that the accuracy, the correct description of the phenomena, and its magnitude are crucial data to be included in LI (Olyazadeh et al., 2016). Traditionally, this information was obtained from conventional methods, such as field surveys or aerial photograph interpretation; however, thanks to the increased availability and coverage of data from remote sensors, these methods have given way to semi-automatic methodologies based on Digital Terrain Models (DTM), the analysis of high-resolution images or the combination of different types of data (Scaioni et al., 2014). Despite this, conventional methods are still mainly used to train the new methodologies and validate their results. We can appreciate a global trend toward increasing efforts in landslide risk assessment through the implementation of landslide databases. However, to this day, these efforts remain absent in most countries due to high cost, intense labor, and time-consuming. Therefore, the development of tools and processes that are accessible, that does not require advanced technical knowledge, and that are low cost, are fundamental tasks to respond to the growing demand for LI –in a framework of climate change– from regions with limited resources, where people and properties are threatened.

Personal smart devices provide the response to such demand. These tools are not only a communication tool but also a device combining several technologies: satellite-based GPS, which allows fast and accurate landslide location; high-quality cameras, allowing immediate graphical documentation of these phenomena; Wireless Fidelity (Wi-Fi); Bluetooth; quad-core processors, data collection and

visualization applications, which based on the above technologies, facilitates the consultation of thematic information and geographic data while presenting the ability to store and transfer data over the network (Liu et al., 2014, Venkatasrinivasa Murthy, 2017). In recent years, the number of such tools available has increased due to the rapid growth of cell phone usage, related infrastructure, and the increasing possibilities for free online education sources in developed and developing countries (Raja et al., 2014, Kocaman y Gokceoglu, 2019), allowing the collection of field data in different fields linked to natural risk management (e.g., forest (Ferster et al., 2013), geomorphological maps (Mantovani et al., 2010), floods (Joy et al., 2019), earthquakes (Liang et al., 2017) or landslides (Olyazadeh et al., 2016)).

Despite the data collection and visualization tools boom (e.g., Open Data Kit, KoBoToolbox, Formhub or Geographical Open Data Kit), their ease-of-use and low-cost, there are not far too many examples of its application for the landslide field survey. ROOMA, developed by Olyazadeh et al. (2016), is one of the few mobile-map applications designed for the fast landslide data collection and to complement conventional remote sensing methods. This application was tested in Nepal in addition to recording landslide characteristics, risk elements were also collected. In many cases, the field survey with ROOMA allowed to improve the level of detail of the delineation of landslide areas; however, a considerable number of small landslides and active landslides in the gullies have not been identified. On the other hand, BEWARE is a platform for interactive landslide event reporting, analyzing and unifying landslide data and multimedia management (Vulović et al., 2017). This platform is made up of two mobile applications for data collection on the field, both on-line and in off-line modes under the android platform. Landslide Monitoring Application (LaMA) is another example of a simple and user-friendly mobile app to collect essential landslide data by non-expert users (Kocaman y Gokceoglu, 2019). Since it is orientated to the collection of information by the civil society, these data are limited mainly to the geo-location, date and time of landslide, effects of the landslide on people, description of damages, photographs and videos of the landslide. Other studies, as the one done by Rosser et al. (2017), contemplates as a future task, the developing of an application for smartphones that enables research teams to report

landslides and capture data in the field, but currently, there is no record of the stage of its development.

In addition, open citizen participatory data collection represents a starting point for field geologists engaged in the production of detailed event landslides inventories, allowing optimization in time and efforts. Volunteered Geographic Information (VGI) has also become a strong emerging field especially in large international initiatives (Goodchild, 2007, Kocaman y Gokceoglu, 2019). Some initiatives like Cooperative Open Online Landslide Repository (COOLR) or the USGS landslide Hazard Program have created a large interest in the scientific and educational world due to its potential for data acquisition, data analysis, and data modelling to represent hazard phenomena that affect territory and population (Baum et al., 2014). NASA's Global Landslide Hazard Assessment for Situational Awareness (LHASA) is a referent in this matter. This project intends to build a global inventory of landslides, where the COOLR is an open platform from which citizen scientists and technicians can report the occurrences that they are aware of (Kirschbaum y Stanley, 2018). The International Consortium on Landslides (ICL) is other non-profit scientific organization for global promotion of understanding and reducing landslide disaster risk, supported, among others, by the United Nations Educational, UNESCO and FAO (Sassa, 2015, 2019).

On the other hand, landslide assessment remains as a crucial task in land management and hazard/risk management, tasks that have been successfully and unsuccessfully undertaken this by all type of stakeholders (Government's, Non-governmental Organizations, Private Sector, and Research Institutes), studies done in a wide spectrum of locations and magnitudes. Even though almost a decade ago, Guzzetti et al. (2012) mentioned in his study the need to provide quality indicators of the inventory maps (completeness, geographical and thematic accuracy); however and despite the technological advances described, this practice remains anecdotal and is not free of problems (Tanyaş et al., 2017, Tanyaş y Lombardo, 2020). Furthermore, despite the tools and methodologies developed for the elaboration, updating, and validation of LI at the regional or medium-large scale level using personal electronic devices, these initiatives are anecdotal in regions like

Latin America.

Natural and anthropogenic landslides are common in the Andes of Ecuador, producing serious and continuous damage. Unfortunately, only a few studies have been conducted in the country (Basabe et al., 1996), and currently, there are neither databases registering these phenomena nor updated inventory maps. Thus, we have developed a mobile application to locate, characterize and typify landslides, using the Open Data Kit (ODK) system, and to undertake the task of gathering landslide data in a massive but controlled way, mainly with three purposes:

1. To increase the number of studies carried out with landslides as a tool to reduce the negative impact of these events in infrastructure, properties and people.

2. To make available to the scientific community, municipal technicians, and civilians a low-cost and easy-to-use tool for the mass collection of landslide data.

3. To obtain current and detailed information (high spatial and temporal resolution) to (1) elaborate and update inventory maps at regional level; (2) train and validate automatic methodologies to obtain these maps at smaller scales; and (3) enrich existing databases (at a regional, national and global level).

1.2 Methods

1.2.1 Design and development of the app system

In order to deliver on the increasing demand for spatial data, different organizations have gathered and displayed data on the web during the last decade. One of the major reasons for your success is the fact that recollecting and publishing the data has become a much easier task. The integration of remote sensing technology, high capacity

computing, the evolution of the internet of things, and GPS location technology has greatly driven the idea of recollecting data through mobile devices, thereby widening the spectrum range of investigation possibilities. Taking into account the development in computer and communication technologies associated with advances in geo-information technologies, the LI development has been improved substantially. Using these advances, a Mobile Application for Regional Landslide Inventories (MARLI) was designed and developed under the Android platform to suit the need for updated and more detailed LI. In this regard, Open Data Kit is an effective tool for collecting data in the field (on-line/ off-line) and it consists of three steps: design data collection form, collect data and export the collected data (Venkatasrinivasa Murthy, 2017). More detailed description of these steps is given below.

1.2.1.1 System architecture

The architecture of the system is based under two basic blocks: collection of data (ODK Collect) and data display (ODK Aggregate). Traditional forms have been replaced by tools that, by means of electronic forms and intelligent mobile devices, allow the collection of data (text, numbers, geolocation, photographs, videos, audio...) (client side - ODK Collect). These data, even without an Internet connection at the time of this data collection, are sent to an online server. This component, ODK Aggregate, allows managing the forms and administrating the collected data, and it is hosted on a own local server (server side - ODK Aggregate). Also, in the server side, we implemented a Spatial Data Infrastructure (SDI) to visualize, manage and analyze the data (data visualization - see section 1.2.1.4) (Figure 1.1).

The advantage of ODK platform is that the tools are open source and are based on open standard XForms to build the forms. XForms is a model view controller based XML markup language. It was developed by the World Wide Web consortium (W3C) to enhance and overcome limitations of other traditional languages such as HTML (Botts et al., 2008). Considering that the expertise of the user is a prominent factor that plays an important role in deciding the functionalities of

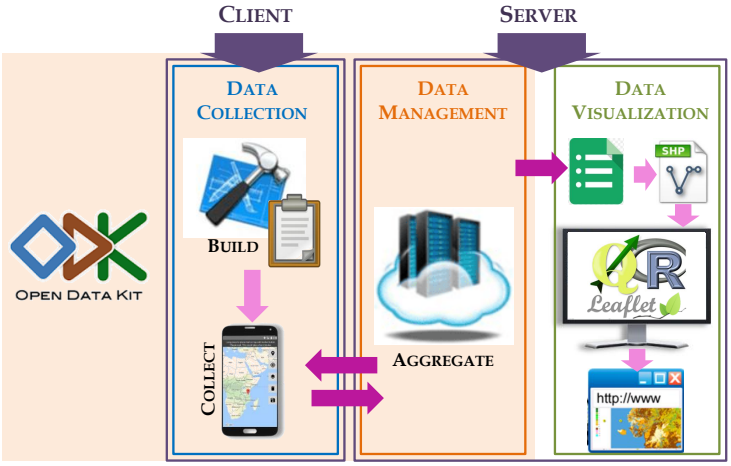

Figure 1.1: Scheme of MARLI architecture.

mobile devices (Venkatasrinivasa Murthy, 2017), for this study, we have implemented two types of forms. The first one called *Citizen Form* and a second one called *Technical Form* aiming to target two profiles types for the landslide data collection. These profiles are as follows: One open to all the community with no regard of expertise on the subject of landslides and a second profile with a technical background on landslide identification, classification and characterization (for more details on the forms, see section 1.2.1.2).

The data are first stored on the smartphone, and then, when the phone is connected to Internet via GSM (Global System for Mobile) or Wi-Fi, the data are uploaded on the server. Finally, the forms stored on the server, which include a unique automatic identifier, are exported to a spreadsheet (CSV format), and then, this file is transformed into a vector format of points from the latitude and longitude fields. In this way, the result of the field data collection can be loaded into a GIS for analysis, editing and processing (process described in section 1.2.2) for subsequent display (section 1.2.1.4). Additionally, it is also possible to export the data to Keyhole Markup Language (KML) format, which is an XML-based markup language for representing geographic data in three dimensions; or export them to JavaScript Object Notation

(JSON), which is based on a subset of the JavaScript Programming Language. This allows a wide possibility of data exchange formats, expanding the possibilities of processing the recorded data.

1.2.1.2 Citizen and technical forms

The design of the forms was based on the study by Kirschbaum et al. (2010), where a difference is made between primary and secondary elements, grouped into 5 categories (location, date-hour, event characteristics, impact information and information source). In addition, the study sought to meet four requirements: (1) it had to take into account an adequate number of fields that were simple enough to collect data quickly and accurately; (2) it could be covered by both technical specialists and civil society; (3) the information recorded could be integrated into existing databases; and (4) it took into consideration the requirements of the National Secretary for Risk Management (SNGR) as a tool to facilitate the making and updating of landslide inventories. Table 1.1 quotes and briefly describes the elements that were finally included in the MARLI forms grouped into the 5 categories cited by Kirschbaum et al. (2010). Additionally, the data collected will be loaded on the Cooperative Open Online Landslide Repository Platform (COOLR).

Table 1.1: MARLI: Primary (•) and secondary (∗) elements (based on Kirschbaum et al. (2010)) in citizen/technical forms.

Group	Element	Form	SN	NS	Field type	References
Location	Relative Location•	CF / TF	1	CF:2/TF:2	Text field	Kirschbaum et al. (2015), Jäger et al. (2018)
	GPS Location•	CF / TF	2	CF:5/TF:3	Location field	Kirschbaum et al. (2015), Rosser et al. (2017)
	Distance to landslide∗	TF	3	CF: /TF:4	Numeric field	
	Direction of the landslide∗	TF	4	CF: /TF:5	Numeric field	
Date/Hour	Date/Hour of report•	CF / TF	5	CF:6/TF:6	Field Date/Hour	Kirschbaum et al. (2015), Olyazadeh et al. (2016), Jäger et al. (2018)
	Report in real time∗	CF / TF	6	CF:13/TF:7	Field Yes/No	Olyazadeh et al. (2016)
Event charact.	Type of the event∗	TF	7	CF: /TF:8	List of options	Kirschbaum et al. (2015), Olyazadeh et al. (2016), Jäger et al. (2018)
	Status of the event∗	TF	8	CF: /TF:9	List of options	Jäger et al. (2018)
	Speed of the landslide∗	TF	9	CF: /TF:10	List of options	Glade y Crozier (1996)
	Landslide triggering event•	TF	10	CF: /TF:11	List of options	Kirschbaum et al. (2015), Olyazadeh et al. (2016), Jäger et al. (2018)
	Landslide category∗	TF	11	CF: /TF:12	List of options	Olyazadeh et al. (2016), Jäger et al. (2018)
	Estimated landslide volume∗	TF	12	CF: /TF:13	List of options	Rosser et al. (2017)

continued on next page

Table 1.1 – MARLI: Primary (•) and secondary (∗) elements in citizen/technical forms (continued).

Group	Element	Form	SN	NS	Field type	References
Impact information	Is there affected population∗	CF / TF	13	CF:14/TF:14	Field Yes/No	Kirschbaum et al. (2015), Jäger et al. (2018)
	Road infraestructure damage∗	CF / TF	14	CF:17/TF:15	List of options	Kirschbaum et al. (2015), Olyazadeh et al. (2016), Jäger et al. (2018)
	Other infraestructure affected∗	TF	15	CF: /TF:16	Field Yes/No	Kirschbaum et al. (2015), Olyazadeh et al. (2016), Jäger et al. (2018)
	Picture of infraestructure∗	TF	16	CF: /TF:17	Multimedia field	
	Hazard level∗	CF / TF	17	CF:19/TF:18	List of options	Olyazadeh et al. (2016)
	Number of fatalities∗	TF	18	CF: /TF:19	Numeric field	Kirschbaum et al. (2015), Jäger et al. (2018)
Information source	Picture landslide∗	CF / TF	19	CF: /TF:20	Multimedia field	
	Name of the event∗	TF	20	CF: /TF:21	Text field	
	Surface-water∗	TF	21	CF: /TF:22	List of options	Glade y Crozier (1996)
	Geology∗	TF	22	CF: /TF:23	Text field	Jäger et al. (2018)
	Land use∗	TF	23	CF: /TF:24	Text field	Olyazadeh et al. (2016), Jäger et al. (2018)
	Picture of land use∗	TF	24	CF: /TF:25	Multimedia field	
	Links to news∗	TF	25	CF: /TF:	Text field	Kirschbaum et al. (2015)

Note: SN = Screen Number, NS = Next Screen CF = Citizen Form, TF = Technical Form (see screens in Figure 1.2).

In addition to the requirements cited, MARLI has two target users. One is the common user with enough knowledge to correctly fulfill the data that the application requires aiming mainly on the location of landslides (citizen form). This form was included, because as other authors have previously stated, the volunteer contributions are considered fundamental to explain the occurrence, magnitude and intensity of landslides in mountainous and rural areas (Kocaman y Gokceoglu, 2019). The other target is the technical operator which can identify, characterize and typify landslides in a more technical matter due to his/her experience and training which translates in high quality data (technical form). In addition, as conducted by Jäger et al. (2018) in his study, both the database and the application are currently upgraded into a bilingual design (Spanish and English). In this way, it is intended to facilitate the integration of MARLI data into regional, national, and continental databases.

The citizen form is destined to all the community (open participatory data collection). The citizen data can provide useful information for technicians, allowing a more efficient investment of resources. In this case, all users of the application can participate in the generation of a LI by providing information in 4 of the 5 categories of elements considered in this study (see Table 1.1):

- The category **location of landslides** includes information relative to the actual location, *relative location* (primary element), where it is asked to specify in a text type field the name of the town/village closest to the place of the event, the province and country. In this category, there is also a field labeled *GPS location* (primary element) that allows users to select the location using the GPS of the mobile device, where in addition to providing latitude, longitude and elevation, it also provides the accuracy of these coordinates. These elements are of special importance because it implicitly gives the location of landslides, and using the density points recollected (amount of data points indicating landslides reports), it is possible to identify hot spots, areas that would be considered for a more specialized intervention.
- In the category **date/hour**, the date and time of occurrence of

the event is recorded (*date/hour of report* - primary element) and the user is asked to indicate whether the previous data actually corresponds to the date of the event by means of a binary type field (*report in real time* - secondary element). This last element is included because sometimes it is difficult to identify the time of occurrence of the event and thus it is possible to avoid errors in the analysis of recorded data.

- In section **impact information**, three elements are included: 1) whether there is a population affected by the landslide (*Is there affected population* - secondary element), where the user must indicate this through a binary type field ("yes"/"no"); 2) to what extent the roads can be used (*Road infrastructure damage* - secondary element), so that the user must select one of the available options to define it (options: free transit, transit with precaution, dangerous transit, road partially closed or road closed); and 3) *hazard level*, where the user must select between three levels of danger (low, medium or high) based on the matrix included in screen 17 of Figure 1.2.

- Within the category **information source**, there is only one element, *picture landslide* (secondary element). In this field, the user can either load photos of the event taken before starting their registration at MARLI and that are stored in the mobile device or take them at that time by using the device's camera.

The technical form was designed under the premise of a technical user. This specialized user has the characteristic that they have a prior knowledge in engineering-geology and have a speciality in landslides hazard management. This technical form was distributed among a group of technicians that collaborated in the creation of the landslide inventory for the Canton Cuenca. These technicians were registered in the tool, and each one was assigned a username and password to access the technical form.

The technical form, in addition to the information included in the citizen form, includes the following elements:

- The category **location of landslides**, in addition to the *Relative location* and *GPS location* fields described above, includes the field *Distance to landslide* and *Direction of the landslide*. These measures are numeric type fields whose values are recorded in meters and degrees, respectively. So, these fields are used to locate the gravitational-center of the landslide mass with respect to the point where the technician who is recording the data is located. This information will be used to correct the location of the highest point of the landslide.

- The category **event characteristics**, which is not active in the citizen form due to its very technical content, includes different fields to characterize the landslide being recorded. First, there is the field *Type of the event*, where the user must select between two options, if it is a new event or a reactivated landslide. This field will be very useful in future processes of updating documented areas. Then, in the field *Status of the event*, the user must choose between four options to describe the current status of the landslide (options: active, reactivable, naturally stabilized or artificially stabilized). In the following field, *Speed of the landslide*, the user must identify the approximate speed of the event by selecting one of the options listed (options: fast, moderate, slow, very slow or extremely slow). This information may be useful in assessing the risk associated with each landslide. The only primary element in this category is the *Landslide triggering event* which seeks to identify the main trigger of the identified landslide. Within the options are rain fall, earthquake, anthropogenic or volcanic activity, but it is also left as an option for the user to identify another trigger not included in the previous options from a text field. Another field present in this category is the *Landslide category*, which refers to the type and characteristics involved the mode of landslide movement. For this, a simplified version of the classification of mass movements developed by Varnes (1978). was used for this purpose. Thus, ten options are included, with the corresponding graphic representation (see screen 11 in Figure 1.2), from which the user must select one (options: rotational, translational, block slide, rock fall, topple, debris flow, debris avalanche, earth flow, creep and lateral spread). Finally, and despite the difficulty in

estimating it (Brunetti et al., 2009), the last field of this block is *Estimated landslide volume*, where the user is asked to select the option that is closest to the landslide volume (options: small - less than 10 m^3, medium - 10 m^3-1000 m^3, large - 1,000 m^3-100,000 m^3, very large - 100,000 m^3-1,000,000 m^3 or catastrophic - larger than 1,000,000 m^3).

- In **impact information**, in addition to the three fields described above in the citizen form, three other elements are included in the technical form: *Other infrastructure affected*, where the user must indicate if in addition to the communication routes there are other affected infrastructures by the event through a binary type field ("yes"/"no"). In the case of selecting the option "yes", the user is asked to describe or list the affected infrastructures through a text type field. The following element is directly related to the previous ones (*Picture of infrastructure affected*), in case there are affected infrastructures, the user is asked to take/upload a photo that reflects the severity of the damage through a multimedia field. Finally, the user ir asked to indicate the *Number of fatalities* that the landslide caused by a numerical field.

- Finally, within the **information source**, in addition to the *Picture landslide* of the citizen form, six more elements are included (all of them, secondary elements). First, the field *Name of the event* asks to assign a name to the event which shall be different from other names in the same region through a text field. To find out this information, people affected or from nearby populations may be consulted. Also included in this category is the element *Surface-water* to report if there is water on the surface. The user is asked to choose between four options: absent, diffuse, concentrated or stagnant. Then, a text field asks the technician to specify the predominant geology in the area of the event (element *Geology*). The following two fields are related to land use. In the first one, *Land use*, the predominant land use is asked to be identified through a text field. In the second one, *Picture of land use*, a multimedia type field, the user can either upload photos or take them at the time of data collection reflecting the land use. Finally, the field *Links to news* asks to include the routes to articles

in the digital press. In cabinet, the above information can be used by incorporating scanned files from the written press.

1.2.1.3 Interface design and options

Figure 1.2 shows how the forms are presented to the users. When the application is opened, the first screen included in Figure 1.2 appears. In this screen, the user must choose between the two forms developed in this study: citizen or technical. In the first case, it will be screen number 1 while in the case of the technical form, authorization verification will be requested. Each field technician will have an independent login. Logins will also be provided to interested municipal technicians. In order to keep track of each technician's work, a field will be added to each technician's record where the login user name will be recorded.

Regardless of the screen, they all have the same interface structure. First, on the left edge of each screen, the five categories proposed by Kirschbaum et al. (2010) are displayed by means of tabs. Inside, a set of circles that correspond to the number of screens included in the categories. So, the user will see "not-filled" those issues that remain to be covered. As soon as the user answer the question on each screen, he/she must save his/her answer (button *Save & Next*, first in the upper right corner) and it will automatically move on to the next screen. When the user reaches the last one, he/she will press the button *Save & Send* to end the registration and send it to the server. The data are uploaded on the server, register by register, when the phone is connected to Internet. It is also possible to go back in the screens in case it is necessary to edit the form, using the button Preview in the lower left corner of the MARLI interface. In that corner, it was also included the button for new landslide registration without the need for new logging. All the available buttons are indicated in the screen number 1 inFigure 1.2.

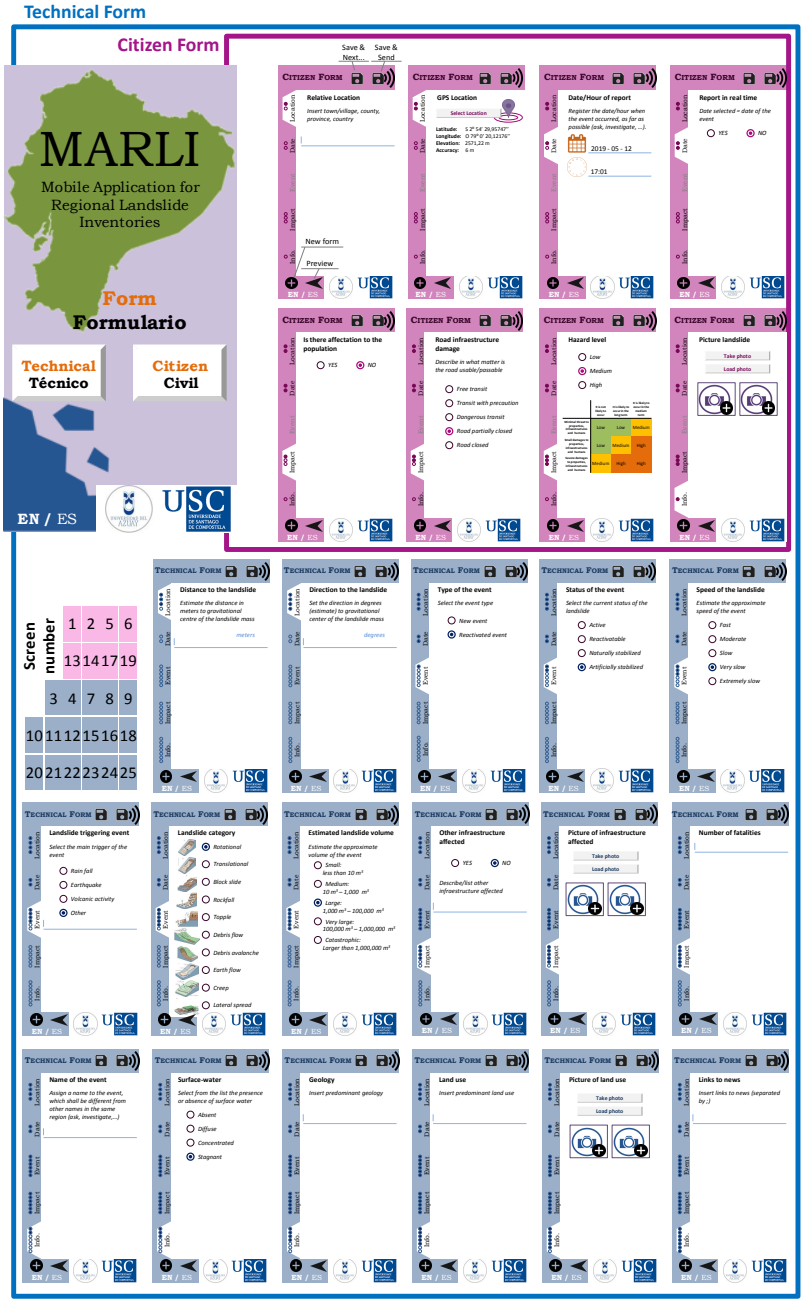

Figure 1.2: Interface of MARLI: citizen form (purple box) and technical form (blue box).

1.2.1.4 Data visualization

First, a script is developed in the R environment (R Development Core Team, 2010), using the R package *leaflet* (v. 2.0.3) via QGIS, in order to display the main landslide characteristics. Then, an interactive map is created using the previous code and the main results of the field survey and the subsequent cabinet analysis. The scheme of script is made up of three parts: (1) the creation of map interface; (2) selection of layers and the legend; and (3) map export for online view. This map is available through Spatial Data Infrastructure of the IERSE (Instituto de Estudios de Régimen Seccional del Ecuador)[1]. As in previous researches (Rosser et al., 2017, Bragagnolo et al., 2020), open-source software is used to achieve two purposes: to make that results obtained within the framework of this study available to the public free of charge and to facilitate researches into assessment of natural disasters.

1.2.2 Cabinet work

In this study, a distinction is made between desk work prior to the field survey, i.e., data collection, planning work to analyze the operation of MARLI; subsequent work to identify, correct or eliminate and complete records, i.e., analysis work after the information has been recorded in the field. As for the tasks of the first group, first of all, the study area is divided into survey quadrants. Each quadrant will be assigned to a pair of field technicians. Then, the guide routes for each quadrant are drawn up based on the cartography and data available (administrative boundaries, orthophotos, topography, geology), and if available, the records captured by civil society using the citizen form.

The tasks of the second group (post-data collection work) start by loading and transforming the records into vector format in order to be able to visualize and edit them in a GIS. The identification and elimination, if any, of duplicate records is then carried out. Knowing that record duplication is one of the most common problems when different

[1] http://gis.uazuay.edu.ec/proyectos/deslizamientos

blocks of data are merged (citizen and technical data) (Jäger et al., 2018), special attention was paid to this point in the previous planning. Despite this, isolated cases of very close points were identified. Despite the difficulty of identifying them, they were analyzed and corrected. Additionally, geology and land use fields were revised and harmonized. On the other hand, the points recorded represent the foot of the slide, but if this is not the case, these points are rectified using satellite images (GeoEye) and *the distance and direction to the landslide* fields. The last steps consisted of setting the head of the landslide according to the contour lines, satellite images and the photographs of the landslide taken in the field. Then, the area affected by each slide is digitized.

Taking as a reference the studies developed by Van Den Eeckhaut y Hervás (2012) and Saleem et al. (2019) and also thanks to the geo-localization of each record, it was possible to assign additional information to each identified landslide. Specifically, data related to landslide dimension such as affected area, length, and width are completed by digitizing on orthoimage or height from top to toe using the DTM. Additionally, the information related to geoenvironmental characteristics was also extended through the use of available thematic layers such as hydrogeology, slope gradient, slope aspect and drainage system. All these variables were obtained from the thematic layers calculated in the framework of the SIGTIERRAS program[2], which depends on the Ministry of Agriculture and Livestock, and available for free download in the geoportal of that program[3].

1.3 Field application, results and discussion

1.3.1 Study Area

The Canton Cuenca is located in the province of Azuay, southern part of Ecuador (South America), and the population of this region is of 636.000 inhabitants. Cuenca covers a surface of about 3.100 km^2 within

[2] http://www.sigtierras.gob.ec
[3] http://geoportal.agricultura.gob.ec/index.php

the occidental and oriental mountain ranges (Figure 1.3). The Canton has a morphology characterized by a series of highlands and plains (approximately 2.580 m over sea level). The predominant lithologies are mainly represented by the sedimentary and clayey materials, adding to a changing climate, ranging from persistent droughts to extensive rainfall (precipitation averages in the order of 940 mm/year, where December to May are considered months of high precipitation and June to November are considered dry months), which encourages the occurrence of landslides.

These phenomena are frequent in Cuenca, they can create problems for the population and cause the destruction of infrastructure. One event that marked the region was the landslide of Tamuga Hill that occurred on the left bank of the Paute River in the southern Andes (see Figure 1.3, *Josefina landslide*). This event, which occurred at the end of 1993, is known as *El desastre de la Josefina* and highlighted the vulnerability of both the infrastructure and the population. Since that event, landslide susceptibility studies and inventories have been carried out in that region, the most relevant being the Prevention-Ecuador-Basin-Paute pilot project (PRECUPA project). This initiative was developed within the framework of international cooperation to support Ecuador in strengthening its capacity to prevent natural disasters (more details in Basabe et al. (1996)). The studies were carried out between 1994 and 1998, recognizing the vulnerability of the Paute Basin to unstable terrain and the need to carry out more studies throughout the basin. In spite of these results, since then no work has been done to update the information generated in this project.

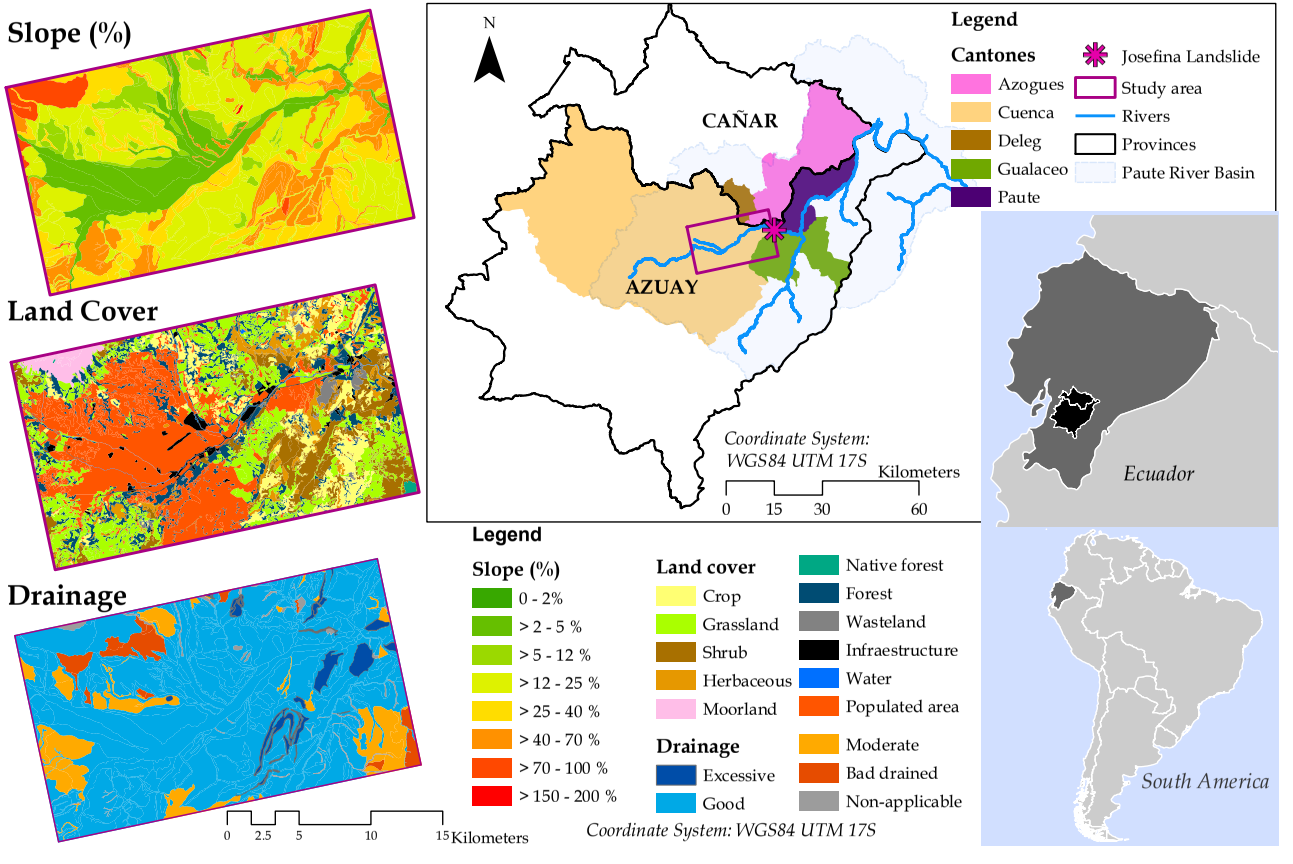

Figure 1.3: Description of study area. The slope, land cover and drainage maps were obtained from SIGTIERRAS project.

Taking into account this background, the study presented here is developed within the area of greatest susceptibility to geological origin phenomena according to the study carried out by Basabe et al. (1996) within the framework of the PRECUPA project. The study area covers 380 km^2 (purple box in Figure 1.3) and affects the cantons of Cuenca, Gualaceo and Paute in the province of Azuay, and the cantons of Azogues and Deleg in the province of Cañar (Figure 1.3). This zone is located within the Paute River basin and includes the area affected by the Josefina disaster. The majority of the surface in the study area presents a slope between 25 and 100% (slope map in Figure 1.3). On the other hand, the majority coverage in the study area is *populated area* (30%), followed by *grassland* (20%), *forest* (15%), *shrub* (12%) and *crops* (10%) (land cover map in Figure 1.3). Finally, in terms of drainage capacity, 80% of the study area has the capacity to easily eliminate water from rainfall, although not quickly. The soils are of medium to fine texture and some horizons can remain saturated for several days, while the water table is found at depths greater than 120 cm (good drainage). In 10% of the surface of the study area, the elimination of water is slow in relation to the supply and the soils have a wide range of textures. The presence of a slow permeability layer, or a high water table (60 - 90 cm deep) (moderate drainage) (drainage map in Figure 1.3).

1.3.2 Analysis of the results

1.3.2.1 Data collection yields

It is widely known that the main limitations in the elaboration of inventory maps are time and technical/human resources (Guzzetti et al., 2012). In this sense, the use of MARLI showed that it is possible to cover wide extensions of surface effectively, besides providing a standard in the information survey, parametrizing the data, and allowing a good characterization of the landslides. The area surveyed corresponds to a polygon of 380 km^2 , which was divided into 36 quadrants of 13.5 km^2 each one (18 North Sector, 18 South Sector). Taking into account the number of landslides, the complexity and accessibility of the sector, an average of one quadrant every two days was established, and an

average of 20 landslides per quadrant. Thus, the inventory undertaken using MARLI application shows a total of 668 landslides (considering duplicate records, 710 landslides) within the study area in a period of less than 2 months. It should be highlighted that this process included the planning, surveying and field, and the works in cabinet.

Table 1.2 compares the performance obtained in this study with other inventories. Based on the ratio of the average number of square kilometers covered per interpreter per month, it can be seen that the MARLI application allows for the management and collection of landslide data in an approximately equal or more efficient manner than most of the studies included in Table 1.2, which mostly use conventional methods. Taking into account these data, it is observed that the efficiency of the inventories is directly proportional to the extent of the area covered by the inventory, except for the inventory conducted by Olyazadeh et al. (2016). On the other hand, the values of the ratio landslides collected per interpreter per month do not vary as much as the previous ratio, and circumstance that coincides with the one identified by Guzzetti et al. (2012) and that depends, mainly, on the scale, the number of experienced personnel, the adequate technology, the complexity of the terrain and the abundance of the landslides.

Table 1.2: Comparison of yields with studies that included field work.

Research	**Method**	**Area**	**Landslides**	**Density**	**Month**	**Rate**		**Attributes**	**Team**
		km^2		$\frac{Lands.}{km^2}$		$\frac{Lands.}{month}$	$\frac{km^2}{month}$		
Cardinali et al. (2000)	PI/FSH	1500	4000	2.67	6	333.3	125	—	2
Guzzetti et al. (2004)	PI/FS	500	1024	2.05	2	256	125	—	2
Ardizzone et al. (2007)	PI/FS	90	70	0.8	0.4	175	225	< 10	1
Galli et al. (2008) - 1987	PI	8456	5270	0.6	9	292.8	469.8	< 10	2
Galli et al. (2008) - 1999	PI	8456	47414	5.6	28	564.5	100.7	< 10	3
Galli et al. (2008) - 2002	PI	78.89	2564	32.5	5	259.4	7.89	< 10	2
Mondini et al. (2011)	PI/FS	60	821	13.7	2	82.1	5.9	< 10	5
Fiorucci et al. (2011)	PI/FS	90	457	5.1	2	228.5	45	< 10	1
Olyazadeh et al. (2016)	MA	123	59	0.5	0.07	421.5	878.6	14	2
MARLI	MA	380	668	1.8	2	167	95	25	2

Note: Method, methodology used to create the inventory (FS - field survey; FSH - field survey by helicopter; PI - photo-interpretation; MA - mobile application); Area, extent of the area covered by the inventory (km^2); Landslides, total number of mapped landslides; Density, landslide density (Lands./km^2); Month, time required to prepare the inventory (month); Rate, average number of landslides and square kilometers per technician per month (Lands./month and km^2/month), respectively; Attributes, total number of fields collected during a field trip; Team, total number of technicians.

1.3.2.2 Qualitative and quantitative results

As already mentioned, in the study area ($\approx$ 5% of Azuay), 668 landslides were recorded and outlined, representing 3.83% of the surface area of the study area with an average density per square kilometer of 45.8 and with an average size landslide of 2.2 ha. Figure 1.4 is prepared to show the types of landslides present in the study area. This figure shows, through a mosaic, the different types of slides in horizontal axis and the different levels of slope in vertical axis. Each block is colored in proportion to the presence of water on the surface. Although MARLI contemplates up to ten different types of landslides, only seven types are present in the study area. The area of each block is proportional to the number of landslides.

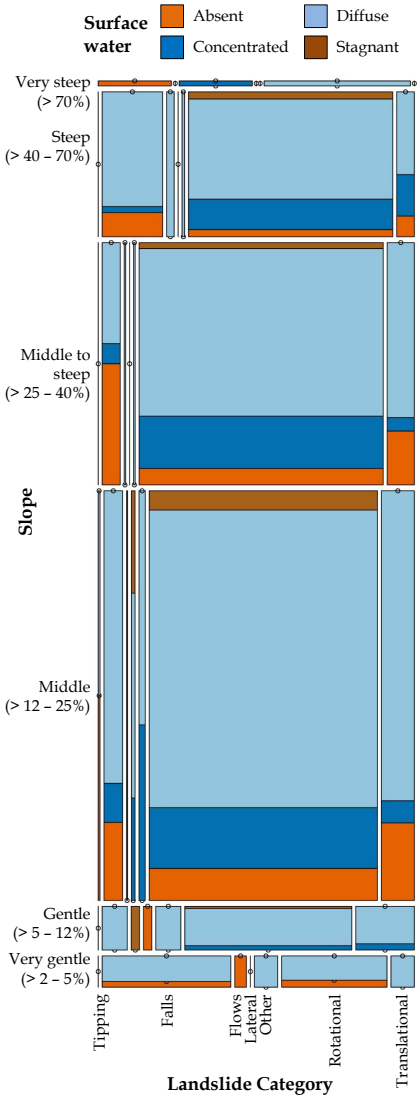

Figure 1.4: Slope, surface water and landslide category.

Most of the identified landslides are of a rotational type and are located in areas which slope varies between 12 and 40% (mediumhigh slope), where the presence of groundwater is mostly diffuse. The fall type slides have a significant weight in areas which slope is between 40 and 70% and in areas with a slope of less than 5%. As expected in high slopes,

the propensity to fall material is strong and even more so if the lithology inherent to the sector corresponds to materials with little cohesion, that is, in such areas, the potential for falling rocks, conglomerates, and soil blocks increases greatly. As for the fall in low slopes, very rare in the area of study, they occur mainly on slopes where anthropogenic actions have occurred, such as roads, or in small cuts, of low height and gentle slopes, where the material has been removed giving rise to the fall in blocks of material.

On the other hand, tipping, flow, or lateral spread landslides are the ones that have less presence in the study area. This fact can be attributed to the lithology in the study area that, although the area is favorable to the occurrence mainly of creeping and rotational type movements, are not so favorable to flow type movements or tipping because of the cohesion of the clays that do not allow the materials to break down easily.

Figure 1.5 is developed to identify the characteristics of areas that are susceptible to landslide occurrence. For this purpose, the different levels of the lithology[4] and slope are represented in the y and x

[4]Lithology legend Figure 1.5: 1. Sandy clays, often reddish and with presence of gypsum, and thick tuffaceous sandstones; 2. Clear laminated shales, with gypsum; locally, sandstones and basal conglomerates with levels of clays and siltstones; 3. Silts, clays, sands, gravels and blocks; 4. Heterogeneous mixture of fine materials and rocky angular fragments of very different sizes; 5. Tobaceous sandstones of medium to thick grain, levels of conglomerates and weak layers of clays, silts and shales; 6. Heterogeneous mixture of fine materials and rocky angular fragments, with absence of stratification and internal ordering structures; 7. Limonites, shales and fine-grained conglomerates; 8. Limonites, shales and fine-grained interstratified sandstones, shales with coal seams, coarse-grained and conglomerate sandstones; 9. Coarse and brecciated andesitic conglomerates, with intercalations of sandstones and tuffaceous siltstones, scarcely lithified and consolidated; 10. Silt and clay (predominant in the distal zone) and sand, gravel and blocks (predominant in the apical zone), in variable proportions and with marked changes of lateral and vertical facies; 12. Volcanic agglomerate with white glass matrix (Llacao) and well stratified volcanic-sedimentary sequence with predominance of tuff (Gualaceo); 13. Sands, silts, clays and conglomerates; 14. Silts, clays, sands, gravels and blocks in variable proportions; 15. Tuffs and agglomerates (dacite, rhyolithic and andesitic) kaolinized, with low percentage of lava; 16. Dark gray massive siltstones and quartz-feldspathic sandstones; limestone, gravel and tuffaceous sandstones; 18. Green andesitic tuffs very meteorized and andesitic to andesite-basaltic lavas; 22. Metavolcanites with

axes, respectively. Additionally, by means of a color legend, the soil cover present in the delimited zones as landslides is shown and its representativeness (surface in hectares) is reflected by means of the size of the points. All these variables were obtained from the thematic layers calculated in the framework of the SIGTIERRAS program.

Based on this figure, a large part of the area affected by landslides is concentrated in areas with slopes between 12 and 40% in populated areas, of pasture, crops or forestry plantations on type 1, 2, 4, 5, 9 and 15 soils (see lithology legend in footnote 4). In areas of a high slope, landslides can occur regardless of land use; however, in less steep terrain, changes in land use can affect the stability of the slope (Hearn y Hart, 2019). In this regard, some researches have shown that anthropogenic intervention is the main agent of landslides in urban areas due to excavations in slope areas, water leakage, and the cultivation of certain species (De Brito et al., 2016). Also, the conclusions of the studies developed by Di Martire et al. (2012) or Sepúlveda y Petley (2015), showing that population density has a strong positive correlation with the density of landslides, increasing the possibilities of affecting people.

With respect to changes in land use, in the last few decades, Ecuador has experienced important processes of informality in the land occupation (Muñoz-Sotomayor et al., 2018), with two different phenomena. On the one hand, the advance of the agrarian frontier due to population growth and the lack of suitable places for people inhabit, which entails the replacement of natural elements, such as native forests, by crops or pastures. This phenomenon causes erosion on the slopes due to agricultural activity, increasing the possibility of landslides. On the other hand, informal settlements on the outskirts of cities, mainly in areas at risk due to slopes, areas of flooding or instability, and on the banks of rivers and streams (De Brito et al., 2016, Rivera Torres y Serrano Fernández de Córdova, 2019). Thus, there are circumstances, identified as critical by Alexander (2012) (location of dense populations in precarious, informal or poor urban settlements), which may lead

weak metamorphism, massive lavas and green phyllites, green schist, quartzite and marbles.

Figure 1.5: Where landslides occur in the study area.

to an increase in the number of deaths from landslides. All of this highlights the vulnerability of the population of these communities, their infrastructure, and the farm areas.

One of the main factors at the local level for the occurrence of landslides is geology/lithology (Karsli et al., 2009, Sepúlveda y Petley, 2015). As discussed in Basabe et al. (1996) and Hungerbühler et al. (2002), in the Paute River basin, the greatest frequency of landslides occurs in areas of sedimentary formations made up of shales, incompetent lake limonite's, expansive clays altered with tuffaceous sandstones, and metamorphic formations made up of fractured phyllites. This information corresponds largely to the data collected in the field. Adding to these lithological factors, the presence of water or high precipitation makes the propensity for landslides greater (Sepúlveda y Petley, 2015).

In addition to being conditioned by factors such as soil, slope, or geology, landslides are also affected by climatic phenomena. Like the results shown at the continental level by Sepúlveda y Petley (2015), the main trigger for these phenomena in the study area is the precipitation, and to a lesser extent, due to anthropic causes or earthquakes as shown in Figure 1.6. Most of the registered landslides are active and present a low-medium level of danger according to the data collected in the field. Although MARLI contemplates up to four states of activity, it is observed that a significant number of landslides are active and present a high level of risk (Figure 1.6). This sample of recent activity should be taken into consideration to carry out prevention tasks since changes in climatic conditions (e.g., increasing precipitation rates) can endanger adjacent areas (Jäger et al., 2018). These factors, along with those identified from the analysis in Figure 1.5, and in the context of climate change in which we find ourselves, re-emphasize, as did Basabe et al. (1996) more than two decades ago, the need to carry out more studies of this nature in Ecuador.

Among the most commonly used variables to analyze the susceptibility to the occurrence of landslides is the distance to rivers and distance to roads (Hearn y Hart, 2019). Figure 1.7 is created to test how close to roads and rivers the recorded landslides are. This was done by

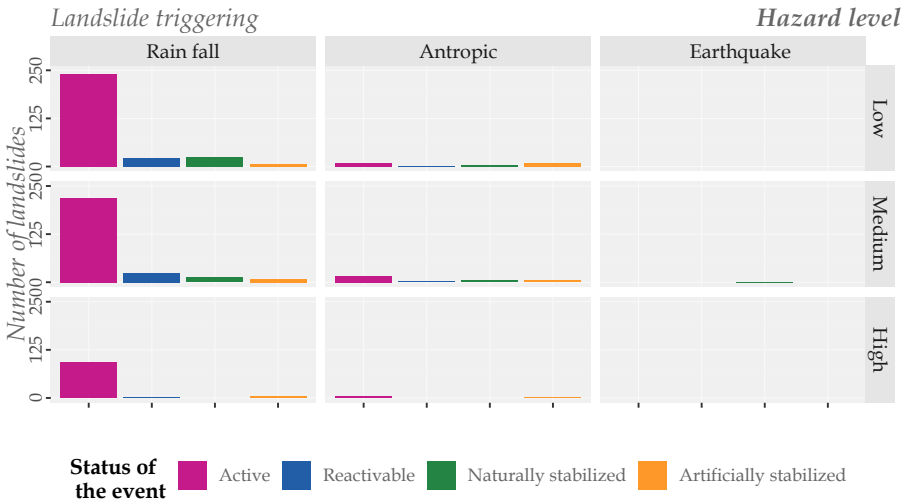

Figure 1.6: Landslide triggering, hazard level and status of the event.

taking into account the courses of the main rivers and the first- and second-order roads. Additionally, populated areas were also considered. Different buffers were applied to each of these vectorial layers, and the percentage of surface affected by landslides that overlap with each layer independently was calculated. From the results of this spatial analysis, it is observed that approximately 25%, 15% and 2% of the surface affected by landslides is located less than 50 m from populated areas, roads, and rivers, respectively. These values amount to 50%, 35% y al 15%, respectively, if the distance is 300 m. These results show that a significant number of landslides threaten populations and infrastructure, exposing communities to material damage and, in the worst case, loss of human life.

Figure 1.8 shows the web map created from the main data collected in the field and subsequent work (blue, orange, and red polygons in Figure 1.8), as well as the landslides recorded in the framework of the PRECUPA project (yellow polygons in Figure 1.8) using the functions of the R leaflet package (map attached as auxiliary information). OpenStreetMap and a Sentinel-2 color composition were used as base maps. The polygons showing the slides recorded by MARLI are

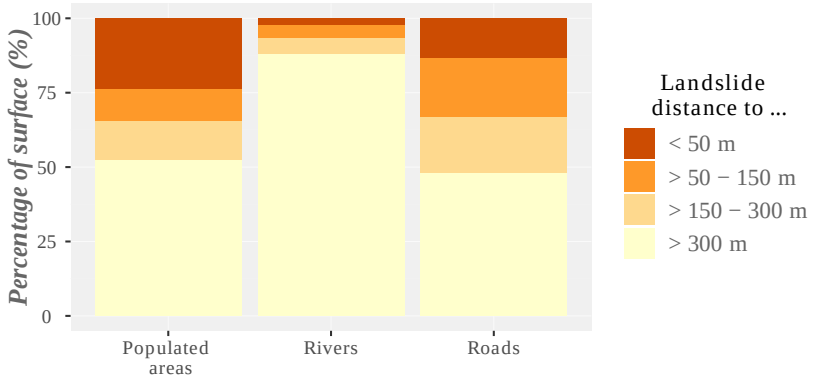

Figure 1.7: Landslide distance to populated areas, rivers and roads.

represented according to the risk levels recorded in the field (low, medium, and high). Additionally, by hovering the cursor over these polygons, the category, the trigger, the speed, and, again, the hazard can be consulted. This web map can be explored by clicking in Figure 1.8, from "MarliLandslide.html" file or by accessing the Spatial Data Infrastructure of University of Azuay (http://gis.uazuay.edu.ec/proyectos/deslizamientos/MarliLandslide.html).

Figure 1.7 shows that a very small percentage of the surface affected by landslides was close to rivers. From the map in Figure 1.8, it can be seen how this low percentage corresponds to the largest and most dangerous landslides (red polygons) and is located in urbanized areas near the course of the Paute River. All of them are located on the southern bank of the Paute River, where the slope and erosion effect is greater so that these active landslides can produce the Paute River dam again, as in the La Josefina landslide (Basabe et al., 1996).

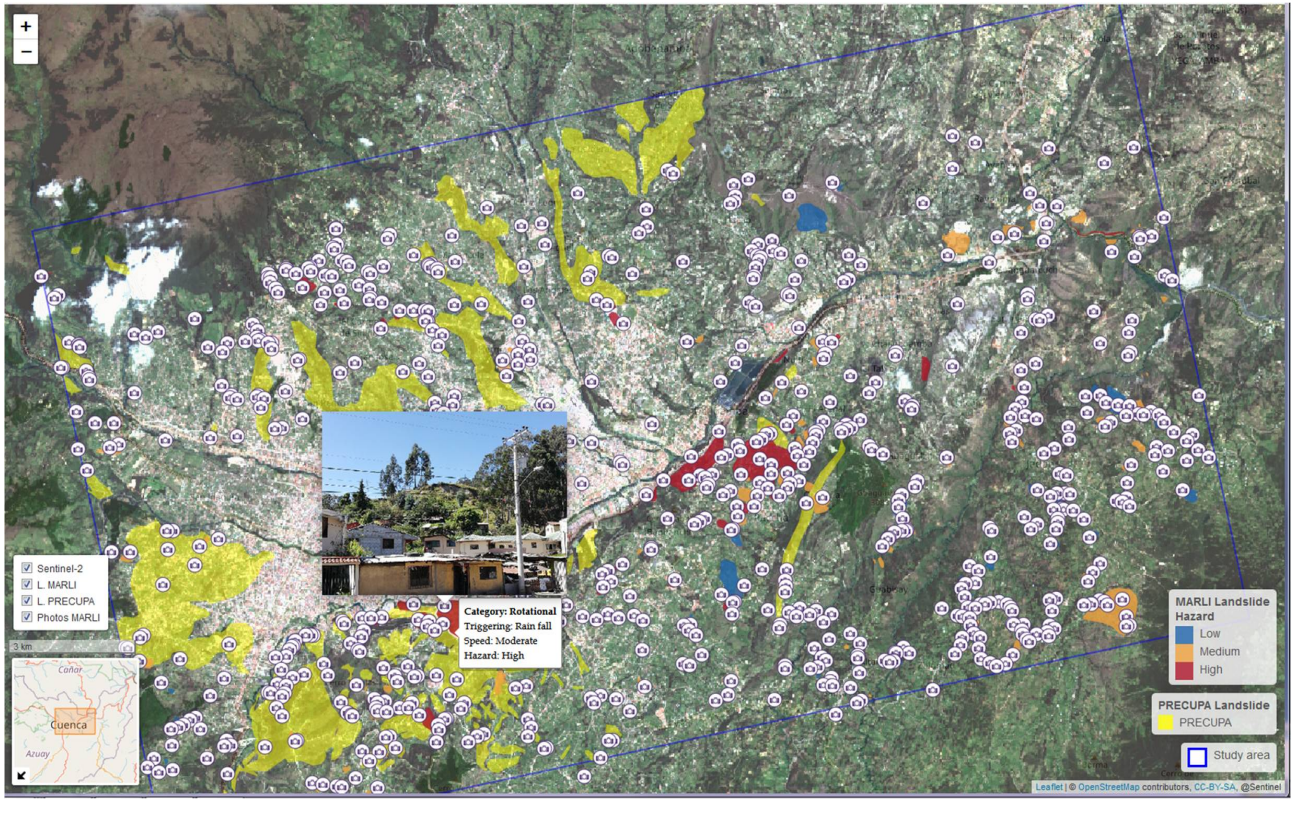

Figure 1.8: Web map using Leaflet package and R software (Download Web map: https://drive.google.com/file/d/1NpYrzLLMhlwZZjrf3wyTPxJXNGYLegwp/view?usp=share_link).

On the other hand, there is also a particularly intense sliding activity, of small volume and mostly of medium or low risk, in the southeast of the study area. These records differ from the landslides recorded at PRECUPA, which are larger and located mainly in the western zone of the study area. This fact can be attributed to the fact that the results of the PRECUPA project were generalized based on existing cartography. However, in the case of MARLI, the landslides and its in situ evidence were located, in addition to having higher resolution cartography and images. Additionally, another possible explanation can be related to the accessibility factor, which at the time of the PRECUPA project was much more reduced than it is today.

1.3.2.3 Comparison with existing databases

In this section, a comparison is made at the regional level between the inventory carried out in the framework of the PRECUPA project in 1996 and that obtained in this study. Table 1.3 includes the statistics for PRECUPA and MARLI landslide inventory maps for the study area. The number of landslides recorded in PRECUPA (130) is multiplied by 5 in the inventory made from MARLI (668), which causes the density of landslides to increase from 3.6 to 45.8 landslides per km^2. However, in the inventory elaborated from MARLI, the surface occupied by landslides in the study area is three times smaller than that registered in the PRECUPA inventory (3.83% y 9.55%, respectively). This same trend is observed in the studies carried out by Galli et al. (2008) and Lupiano et al. (2019), where the surface occupied by landslides also decreases as the completeness of the inventories increase. The improvement of inventories may be due to the methods used, the increased resolution of the information layers employed, and the technological advances that have occurred in the last two decades.

Afterward, the degree of cartographic matching between the two maps, using the method proposed by Carrara (1993) and later used by Galli et al. (2008), is assessed. For that, the overall error index (Eq. 1.1) and the degree of matching (M) (Eq. 1.2) are calculated.

Table 1.3: Statistics for PRECUPA and MARLI landslide inventory maps for the study area (area = 380 km^2) (based on Galli et al. (2008)).

Characteristics	**PRECUPA**	**MARLI**
Number of mapped landslides	130	668
Percent of landslide area (%)	9.55	3.83
Landslide density (L/km^2)	3.6	45.8
Smallest mapped landslide (ha)	0.013	0.002
Largest mapped landslide (ha)	621.9	109.1
Average size of mapped landslide (ha)	27.9	2.2

$$E = \frac{(LI_1 \bigcup LI_2) - (LI_1 \bigcap LI_2)}{(LI_1 \bigcup LI_2)} \; x \; 100 \tag{1.1}$$

$$M = 100 - E \tag{1.2}$$

Where $\mathrm{LI}_1 \bigcup LI_2$ is the geographical union of the two landslide inventories and $\mathrm{LI}_1 \bigcap LI_2$ is the geographical intersection of the two inventories. If the the two inventories are about equal, the cartographic matching is perfect (M=1) and the error is minimal (E=0).

Table 1.4 shows the quantitative comparison of the PRECUPA and MARLI inventories. As in the research of Galli et al. (2008), the geographical unions and intersections with due regard to the buffers of 10 m, 50 m y 100 m around the landslides are calculated in order to mitigate the discrepancies associated with the production of the inventories. According to Table 1.4, if we combine the inventories PRECUPA and MARLI, the area affected by the landslide in the area of study amounts to 12.7%, while in 1996 (PRECUPA) it was 9.55% (Table 1.3). These data can be taken as an indicator of the increase of instability in the region, caused, besides by the geological character of the area and the presence of water that saturates and alters the fine granular layers (Basabe et al., 1996), by the increase of the anthropic activity during the last two decades (its population increased 50% since 2001 according

to data of the National Institute of Statistics and Censuses[5]).

Table 1.4: Quantitative comparison of PRECUPA and MARLI inventories.

	Buffer size (m)			
	0	10	50	100
PRECUPA $\bigcup$ MARLI (km^2)	48.33	53.26	64.81	101.71
PRECUPA $\bigcap$ MARLI (km^2)	1.47	1.89	3.32	9.50
E (Mapping error) (%)	97.0	96.5	94.9	90.7
M (Mapping match) (%)	3.0	3.5	5.1	9.3

Taking into account the value of the mapping match index with the null buffer size, it is concluded that both inventories present few similarities as they share only 3% of the surface that presents landslides. This value is close to 10% when a 100 m buffer is applied (Table 1.4). Recently, Jäger et al. (2018) showed in his study that a low overlap between slides from different inventories may indicate a low propensity for remobilization. Similar values to those obtained in this study were reported by Carrara (1993) ($\approx$ 20%). These authors considered that these results were due to the fact that the inventories they compared represented different morphologic features. AsGalli et al. (2008), we consider that this may be one of the reasons for the discrepancies obtained, but as recently reported by Lupiano et al. (2019), and due to the temporal distance between both inventories, it may also be due to the type and quality of the available data, methods used, mapping scale, type of landslides or their occurrence linked to certain triggers (rain, earthquakes, ...). Another aspect that may be related to this disparity between PRECUPA and MARLI is the "effect" generalization due to the characteristics of the data. In PRECUPA, much larger areas were delimited because the cartography and images available at the time presented a lower resolution and level of detail than those used in MARLI.

[5] https://www.ecuadorencifras.gob.ec

1.3.3 Disadvantages and advantages of the mobile tools

The conventional methods (systematic interpretation of aerial photographs and field checks and investigations) and the new methods based on the new technologies (mobile applications) for the characterization of landslides, used to prepare landslide inventory maps, at medium-large scales, share a number of limitations: the size of the landslide, the viewpoint of the investigator (local perspective) and the old landslides are often partially covered by forest (Guzzetti et al., 2012). Additionally, the main challenges facing the previous methods are related to: 1) the available resources (equipment and staff), 2) the cost and timing per unit area, 3) the possibility of carrying out a cross-check process, 4) the characteristics of study area (morphology, hydrography, anthropic elements and land-use or land-cover) and 5) the integration of registers/maps from several (previous) periods/events. Table 1.5 shows the major limitations and advantages of both methods with regard to such challenges.

Table 1.5: Field surveys: Limitations (-) and advantages (+) of conventional methods and mobile tools..

Conventional methods	**Mobile apps**
- The need to have experienced investigators and technical resources to carry out the tasks of lifting and processing of the data collected in the field. This limitation is also directly related to the level of subjectivity that characterizes any method of landslide inventory gathering (Lupiano et al., 2019)	+ Open source tool (Rosser et al., 2017). + Easy or effortless data manipulation and commutation with other data formats like Arcgis, Qgis, R-statistics, map server, Google Earth, ... and recorded data could be transmitted to the risk management agencies at real time (Liu et al., 2014). + The rapid growth of the cell phone usage favors the accessibility and use of this tool unlike other tools used so far (e.g. PDA) (Liu et al., 2014). + Thanks to institutions such as NASA, which are considering the possibility of employing the volunteer contributions as a landslide data collection stage, will increase the demand for applications such as MARLI (Kocaman y Gokceoglu, 2019).
- Very expensive and time consuming affecting directly the amount of landslides and the area that are possible to survey effectively.	+ Increased possibility for surveying larger areas with low cost in time consumption. + Due to the landslides are local phenomena, they have often been undervalued (Foster et al., 2012). The use of mobile applications and the volunteer contributions to landslide geodata collection will allow to overcome this shortcoming,reduce the cost of data acquisition while improving the academic and public understanding of geographical and ecological processes (Kocaman y Gokceoglu, 2019).
- To apply a cross-check process on the data collected with conventional methods is almost impossible.	+ It is possible to collect much more data and observations from the same event and/or location lwhich would make it possible to carry out a cross-check process. In addition, it would be possible to address current limitations in the availability of massive field work and detailed surveys of the study areas in developing countries with lacking infrastructure. Having this information would allow you to easily and quickly create products such as landslide susceptibility maps using open-source GIS-integrated tools (Bragagnolo et al., 2020).

continued on next page

Table 1.5 – Field surveys: Limitations (-) and advantages (+) of conventional methods and mobile tools (continued).

Conventional methods	Mobile apps
- It is often impossible to obtain accurate and representative data from the landslides occurring in mountainous and/or rural areas because of access limitations, no internet connection, or no access to high resolution imagery (Kocaman y Gokceoglu, 2019)	- Data recorded from mobile apps will be limited to accessible areas, requiring the completion of inventory maps using remote sensing techniques (Kocaman y Gokceoglu, 2019). + Despite this, it is possible to partially address the problem of accessibility to places of difficult access, as the event can be reported by providing an approximate location and then, from laboratory work, adjust its location and size. - Relies on the battery capacity of the mobile device. + Offline - Online application helps to map the landslides, especially in rural areas where internet is not available (Olyazadeh et al., 2016). It allows offline data collection and upload when the user is again online. + Designed to be adaptable in networking environments with high latencies, low bandwidths, and long periods of disconnected operation.
- The effective integration of captured records and digitized in different periods depends on the quality and completeness of the data (Rosser et al., 2017), the scale, the technical differences of capture and experience of the staff in charge of carry out the collection and processing of data in each period or event (Venkatasrinivasa Murthy, 2017)	-Integration of records captured by mobile applications with existing data can be difficult due to differences in the level of detail of the recorded information. - In the particular case of MARLI, there may be difficulties in integrating registered landslides by means of citizen and technical forms. + Faster and easier data recollection and storing of data and information and easy to carry (Liu et al., 2014). Data standardization and new data to be is easily uploaded (Rosser et al., 2017).) In this way, it is possible to integrate new records into the database, allowing a better spatial and temporal characterization of landslides (Latini y Köbben, 2005). + A single tool allows to register different types of data (e.g. photos, videos, links to news, geolocation, text...) and to integrate them automatically in a database.

1.4 Conclusions

Several studies have shown that regions of Central and South America will become more vulnerable to landslides because of the increased frequency of extreme weather events. Despite the history of disastrous landslides in Ecuador, with the consequent loss of human lives, the prevention studies have been insufficient. This research is the first attempt to inventory landslides at the regional level two decades after the Josephine disaster. This study describes the development of MARLI, a simple but efficient open-access platform to report landslide events using ODK system. Its design makes reporting fast, simple and cost-effective with an added benefit, and a specialized knowledge is not required for its use. MARLI provides two types of forms: one open to all citizens (no prior knowledge), group can provide very useful and updated information, and a second form for specialized users. The user interface of MARLI, designed in accordance with the needs and capacities of different users, allows easy input of information into the database.

The results of this research show that the surface affected by landslides has increased during the last two decades. This circumstance may be a consequence of the processes of informality in land occupation that occur in Ecuador, either due to the advance of the agricultural frontier or the existence of informal settlements on the outskirts of cities. Additionally, the analyses carried out revealed a significant number of landslides registered with MARLI threaten populations and infrastructure, exposing the community to personal and material damage. This information can be taken as indicator of increased instability in the region, showing the need to monitor these phenomena in relation to territorial dynamics and factors derived from climate change.

The use of free tools, such as leaflet, R, and QGIS, together with spatial information, such as OpenStreetMap or Sentinel-2 images, made it possible to contextualize the data taken in the field, carry out spatial analysis and share research results in a simple, clear and low-cost way. This information is helpful to land use planners, policy- makers and network operators in their effort to manage landslide hazards. These

tools are also crucial to increase the possibilities of research centers and institutions with limited resources to develop tools in order to mitigate the impact of landslides, improve interoperability by democratizing information and bring research results closer to both society and institutions. In addition, the existence of local landslide databases and making them available for the wide public can facilitate the application of landslide susceptibility mapping methods. Achieving this objective relies on the process of creating, maintaining, and updating landslide databases as a well-consolidated practice.

While the results and findings from this study are not sufficient as susceptibility analyses, they should not be ignored. Additionally, they can be used to carry out a comprehensive assessment of future landslides and, in turn, constitute a fundamental input for the formulation of mitigation strategies, appropriate and timely response, as well as the elaboration of reconstruction plans in the face of an increased occurrence of such phenomena.

CHAPTER 2

Multitemporal relative landslide exposure and risk analysis for the sustainable development of rapidly growing cities

In recent decades, developing countries have experienced an increase in the impact of natural disasters due to both ongoing climate change and the sustained expansion of urban areas. The intrinsic vulnerability of settlements, due to poverty and poor governance, as well as the lack of tools for urban occupation planning and mitigation protocols, have made such impacts particularly severe. Cuenca (Ecuador) is a significant example of a city that in recent decades has experienced considerable population growth (i.e exposure) and an associated increase in loss due to landslide occurrence. Despite such effects, updated urban planning tools are absent so that an evaluation of multitemporal exposure to landslides and related risk is required. In this perspective, a potential urban planning tool is presented based on updated data depicting the spatial distribution of landslides and their predisposing factors, as well as population change between 2010 and 2020. In addition, a multitemporal analysis accounting for changes in exposure between 2010 and 2020 and an estimation of relative landside risk was carried out. Due to the absence of spatially distributed population data, energy supply contract data have been used as a proxy of the population. The results indicate that the current higher exposure and related relative risk is estimated for parishes (*parroquias*) located in the southern sector of the study area (i.e., *Turi*, *Santa Ana*, *Tarqui*, *Nulti*, *Baños* and *Paccha*). Moreover, the exposure multitemporal analysis indicates that most parishes located in the hilly areas that bound the city centre (i.e., *Sayausi*, *San Joaquin*, *Tarqui*, *Sidcay*, *Baños*, *Ricaurte*, *Paccha* and *Chiquintad*) are experiencing sustained population growth and will

be potentially exposed to an increased risk with a consistently growing trend. The obtained relative risk map can be considered a useful tool for guiding land-planning, land management, occupation restriction and early warning strategy adoption in the area. The methodological approach that is used, which accounts for landslide susceptibility and population variation through proxy data analysis, has the potential to be applied in a similar context of growing-population cities in low- to mid-income countries, where data usually needed for a comprehensive landslide risk analysis is non existing or only partially available.

Keywords: Landslide susceptibility, Machine learning algorithm, Relative risk assessment, Cuenca, Ecuador, Latin America.

2.1 Introduction

In recent decades, ongoing climate change, associated with global population growth and the related expansion of urbanized areas has been responsible for an increase in the frequency and impact of natural disasters due to floods, landslides and wildfires (Knox, 1993, Xu et al., 2013, Arnell y Gosling, 2016, Gariano y Guzzetti, 2016, Di Napoli et al., 2020b). Developing countries have experienced more severe impacts because people are often concentrated in high-hazard urban areas where housing is highly vulnerable due to poor construction and early warning systems are commonly absent (Zorn, 2018, Aguirre-Ayerbe et al., 2020). The significance of such an impact can be easily understood considering that between 1996 and 2015, approximately 90% of disaster-related deaths occurred in middle- to low-income countries (http://reliefweb.int/report/world/poverty-death-disaster-and-mortality-1996-2015).

Vulnerability factors, such as poverty, poor governance, and the lack of experience in facing natural disasters are responsible for this disproportionate effect (i.e., the death concentration in developing countries; Petley (2012a). The lack of tools for urban occupation planning, recommendations, and mitigation protocols is an additional element of vulnerability that particularly applies to rapidly growing urban areas prone to floods and landslides. For this reason, evaluating and preventing the exposure to geohazards, in terms of susceptibility and hazards, is a fundamental step for adequate environmental planning and management, as shown by several scientific contributions in this field (Goetz et al., 2015, Guerriero et al., 2018, 2020b,a, Lombardo et al., 2020, Segoni et al., 2020, Di Napoli et al., 2021, Allocca et al., 2021, Novellino et al., 2021).

In Latin-American countries, between 2004 and 2013, 611 landslides triggered by rainfall and earthquakes were responsible for approximately 12,000 deaths (Sepúlveda y Petley, 2015). A relevant example is an event that occurred in 2017 in the city of Mocoa in southern Colombia, which killed more than 300 people and destroyed 130 houses (García-Delgado et al., 2019). While the spatial distribution of such events is consistently

related to a combination of slope morphometry, rainfall distribution and population density, poverty is a factor controlling the impact on people and is particularly relevant in urban areas of developing countries. Indeed, the presence of informal settlements and their localization has a large impact on the number of fatalities. In such conditions, landslide susceptibility and risk maps are useful tools to develop land-planning strategies for preventing such impacts and supporting the sustainable development of cities (Musakwa y van Niekerk, 2015, AlQahtany y Abubakar, 2020).

Landslide susceptibility indicates the probability of a slope failure occurring in an area depending on its geological, geomorphological, structural and vegetation cover peculiarities (van Westen et al., 2003, Guzzetti et al., 2006, Reichenbach et al., 2018). It differs from hazard, since it does not directly consider any evaluation of the expected magnitude of an event and its recurrence time (Fell et al., 2008). A landslide susceptibility map spatially reproduces the landslide occurrence likelihood, providing an overview of areas that need recommendations from a settlement development perspective (Chen et al., 2020, Di Napoli et al., 2020a, Zhang et al., 2020, Arabameri et al., 2022). Landslide risk depends on the characteristics of elements at risk, their vulnerability and the temporal-spatial probability of the occurrence of a damaging landslide event. Risk maps are powerful tools because they also consider the characteristics of exposed elements and provide potential damage scenarios (Bignami et al., 2018, Novellino et al., 2021). In general, landslide risk is evaluated through a multistep analysis: i) hazard identification, ii) hazard assessment, iii) inventory of elements at risk and exposure, iv) vulnerability assessment and v) risk estimation (Dai et al., 2002, Glade et al., 2006, van Westen et al., 2008, Corominas et al., 2014). Due to the frequent lack of landslide occurrence timing data, the risk is often evaluated by adopting a simplified approach based upon susceptibility scenarios rather than hazard (Ercanoglu, 2008, Fell et al., 2008, Arabameri et al., 2017). As an alternative, hazard can be estimated based on the return period of landslide triggering events (Grelle et al., 2014). A further element of simplification generally relates to vulnerability estimation, and could be very challenging to be correctly estimated and might cause diffuse under-or over-estimation of landslide risk, especially for heterogenous settlements (Glade, 2003, Li et al., 2010,

Mavrouli et al., 2014). The concept of relative risk applies well to regions where a reduced complexity estimation is preferred due to limits in data availability, such as in rapidly growing urban areas of developing countries (Andrejev et al., 2017).

The city of Cuenca (Ecuador) is an example of a rapidly growing city that in recent decades has experienced a sustained increase in population, having reached 637,000 people. The magnitude of the change can be estimated by considering that thirty years ago the total population was approximately 200,000 people. Due to this growth, the urban area has consistently expanded from its original position within the Tomebamba River floodplain and now occupies surrounding hilly slopes. Such slopes are prone to landslides, so that damage to settlements and infrastructures are very frequent, preventing the sustainable and safe development of the city (Miele et al., 2021). On this basis, an analysis of the multitemporal variation of exposure, as a function of population growth, and the relative landslide risk in the city of Cuenca was completed to provide:

1. An updated overview of the exposure and relative landslide risk to the population.

2. A general tool for supporting land planning in rapidly growing cities suffering the effects of natural hazards due to the lack of planning instruments

Such a tool can be used to identify areas where the relative landslide risk is higher and, at the same time, the most suitable areas for urbanization. Indeed, for the city of Cuenca, a first attempt of natural hazard assessment dates back to the early 1990s with a pilot project called PRECUPA (PRevention ECuador CUenca PAute). From the perspective of the analysis, an integrated method consisting of i) machine-learning-based susceptibility assessment by using Maximum Entropy algorithm, ii) energy supply contract analysis for exposure quantification and iii) relative risk estimation, was used.

2.2 Study area

The study area comprises the city of Cuenca and the surrounding hilly area that has been increasingly occupied by settlements (Figure 2.1). Cuenca is the capital of the Azuay province of Ecuador and extends over an area of approximately 124 km^2. In 1999, the historic centre of the city was included on the UNESCO World Heritage Site list due to its importance as a cultural and governmental centre of the Cañari and Inca civilizations, and as an example of renaissance urban planning in the Americas during the Spanish colonial period.

The city lies within an inter-Andean valley, which formed following compressional deformation controlled by major NE-trending faults (Noblet et al., 1988, Hungerbühler et al., 2002). The geology of this area is represented by Mesozoic marine and subaerial sedimentary deposits that cover the Paleozoic metamorphic basement (Noblet et al., 1988). The sedimentary series is more than 2400 m thick and is composed of two main sequences separated by a regional unconformity. The lower sequence consists of fluvial and brackish delta plain deposits containing ubiquitous metamorphic pebbles from the Cordillera Real. From the bottom, this series is made up of the *Biblián*, *Loyola*, *Azogues* and *Mangan Formations*, which include sandy clays, laminated shales with gypsum, tuffaceous sandstones, siltstones and conglomeratic sandstones. The upper sedimentary sequence is composed of volcanic clast-bearing rocks of the *Turi* Formation, which is divided into the *Turi* and *Santa Rosa* Members, and consists of tuffaceous coarse sandstones, volcanic clast-supported conglomerates, matrix-supported volcanic breccias and minor tuff layers. Furthermore, the late *Miocene* volcanic series of the *Tarqui* Formation crops out in the area that unconformably covers a wide range of volcanic and Tertiary sedimentary formations. The *Tarqui* Formation is formed by two members: i) the *Tarqui* Member, which is formed by poorly consolidated and intensely weathered red volcanic airfall deposits and ii) the *Llacao* Member, which is represented by debris-flow deposits of volcanoclastic materials (Steinmann, 1997).

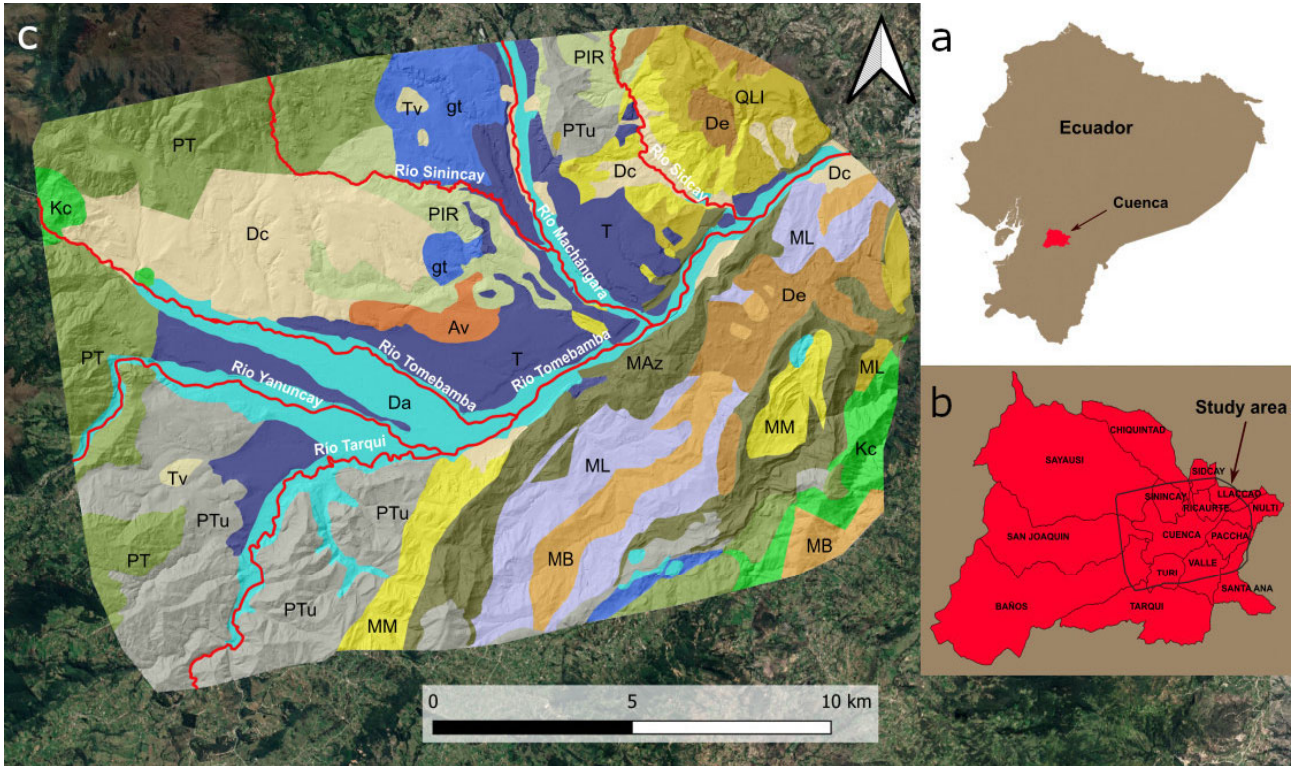

Figure 2.1: a) Geographic location of the study area; b) Azuay parishes; the box shows the location of the considered area for the analysis; c) Cuenca geological map (refer to Table 2.1 for the code descriptions of lithologies). Red lines represent the four principal rivers that cross Cuenca town.

This area is known for frequent landslides involving settlements and infrastructures (Figure 2.2). For instance, the buildings of the Faculty of Philosophy of the University of Azuay are consistently affected by slow-moving landslides and periodically damaged by slope deformation (Sellers et al., 2021a). On March 29, 1993, a large landslide (20 million m^3) occurred northeast of Cuenca city, damming the Paute river and causing the formation of an artificial lake that flooded fertile land and destroyed houses, roads, railways and a regional thermoelectric plant (Plaza et al., 2011). In addition, the segment of the Pan-American Highway crossing the city is continually affected by landslides that induce damage and, in some cases, accidents (Miele et al., 2021). The high frequency of landslides is related to the significant yearly rainfall amount (approximately 900 mm), the extremely high frequency of earthquakes of significant magnitudes (ranging from 4.0 to 4.9 Mw according to Ecuador's Geophysical Institute, https://www.igepn.edu.ec/) and the predisposing effects of slope morphologies and geological characteristics or rocks forming slopes.

Figure 2.2: a) House completely destroyed by a mass movement; b) house with considerable disjunction, floors inclined and walls out of plumb due to a landslide; c) an example of low-risk perception by the local population. The structure was built close to a subvertical rock wall which is very prone to mass movements such as rockfalls, topples and slides (photo: M. Ramondini).

2.3 Data and methods

To evaluate the relative landslide risk to the population of the city of Cuenca and the multitemporal variation of exposure in terms of population growth, a procedure consisting of machine-learning-based susceptibility analysis, population growth estimation through energy supply contract analysis and relative risk evaluation was executed (Figure 2.3). Below, the detailed data and methods used for the analyses are provided.

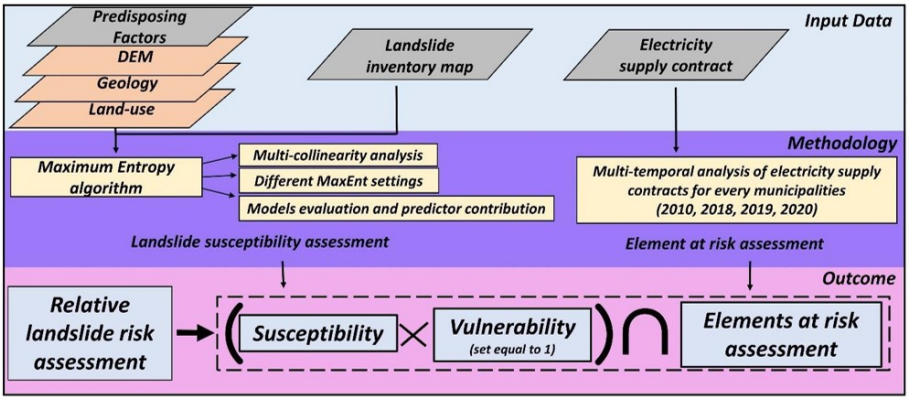

Figure 2.3: Flowchart showing the methodology for relative landslide risk assessment.

2.3.1 Landslide inventory map

From the perspective of evaluating the relative landslide risk to people, the assessment of susceptibility to landslides was carried out using the available landslide inventory map (LIM) prepared by Miele et al. (2021). The LIM is composed of 710 landslides obtained by : i) field surveys, following the approach presented in Sellers et al. (2021b); ii) photo interpretations; iii) interferometric data obtained from the processing and interpretation (Di Martire et al., 2016, Guerriero et al., 2019, Ammirati et al., 2020) of Sentinel-1A and Sentinel-1B images (ascending and descending passes) acquired between October 2016 and May 2019 using the Coherent Pixel Technique - Temporal Phase

Coherence (CPT-TPC) approach (Mora et al., 2003, Iglesias et al., 2015). The landslide database contains useful information regarding the type of movement according to Cruden y Varnes (1996), state of activity, location, triggering factor (i.e., precipitation or anthropic), geology, land use, velocity and further information (such as the field survey date, induced damages and fatalities; Sellers et al. (2021b). In the database, it is possible to recognize rockfalls (72 - 10.1%), topples (3 - 0.4%), flows (8 - 1.1%), spreads (5 - 0.7%), rotational slides (550 - 77.1%) and translational slides (72 - 10.1%) (Figure 2.6). The mass movements represent the principal hazard of the area since they affect the urban area damaging road networks and buildings. Landslide initiation is mainly related to intense or prolonged rainfall.

Geostructural discontinuities notably influence the occurrence of gravitational phenomena involving rock masses, such as falls, topples and planar slides. Rockfalls and topples affect steep artificial slopes around the main infrastructures (Miele et al., 2021). In fact, these phenomena mainly occur where anthropogenic actions have caused cuts linked to the construction of infrastructures. The high slope angles represent an essential element in favouring translational slides (Raso et al., 2021), whose action is often enhanced by diffuse and/or concentrated erosion.

2.3.2 Susceptibility analysis

Considering the mapped landslides and various predisposing factors (and defined covariates), the landslide susceptibility was estimated using a machine-learning algorithm (Lombardo et al., 2016, Di Napoli et al., 2020b, 2021).

From this perspective, eleven covariates namely, i) Slope Steepness (Zevenbergen y Thorne, 1987); ii) Eastness (Lombardo et al., 2020); iii) Northness (Lombardo et al., 2020); iv) Planar and v) Profile Curvatures (Heerdegen y Beran, 1982); vi) Topographic Wetness Index (Beven y Kirkby, 1979); vii) Relative Slope Position (Böehner y Selige, 2006); viii) Distance to streams; ix) Distance to roads; x) Land Use and xi) Geology were selected (Appendix A.1). Numerical covariates were derived from

a 10×10 m Digital Elevation Model (DEM) resampled from an original 3×3 m DEM. In contrast, categorical covariates, such as Land use and Geology were derived considering available data from the National Institute of Geology and Energy (https://sni.gob.ec; Table 2.1).

Table 2.1: Land use and geological code descriptions.

Land Use		**Geology**	
Code	***Class***	***Code***	***Class***
1	Bare area	1	PT - Tarqui Fm
2	Forest	2	gt - Alluvial deposit
3	Crop	3	PIR - Santa Rosa Fm
4	Moorland	4	PTu - Turi Fm.
5	Urban area	5	MM - Mangan Fm.
6	Shrub vegetation	6	MB - Biblian Fm.
7	Water course	7	Da - Alluvial deposit
8	Corn cultivation	8	ML - Loyola Fm.
9	Natural grassland	9	De - Colluvial deposit
		10	Kc - Celica Fm.
		11	MAz - Azogues Fm.
		12	Tv - Travertine
		13	T - Fluvial terrace
		14	QLI - Llacao Fm.
		15	Dc - Colluvial deposit
		16	K7 - Yunguilla Fm.
		17	Av - Varvada clays

The abovementioned covariates were tested for multicollinearity, which represents the occurrence of high intercorrelations among two or more independent variables. When collinearity issues arise, the concerned variables should be removed because they imply a redundancy in a model (James et al.). The Variance Inflation Factor (VIF), by using the R *usdm* package (Naimi et al., 2014), was employed to test multicollinearity. As a rule of thumb, a VIF value that exceeds 5 or 10 indicates severe issues (James et al.).

Landslide susceptibility was assessed using the MaxEnt modelling algorithm (Elith et al., 2011). MaxEnt is a Presence-Only (PO) spatial distribution method that addresses only locations where landslides are

present (Zhao et al., 2022). It makes use of occurrence data and a large (typically 10,000) number of points throughout the study area, which are referred to as background points. To reconstruct the potential distribution of an event, MaxEnt calculates two probability densities: for all presence and background points (Guillera-Arroita et al., 2014). The resultant probability occurrence map anges from 0 (no landslide probability) to 1 (highest landslide probability).

Since MaxEnt predictions are sensitive to initial modelling settings (Merow et al., 2013), different MaxEnt implementations were evaluated through the *ENMeval* R package (R Core Team, 2021) to detect the settings that optimize the trade-off between goodness-of-fit and overfitting (Muscarella et al., 2014). In fact, in MaxEnt it is possible to set up two main parameters: 1) feature classes and 2) regularization multipliers (for further details consult Elith et al. (2010) and Merow et al. (2013). For the analysis, regularization values between 0.5 and 10, with 0.5 steps were investigated, and the following feature classes were considered: linear, linear + quadratic, hinge, linear + quadratic + hinge, linear + quadratic + hinge + product, and linear + quadratic + hinge + product + threshold (Muscarella et al., 2014).

Model evaluation was executed using a spatial block cross-validation scheme (Muscarella et al., 2014). This method converts part of the occurrence and background points into evaluation bins and uses them to reduce the spatial - autocorrelation between training and validation points (Hijmans, 2012, Wenger y Olden, 2012). The block cross-validation scheme was able to assess model transferability, i.e., the ability to extrapolate predictions into new areas (Roberts et al., 2017) and to penalize models based on meaningless predictors (Fourcade et al., 2018).

Because no consensus currently exists regarding the most appropriate metric or approach to evaluate the performance of models (Fielding y Bell, 1997, Peterson et al., 2011, Warren y Seifert, 2011), different statistical approaches were adopted for the models' predictive performance with presence-background data (Muscarella et al., 2014). In this case, the best model reliability-combination was chosen following three criteria: i) the lowest delta Akaike Information Criteria (ΔAIC_c) (Hanley y McNeil, 1982), ii) the Area Under the Curve plot based on the training

data (AUC_{train}) (Hanley y McNeil, 1982) and iii) the difference between training and testing AUC (AUC_{diff}) (Warren y Seifert, 2011).

Moreover, the Landslide Ratio of each predicted landslide susceptibility class (LR_{class}) was employed as a further performance evaluation of the landslide model. The LR_{class} formula is as follows (Eq. 2.1):

$$LR_{class} = \frac{\%\ of\ contained\ sites\ in\ each\ susceptibility\ class}{\%\ of\ predicted\ landslide\ areas\ in\ each\ susceptibility\ class} \tag{2.1}$$

This index was developed specifically to deal with situations when landslide boundaries are not available but their locations are known. The advantage of LR_{class} index is to consider both the predicted stable and unstable areas and thus significantly decrease overprediction. A larger value of LRclass corresponds to a lower over-prediction by the model (Park et al., 2013).

Predictive performance estimation is only a partial metric of model goodness. Predictor contributions represent a further key step that should be assessed to comprehensively estimate the validity of a model. In this contribution, the investigation has been carried out considering 1) predictor importance and 2) percentage contribution (Oke y Thompson, 2015). Predictor importance represents the degree to which single environmental variables are contribute to the final model so that the percentage contributions for all predictors in a model sum to 100% (Phillips y Dudík, 2008). A large permutation importance decrease indicates that the model depends heavily on that variable (Phillips, 2017). A very useful and detailed explanation was given by Bradie y Leung (2017).

2.3.3 Electricity supply contract analysis

The exposure and the relative landslide risk evaluation was completed by considering the population as the element at risk. To account for population growth, a multitemporal assessment was executed

considering data representative of the population distribution in the study area in 2010, 2018, 2019 and 2020 (the only available years). Although population data and their future projections are available in absolute terms for the city of Cuenca, the spatial distribution in the parishes that form the city of Cuenca is not available. Such data are notoriously essential in any landslide risk evaluation. To provide proxy data on inhabitant allocation, the distribution of energy supply contract data derived from the IERSE (Instituto de Estudios de Régimen Seccional del Ecuador - Institute of Studies on the Sectional Regime of Ecuador, http://ierse.uazuay.edu.ec/), were used. Although it does not correspond to the number of people living in each sector of the city, the utilities' availability (i.e., energy supply contracts) was exploited as a proxy of the population and can be considered as alternative data from a relative risk assessment perspective. Energy supply contract data consist of georeferenced points corresponding to different address and therefore to a different housing unit. Each point correspond to a single unit and the potential of such data is related to their public availability. For each parish such information was aggregated and associated with the specific area and used for relative risk evaluation. Figures 2.4a-d depict the distribution of such data at the parish scale between 2010 and 2020 while their variation in comparison with the year 2010 is showed in Figures 2.4e-g.

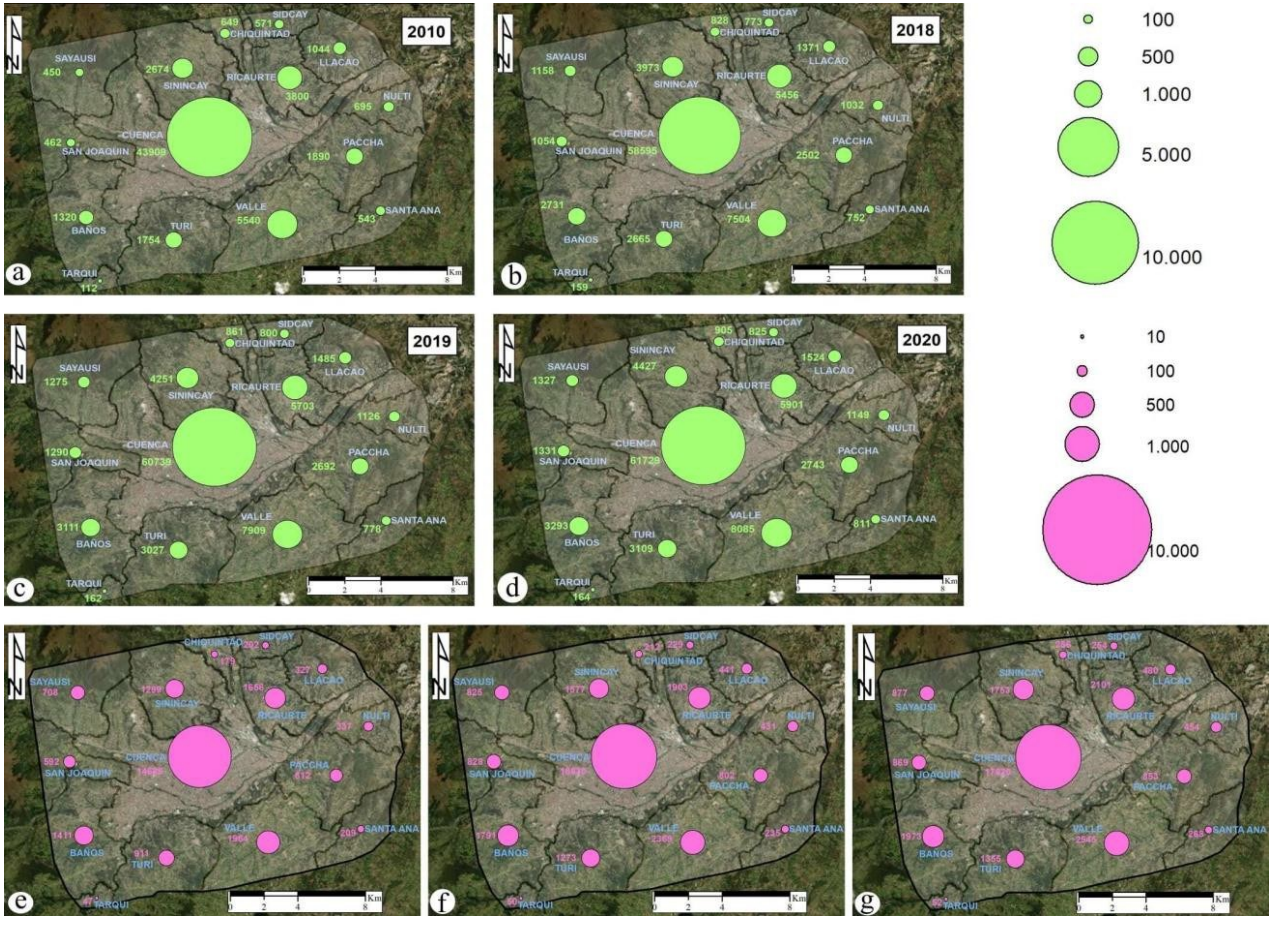

Figure 2.4: a), b), c) and d) Evolution of multitemporal parishes via analysing energy supply contracts from 2010 to 2020; e), f) and g) variation in energy supply contracts, in 2018, 2019 and 2020, respectively, compared to 2010.

2.3.4 Exposure and relative risk analysis

Considering the risk definition introduced by Varnes (1984) as "the expected number of lives lost, persons injured, damage to property and disruption of economic activity due to a particularly damaging phenomenon for a given area and reference period", landslide risk can be assessed qualitatively (Wang et al., 2013) or quantitatively (Chang et al., 2021). Generally, for a wide area, where the quality and quantity of available data are inadequate for quantitative analysis, a qualitative risk evaluation may be more appropriate (Andrejev et al., 2017). In presence of data that might support a simplified quantitative exposure estimation, the relative risk could be assessed. In the context of the proposed analysis, data from susceptibility analysis and energy supply contracts, and their variations between 2010 and 2020 (i.e., 2010, 2018, 2019 and 2020), were used as a basis for multitemporal landslide exposure evaluation and risk estimation over the study area. The evaluation was completed by considering only the risk for people, so that exposure analysis accounted for people distribution.

For the city of Cuenca, the use of energy supply contracts as a proxy of people distribution fits the choice of evaluating the multitemporal exposure and landslide risk in a relative manner. Indeed, while exposure analysis is completed considering the distribution of elements at risk for each landslide susceptibility class, relative risk is estimated using the matrix of Figure 2.5 which relate susceptibility to landslide and exposure (Andrejev et al., 2017). The outcomes of exposure analysis were expressed in the form of histograms, representing the number of energy supply contracts located in each susceptibility class. The histograms were obtained by using the Sturges method (Sturges 1926), which highlights how different Cuenca sectors underwent an increase in contracts over time and, therefore, also in

	Susceptibility				
Exposure	S1	S2	S3	S4	S5
E1	**Very low**				
E2		**Low**			
E3			**Medium**		
E4				**High**	
E5					**Very high**

Figure 2.5: Matrix used for relative landslide risk analysis of the city of Cuenca.

exposure. For the relative risk estimation, a matrix-based approach, allowing to determine a specific risk class for each association of susceptibility class and exposure class, was adopted. Specifically, a 5 by 5 classification matrix (Figure 2.5) was developed accounting for classified exposure data, in terms of concentration in each cell of susceptibility map (see Appendix A.2), through the natural break criterion. Exposure classes considered for the analysis are: E5 - 0 to 1 , E4 - 1 to 2 ,E3 - 2 to 3 ,E2 - 3 to 6, E1- 6 to 11. In particular, in this analysis was employed last available information referred to 2020. As a final product, a relative risk raster map (10 m single sided pixel dimension) was produced. In the context of this analysis the vulnerability was implicitly considered equals to the unit.

2.4 Results and discussion

2.4.1 Multicollinearity examination

Table 2.2 shows the results of multicollinearity analysis carried out through VIF estimation and its comparison with a predefined threshold value. In this regard, it must be noted that there is no unequivocal and approved threshold in the scientific literature. However, it is generally accepted that VIF values higher than 10 indicate severe collinearity (Hair et al., 2010), even though this rule of thumb lacks a theoretical basis (Gómez et al., 2016).

The employment of many environmental covariates might lead to overfitting problems, but, in this work, the individual predisposing factor values differ considerably from the aforementioned threshold. Based on Table 2.2, the highest VIF value is 2.02, corresponding to the Topographic Wetness Index, while the smallest VIF values are 1.01 and 1.02, which are associated with Northness and Eastness, respectively. Accordingly, there are no environmental variables that exceed the critical value, and thus, these results satisfy the criterion (VIF < 10) indicating that there is no multicollinearity among the landslide PFs.

Table 2.2: Multicollinearity analysis for the landslide environmental factors.

Environmental Variables	Slope steepness	Eastness	Northness	Planar curvature	Profile curvature	Topographic Wetness Index	Relative Slope Position	Distance to stream	Distance to road
Variance Inflation Factor	1.72	1.02	1.01	1.39	1.30	2.02	1.39	1.12	1.19

2.4.2 Landslide susceptibility

Figure 2.6 shows the landslide susceptibility analysis outcome subdivided into five classes through Natural Breaks classification (Jenks, 1967). This is accomplished by seeking to reduce the standard deviation within each class and maximizing that between the classes themselves (Basofi et al., 2018, Novellino et al., 2021). The percentage of susceptibility classes is summarized in Table 2.3.

As shown by the map, the most susceptible areas in Cuenca are located on mountainsides that border the city. In these portions, slopes are steep and concave, and roads create local discontinuities. The central part of the map is characterized by very low and low susceptibility zones and represents the Cuenca urban area located in the plain which is characterized by the presence of alluvial deposits and different terrace orders. Along the *Tomebamba* riverbanks, as well as of the other rivers of the area, due to their erosive action that affects the foot of the slopes, there are sectors predisposed to landslides with a medium to very high susceptibility. Periurban and rural areas, instead, are in medium- to very high-susceptibility areas where there are steeper mountainsides.

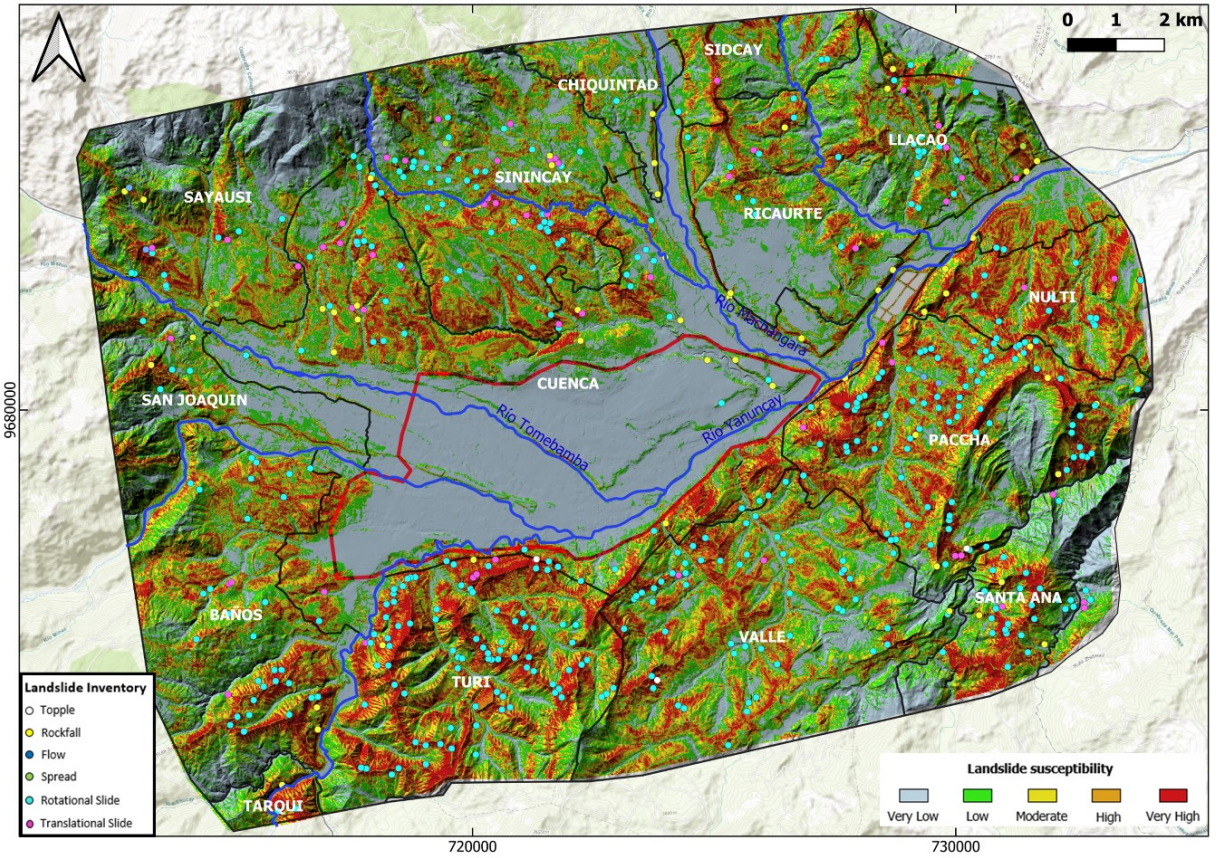

Figure 2.6: Map showing landslide susceptibility classes and inventoried landslides in the study area. Landslides are represented by points (data source modified from Miele et al. (2021)). Parishes boundaries are shown by black artworks.

Table 2.3: Summary of MaxEnt outcomes in landslide simulations.

Susceptibility classes	**Landslide site (a)**	**% of landslide site (c)=a/b**	**% of predicted area (d)**	**LR_{class} (e) = c/d**	**% of LR_{class} = e/f**
Very low	14	3.0	30.6	0.1	1.4
Low	44	9.4	23.9	0.9	5.3
Moderate	63	13.5	19.4	0.7	9.4
High	118	25.2	15.5	1.6	21.9
Very high	229	48.9	10.6	4.6	62.0
Sum	468 (b)	100	100	7.9 (f)	100

2.4.3 Susceptibility model validation

According to Swets (1988), the obtained models achieved fair- to- good predictive performance, with AUC values ranging from 0.763 to 0.866 (Figure 2.7). The lower value is associated with models with linear or linear + quadratic features and high regularization values (i.e., 9.5 and 10). The higher value is associated with a model that contains all features and low regularization values (i.e., 0.5 and 1).

AUC_{diff} values scored from 0.06 to 0.14. Among the resulting 120 combinations, the one reporting the lowest ΔAIC_c was chosen. The selected model is characterized by the following: linear + quadratic + hinge + product + threshold features, AUC value of 0.82, average AUC difference value of 0.08 and ΔAIC_c value equal to 0 (for further information, refer to Appendix A.3).

The LIM availability allows an assessment of the model performance that considers field data. By Intersecting the landslide detachment points and the final susceptibility map, it is possible to achieve information about the number of landslides and their distribution into each different landslide susceptibility class. Subsequently, the areal extent of the susceptibility classes was calculated. Areas characterized by high and very high susceptibility involve 15.5% and 10.6% of the total

study area, respectively (Table 2.3). Very low and low susceptibility classes cover approximately 55% of the study area, particularly in the central sectors, namely, Cuenca city. The remaining portions are assigned to the moderate (19.4%) class. Moreover, the highest concentration of landslides can be found within the highest susceptibility class values (high, 25.2%, and very high, 48.9%).

In addition, approximately 3% are in the very low susceptibility class and the remaining 22.9% are distributed in the low class (i.e., 9.4%) and moderate class (i.e., 13.5%). The last column of Table 2.3 highlights the LR_{class} percentage for each susceptibility class. The highest LR_{class} value corresponds to the very high susceptibility class and more than 80% are in the high and very high susceptibility classes. This evidence roughly implies that, if a landslide occurs, then the predicted susceptible area has approximately an 80% chance of including the landslide itself.

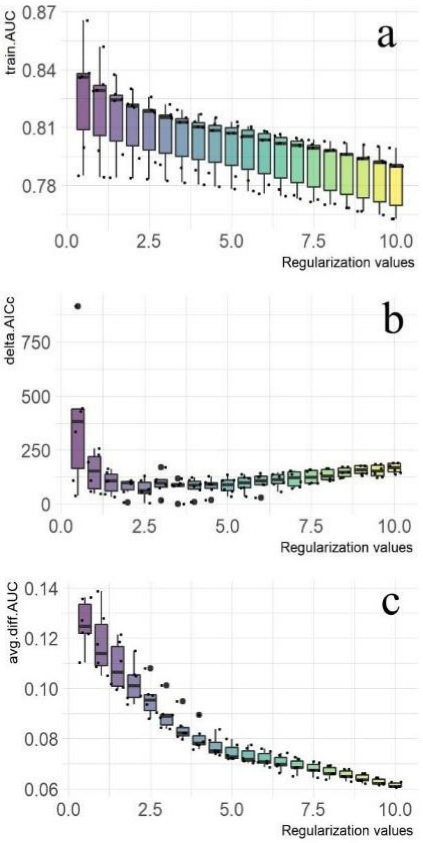

Figure 2.7: a) Boxplot of AUC training data (AUC_{train} - train.AUC); b) lowest difference between the best model and every other model in the dataset (ΔAIC_c - $\Delta AICc$); c) difference between the training and testing AUC (AUC_{diff} - avg.diff.AUC).

The spatial aggregation of the susceptibility map confirmed that the largest part of the study region has a low susceptibility to landslide events. Approximately the 75% of

actual landslides were localized in the high and very high susceptibility classes. Moreover, the higher susceptibility classes showed higher values of LR_{class} percentages. These outcomes show significant quantitative agreement between the simulated scenario and the landslide inventory map. All the produced analyses permit zoning of the complex territory of the Cuenca area to identify the spatial probability of landslide initiation in areas characterized by specific conditions that materialize by the considered environmental variables. Moreover, landslide density is characterized by an increasing trend when passing from the lowest to the highest classes of susceptibility. These observations underline that, despite the limited area extension of the very high susceptibility class, most of the surveyed landslides are within the latter.

2.4.4 Factors predisposing slope instability

As the last outcome, the variables' contribution was evaluated. This result allow us to understand which variables have greater importance in the final models' implementation. Table 2.4 presents the impact of each variable. In particular, the results reveal that the main conditioning variables (i.e., the variables that assume a fundamental role in the final landslide susceptibility) are slope steepness, distance to roads and planform curvature. Therefore, a model with a higher fit is achieved through the aforementioned variables. In general, when the percent contribution is observed, a good spread of values is desirable. Conversely, if the contribution of a variable is high in the model (i.e., higher than 70%), something is not correct and that variable is not encompassing many variations or is correlated with other variables. Other variables, such as distance to streams, land use, geology and relative slope position show noteworthy values in the model. Last, low values close to zero are assigned to eastness, northness, profile curvature and the Topographic Wetness Index.

Primary roles in slope stability are related to slope steepness, which influences water infiltration and modulate gravity force (Huat et al., 2006). Particular conditions are related to the presence of road cuts, where steep slopes and slope unloading related to the excavations for

the roads construction that influence slope stability. An additional fundamental covariate contribution to the slopes' stability of this area is represented by the planar curvature that adjusts the convergence or divergence of water in the direction of landslide movement and landslide material (Ohlmacher, 2007). Furthermore, in the Cuenca territory, hillsides with low planar curvature values are the most susceptible to earth and debris flows and earth and debris slides. Indeed, this factor is used to identify gullies (Wieczorek et al., 1997), and debris flow initiation areas can be recognized where the curvature values are negative (Park et al., 2016). Finally, other important predisposing factors to slope stability are geology and land use (e. g. Glade (2003), Cevasco et al. (2014). Unconsolidated material, such as alluvial and colluvial deposits or pyroclastic lithologies derived from the near volcanic activity, covers the surrounding mountainous landscape, resulting in a very high susceptibility to sliding.

Table 2.4: Variable contribution values of environmental factors.

Environmental Variables →	Slope steepness	Eastness	Northness	Planar curvature	Profile curvature	Topographic Wetness Index	Relative Slope Position	Distance to stream	Distance to road	Geology	Land use
% contribution	26.6	1.7	0.1	19.5	0.8	0.2	6.1	6.0	20.3	9.1	9.4
Permutation importance	26.6	0.7	0.4	15.7	0.8	0.1	1.5	5.5	26.6	8.2	10.6

2.4.5 Exposure and relative risk assessment

Figure 2.8 provides an overview of the exposure in each parish updated to 2020 (i.e. number of energy supply contracts for each susceptibility

class). In this way, the parishes with higher exposure to risk were identified. As observed from the inset graphs, the exposure is higher in boroughs that surround the southern portions of Cuenca, namely *Turi*, *Santa Ana*, *Tarqui*, *Nulti*, *Baños* and *Paccha*. Such boroughs show a higher number of energy supply contracts (i.e., element at risk) in high and very high landslide susceptibility classes. In Contrast, the northern sectors of the study area report a lower number of energy supply contracts included in the higher landslide susceptibility classes. Last, the central portion of the study area, in which the city of Cuenca is located is characterized chiefly by very low and low exposure to landslides. However, recently, as shown in Figures 2.4 and 2.8, the city of Cuenca and its neighbouring areas have experienced a substantial demographic increase, which has led to the construction of buildings in notoriously very high susceptibility areas. Similar problems can be easily found in other rapidly expanding cities where the construction of new boroughs occurs in hilly and mountainous areas that are more prone to instability (Di Martire et al., 2012). This condition is evidenced by the high number of energy supply contracts falling in the highest susceptibility classes.

Since the city has experienced a consistent growth of population between 2010 and 2020 (Figure 2.4), with a sustained occupation of peri-urban hilly areas characterized by higher susceptibility in comparison to the centre of the city, a detailed exploration of the spatial and temporal rates of change for both energy supply contracts and related exposure for each parish is reported in Figure 2.9. In particular, in Figures 2.9, graphs "a" highlights energy supply contracts for each landslide susceptibility class, yielding the percentage of the change in the exposure to landslides from the reference year 2010 to 2020 (i.e., 2018, 2019 and 2020), while the same rates in terms of the total exposure (i.e., normalized to the total 100%) are given in graphs "b". In addition, the relative areal extensions of different susceptibility classes are also reported on graph "a" (violet bar). In the reference period, the parishes of *Sayausi*, *San Joaquin*, *Tarqui*, *Sidcay*, *Baños*, *Ricaurte*, *Paccha* and *Chiquintad* experienced a higher increase in energy supply contracts located in the very high susceptibility class corresponding to an increase in the exposure to landslides (Figure 2.9). Such an increase, in comparison with 2010, ranged between 33% of Paccha and 300% of *Sayausi*. Conversely, the

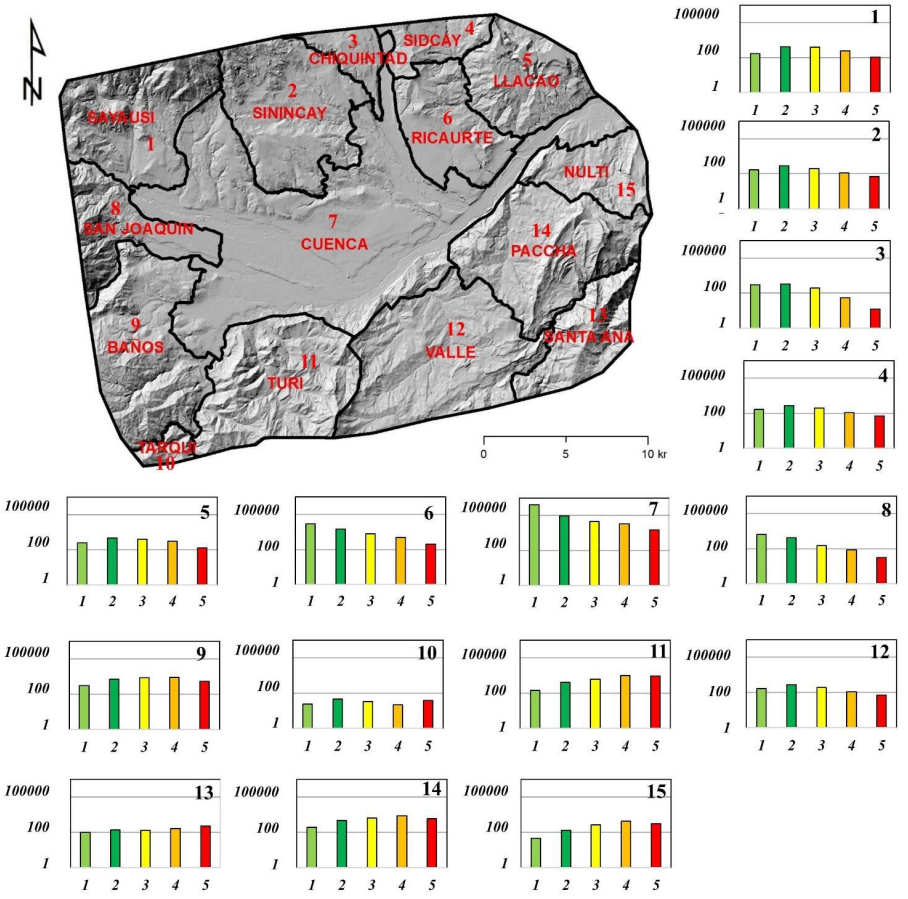

Figure 2.8: Landslide exposure analysis outcome. The graphs, on a logarithmic scale, highlight the energy supply contract numbers for each susceptibility class (1: very low; 2: low; 3: moderate; 4: high; 5: very high) in each considered parish. The numbers in the upper-right corner of the graphs represent the parishes of the studied area.

parishes of *Turi*, *Nulti*, and *Cuenca* experienced a higher increase in energy supply contacts located in the very low to medium susceptibility class. Such an increase, in comparison with 2010, ranged between 20% of Cuenca and 100% of *Nulti*.

However, in absolute terms, the districts of *Tarqui*, *Turi*, *Nulti* and

Santa Ana show the highest exposure, with the highest number of energy supply contracts located in high susceptibility areas between 2018 and 2020. Conversely, the boroughs of *Sayausi*, *Sidcay*, *Ricaurte*, *Cuenca* and *Chiquintad* show the lowest exposure, with the lowest number of energy supply contracts located in high susceptibility areas in the same period. In the Appendix A.2, it is possible to consult the tables that quantitatively represent the graphs shown in Figure 2.9.

Figure 2.10 depicts the outcome of the relative risk estimation in the form of a risk map. It shows five classes of landslide risk for the studied area. Especially, the centre of Cuenca city is located within a very low risk zone because of a the significant number of buildings and infrastructures built up in a flat area characterized by very low landslide susceptibility. However, some areas with higher landslide risk correspond to the banks of the rivers that pass through the historic centre of the city. Overall, the low-risk class (green pixels) is observable in correspondence of low inclined slopes of the hills surrounding Cuenca where the landslide susceptibility is generally low. On the other hand, steep slopes are generally characterized by medium to high degrees of landslide susceptibility. In these areas, the analysis pointed out a large number of energy supply contracts and, consequently, a final estimates of elements at risk. These slopes are generally colored with orange and red pixels indicating the high to very high risk. In particular, the Southern sector of the study area is characterized by the highest relative landslide risk.

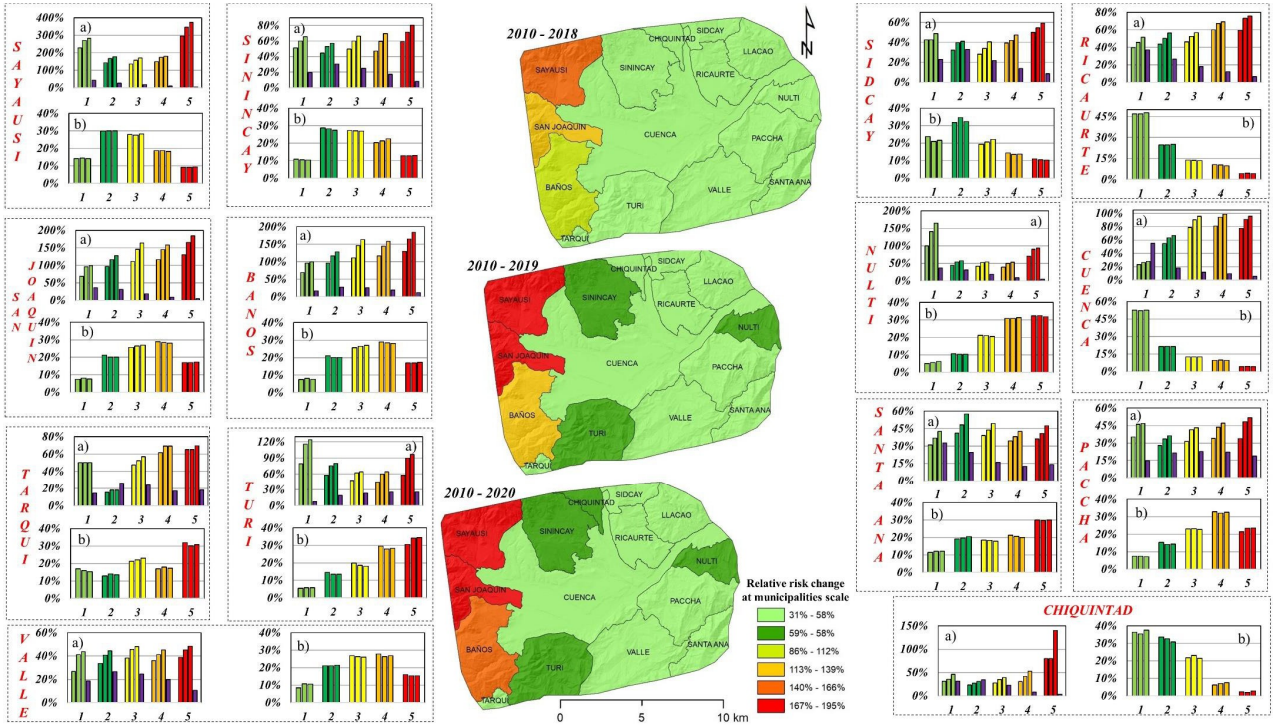

Figure 2.9: Multitemporal evolutionary perspective of exposure to landslides from 2010 to 2020. Graphs "a" highlight the variation, in percentage terms, of the energy supply contract for each landslide susceptibility class for the considered years (i.e., 2018, 2019 and 2020); graphs "b" represent the same rate in terms of relative risk, namely, normalized to the total, i.e., 100%. The coloured bars of the histograms indicate the different susceptibility classes ranging from very low to very high, and the violet bar, included in histogram "a" specifies the landslide susceptibility class areal extent. In the middle, maps of relative risk change for each parish of the study area are given during the time span considered.

In the last decade, landslide susceptibility analyses have also been conducted in emerging and developing countries (O'Hare y Rivas, 2005, Klimeš y Rios Escobar, 2010, de Luiz Rosito Listo y Carvalho Vieira, 2012, Jamalullail et al., 2021). Several attempts have been made to estimate landslide risk in various contexts where demographic growth is very pronounced (de Luiz Rosito Listo y Carvalho Vieira, 2012, Rahman, 2012, Rojas et al., 2013, Alcántara-Ayala y Moreno, 2016). Considering the high growth rate recorded in the last few years, it is appropriate to assess the exposure of the landslide risk over time. This type of analysis makes it possible to identify the most critical areas and sectors of the city of Cuenca in terms of risk evolution due to population growth. The outcome of the analysis represents a significant land planning tool for the definition of urban occupation plans, land-use recommendations, and mitigation protocols that should be applied to reduce the impact of a landslide occurring in urban areas (Klimeš et al., 2020, Sultana y Tan, 2021). The problem of landslides involving settlements and claiming human lives is of particular significance in low- to mid-income countries because people are often concentrated in high-hazard urban areas and vulnerability factors, such as poor building of housing, poor governance, the lack of experience in facing natural disasters and the absence of early warning systems, consistently exacerbate landslide impacts (Petley, 2012a, Zorn, 2018, Aguirre-Ayerbe et al., 2020).

This qualitative procedure for evaluating the landslide exposure in Cuenca attempts to provide information for risk assessment, which is useful in a preliminary stage of regional planning or for more detailed studies on high-exposure areas. Therefore, the procedure proposed in this study can be implemented when not all the information that is useful for risk assessment is attainable. Exposure quantification, which is a basic input in spatial and risk reduction planning, is the main objective of this study. It is important to mention that, as not all the information is available, landslide risk values are not expressed in absolute terms, but relative landslide risk may be a good proxy for districts that have encountered, in the last decade, a population growing into very high-risk territories. Notwithstanding the limitations, this study has allowed us to estimate which areas are more prone to instability, which areas have a high relative landslide risk and to establish future risk by consulting the trends in the different parishes.

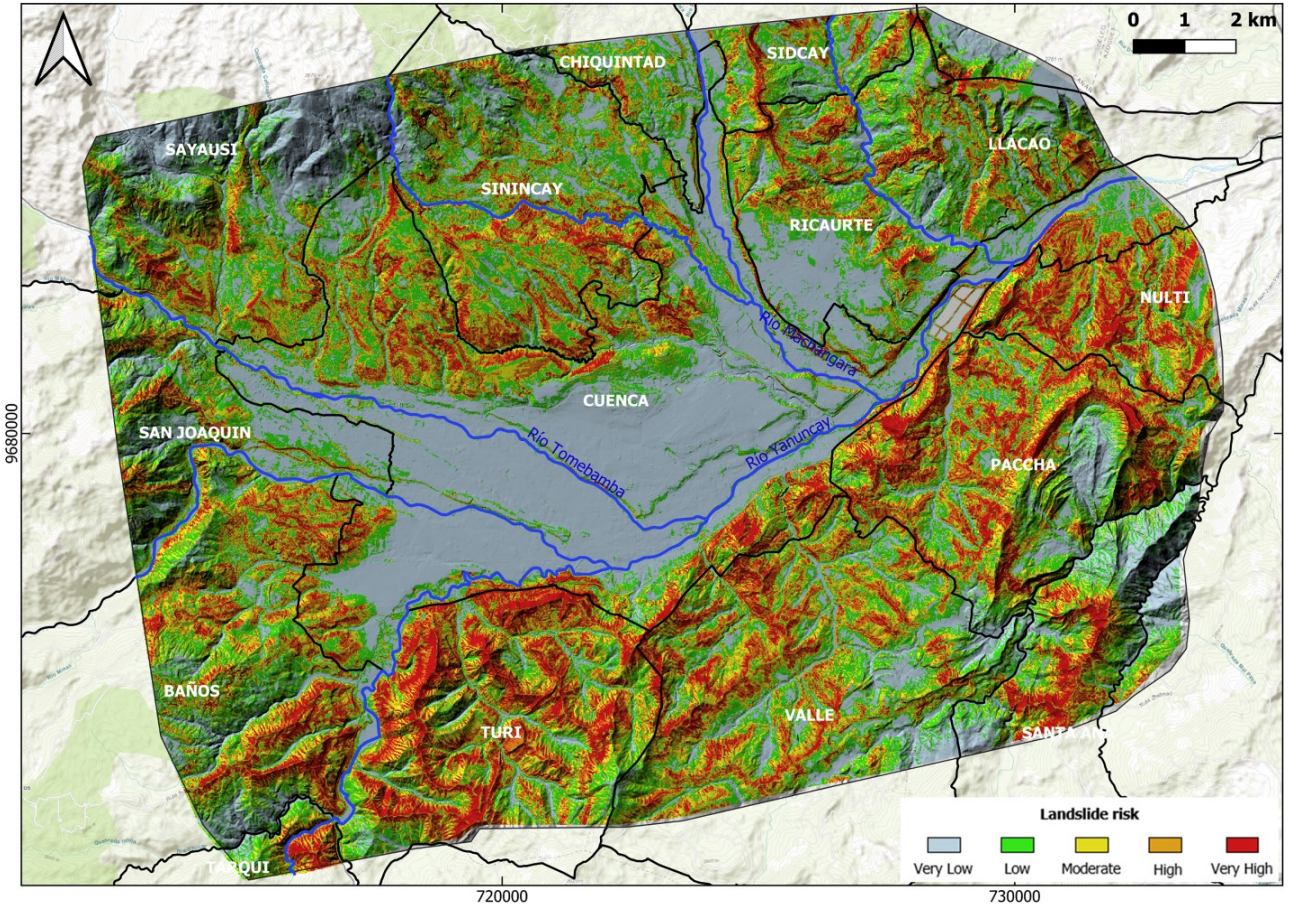

Figure 2.10: Landslide relative risk map (10×10 m) derived by the proposed procedure. The exposure map representing the density of energy supply contracts in 2020 used in the final relative risk map creation was included in Appendix A.4.

2.5 Conclusions

In this paper, an analysis of the exposure to landslides, its multitemporal variation between 2010 and 2020, and related relative risk for the city of Cuenca in Ecuador (Latin America) has been presented. This study provides insights into important issues, such as *i)* the effect of the sustained expansion of urban areas due to population growth on landslide exposure variation and *ii)* the reduced complexity method of risk assessment in the presence of partial data only (i.e., landslide susceptibility rather than hazard, and energy supply contracts rather than population distribution or exposure). The results indicate that the current higher exposure and related relative risk is estimated for districts located in the southern sector of the study area (i.e., *Turi*, *Baños*, *Santa Ana*, *Nulti*, *Tarqui* and *Paccha*). In addition, by carefully observing the study area is possible understand how most boroughs of the city are located in the hilly areas that bound the centre (i.e., *Sayausi*, *San Joaquin*, *Tarqui*, *Sidcay*, *Baños*, *Ricaurte*, *Paccha* and *Chiquintad*); these boroughs, which are experiencing sustained population growth, could be exposed to an increased risk with a sustained growth trend. This is also connected to the overall high vulnerability of settlements that, in many cases, is related to the presence of modest buildings and the absence of early warning systems.

The obtained results can be considered a relevant tool for future land planning in the town of Cuenca, despite their resolution, being limited to the parish area. The proposed method, using potentially available data for mid- and low-income countries (i.e., landslide inventory and a proxy of population distribution), has the potential to be applied in many contexts where a minimum dataset is available or can be developed on the basis of either field or remotely sensed data. The results of the risk analysis are useful for ranking the parishes based on increasing risk and for supporting decision-makers in prioritizing funding for risk mitigation measures.

CHAPTER 3

An integrated approach for rockfall susceptibility assessment along linear infrastructure in Cuenca (Ecuador)

Rockfalls are considered the major hazard in mountain areas worldwide partly because of their direct consequences on the territory and the population. Rockfall susceptibility mapping is critical both for the previous evaluation of the impact of the implementation of infrastructures and to establish, a posteriori, restrictions in relation to land use around these areas, with the main purpose of preventing the loss of human lives and tangible property. Thus, in this research, a novel hybrid approach based on the trajectory count per grid cell produced by QPROTO tool is developed and used to calculate the rockfall susceptibility. Then, the susceptibility results are used for various purposes: 1) to identify rockfall source points; 2) to evaluate the rockfall susceptibility, 3) to classify the physical consequences of rockfall events on Molleturo road, and 4) to analyze the DEM resolution influence on the accuracy of results. The DEM resolution effect on the results was not unique: the use of coarse DEM resolution is the most appropriate for the identification of source points (accuracy $\approx$ 84%), while the DEM_{10m} allows obtaining the best precisions in the elaboration of susceptibility maps (AUC = 0.75 for all rockfall and AUC = 0.88 for small rockfalls). The results of this study are a valuable help to local authorities since they will allow them to design mitigation measurements, develop slope monitoring plans and increase highway user safety and the local population resilience.

Keywords: MARLI rockfall inventory, QPROTO, rockfall source points, CART analysis, rockfall vs. subsidence.

3.1 Introduction

Landslide detection, inventory, susceptibility, and hazard zoning examples have been present since the 1970s. Within the last few decades, different techniques and maps have been used to represent the cartographic location and distribution of landslides (Parise, 2001). Various information sources, types, scales, and mapping techniques are available, so there is implicit knowledge needed to fulfill landslide detection and inventory development. The scope and scale of how to communicate susceptibility and hazard information are predominant requirements of the end-users; this is, decision makers or people directly affected by natural or anthropic events of this type. Landslide inventory maps are essential to assess landslide susceptibility and analyze slope stability. Remote sensing techniques play a crucial role in natural disasters in terms of quick response and mitigation. Optical satellite images can provide visual data to construct landslide inventories (Guzzetti et al., 2012). However, landslide inventory maps produced by traditional methods such as aerial photograph interpretation, topographic map analysis, and fieldwork are frequently subjective and incomplete. Some of the first scientific approaches to using spatial data in a digital context for landslide detection and inventory are in California (Brabb et al., 1972) and Italy (Carrara et al., 1977). Currently, most landslide susceptibility research uses digital tools such as Geographic Information Systems (GIS) and remote sensing data acquired from active or passive sensors (Metternicht et al., 2005, Niethammer et al., 2012). Knowing this, it is intuitive to the type of spatial analysis that can be undertaken; a clear example is one stated by Van Westen (2004), where the author proposes a complete schematic view for landslide risk management.

Unlike other types of landslides, rockfall events are commonplace geomorphological processes that often arise when infrastructure is developed. The rockfall phenomenon, represents a major hazard in mountain areas worldwide and a major threat to infrastructure, transportation lines, and people, is unpredictable, fast, often punctual, and involves small volumes with high energy and long runout distances

(Cignetti et al., 2021, Leine et al., 2021). The characteristics of these phenomena, which make it difficult to develop methods for their prediction and modeling of their behavior, together with the difficulty in capturing data and modeling the terrain in mountainous and inaccessible areas; the technical complexity of the layout of communication routes in these areas; and the territorial dynamics characterized by the colonization of these infrastructures, transform them into extremely dangerous and harmful events, with consequent human lives and economic losses. Despite their often relatively small size, rockfalls are among the most destructive mass movements (Guzzetti et al., 2002). Determining mechanisms to predict and model these phenomena are essential to design mitigation measurements, developing slope monitoring plans, and increasing highway user safety and local population resilience.

As in other disciplines, the advances in geometry, which made possible the development of reference systems; advances in cameras and the development of Global Positioning Systems (GPS); the development of aviation and remote sensing; the Internet and advances in the field of information technology, computing, and mobile devices... have provided us with a new point of view of the world, revolutionizing both the way of capturing it on a plane, as well as the type of data used to achieve it, as well as the methods used to acquire the latter and extract information from them. This democratization of information and knowledge puts within our reach the possibility of adopting the role of creators of tools for the registration, generation, or extraction of information beyond the limited role of users that we have maintained for decades. Proof of this is that the availability of various software tools that enable modeling rockfalls at different spatial scales has increased significantly. Thus, the use of algorithms, tools, and software to automatically carry out rockfall simulations in short times with robust procedures has become popular in determining runout distance, jump height, kinetic energy, and impact force and consequently identifying potential rockfall areass (Guzzetti et al., 2002, Dorren et al., 2006, Castelli et al., 2021, Leine et al., 2021). At the same time, these developments have allowed empirical and experimental prcedures to be left behind, as well as simple and computationally efficient 2D models to make way for 3D rockfall simulation with complex shape models. However, despite all

these developments, the availability of free, user-friendly, and easily executable tools that can be integrated with other functions continues to be a pending task. Among the few tools that meet these characteristics is QPROTO. Based on the cone method developed by Jaboyedoff y Labiouse (2011) and implemented by Castelli et al. (2021), this tool identifies the areas that are most exposed to a rockfall phenomenon considering the topography and several empirical parameters. QGIS is a free and open-source Geographic Information System and is widely used in those fields where data processing and visualization with a spatial component are fundamental processes; it is the communication and execution platform that QPROTO uses for its easy use.

The vast majority of methods developed to identify areas susceptible to be affected by rockfalls, including the cone method on which QPROTO is based, require previously identifying the so-called source points. These points are considered the origin of the rockfall and, therefore, the location from which identification of the most exposed areas is carried out in the event of the occurrence of said phenomenon. Usually, those points that correspond to actual source points, identified in the field or by photo interpretation once the landslide has occurred, are used to validate the operation of these methods (Guzzetti et al., 2004, Agliardi et al., 2009, Castelli et al., 2021). Before a rockfall, specific areas predisposed to these phenomena can also be identified in the field and used to predict the area, infrastructures, or buildings that may be affected (Cignetti et al., 2021, Torsello et al., 2022). Frequently, these studies are carried out on a local scale. However, identifying such points is considered a challenge if the intention is to carry out a survey at a medium-large scale (Loye et al., 2009, Torsello et al., 2022), among other motifs, due to the main methods of the rockfall analysis on large areas are designed to be applicable only along previously defined falling profiles (Losasso et al., 2017) or the visual identification of all of the potential source points over a large area would be impossible in a reasonable time (Alvioli et al., 2021). Thus, in these cases, the complexity and characteristics of the methods used to identify source points are directly related to the availability of information and its level of detail. Thus, a relatively widespread and straightforward methodology based on using factors such as the slope, rock properties, distance to roads or urban areas, the combination of several factors or even operational variables

such as the computation time, establishing reference thresholds based on the experience of professionals or analysis of the characteristics of the reference data (Losasso et al., 2017, Miele et al., 2021, Torsello et al., 2022). However, studies where probabilistic or hybrid models are applied, are much less frequent(Fanos y Pradhan, 2018, Rossi et al., 2021). Although the effectiveness of rockfall simulation methods has been demonstrated with these methodologies, more studies are needed to analyze, either based on real data or theoretically, the characteristics of the source points, both to check if the establishment of a simple threshold for their selection is enough and to improve the efficiency of data processing in large areas.

Another of the points to which special attention is paid when using this type of method on a regional scale is the data sets used. In this regard, the Digital Elevation Model (DEM) is one of the essential data used in rockfall susceptibility mapping, and choosing the appropriate level of detail, that is, the spatial resolution, another of the critical points that influence the correct and efficient identification of rockfall events. Thus, the spatial resolution that provides the best agreement between precision, level of detail, and efficiency can be seen as the ideal resolution. This point is considered even more decisive when using, in large areas, methods whose main data source is this type of model. Thus, in these cases, time and processing capacity can limit the obtaining of results. Previous studies have shown, in some cases solely through indications, that the resolution of DEMs and their influence when identifying landslide events are closely related, among other factors, to the size of these phenomena (Wubalem, 2022), the lateral dispersion of rockfall trajectories due to the terrain's morphology and its level of complexity (Zieher et al., 2012, Bühler et al., 2016, Moos et al., 2018) or even with the method used for its identification. In this sense, few studies have explored the effects of the spatial resolution of DEM on landslide susceptibility mapping (Meena y Nachappa, 2019, Qiu et al., 2022, Wubalem, 2022) and almost non-existent those who have done so in the particular case of the rockfall (Zieher et al., 2012, Bühler et al., 2016, Žabota et al., 2019).

Considering the above and the lack of a useful and updated products for highway safety management from a rockfall risk perspective, our

primary goal is to increase the efficiency and precision of data processing to obtain rockfall susceptibility maps at medium-large scale (wall-to-wall) by combining existing tools and not only by specific areas. For this, in this research

1. A novel hybrid approach that integrates the QPROTO tool and various functions of the R software is applied for automatically identifying the areas which might be affected by rockfall.
2. The factors that characterize the source points are analyzed to increase the efficiency and precision of data processing to obtain rockfall susceptibility maps.
3. A methodology for the differentiation between rockfall and subsidence phenomena in relation to the layout of a communication route is developed.
4. The influence of DEM resolution on the accuracy of the results is analyzed.

3.2 Materials

3.2.1 Study area

The study area is situated in Cuenca canton in the province of Azuay, southern part of Ecuador, between the Andes Mountains, at an elevation ranging from 200 to 4500 meters above sea level (Figure 3.1). This canton covers a surface of about 3190 km^2 and has a lithology characterized by the Tarqui formation (90% of the Molleturo area). The population of this region is in the range of 680,000 inhabitants. The zone presents a changing climate, ranging from persistent droughts to extensive rainfall (precipitation averages 940 mm/year, where December to May are considered months of high precip-itation and June to November are considered dry months), which encourages the oc-currence of landslides.

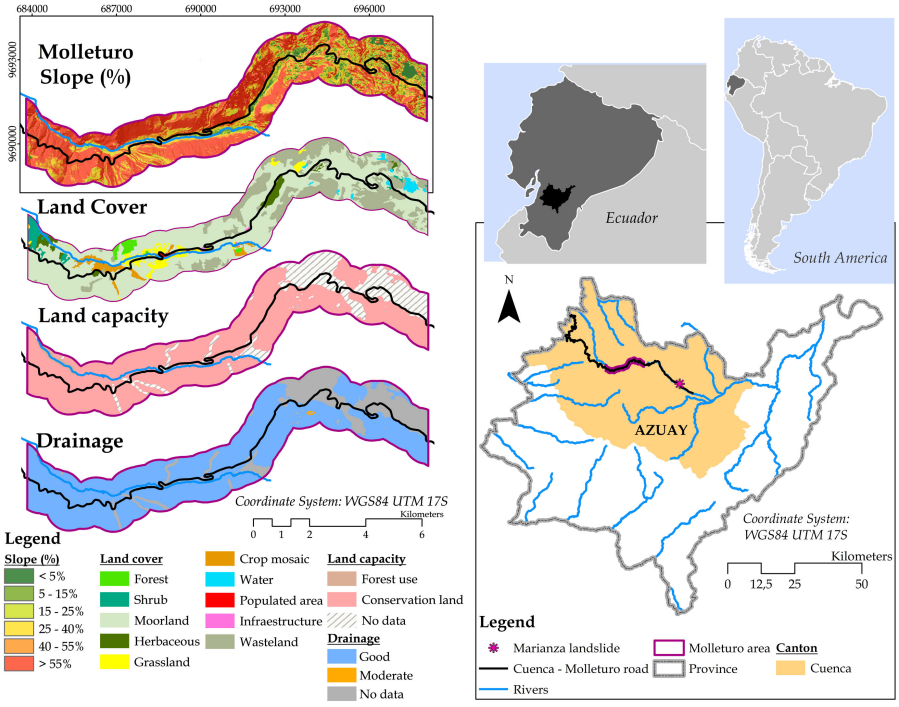

Figure 3.1: Description of Molleturo study area including the slope, land cover, land capacity and drainage maps. The study area is the buffer zones (800 m) (magenta polygon) surrounding the Cuenca - Molleturo (black line) road.

Cuenca - Molleturo road (continuous black line in Figure 3.1), one of the main access routes to Cuenca, is typically affected by landslides, creating problems for the popula-tion and causing the destruction of this infrastructure. The Marianza landslide was the last event in the area (march 2022, magenta star in Figure 3.1), leaving a balance of four victims, with more than 400 displaced people after heavy rains. Considering this back-ground, one section of this road is selected to develop the study presented here. This section is located on the Cuenca - Molleturo road, with a length of 21.7 kilometers. To analyze the potential slope instability, a buffer zone of 800 meters surrounding it was considered (magenta polygon in Figure 3.1). High slopes characterize this area; approx-imately 70% of the surface of the study area has a slope greater than 40%. The "moorland" and "wasteland" covers are the

predominant ones in the Molleturo area (65.3% and 23.8%, respectively), where the majority of the surface is destined for conservation (77.2% of the surface in relation to the of the study area). However, small populated regions (0.4% of the surface), forest plantations and shrub and herbaceous vegetation (1.2%, 2.2%, and 2.4%, respectively) are also present in the study area.

3.2.2 Datasets

3.2.2.1 Field data

Rockfall inventory was created using the MARLI application (Sellers et al., 2021b), and it is employed to assess the rockfall susceptibility results. MARLI was used to record both active rockfalls and events that have taken place in the past, for which there is still physical evidence on the ground. However, the complex terrain of the study makes the recognition and mapping of the rockfall areas highly difficult. For this reason, detailed identification and mapping of these areas have been limited to a few test locations. The registration of the data used in this study took place in August 2022; its characteristics are shown in Figure 3.2.

The rockfalls are recorded as points that represent the foot of the slide. After the field survey, the rockfall's head (source point) is set according to the contour lines, satellite images and the photographs of the rockfall taken in the field, and the area affected by each slide is digitized. Finally, 21 active and historical rockfalls were recorded, which cover a region of around 360 ha, 12.5% of the study area. The active rockfalls account for 52.4% of the total rockfall recorded by MARLI, representing 26% of the total area mapped as areas affected by rockfall. To carry out the rockfall susceptibility assessment, the centroids of the digitized polygons, representing the affected area of each rockfall recorded with MARLI (red and orange polygons in Figure 3.2) were calculated, and the same number of "non-rockfall" points were randomly generated (points located outside said polygons and within the study area). This set of points is considered the validation sample.

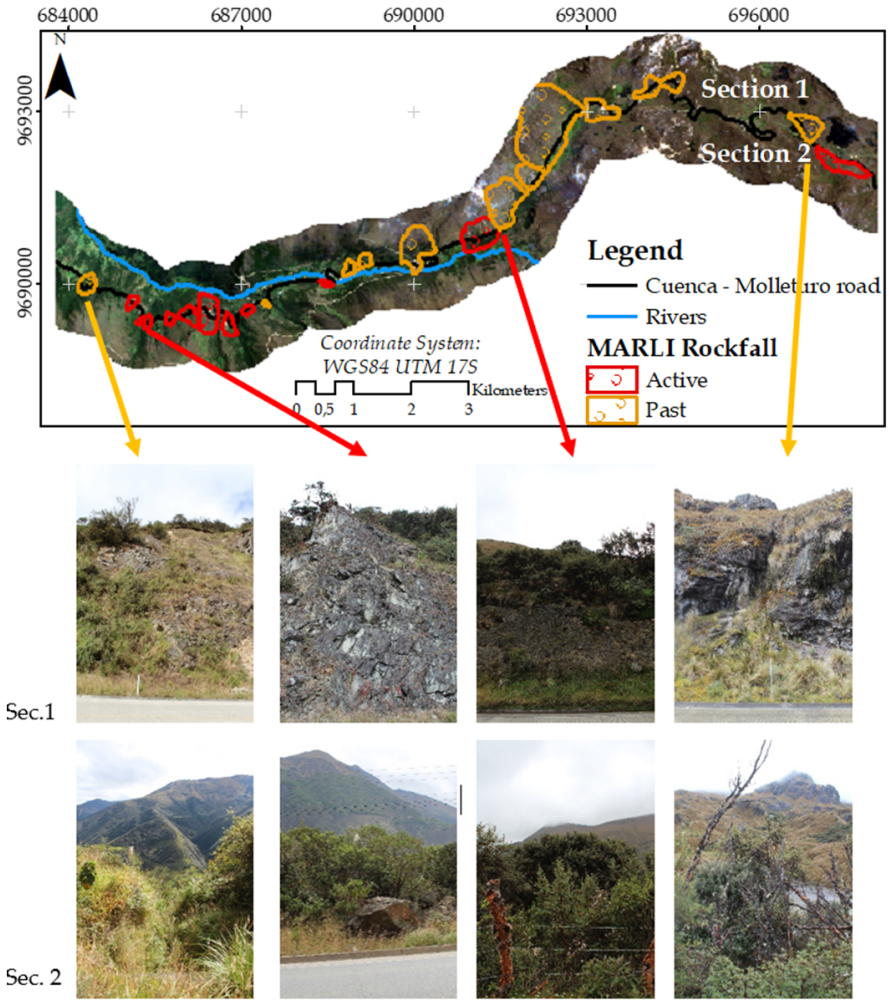

Figure 3.2: Rockfall inventory using MARLI application and photograph examples from the road.

In addition to the data above, photographs were taken to the left and right at different points along the road to validate the results of the classification of conditions, rockfall or subsidence, in its various sections (Figure 3.2).

3.2.2.2 GIS data

The factors considered in this survey to characterize the source points derived from the QPROTO tool and improve the process efficiency are all static factors, i.e., factors that are unlikely to change within a short period of time (Tyoda, 2013). Such factors are described below, and their essential characteristics and data source are included in Table 3.1.

Table 3.1: Characteristics of employed GIS data.

GIS data	**Source**	**Processing software**	**Date**	**Scale Resol.**
Elevation	MAG SIGTIERRAS	—	2014	3 m
Slope (%)	...from DEM MAG SIGTIERRAS	ArcMap 10.8.1. Slope function	2014	3 m
Slope length	...from DEM MAG SIGTIERRAS	QGIS 3.16.16. *LS factor* function	2014	3 m
Curvature	...from DEM MAG SIGTIERRAS	ArcMap 10.8.1. *Curvature* function	2014	3 m
Aspect	...from DEM MAG SIGTIERRAS	ArcMap 10.8.1. *Aspect* function	2014	3 m
TWI	...from DEM MAG SIGTIERRAS	ArcMap 10.8.1. *Raster calculator* function	2014	3 m
TPI	...from DEM MAG SIGTIERRAS	ArcMap 10.8.1. *Raster calculator* function	2014	3 m
Land Use	MAE-MAGAP	—	2009-2015	1:25,000
Drainage	MAG	—	2009-2015	1:25,000
Distance from rivers	...from river layer	ArcMap 10.8.1. *Euclidean direction* function	2013-2014	1:25,000
Distance from roads	...from road layer	ArcMap 10.8.1. *Euclidean direction* function	2013-2014	1:25,000
Distance from urban areas	...from Land Use layer	ArcMap 10.8.1. *Euclidean direction* function	2013-2014	1:25,000
Geology	MAG	—	2009-2015	1:25,000

- *Elevation*: this factor is one of the most commonly used factors for landslide susceptibility mapping because the altitude determines the spatial distribution of landslides, they generally take place at high altitudes, and this factor plays a significant role in both precipitation conditions and vegetation cover types (Pourghasemi y Rahmati, 2018, Pourghasemi et al., 2018, Juliev et al., 2019). The Molleturo area's elevation ranges from 2605 m to 4352 m.a.s.l. with a mean of 3770 m.a.s.l (see Figure 3.3a).

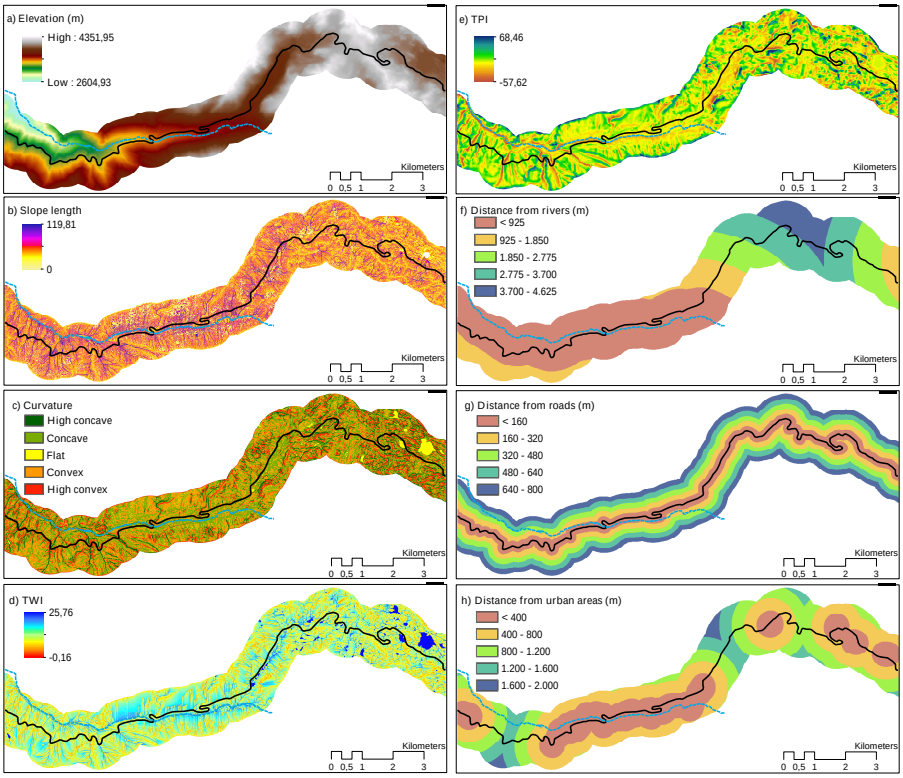

Figure 3.3: Factors used to analyze the rockfall susceptibility mapping: a) elevation, b) slope length, c) Curvature, d) TWI, e) TPI and distance from ... f) rivers, g) roads and h) urban areas.

- *Slope (%)*: this factor is related to the landslide occurrence because of its linkage with the management of both the underground flow and the shear forces acting on hill slopes and the concentration

of the soil moisture (Dou et al., 2015, Pourghasemi y Rahmati, 2018). In this study, the slope is the main factor used to obtain the rockfall susceptibility, and it is calculated from DEM (3 x 3 m) (see Figure 3.1).

- *Slope length (LS factor)*: This factor measures the sediment transport capacity of overland flow and, together with the slope, affects the soil loss and hydrological processes (Pourghasemi et al., 2012, Pourghasemi y Rahmati, 2018). Slope length is defined as the distance from the point of origin of overland flow to the point where either the slope gradient decreases enough that deposition begins or the runoff water enters a well-defined channel that may be part of a drainage network or a constructed channel (Smith y Wischmeier, 1957). In the current study, the LS factor was extracted from DEM using SAGA software according to Eq. 3.1 (Moore et al., 1991), and its values range between 0 and 119 (see Figure 3.3b).

$$LS = \left(\frac{A_S}{22.13}\right)^{0.4} \cdot \left(\frac{\sin\beta}{0.0896}\right)^{1.3} \tag{3.1}$$

  where, A_S (m^2) is the specific catchment area and β is in degree.

- *Curvature*: The curvature is defined as a three-dimensional feature of a two-dimensional surface and represents the deviation from the flat surface. The curvature is one of the most important landslide causative factors, and it controls the water flow on earth's surface, affecting landslide occurrences and the presence of open or closed fractures (Kornejady et al., 2017, Pham et al., 2017, Zhao et al., 2022). The curvature values of Molleturo area range between -74.89 and 44.47 and grouped into five classes: High concave [-74.89, -2), concave [-2, -0.05), flat [-0.05, 0.05), convex [0.05, 2), high convex [2, 44.47] (see Figure 3.3c).

- *Aspect*: The aspect layer shows the compass direction that the downhill slope faces for each location. This factor controls evapotranspiration and soil moisture since more sunlight radiation increases evapotranspiration while soil moisture decreases (Dou et al., 2015, Zhao et al., 2022). In the southern hemisphere, the

orientation north receives the greatest insolation, which is present in 18% of the study area.

- *Topographic wetness index (TWI)*: Generally, TWI is used to quantify the topographic influence on hydrological processes. The flow accumulation theoretical measure describes this index. Although several studies have shown that the influence of this factor is slight on the landslide susceptibility mapping (Lombardo y Mai, 2018, Pourghasemi et al., 2018, Zhou et al., 2018), TWI is considered in this study because the altitude range is much higher in our study area, which could increase its influence on the landslide frequency. The following steps were necessary to determine the TWI: 1) to compute the flow direction (fd); 2) to obtain the flow accumulation (fa); 3) to calculate the slope layer (rad) from DEM (slp); 4) the slope tangent is calculated (tan_slp); 5) the flow accumulation is scaled (fa_sc) and finally, 6) TWI is obtained from Eq. 3.2 (see Figure 3.3d).

$$TWI = ln(\frac{fa\_sc}{tan\_slp}) \tag{3.2}$$

- *Topographic position index (TPI)*: TPI is a morphometric property used to subdivide landscapes into morphological classes based on topography. This factor is calculated by measuring the relative topographic position of the central point as the difference between the elevation at this point and the mean elevation within a predetermined neighborhood (Reu et al., 2013) (Eq. 3.3).

$$TPI = int(DEM - focalmean(DEM, rectangle, 65)) \tag{3.3}$$

  Positive TPI values represent locations that are higher than the average of their surroundings (ridges); negative TPI values represent lower locations than their surroundings (valleys) and values near zero are either flat areas or areas of constant slope (see Figure 3.3e) (Pourghasemi et al., 2018).

- *Land use*: This layer shows the type of use that society gives to the different types of land cover, cyclical or permanent, to

meet its needs. This layer has five levels, but data referring to level II updated by the MAE and MAGAP were used in this study. The following categories are found in the study areas: *Shrub*, areas with a substantial component of native non-tree woody species, including degraded areas in transition to dense canopy cover; *Herbaceous*, areas made up of native herbaceous species with spontaneous growth, which do not receive special care and are used for sporadic grazing, wildlife or protection purposes; *Grassland*, herbaceous vegetation dominated by introduced species of grasses and legumes, used for livestock purposes, which require cultivation and management for their establishment and conservation; *Crop Mosaic*, they are groups of cultivated species that are mixed with each other and that cannot be individualized; and exceptionally may be associated with natural vegetation; *Forest*, wooded surface that is obtained artificially by planting native or exotic species, which have the same years of life and present a homogeneous separation; *Moorland*, vegetation located on the upper limit of the forest, in the upper and sublevel montane floors, which is characterized by predominantly herbaceous and shrubby vegetation; *Natural water*, surfaces permanently covered by water of natural origin; *Populated area*, area of human settlement that contains a concentration of houses and other structures, fixed or light, that serve as residence; *Infrastructure*, spaces built or created by man that generate a service and that include physical infrastructure works; *Wasteland*, areas generally devoid of vegetation, which due to their edaphic, climatic, topographic or anthropic limitations, are not exploited for agricultural or forestry use, however, they may have other uses (see Figure 3.1).

- *Drainage*: This layer shows how quickly excess water is removed relative to inputs (see Figure 3.1). Although it presents five levels, in the study areas, there are only three: good, easy removal of precipitation water, although not quickly, some horizons can remain saturated for a few days after a water supply and the water table is at depths greater than 120 cm; moderate, slow removal of water in relation to the contribution, some horizons can remain saturated for more than a week after the contribution of water

and present a layer of slow permeability, or a high water table (60-90 cm deep).; no data indicates that the attribute does not apply to the object.

- *Distance from rivers, roads and urban areas*: the Euclidean distance function included in ArcMap 10.8.1. was used to calculate, for each cell, the straight-line distance to the closest source feature datasets: rivers, roads and urban areas, respectively (Figures 3.3f-h).

- *Geology*: See the next section for detailed information on geological characteristics (see Figure 3.4).

3.2.2.3 Geological Setting

The spatial distribution of the different geological formations, the composition of the relief forms in terms of their rocky substrate (lithology), and the surface formations in the study area are included in Figure 3.4 (source: MAG). The Tarqui formation, attributed to the late Miocene period, covers a large part of the southern highlands of Ecuador, consisting of slightly consolidated and altered volcanic deposits, it is the most predominant in the study area, with approximately 2600 hectares, representing 89.4% of the total study area (2893 ha) (Figure 3.4). Pyroclasts predominate in the sequence, consisting of agglomerates ranging from rhyolitic to andesitic, tuffs, volcanic ash, and ignimbrites, most of which are heavily kaolinized and or silicified. Dacitic to rhyodacite lavas forms a subsidiary part of the Tarqui succession; minor non-volcanic sedimentary horizons appear sporadically. The thickness of the formation reaches 1200 meters. Fossil wood is aged around 25,000 and 34,000 years, indicating the upper Pleistocene's age. Pyrite is widely developed, and some veinlets break through the fossilized wood (Bristow, 1973, Steinmann, 1997). The remaining 10.6% comprises glacial origin deposits, alluvial, colluvial deposits, hillside deposits, and mixed and intercalations-mixtures of those previously described.

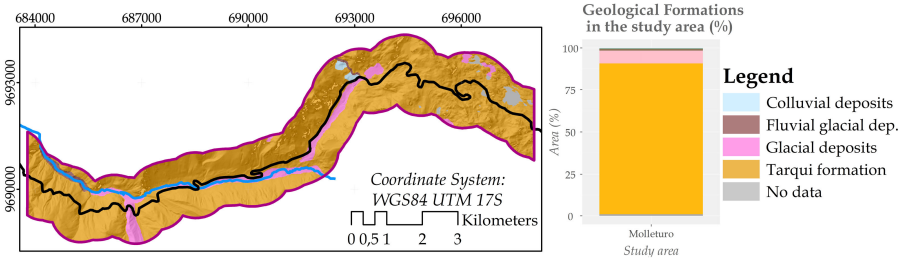

Figure 3.4: Geological formations in the study area (the total study area = 2893 ha).

3.3 Methods

3.3.1 Rockfall susceptibility mapping

To produce the rockfall susceptibility maps of the study area, the QGIS-based plugin QPROTO (QGIS Predictive ROckfall TOol), recently created by Castelli et al. (2021), was used. However, due to the limitations of QPROTO in processing large amounts of data, several functions and processes were designed, implemented, and executed in the R software (R Core Team, 2021). Thus, the methodology to obtain the rockfall susceptibility maps is composed of 4 steps: 1) pre-processing using R software; 2) identification of areas that could be affected by rockfalls using QPROTO; 3) post-processing of rockfall results in R software; and 4) classification of the infrastructure sections affected using QGIS software. Each step is detailed below.

3.3.1.1 Step 1: Pre-processing

As mentioned, QPROTO presents a direct relationship between the input data size, execution time, and memory and disk space, limiting its use to files/zones that are not excessively large. In addition, this tool can present errors when processing areas with "valley orography". To address these drawbacks, an 800 m buffer was applied to both sides of the tracks (Figure 3.5b), and then, this area was divided into sections:

first around the track axis to avoid "valley effect" errors, sections 1 and 2 (Figure 3.5b); and secondly, each of these sections in "equal parts" taking the axis of the road as a reference to avoid the use of files that are too large (Figure 3.5c). This buffer ensures that the simulations using QPROTO will include all source points that could develop into rockfalls.

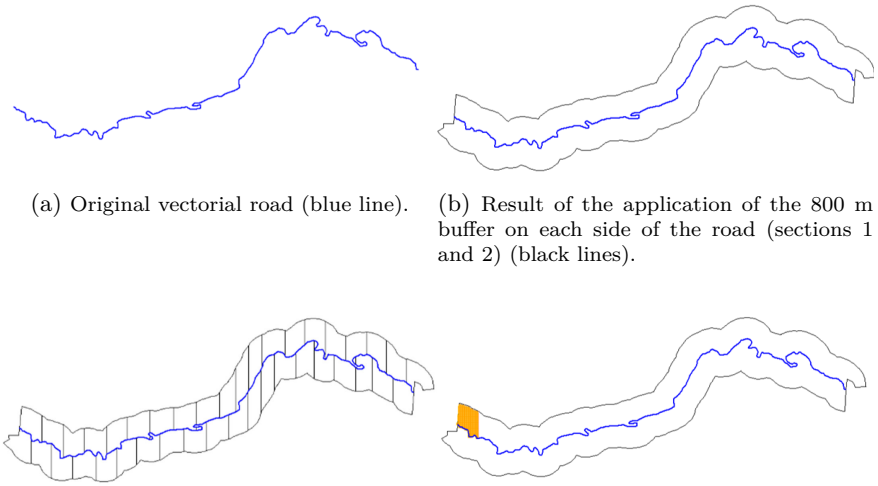

(a) Original vectorial road (blue line).

(b) Result of the application of the 800 m buffer on each side of the road (sections 1 and 2) (black lines).

(c) Subdivisions of each section in "equal parts" taking the axis of the road as a reference.

(d) Points belonging to division 1 of section 1 (orange points).

Figure 3.5: Pre-processing steps.

Next, from the DEM of each area, the slope and aspect layers are obtained, and the mentioned DEM is transformed from raster format to points (vector layer). Then, the values of elevation, slope and aspect, as well as the values of detachment propensity and boulder mass necessary for processing in QPROTO (such parameters will be described in the next section) are assigned to each point. In this case, the detachment propensity was set equal to 1 as Castelli et al. (2021) did in their study, while the boulder mass was set up in accordance with the geology. All geological formations in the study areas require the assignment of a value of 1000 kg in this parameter. Finally, from the previous sections of the

study area, the point layer is divided into as many parts as sections, and the resulting vector files are saved in shapefile format (Figure 3.5d). The DEM of the study area and each of the point files, together with their associated attributes, will be the input data of the QPROTO plugin.

3.3.1.2 Step 2: QPROTO

QPROTO, based on the cone method developed by Jaboyedoff y Labiouse (2011) and implemented by Castelli et al. (2021), identifies the areas most exposed to a rockfall phenomenon considering the topography and several empirical parameters. The algorithm adopts a simplified energy assumption in which the falling block path is summarized by an equivalent sliding motion of the boulder along a straight line (i.e., the energy line) linking the more distant observed fallen block to the slope apex (i.e., the shadow angle method) Castelli et al. (2021), Miele et al. (2021). Further information on the rockfall calculation can be found in Castelli et al. (2021). Two input layers are necessary to execute QPROTO: a DEM (m) in raster format and a set of source points representing a single block (vectorial point layer). Then, each source point is used to start a viewshed analysis, and a visibility cone is determined in the vertical and horizontal plane. Although in previous studies only points located in the steepest areas of specific sectors of the study area were used Miele et al. (2021), probably to reduce processing costs, in this case and with the purpose of obtaining the rockfall susceptibility map of the totality of the surface object of study, as many points as cells presenting the DEM were used. In addition, considering all the points to calculate the rockfall susceptibility will allow us to analyze the characteristics of the actual rockfall source points. In this way, the processing efficiency will be improved in future studies. In addition to the input layers, it is necessary to set a series of parameters, some of which are extracted from the vector layer of points:

- *ID*: Identifying a number of the source point from input point layer.
- *Elevation*: Elevation from input point layer (m).

- *Aspect*: Dip direction of the slope from the input point layer, ranging between 0-360 (°). It defines the orientation of the cone.
- *Detachment Propensity*: Propensity index to detachment, ranging between 0-1. A value of 1 is set for all points using the input point layer in this study.
- *Boulder mass*: Boulder mass from input point layer (kg). A value of 1 is set for all points in this study.
- *Energy Line Angle*: The energy line angle of the cone having an apex in each source point, ranging between 0-90 (°). Recommended values between 20°-50°. Optionally, a fixed value can be used for quick analysis. The slope values from the input point layer were used in this case.
- *Lateral spreading angle*: Lateral dispersion angle of the cone having an apex in each source point, ranging between 0-90 (°). Recommended values between 0°-30°. Optionally, a fixed value can be used for quick analysis. In this case, a value of 10 has been indicated in Fixed value of the Lateral Spreading Angle field.
- *Visibility Distance*: Distance to which the analysis can be extended (m). In this case, a value of 800 was established.

Finally, the QPROTO plugin provides several output files, concretely ten raster files and a point shapefile. The first raster (count) shows the number of source points that can view each cell. The second raster (susceptibility) shows the sum of all the detachment indexes of the source points that can view from the considered cell. The following three raster maps (v_min, v_mean and v_max) include the minimum, mean and maximum computed block velocity. The next three rasters, energy maps, (e_min, e_mean and e_max) are obtained based on these last three rasters. Two time-independent hazard maps (w_en and w_tot_en), are provided by multiplying the detachment index and the kinetic energy in each cell of the runout area. In addition to these outputs, the *Finalpoints* vector shapefile shows details on points located in the runout zone (Castelli et al., 2021). In this study, only this last file has been used because the block processing methodology adopted

produces overlaps between the rasters, making it impossible to correctly visualize and interpret the results. The post-processing tasks based on *Finalpoints* vector shapefile are detailed in the next section.

3.3.1.3 Step 3: Post-processing

Block processing generates as many *Finalpoints* files as point blocks have been processed using QPROTO. Table 3.2 shows the main fields included in the attribute table of *Finalpoints* shapefile.

Table 3.2: Main fields included in the attribute table of *Finalpoints* vector shapefile.

Fields	Description	Observations
ID_IN	ID of rockfall source point from ID field of input point layer.	The more times an ID is repeated, the larger the magnitude of the area affected by the rockfall event originating from that point is expected to be. Points with such IDs are considered QPROTO source points (vertices of the visibility cones defined in QPROTO) and are not included in the *Finalpoints* shapefile.
V	Computed block velocity.	
E	Energy.	
W_EN	Time-independent hazard values.	
Count	The number of source points that can view each cell.	The higher the value of this field, the greater rockfall effect is expected in the cell that contains those points.

Once all the blocks have been processed, *Finalpoints* files are merged into a single shapefile that is transformed into raster format so that the value of each pixel corresponds to the number of points located in each one, or what is the same, the sum of the *Count* field of the points resulting from the processing of each block. Then, each grid cell shows the total number of times that a rock trajectory crosses

it. For this, the *rasterize* function of the *raster* package was used (Hijmans, 2022) (Hijmans 2015) (parameter fun = "count") included in R software (R Core Team, 2021). This raster layer is considered the susceptibility map and five categories are differentiated (very low, limited, medium, high and very high) using the Jenks natural breaks classification. Natural break was also used by Arabameri et al. (2019) as the best classification method for numerical variables, and it was used int his study because its different from the geometrical interval method used in previous studies (Pham et al., 2016, Chen et al., 2017, 2018); it allows to identify logical break points in a data set, by grouping similar values that minimize differences between data values in the same class and maximize the differences between classes. Class ranges are tailored to one data set, so comparing maps for different data sets is difficult. To address this disadvantage, the Jenks natural breaks method was applied to the susceptibility map using DEM_{10m} and taking into account the minimum and maximum values of their intervals, the class ranges of susceptibility maps using DEM_{20m} and DEM_{30m} were extrapolated.

3.3.1.4 Step 4: Rockfall direction and classification

To complete the susceptibility map obtained from the methodology described in the previous sections, the aspect layer is used to indicate the direction in which the rockfall occurs. To do this, the orientation values using the aspect layer were assigned to each resulting point of QPROTO. Finally, this information is incorporated into the susceptibility map.

On the other hand, the physical consequences that rockfall events have on infrastructures can be classified, in a generic way, into two types: rockfall, when the rockfall deposit is located on an infrastructure, and subsidence, when the crack in the hillside or source point occurs at the edge of the infrastructure giving rise to undermining (Figure 3.6a). To differentiate these events from the information provided by QPROTO and subsequently post-processed, a classification process was developed using various functions of the R software (Figure 3.6b). First, the axis of the road (polyline) was transformed to points with a separation between points of 10 m and the elevation value was assigned from the DEM

layer. Next, from the axis points, their mirror points were located on each side at a distance of 30 m using the methodology described in (Buján et al., 2021). Each point on the axis is assigned its mirror points' elevation and susceptibility value. Finally, based on some simple decision rules, the points of the infrastructure that can be affected by rockfall or subsidence are identified. This classification is made taking into account independently the data relative to each side of the road, that is to say, that the same point of the axis can be affected by rockfall and subsidence. The decision rules used are based on the elevation and susceptibility values, so that a point will be identified as a rockfall if the susceptibility of its mirror point is classified as high or very high and the difference in elevation between that point and its mirror point is negative; it will be classified as subsidence if the susceptibility of its mirror point is classified as high or very high and the elevation difference between said point and its mirror point is positive; otherwise, said point will be classified as "no rockfall" since the occurrence of such phenomena is not expected.

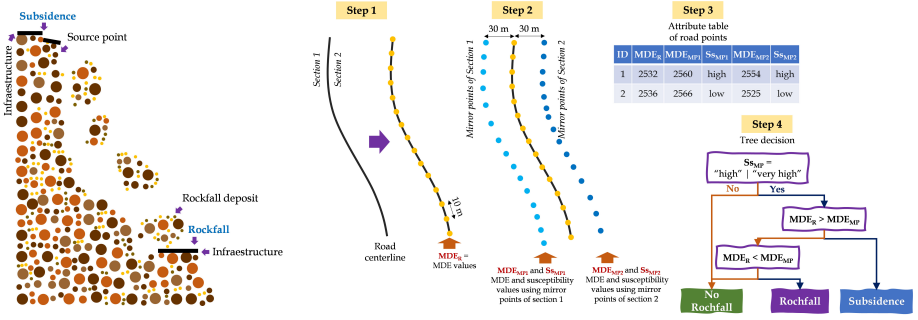

(a) Subsidence vs. rockfall.

(b) Rockfall classification overview.

Figure 3.6: Rockfall classification.

3.3.2 Analysis of factors to identify rockfall source points

The first step to assess the rockfall susceptibility consists of the spatial identification of the involved areas. Generally, such identification is

carried out through exhaustive fieldwork or using existing inventories. In these areas, those points will be considered the origin of the rockfall, the so-called source points. In the case of using predictive methods, these points are fundamental for delimitating the areas that would be more exposed to an event of this type. When we carry out studies at a regional level, the complexity, the execution time and the costs linked to identification source points increase considerably. That is why in these cases, points are selected taking into account factors such as the slope or the properties of the rocks.

To apply the methodology described and tested in the study area to the route of the Cuenca - Molleturo road (109 km), this study seeks to identify those factors that best define the source points and the corresponding thresholds. In this way, it will be possible to improve processing efficiency for large areas. To do this, based on the results obtained from QPROTO using all the possible points in the study area, the source points that said tool has actually used to calculate the areas that can be affected by rockfalls are identified (*ID_IN* field in the attribute table of *Finalpoints* vectorial shapefile). Those source points whose cone surface is less than 1 ha are discarded as they are considered to be of little relevance. Next, the points resulting from this filtering are assigned the value of each factor described in section 3.2.2.2 using the *extract* function included in the R *raster* package (v 3.5-15) (if factor is a continuous variable, method = "bilinear", otherwise method = "simple") (Hijmans, 2022).

Then, a predictive analysis is carried out using a decision tree, one of the most common tools. Concretely, this analysis was conducted using CART (Classification and Regression Tree) analysis, implemented with the rpart function included in the R *rpart* package (v 4.1-15) (Therneau y Atkinson, 2019). Due to the fact that the points that are considered source points represent only 4% of all the points processed (imbalance dataset), the strategy of reducing the sample of non-source points was applied to balance the obtaining of the model, as otherwise, a high degree of precision in the majority category and a low recall in the minority category would be obtained. Then, as input data, $\approx$ 8% of the previous points were used ($\approx$ 2500 points). CART analysis is used because it is a robust method that does not require

the data to follow a specific statistical distribution and is capable of handling data that contain outliers and non-significant predictors (Bater y Coops, 2009, Montealegre et al., 2015, Buján et al., 2019). This method identifies a series of independent variables as predictors of an independent categorical variable. In this study, the thirteen factors were considered independent variables (see Table 3.1), whereas the type of point (source or non-source point) was considered the dependent variable. A diagram representing the data division into homogeneous groups based on independent variables is the result of this analysis.

Finally, the results were tested using a confusion matrix by comparing detected source points and real source points. The detected points can be classified into four types of results: true positive (TP) and true negative (TN), are the number of points that are correctly classified; false positive (FP) and false negative (FN) are the numbers of points erroneously classified. Based on these possible results, the statistical metrics used to assess the identification of source points were included in Table 3.3. The assessment of source point/rockfall identification is considered ideal when FPR = 0 and TPR = 1, i.e., the model produces no false or missing predictions. However, if both the TPR and FPR values are high, over-prediction may occur. Then, the True Skill Statistic (TSS) is used as a complementary statistic, so that TSS = 1 is the ideal performance (TPR = 1 and FPR = 0) (Qiu et al., 2022). To evaluate which resolution of the DEM is more appropriate to identify the source points, this evaluation considered DEMs with different resolutions. To do this, the original DEM (resolution = 3 m) was resampled into three DEMs with different resolutions (10 m, 20 m and 30 m). According to Qiu et al. (2022), the bilinear interpolation method was used for the resampling.

3.3.3 Rockfall susceptibility assessment

Although there is no consensus regarding the most appropriate approach to evaluate landslide susceptibility, in addition to the above mentioned

Table 3.3: Proposed statistical metrics to assess the identification of source points and the rockfall susceptibility mapping.

Metrics	Equation	Description	References
Accuracy	$\frac{TP+TN}{TP+FP+FN+TN}$	Proportion of points correctly classified.	(Tien Bui et al., 2016, Chen et al., 2017, Orhan et al., 2022)
Specificity	$\frac{TN}{TN+FP}$	Proportion of detected non-source points that are correctly classified as non-source points.	
Sensitivity (TPR)	$\frac{TP}{TP+FN}$	Proportion of detected source points that are correctly classified as source points.	
NPV	$\frac{TN}{TN+FN}$	Probability of points that are correctly classified as non-source points.	
FPR	$\frac{FP}{TN+FP}$	Proportion of detected non-source points that are not correctly classified as non-source points.	(Sarma et al., 2020, Palazzolo et al., 2021, Qiu et al., 2022)
TSS	$TPR - FPR$	Compares the number of correct forecasts, mi-nus those attributable to random guessing, to that of a hypothetical set of perfect forecasts.	

TP = true positive, TN = true negative; FP = false positive; FN = false negative; TPR = True positive ratio; NPV = Negative Predictive Value; FPR = False Positive Ratio; TSS = true skill statistic.

statistical criteria (section 3.3.2), the Receiver Operating Characteristics (ROC) curve, and consequently the Area Under the Curve (AUC), based on the training and/or testing data are the most common metrics used to assess the predicted results (Chen et al., 2017, Orhan et al., 2022). The ROC curve is a graph based on the Specificity (x-axis), the number of "non-rockfall" pixels that have been classified correctly as "non-rockfall" class, and Sensitivity (y-axis), the number of "rockfall" pixels that have been classified correctly as "rockfall" class (Tien Bui et al., 2016, Orhan et al., 2022). From this graph, the AUC is calculated and is used to evaluate quantitatively the overall performance of rockfall method. Its values are in the range 0 - 1, where an AUC value of 0 indicates a non-informative model, while a value equal to 1 indicates a perfect rockfall

model (Chen et al., 2017, Arabameri et al., 2019). For this propose, the *rocit* function included in the R *ROCit* package (v.2.1.1) was employed (Ahmed Khan y Brandenburger, 2020) and centroid points of rockfall areas recorded from the MARLI tool were used as input data.

3.4 Results and discussion

3.4.1 Effects of factors on the susceptibility processing

The result of the CART analysis (Figure 3.7) shows that TPI, Slope and Distance from rivers are the factors that best define the location of rockfall source points in the study area using QPROTO tool.

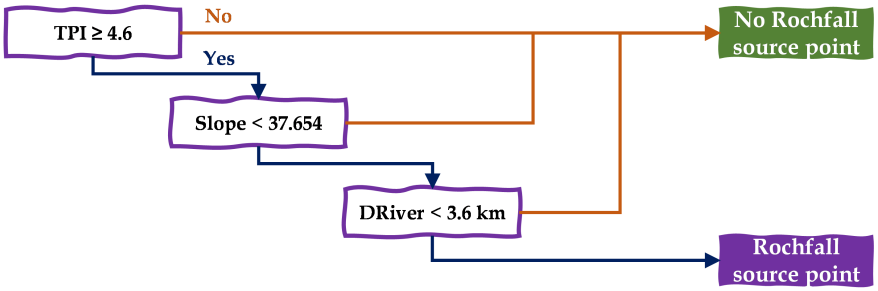

Figure 3.7: CART analysis result.

The factors and thresholds identified in this study for the location of source points differ considerably from those used at the medium-large scale in previous studies. Specifically, Torsello et al. (2022) and Miele et al. (2021), where QPROTO was also used to analyze slopes potentially prone to collapse, set a value of 45° slope as a minimum threshold to identify rockfall source areas. However, in the present study, as long as the TPI is greater than or equal to 4.6, a slope value of 37.65° was identified as maximum value for locating rockfall source points. Finally, the identification of source points is refined considering the distance to the rivers (< 3.6 km) (Figure 3.7).

Based on the above factors and thresholds, a classification process

(a) Using DEM_{10m}

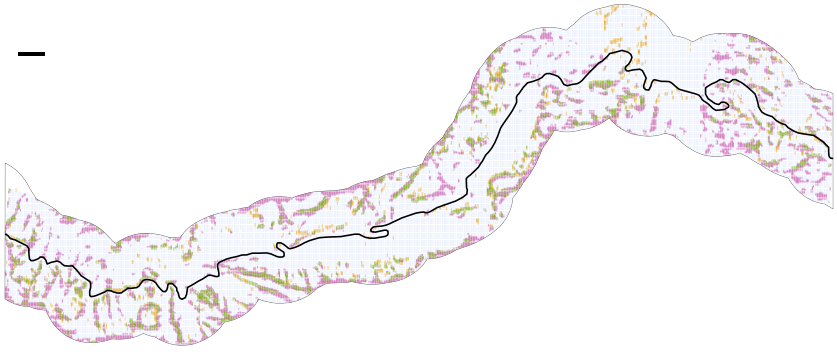

(b) Using DEM_{20m}

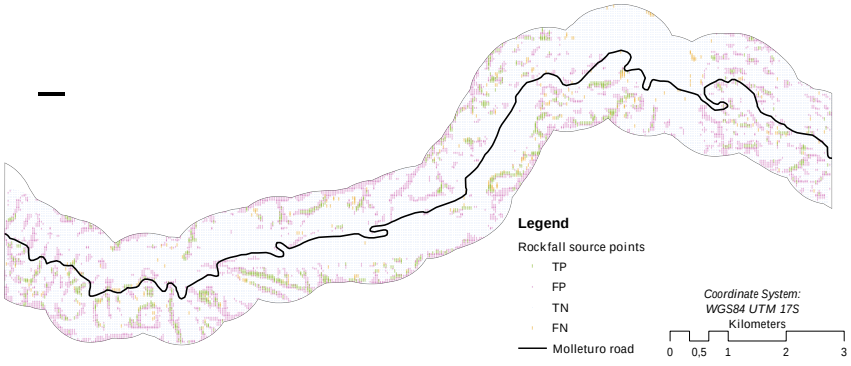

(c) Using DEM_{30m}

Figure 3.8: Predictive analysis results of rockfall source points.

was carried out to identify the source points whose qualitative result is shown in Figure 3.8, differentiating between true positive (TP), true negative (TN), false positive (FP), and false negative (FN) from three DEMs with different resolutions: 10 m (Figure 3.8a), 20 m (Figure 3.8b) y 30 m (Figure 3.8c). Analyzing the qualitative results of identifying rockfall source points (Figure 3.8), it is verified that a considerable number of FPs are located on the edges of the study area, probably due to the values that the TPI variable takes in these areas (Figure 3.3e). These errors may be due to the edge effect, i. e., due to the absence of information in an important part of the calculation/analysis window. A possible option to alleviate this error would consist of increasing the analysis buffer, identifying the source points in that enlarged area, but only considering for subsequent calculations and analyses of those points within the initial 800 m buffer. Thus, the edge effect would be eliminated, and an increase in precision would be expected as a consequence of the reduction in commission errors.

Taking into account the total points processed in this study (DEM_{10m}, 293,477 points; DEM_{20m}, 73,366 points and DEM_{30m}, 32,616 points), the number of points identified as source points (TP + FP) from the CART analysis (DEM_{10m}, 50,899 points; DEM_{20m}, 13,247 points and DEM_{30m}, 6103 points) representing approximately 18% of the points processed and approximately 70% of the real source points. Thus, the points to be processed would be reduced by more than 80% and, therefore, the processing time, a factor considered decisive when obtaining results at a medium-large scale. However, if only the minimum slope threshold of 45° had been taken into account, which was used in the aforementioned studies (Miele et al., 2021, Torsello et al., 2022), said reduction would have been approximately 95%, but only 0.5% of the real source points would have been identified. Thus, the establishment of a threshold angle, above which the hillslope may be considered potentially a rockfall source area, allows the rapid identification of source points and a more efficient processing; however, it has been at the expense of not analyzing the vast majority of the areas potentially susceptible to the occurrence of rockfall using QPROTO. These results show that the source points selected by QPROTO are not found in the areas with the steepest slope but quite the opposite (according to the result of the CART analysis included in Figure 3.7, Slope $< 37.65°$). An

explanation for this circumstance could be expected for several reasons, for example, moderate slope areas show characteristics favorable to rockfall occurrence due to anthropic activities (e.g., Molleturo road construction). However, it can also be due to a technical factor from using a raster (2D) DEM. In a raster image, only a few cells are needed to represent the transition from a moderately flat to a steep area, for example, an almost vertical wall. Thus, source points can be seen displaced to cells with moderate slope, contiguous to those with high slope. Note that these results are particular to the QPROTO tool, and it would be necessary to replicate said analysis in case you want to use other tools, such as STONE.

Additionally, statistical metrics, which represent the agreement between reality and the automatic classification result, have been calculated and included in Table 3.4. Such metrics were calculated from the results of DEMs with different resolutions. The high accuracy value obtained, approximately 85%, shows the success of both source point identification and non-source points regardless of the DEM resolutions, in general terms. This accuracy value is consistent with findings of Rossi et al. (2021) (mean accuracy $\approx$ 90%) using a DEM of 5 m resolution. Analyzing this result in more depth, it can be verified that almost all non-source points are correctly identified from the proposed method (NPV $\approx$ 98%), and $\approx$ 85% of the non-source points detected, they really are (specificity values). In Figure 3.8, this result can be observed qualitatively: in blue, the non-source points correctly identified (TN) and in yellow, the few commission errors committed (FN). However, in the case of source points (sensitivity values), the number of detected source points (that really are) varies inversely with the resolution of the DEM used; that is, the higher the level of detail of the DEM, the lower the percentage of source point detection, being $\approx$ 60% in the case of using the DEM_{10m} and 77.17% in the case of using the DEM_{30m}. These results are supported by the values of TSS ($\approx$ 45% using the DEM_{10m} and $\approx$ 60% using DEM_{30m}) and show that the source points used by QPROTO for rockfall susceptibility estimation are more accurately identified from the proposed methodology if a less detailed DEM is used. This inverse relationship between the sensitivity values and the resolution of the DEMs was also observed by Žabota et al. (2019) in their study, where the $DEM_{12.5m}$ and DEM_{25m} were more effective

at predicting the source area compared to DEM_{1m}, although correct prediction of source areas does not exceed 50%.

Table 3.4: Statistical metrics from confusion matrix from three DEMs.

	DEM resolutions		
Metrics	**10 m**	**20 m**	**30 m**
Accuracy (%)	83.66	84.14	83.32
Specificity (%)	84.75	84.80	83.56
Sensitivity (%)	60.96	71.72	77.17
NPV (%)	97.84	98.26	98.95
FPR (%)	15.25	15.20	16.44
TSS (%)	45.71	56.52	60.73

FPR = False Positive Ratio; TSS = true skill statistic.

3.4.2 Rockfall susceptibility mapping

Rockfall susceptibility maps were constructed using the QPROTO tool and DEMs with different resolutions and reclassified into five categories based on trajectory count per cell: very low, limited, medium, high and very high rockfall susceptibility (Figure 3.9). The rockfall direction was also included in four subareas (rockfall example 1-2 and rock subsidence example 1-2, Figure 3.9). As expected, the higher the level of detail of the DEM used, the higher the level of detail with which the data of rockfall events are displayed (Figure 3.9a vs. Figure 3.9c). However, despite the obvious loss of detail in the representation of the rockfall susceptibility using the coarse-resolution DEM (Figure 3.9c) with respect to the results derived from using the highest resolution (Figure 3.9a), the use of the coarse-resolution DEM could favor the graphic interpretation of the results by showing the rockfall events in a clear and simplified way. Additionally, from the analysis of these results (Figures 3.9a, 3.9b, and 3.9c), there are no evident spatial differences (location) between the areas represented by each of the susceptibility categories using one or the other DEM. However, differences are observed

in the extent of the area that can be affected by each event and the magnitude (level of susceptibility) with which they are represented. In other words, in general, the number of rockfall events does not vary considerably as the resolution of the DEM varies; however, the level of detail of the DEM does seem to influence the surface that can be affected by these events both in total (transit + deposit areas) as in relation to each susceptibility class.

In the study carried out by Qiu et al. (2022) it is also observed that generally, the surface of the area considered unstable and extremely unstable does not vary when increasing the level of detail of the DEM when going from a resolution of 30 m to one of 5 m. However, unlike the results obtained in our study, neither is the proportion of each one, where $\approx$ 35% of the study area is considered unstable, and $\approx$ 10% is considered extremely unstable regardless of the resolution of the DEM. The explanation for this difference is possibly found in the method used to represent the susceptibility. While Qiu et al. (2022) use the Factor of safety, typical of the Scoop3D tool, in our study, the level of susceptibility is based on the count attribute distinct of QPROTO, where the increase in resolution and, therefore, the number of cells have a determining role. Thus, the thresholds are established to identify each susceptibility category since modifying these thresholds increases/decreases the number of pixels belonging to one or another category. Contrary results are shown by Zieher et al. (2012), where they observed how simulations with coarser resolutions (DEM_{10m} and DEM_{20m}) lead to lateral overestimations of the rockfall-affected area. Analyzing these results together with the DEMs used in one of the examples included in the mentioned study (see Figure 4 in Zieher et al. (2012)), it is verified how there is an evident loss of detail if the DEM_{5m} is compared with the DEM_{20m}, observing in this last case an excessively smooth surface. For the example in question, this circumstance is aggravated due to the orography of the area affected by the rockfall event (area flanked on both sides by very steep terrain) so that when smoothing the surface, said flanks are also smoothed, perhaps excessively, producing an "overflow effect" that leads to an increase in the surface affected by the rockfall event. Likewise, in a complementary way, Bühler et al. (2016) indicated in their study that the high level of detail of the terrain roughness presented by the higher resolution DEMs can have a high

impact on the trajectories of rocks, slowing down the fall of rocks and therefore resulting in a smaller affected area. The rockfalls identified in our study area do not present the morphology of steep flanks (an example is shown in the photograph of rock subsidence example 1 included in Figure 3.9), nor are DEMs available with a sufficient level of detail, which could be one of the reasons why an inverse relationship between the area affected by rockfall events and the level of detail of the DEMs is not observed in our study.

This comparison of results where the DEMs with different levels of detail present positive and negative aspects depending on the objective, the magnitude of the landslides, and processing requirements, has already been revealed, partially, in previous studies, although in relation to landslides in general and not to rockfall in particular. Thus, in some studies, the higher resolution involves better landslide simulation results (coarse resolution can produce over-estimations of the rockfall-affected area) (Sarma et al., 2020), while in other cases, the high-resolution DEM does not produce the best results (over-prediction, high processing time,...) (Schlögel et al., 2018, Meena y Nachappa, 2019) or the results are not conclusive (Qiu et al., 2022). Probably, this disparity of conclusions might be due to, as indicated by Wubalem (2022) in his study, the size of average landslides and the quality of DEM and landslide inventory data used. Additionally, the operational characteristics of the method or tool used to identify and simulate the occurrence of these events may also have a relevant role in the direction and magnitude of the effects that the resolution of the DEMs may have on the results. However, to the best of our knowledge, no studies have focused on investigating the influence of DEM spatial resolution using several methods/tools on rockfall modeling. Probably the main cause of this knowledge gap lies in the limited offer of user-friendly open-source tools.

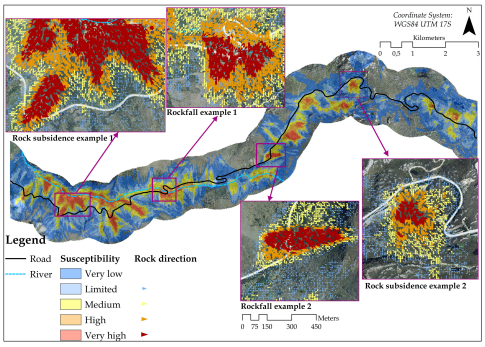

(a)

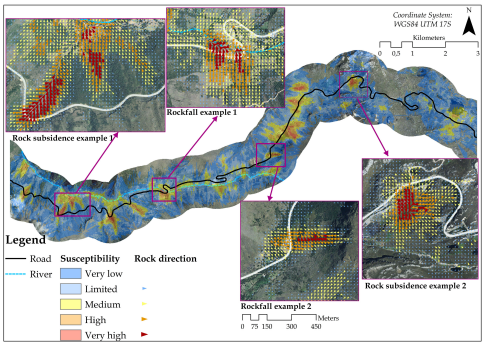

(b)

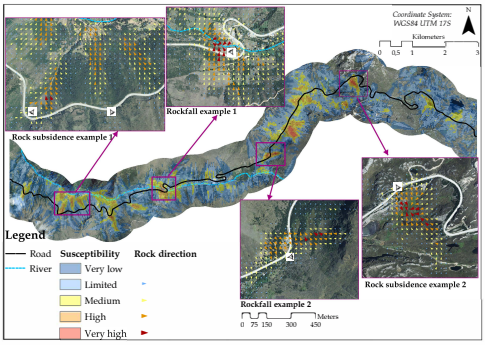

(c)

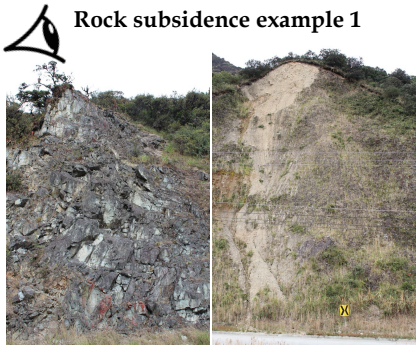

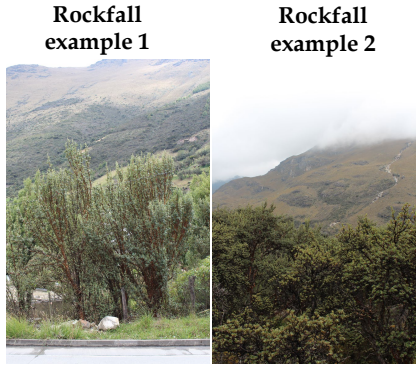

Figure 3.9: Qualitative results for Molleturo with a resolution of a) 10 m, b) 20 m, and c) 30 m. Note: The susceptibility legend was scaled based on the maximum values of each resolution to maintain consistency between the different results.

Figure 3.10 shows the distribution and characterization of rockfall susceptibility classes using DEM_{10m}. It can be observed that ≈ 40% of the study area belongs to limited, medium, high or very high rockfall susceptibility (rockfall-prone areas). Specifically, the high and very high susceptibility classes account for ≈ 8%, and the limited and medium susceptibility classes account for 19.62% and 11.26% of the study area, respectively. These proportions differ from those obtained using DEM_{20m} (≈ 5%, 21.11% and 12.19% respectively) and DEM_{30m} (≈ 2%, 27.35% and 8.78% respectively). However, other studies found homogeneity in the susceptibility classes' proportions using different DEMs resolutions (Qiu et al., 2022, Wubalem, 2022). The results show that the slope is moderate to high ($> 15°$) in 75% of the rockfall prone areas (top left graph, Figure 3.10), where the majority of land cover classes are moorland (65.14%), wasteland (11.49%) and grassland (6.62%) (bottom left graph, Figure 3.10). In relation to the slope, previous studies also showed that the most susceptible areas to landslides are associated with a moderate slope of the ground (Pham et al., 2016, Arabameri et al., 2019). In keeping with these results, the majority of the rockfall-prone regions are located close to the urban areas (< 400m, 45.58% of the rockfall-prone area) (top right graph, Figure 3.10) and the roads (< 320 m, 63.52% of the rockfall-prone area) (bottom right graph, Figure 3.10). These results show that the location of rockfall-prone areas had a strong relationship with human activities such as road construction, agriculture activities, or land use changes related to new settlements along roads, which negative effect stability and increased the probability of rockfall occurrence. These results also agree with the findings of Arabameri et al. (2019).

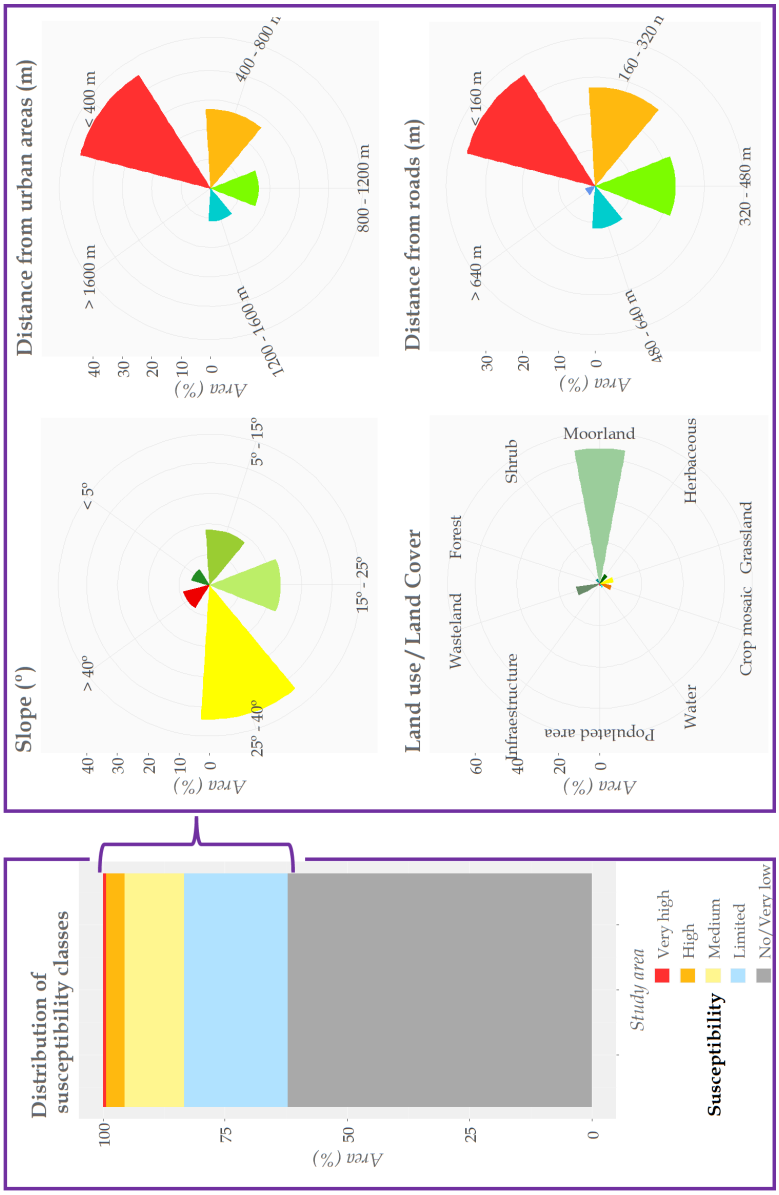

Figure 3.10: Distribution and characterization of rockfall susceptibility classes (data from results using DEM_{10m}).

The general performance of the rockfall models based on the ROC curve method is presented in Table 3.5. It can be observed that the QPROTO tool achieves good performance for rockfall susceptibility assessment using the MARLI validation dataset for three DEM resolutions (AUC $>$ 0.7). The susceptibility maps using DEM10m achieved the best results (AUC = 0.75), followed by the map using DEM_{20m} or DEM_{30m} (AUC = 0.73). These results can be interpreted as the precision of the maps is independent of the resolution of the DEM. However, taking into account the recommendations made in previous studies on the need to complete the analyzes with additional metrics (Sarma et al., 2020, Qiu et al., 2022), taking into account the sensitivity values, it is observed that using the DEM_{30m} obtains 14 percentage points less than if the DEM_{20m} is used and almost 20 percentage points less than if the DEM_{10m} is used. Taking these results into account, the susceptibility map using the DEM10m achieved the highest performance for the classification of rockfall (sensitivity = 72.73%). Nevertheless, the highest performance of the identification of non-rockfall areas is achieved using DEM_{30m} (specificity = 90.91%). Additionally, the best can be assumed as the one closest to the ideal performance point (FPR = 0%, sensitivity = 100%), which is FPR = 22.73% and sensitivity = 72.73% (TSS = 50%). Thus, the DEM_{10m} achieved the highest performance for the identification of rockfall in the study area, in general terms. As Zieher et al. (2012) showed in their study, in this case, the minimum size of the identified rockfalls increases as the resolution decreases. This circumstance is coupled with a reduction in the number of rockfall events identified. Circumstance that reflects the sensitivity values obtained using the DEMs with different resolutions (the lower the resolution, the lower the number of correctly identified rockfalls).

These results are also consistent with the findings of Cignetti et al. (2021), where a rockfall susceptibility map was calculated using the combination of several factors among which stand out the slope, the lithology, and a DEM_{10m}, obtaining a success AUC value of up 0.75. Also Alvioli et al. (2021), using the model STONE Guzzetti et al. (2002), they calculated a national rockfall probability map related to several topographic units. Considering the results of all topographic units, they managed an average sensitivity of 75%, a value similar to that obtained in this study without considering the rockfall size ($\text{Sensitivity}_{DEM10m}$ =

72.7%). In the case of considering only those smaller rockfalls (<10 ha), the susceptibility value reaches 100%, while it drops to 40% when large rockfalls are considered.

Table 3.5: Statistical metrics from confusion matrix from three DEMs.

Rockfalls→	**All**			**Small (<10 ha)**			**Large (>10 ha)**		
Resolutions→ Metrics↓	**10 m**	**20 m**	**30 m**	**10 m**	**20 m**	**30 m**	**10 m**	**20 m**	**30 m**
AUC	0.75	0.73	0.73	0.88	0.75	0.75	0.55	0.70	0.70
Specificity (%)	77.27	77.27	90.91	75.00	66.67	83.33	70.00	90.00	100.00
Sensitivity (%)	72.73	68.18	54.55	100.00	83.33	66.67	40.00	50.00	40.00
FPR (%)	22.73	22.73	9.09	25.00	33.33	16.67	30.00	10.00	0.00
TSS (%)	50.00	45.45	45.46	75.00	50.00	50.00	10.00	40.00	40.00

AUC: Area under the ROC curves; FPR = False Positive Ratio; TSS = true skill statistic.

As mentioned in the previous paragraph, in a complementary way, the metrics of rockfall susceptibility assessment were also calculated based on the size of the rockfalls identified in the field. Thus, a difference was made between the rockfalls that affect an area of less than 10 ha, the so-called small rockfalls, and those that exceed this area, the so-called large rockfalls (Table 3.5). Based on these results, it can be seen that in the case of trying to identify small rockfall, the DEM_{10m} (fine DEM resolution) is the best option since, based on the AUC value of prediction curves, excellent performance is obtained (AUC $\approx$ 0.9) (reference levels defined in Wubalem (2022)), correctly identifying all the rockfall events recorded in the field (sensitivity = 100%). Although a considerable improvement in the results is observed when the fine DEM resolution is used for the identification of small rockfalls in comparison with the results obtained from the entire validation sample (AUC_{ALL} = 0.75 vs. AUC_{Small} = 0.88; $Sensitivity_{ALL}$ = 72.7% vs. $Sensitivity_{Small}$ = 100%; TSS_{ALL} = 50% vs. TSS_{Small} = 75%), this is not the case when DEMs with a lower level of detail are used. While the sensitivity values do show an evident improvement in the detection of small rockfalls (using DEM_{20m}, $Sensitivity_{ALL}$ =68.2% vs. $Sensitivity_{Small}$ = 83.3%; using DEM_{30m}, $Sensitivity_{ALL}$ =54.6% vs. $Sensitivity_{Small}$ = 66.7%), the

values of the AUC (using DEM_{20m}, AUC_{ALL} =0.73 vs. AUC_{Small} = 0.75; using DEM_{30m}, AUC_{ALL} =0.73 vs. AUC_{Small} = 0.75) y TSS (using DEM_{20m}, TSS_{ALL} =45.5% vs. TSS_{Small} = 50%; using DEM_{30m}, TSS_{ALL} = 45.5% vs. TSS_{Small} = 50%) are similar in both cases. On the other hand, it would not be appropriate to use fine DEM resolution to identify rockfalls whose potential affected areas by these events (source, transport, and the depositional regions) exceed 10 ha (for large rockfall, TSS_{DEM10m} = 10% vs. TSS_{DEM20m} = TSS_{DEM30m} = 40%). Although in the study area, ≈ 35% of the rockfalls recorded in the field occupy an area greater than 10 ha, the occurrence of phenomena of this magnitude is not common since, generally, the rockfall volume ranges between 10^{-2} to 10^{2} m^3 (Fanos y Pradhan, 2018). Although previous studies have shown a similar relationship between the DEM resolution and the landslide sizes (if the landslides cover a larger area, coarser DEM resolutions result in better landslide susceptibility mapping than finer resolutions), they are not specific to rockfall events (Wubalem, 2022). Although it would be necessary to have a larger validation sample and to carry out a study that delves deeper into the rockfall resolution-size relationship, these results can be taken as indicative of the need to consider rockfall characteristics, specifically its size, when choosing the level of detail of the DEM used to estimate rockfalls using QPROTO.

3.4.3 Rockfall and subsidence mapping

After dividing the road axis into sections of 20 meters, the decision rules described in section 3.3.1.4 were applied to each of these sections, differentiating between each side of the road (to the north, section 1, and to the south, section 2). Thus, each section was classified as rockfall or subsidence. Figure 3.11 includes the qualitative result of this process when using the DEM_{10m}, while the percentage of the road affected by rockfall events is included in Table 3.6.

Unfortunately, available data was insufficient to perform a quantitative validation of the result included in Figure 3.11. However, a graph analysis was developed. For this, the results included in Figure 3.11 were analyzed together with the susceptibility values and the data collected in

the field (four example sites in Figure 3.9), so that the high level of agreement reached between the characterization of the sections of track and reality could be established. Thus, in the case of rock subsidence example 1 (upper-left-corner picture in Figure 3.11), it is observed how correctly the sections of the road at the beginning and exit of the curve would be affected by subsidence on the edge corresponding to section 1 (lane located to the north) while the central section of the curve would also be affected by rockfall on its edge corresponding to section 2 (lane located to the south). A more complex and dangerous situation for the population is observed in the case of rockfall example 1 (upper-center picture in Figure 3.11). On the one hand, the section that is to the south of the water course, at its beginning, presents a risk of subsidence on the edge where the river is located (section 1), increasing said risk along the edge of section 2, the possibility of rockfalls as the road approaches the junction with the said watercourse. Next, the next stretch of track is located to the north of the watercourse, where the possible affectation of subsidence on its edge with section 1 and landslides on the edge corresponding to section 2 transitions to possible affectation by subsidence only due to the edge of section 2, again the place where the Molleturo river is positioned. Additionally, in this section, there are small settlements whose origin dates back to the construction of the road. These results, on the one hand, support the idea of the influence that the existence of populations and watercourses near a communication route can exert. On the other hand, they urge to reinforce the rockfall preventive, security, and control measures in said areas. In the case of rockfall example 2 (bottom-center picture in Figure 3.11), this section of the track would be devastated by a rockfall whose origin is located to the East of said track. Thus, the edge corresponding to section 2 would be affected mainly by rockfalls, while on the edge of section 1, the phenomenon of subsidence would occur due to the displacement of material from the East of the area and would be seen deposited on that edge.

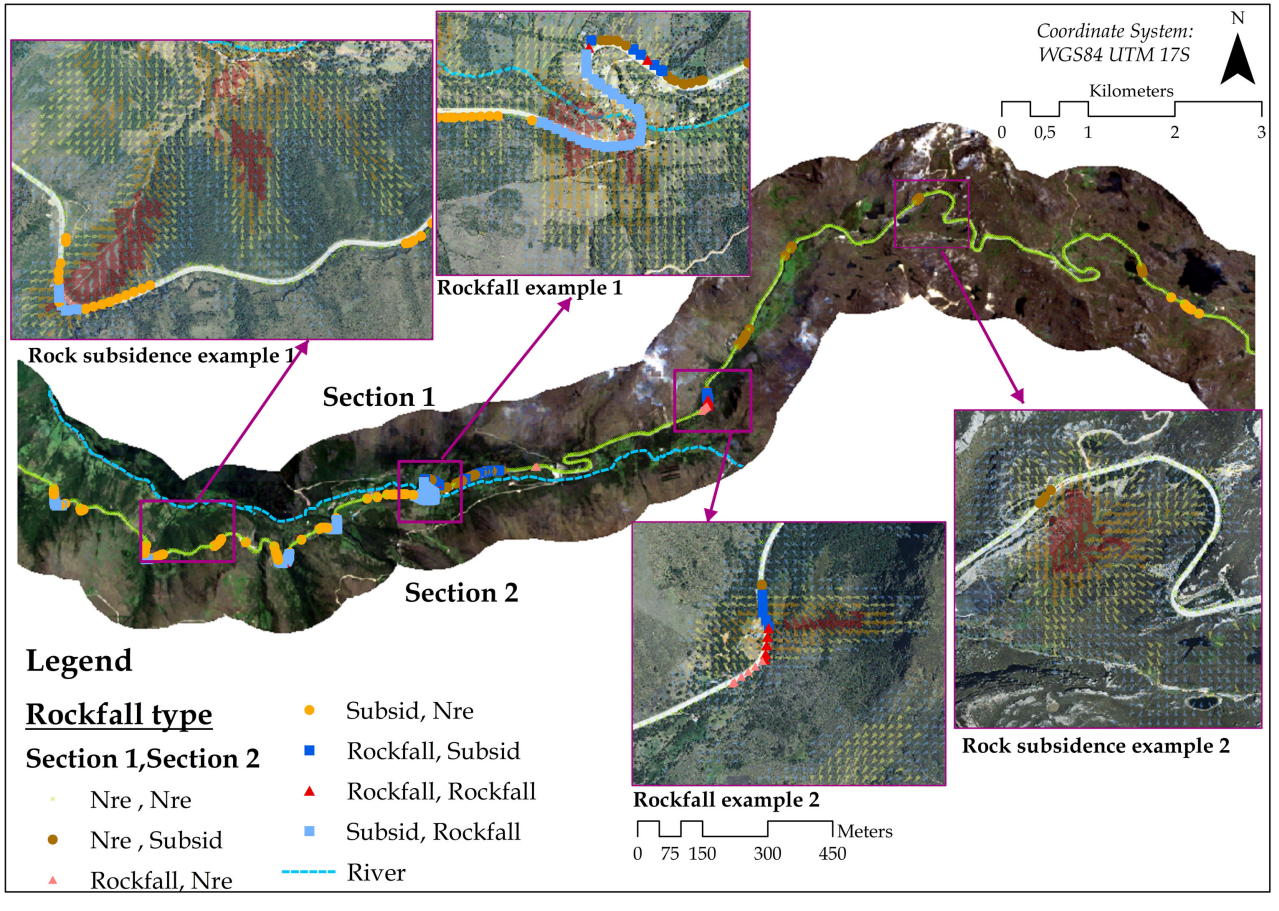

Figure 3.11: Classification of road stretches by the event type: rockfall or subsidence (results using DEM_{10m}).

Table 3.6: Percentage of the road affected by rockfall events.

Event type in … Section 1	Section 2	% Road area
No rockfall events (Nre)		80.8%
		0.0%
		4.3%
		0.6%
		5.9%

Event type in … Section 1	Section 2	% Road area
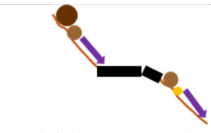		1.8%
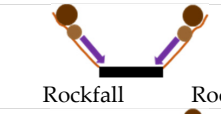		0.6%
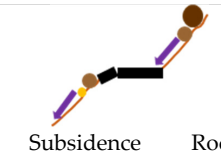		6.0%
		0.0%

Based on the quantitative results (Table 3.6), 20% of the route of the study route is affected by some type of rockfall event, most of them located in the western area where the Molleturo river flows, while the number of rockfall events is much lower on the East Side (Figure 3.11). Most of the surface of this last zone has no vegetation (wasteland is the majority cover according to Figure 3.1) and is characterized by much lower terrain slopes than in the case of the western zone (see Figure 3.1). Based on the results included in Table 3.6, it is verified how the Subsidence-Subsidence and Nre-Rockfall combinations are not found in the study area (Nre-No rockfall events). The first one is very unusual due to the morphology that the land in the vicinity of the road should have (inverted V where the road would pass through the vertex). On the other hand, the most frequent combinations are Subsidence-Rockfall (6.0%) and Subsidence-Nre (5.9%), both types located mainly when the course of the Molleturo river is located to the north of the

study road. Another of the predominant combinations is Nre-Subsidence (4.3%), whose location is also close to the Molleturo River, but in this case when said watercourse is located to the south of the study road (Figure 3.11). Other combinations present in the study area but with less representation are Rockfall-Subsidence (1.8%) and Rockfall-Rockfall (0.6%), the latter being very unusual since the road is crossed by steep slopes and height, particular cases where the construction of tunnels is projected.

3.5 Conclusions

The different procedures and analyses described and developed in this study have shown, firstly, how the rockfall source points selection method, based on a CART analysis, allows a more rigorous selection of source points than in the case of previous studies using simple slope thresholds while increasing processing efficiency. Thus, selecting more than 70% of the real source points is possible, reducing the processing time by more than 80% in relation to the time necessary to process all possible points under the same conditions of the DEM input. The TPI, Slope, and Distance from rivers factors have been decisive for identifying these points, highlighting that these source points are found in areas close to rivers where the slope is less than 37.65° as long as the TPI is greater or equal to 4.6. Additionally, it was observed how the identification of the source points used by QPROTO for the estimation of rockfall susceptibility is carried out more precisely from the proposed methodology if the coarse-resolution DEM is used.

On the other hand, in general terms, identifying the location of rockfall events is not affected by reducing the resolution of the DEM used by QPROTO to identify areas susceptible to rockfall. However, both the surface of the area that can be affected by each event and the magnitude with which it is represented show a direct relationship with the resolution of the DEM, i.e., the lower the resolution, the lower the surface and magnitude with which each rockfall event is represented. Thus, it is difficult to draw generic conclusions regarding the most appropriate

resolution for rockfall susceptibility mapping. However, based on the results obtained, it could be said that for the selection of source points, the coarse DEM is the most appropriate, while for rockfall susceptibility mapping, the DEM with the highest level of detail provides the best precision if the rockfall events have a size of less than 10 ha. Otherwise, the use of DEMs with a lower level of detail is more appropriate. In the line of improving efficiency, the comparison of results using DEMs with different resolutions (DEM_{10m}, DEM_{20m}, and DEM_{30m}) has shown that the results obtained using DEM_{20m} and DEM_{30m} present accurate results and graphically more manageable, readable and interpretable than in the case of using the DEM with the highest level of detail (DEM_{10m}).

The result of the classification of road sections according to the type of condition, where the rockfall susceptibility maps have been taken as a reference, has showed that 20% of the route of the road under study may be affected by some type of rockfall event. At the same time, it is considered a novel, versatile product (possibility of being used regardless of the model used to estimate susceptibility) and that can be very useful for the effective and efficient implementation of the rockfall preventive, security, and control measures, in the study area.

The analyzes that revolve around the influence of the resolution of the DEMs on the different results obtained in this research have completed results achieved in previous studies. However, the research proposed has surfaced new unknowns: What relationship exists between the resolution/quality of the DEM, the type of rockfall morphology, and the method used to estimate the susceptibility to the occurrence of such events? Undoubtedly, the answer to this question involves increasing efforts to make available the tools that allow rockfalls to be estimated/predicted and to develop methods that enable landslide inventories to be developed more efficiently.

As a final reflection, the analyzes carried out in this study are considered particularly relevant both for the prior evaluation of the impact of the implementation of infrastructures, the particular case of communication routes, in environments prone to the occurrence of rockfall events, which would allow to modify the construction

conditions and/or deploy the most appropriate prevention measures for the identified risk circumstances; as well as to establish a posteriori restrictions in relation to land use around these areas, with the main purpose of preventing the loss of human lives and material goods, as well as the consequent disconnection to which the cities that benefit from said infrastructures. Additionally, these results will also help researchers consider the effects of DEM resolution on identifying rockfall source points, the rockfall susceptibility mapping, or the identification of road sections that can be affected by rockfall or subsidence phenomena using automatic prediction tools.

CHAPTER 4

Ground Deformation Monitoring of a Strategic Building Affected by Slow-Moving Landslide in Cuenca (Ecuador)

The prevention and mitigation of slope instability requires effective technologies to reduce the vulnerability of existing structures. Landslides are global phenomena, caused by natural geological phenomena or induced by anthropogenic sources. Slow and intermittent landslides result in a significant number of losses, as well as physical damage and extensive economic losses to private and public property. The physical vulnerability of buildings to landslides is a term used to describe their potential for physical loss when they are affected by movements induced by unstable terrain. Therefore, monitoring plays a key role in the management of natural hazards and assumes a fundamental task to provide cost-effective solutions to mitigate or minimize physical and economic losses. Remote sensing techniques proved to be powerful investigative tools due to their high spatial and multi-temporal coverage, rapid data acquisition and overall reasonable costs. The main aim of the present issue is to provide a general methodology that can be used to predict the spatial and temporal evolution of a slow landslide. In particular, this work analyses a slow-moving phenomenon which affects the University of Azuay (Cuenca - Ecuador). Multi-level analysis integrated with innovative monitoring techniques and geophysical analysis methods lay the foundations for greater accuracy for the prevention and prediction of such phenomena.

Keywords: DInSAR, Geophysical survey, Landslide, Monitoring, Ecuador.

4.1 Introduction

Natural disasters increased in frequency and intensity on a global scale and affected a large part of the world's population, causing human and economic losses and a quality of life that led to the emergence of a number of problems. The countries of Latin America and the Caribbean are the territories most affected by natural phenomena such as earthquakes, landslides, volcanic eruptions, tsunamis and hurricanes. Landslides are among the most important and frequent natural disasters: in fact, after earthquakes, they cause the highest number of victims and damage to artificial structures. For this reason, the evaluation and prevention of the risk of landslides is the fundamental step for a correct planning and management of the territory, as shown by the growing scientific evidence in this field (Albano et al., 2016, Di Martire et al., 2016, Infante et al., 2019, Confuorto et al., 2017). The continuous development of urban contexts led populations to build structures and infrastructures even in unstable areas. An example is the city of Cuenca, Ecuador, which is continuously expanding, and for this reason the local population builds in areas with steep slopes that are at high risk of landslides. The city of Cuenca is located in the highlands of Ecuador at about 2,560 m above sea level, with a urban population of about 400,000 inhabitants rising to 700,000 in the larger metropolitan area. The high slopes, heavy rainfall, poor soil resistance of the city of Cuenca, combined with the high seismicity of the city, lead us to consider a high vulnerability to catastrophic events. In this context, the monitoring of structures plays an increasingly important role in the context of life and management of these natural hazards. Therefore, it is necessary to study the evolution of such events and consider their consequences. Actually, the prevention, forecasting and monitoring of these phenomena are the most suitable tools to minimize side effects. The development of unstable areas in urban contexts has developed a growing interest in innovative approaches to provide information on the temporal and spatial evolution of their interaction with existing buildings. Among the different types of remote sensing techniques, Differential Interferometry SAR (DInSAR (Franceschetti et al., 1992)) complies very well with these needs. In particular, mean displacement rate maps can significantly

influence spatial planning and urban development, especially in areas not yet affected by landslides, allowing the updating of landslide risk maps of the area. In addition, it is of fundamental support to monitor buildings already affected by landslides and for post-event damage assessment. The high accuracy and reliability of satellite data needs to be compared with traditional in situ monitoring and validation techniques in order to validate the data and allow more accurate interpretation. The present study develops in detail an analysis integrated with remote sensing and geophysical investigations carried out at the University of Azuay in Cuenca (Ecuador). This work aims at offering a general methodology to define future damage conditions and local subsidence of buildings within landslide affected areas. This structure is of strategic importance and to date is the most important University in the province of Azuay located in the south-east of Cuenca. Its construction dates back between the end of 1982 and 1984 on unstable slope due to the slow movement from the north of the study area. In this essay will therefore be analyzed phenomena of slow movement that generally do not cause loss of life, but meaningful damage to existing structures and infrastructure with cracks and fractures, such as the building of the Faculty of Philosophy of Azuay which is the most affected. For this purpose, an integrated monitoring and analysis system has been implemented both on a territorial and detailed scale, highlighting the importance of the DInSAR technique as an additional monitoring technique and as an alternative method, at least in the preliminary assessments of the phenomena, to traditional terrain monitoring systems. The present work is structured as follows: the first section will deal with the geological setting of the area where the University of Azuay is located; then the methodologies used and the data already available will be described. Finally, the achieved results and the conclusions will be presented.

4.2 Area of study and Geological Setting

Cuenca is located in the southern part of Ecuador, in the province of Azuay between the two main cordilleras of the Andes at an elevation that ranges from 200 meters above sea level to 4500 m above sea level. The study area is bounded to the east on edge of the Eastern Cordillera (Litherland et al., 1994) and to the west by uplifted Tertiary volcanic arc. The Cuenca basin is filled with Mesozoic marine and subaerial deposits set above a Paleozoic metamorphic basement. This depression is subsequent compressional deformations controlled by major NE-trending faults (Bristow y Guevara, 1980, Noblet et al., 1988, Hungerbühler et al., 2002). The basin fill occurred in two different periods. The first period is characterized by almost continuous sedimentation in a deltaic to marine/brackish environment, with a dominant source by flow directions, fades relations and metamorphic clasts derived from the Eastern Cordillera. The second period is characterized by coarse-grained fluvial and alluvial sediments derived from the west, which were deposited unconformably on the older deformed deltaic deposits. In the University of Azuay area three geological formations can be distinguished (Figure 4.1).

The late Miocene to Plio-Pleistocene Tarqui Formation (TF) is about 300 m thick and abounds in the eastern part of the University of Azuay. A large variety of lithologies, including rhyolitic to andesitic volcanic breccias, ash-flow tuffs, pyroclastic flows, ignimbrites and many airborne tuffs are observed. The intermediate to acid pyroclastic deposits in the upper part of this formation are often altered to dark red and purple kaolinitic clays (Hungerbühler et al., 2002).

The Mangan Formation (MF) is also present in the area of study with a lithology are composed by brown sandstones, green and red shales usually laminated associated with the coal deposits (de Eficiencia Energética, 2000) related to the tertiary period middle

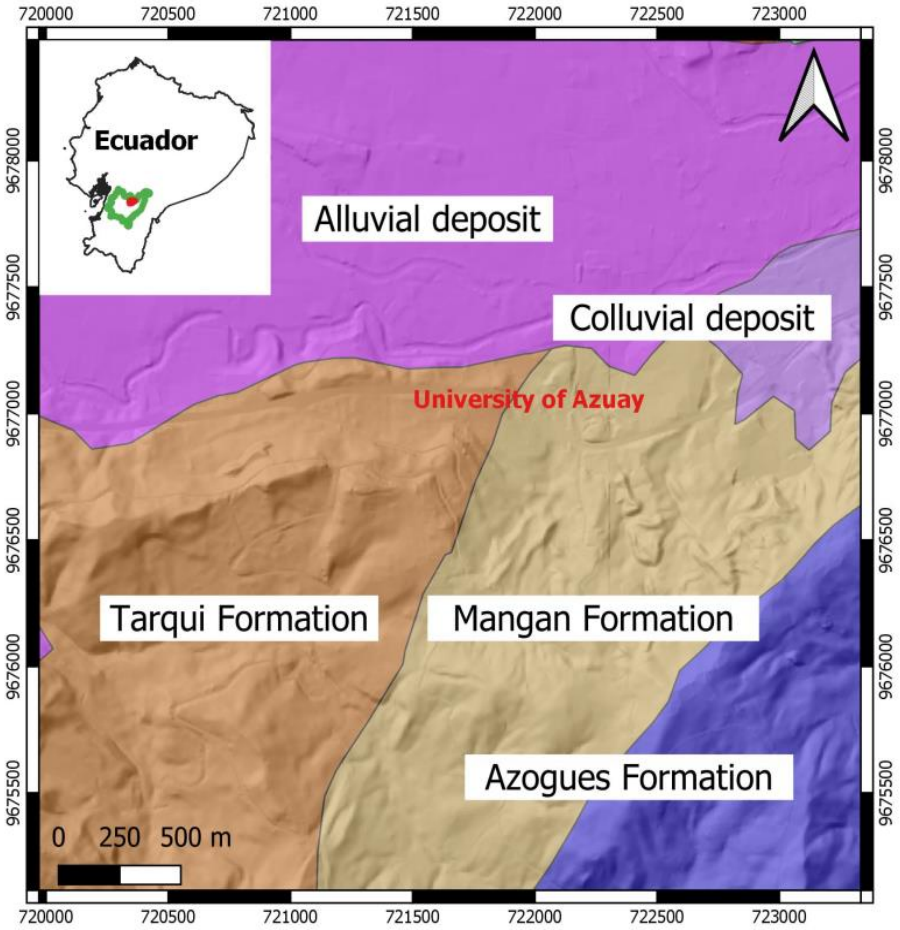

Figure 4.1: Geological sketch map of the study area. Azuay Province limit (green), Cuenca city limit (red).

Miocene. The Azogues Formation (AF) materials are organized in a fluvio-lacustrine ambient. Thematerials present in theformation aremostly brown composed of thick sandstones, shales, conglomerates, clays strata usually not having more than 1 m of thickness and characterized by spheroidal weathering frequently found to the south.

4.3 Data

4.3.1 Amenaza de PRECUPA

An event that marked Cuenca city was the landslide of a part of Tamuga hill, known as the "Josefina disaster", which occurred at the end of March 1993 Figure 4.2). After this event, in the period between 1994 and 1998 the PRECUPA project was born: it shortened PRevention-Ecuador-CUenca-PAute, which was developed within the framework of international cooperation to support Ecuador in strengthening its capacity in the prevention of natural catastrophes Figure 4.3.

Figure 4.2: Josefina Landslide.

The aim was to apply, develop and implement monitoring methodologies and networks that allow the evaluation of different phenomena, their degree of hazard and risk areas, and the application of the results to reduce impacts, based on the transfer of technology that serves the country and is projected in the region. Since then, this information has not been updated. At this preliminary stage, the University of Azuay had already been in the landslide risk area in 1994. This work confirmed this risk and contributed to the redefinition of the boundaries of the risk areas.

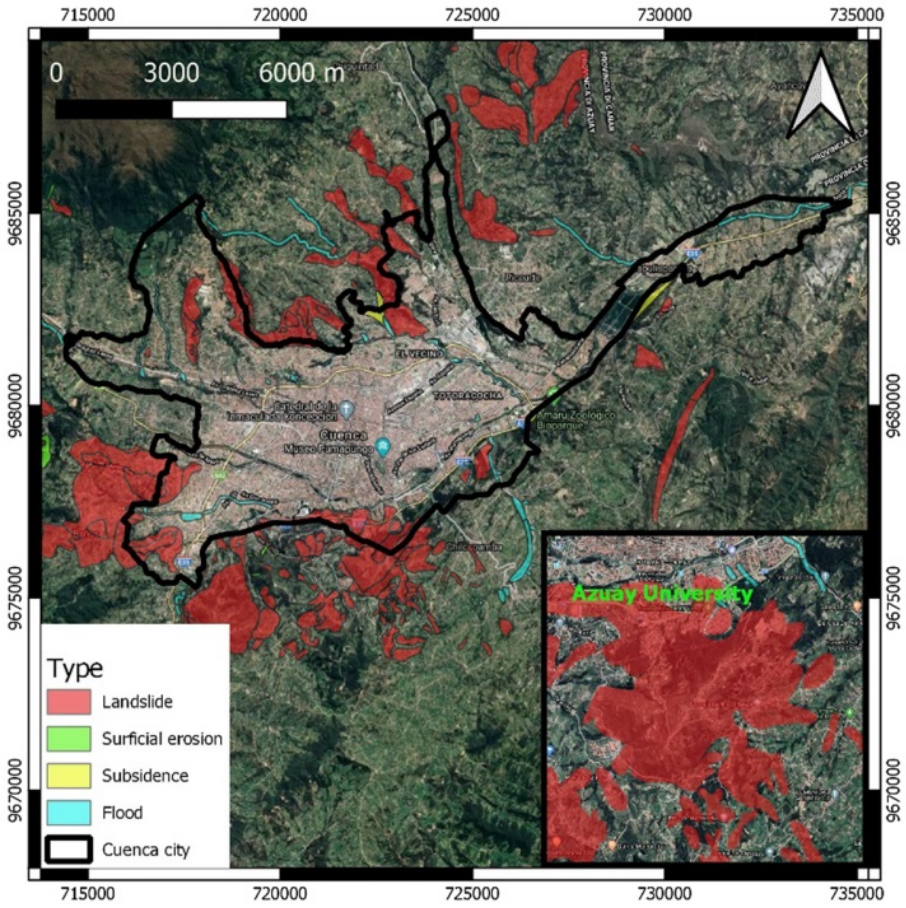

Figure 4.3: Amenaza de PRECUPA map.

4.3.2 DInSAR Data

Thanks to the interinstitutional collaboration agreement between University of Naples "Federico II" and University of Azuay it was possible to obtain 79 SAR images, acquired from the constellation of satellites Cosmo-SkyMed, related to the period March 2016 - January 2018 (in ascending geometry), through a research project with ASI (Italian Space Agency). On this site the available images were processed with the application of the Coherent Pixels technique (CPT (Mora et al., 2003);

(Iglesias et al., 2015) implemented in SUBSOFT software, developed at Universitat Politecnica de Catalunya (UPC - Barcelona). Co-registered images were processed, and all possible interferogram pairs (235) with spatial baseline lower than 300 m were identified. This threshold for spatial baseline values allowed to minimize the error induced by spatial decorrelation. A Digital Elevation Model (DEM), with cell resolution of $3mx3m$, extracted from the regional topographic cartography, was used in order to remove the effect of topography on the interferometric phase. The mean coherence map, which allows to evaluate the reliability of the derived measurements, was then elaborated. A 0.7 coherence threshold was set, in order to identify the points to use for further analyses. This value allows to obtain a phase standard deviation equal to 15°, using a $3x3$ multilook. Finally, the LoS mean displacements rate map and time series of deformations was elaborated. Thanks to the high density of space-time information guaranteed by Cosmo-SkyMed images, it was possible to reconstruct, for each building, the deformation behaviour over time. It represented a valid support, with a view to optimizing time and investigation costs, to the forecasting and prevention of disruptions for the entire decision-making system operating in the field of land management.

4.4 Methods

4.4.1 DInSAR Method

In this work, DInSAR technique was used to assess the displacements in the Azuay University buildings, which are affected by slow-landslide movement. DInSAR is a technique based on the analysis of signal phase differences between two radar images acquired on the same area at different times (Franceschetti et al., 1992). Such technique is used to measure the deformations of the Earth's surface, projected along the Line of Sight (LoS) of the sensor, calculating the difference of phase (interferogram) between two different images related to the analyzed area, acquired in moments of time (time baseline) and from different orbital positions (space baseline). The phase difference $\delta\phi$int is a

function of a series of parameters linked by the following relationship (Hanssen, 2001):

$$\delta\phi int = \delta\phi flat + \delta\phi topo + \delta\phi mov + \delta\phi atm + \delta\phi noise \tag{4.1}$$

where $\delta\phi$ flat is the contribution due to the flat earth, $\delta\phi$ topo is the contribution due to the presence of the topography, $\delta\phi$ mov is the actual contribution due to any movements, $\delta\phi$ atm is the phase difference due to the presence of the atmosphere and finally $\delta\phi$ noise is the contribution due to spatial and temporal decorrelation. Finally, the outcomes of the interferometric chain are: a) mean displacement rate map and b) time series of deformation along the time span investigated.

4.4.2 Geophysical Survey

The geophysical survey, by means of electrical and seismic tomography of refraction and reflection, was carried out in order to know the composition and general features of the subsoil and their properties where the electrical tomography showed to be well adapted to supply information on the depth, thickness and characteristics of geological level (García-Cortés et al., 2008). Seismic refraction establishes the elastic parameters of the materials present in the crust and upper mantle, through seismic velocities in the different horizons of the materials (Fernández Viejo, 1997). These tests define the values of the shear wave velocities Vs and compression wave velocities Vp, which, according to the layer or material, will have a different value.

4.5 Results

4.5.1 DInSAR Results

The area investigated by interferometric technique covers the central-southern sector of the city of Cuenca, where the campus of the University of Azuay is located. The area is about 10 km^2 and the processing allowed to identify about 24,000 targets with a density of about 2400 targets/km^2. The mean displacement rate map was obtained Figure 4.4) from the processing of the interferometric data. The points represent the mean velocity, on the basis of which it is possible to distinguish stable areas from the unstable ones indicated with the green and red dots respectively. It can be noted that the University of Azuay is characterized by a greater concentration of red targets indicating potential ground displacement.

Starting from the interferometric results, taking into account that this area has already been classified as risk area (Amenaza de PRECUPA map) since 1994, it was possible to refine the risk zone of this area Figure 4.4. Within the identified area, about 400 targets were identified, characterized in some cases by maximum velocities of about 1.5 cm/year.

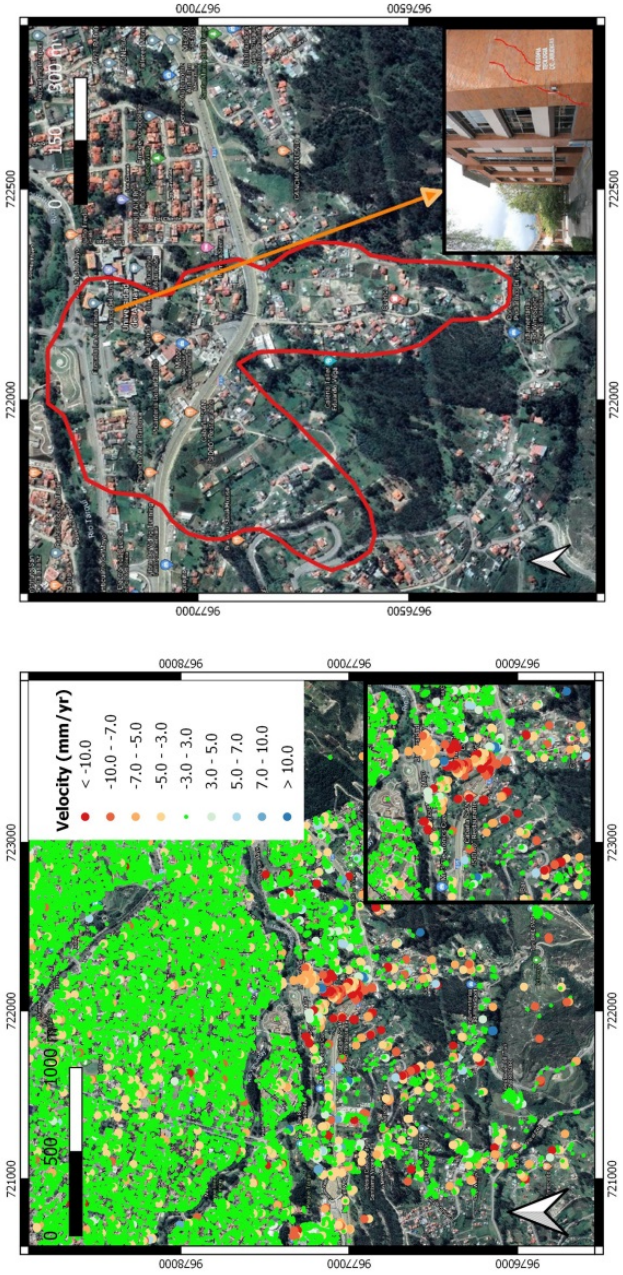

Figure 4.4: Mean displacement rate map and Area affected by slow-moving landslide.

4.5.2 Geophisical Results

Electrical Tomography

The electrical tomography consisted in 32 electrodes, covering a length of 155 m. They start from the upper part of the campus, giving different resistivity values between 3 and >80 ω as shown in Figure 4.5, where at a depth of about 17 m from the ground level there is a low resistivity material, as well as blocks of higher resistivity that were displaced.

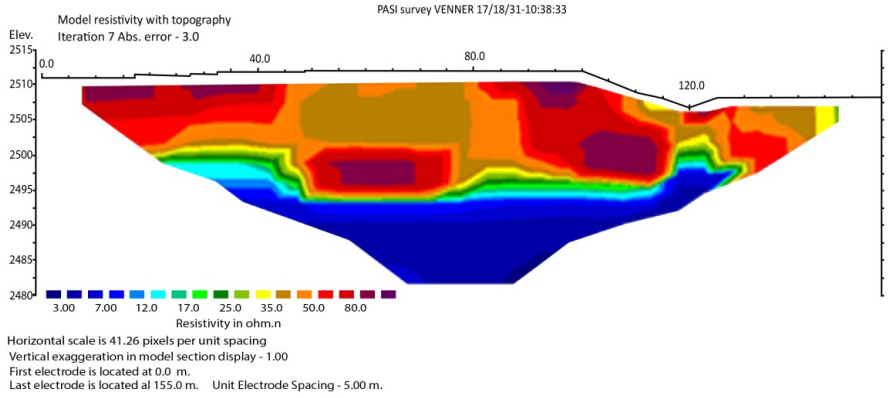

Figure 4.5: Electrical tomography cross section.

Seismic Refraction and Reflection

Here a 23-m line analysis was taken inside the campus of Universidad of Azuay and a 36-m line outside the campus, where 24 geophones were used, varying the spacing depending on the space conditions of the area, using the same configuration for the ReMi and MASW tests, while, for the ESAC test, a perpendicular configuration was used. With these tests, the values of the shear wave velocities Vs and compression wave velocities Vp are obtained, as well as the Poisson module that helps with the detection of groundwater level since its behavior is directly related to the humidity and density of the ground Suárez et al. (2008). Cross sections of geophysic lines are represented in Figure 4.6 and Figure 4.7, where a consistent water saturation, starting at about 5 m depth in both lines, lines, was identified.

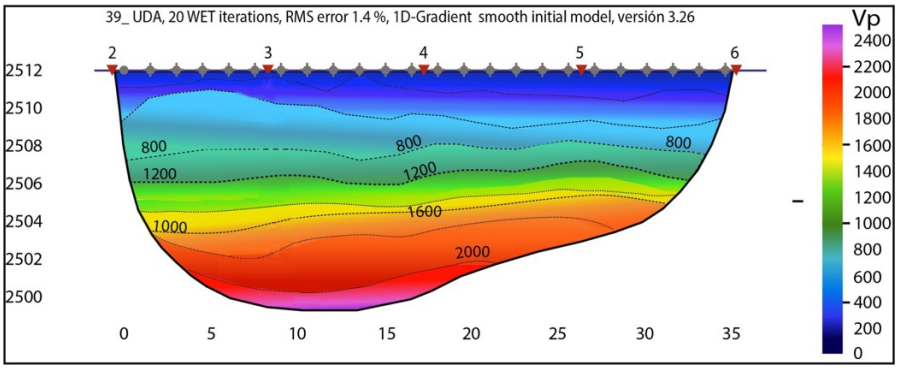

Figure 4.6: Stratification of the seismic line outside the Campus

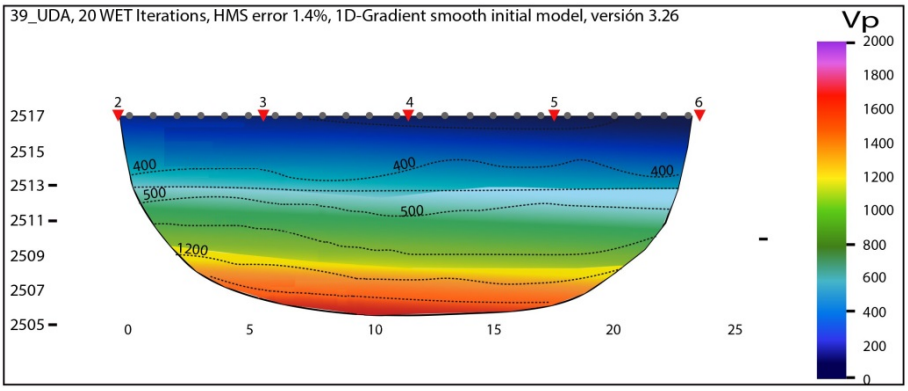

Figure 4.7: Stratification of the seismic line inside the campus

4.6 Conclusion

The prevention and mitigation of slope instability requires effective technologies to reduce the vulnerability of existing structures. Subsidence and landslides in particular, are widespread phenomena at global level, caused by natural geological and climatic processes or induced by anthropogenic sources. The Andean region of Ecuador is susceptible to landslides due

to its propitious characteristics of slope, geology, climate, among other things; these events affect the center of towns and infrastructures and should be considered in urban and rural planning. Slow and intermittent landslides cause a significant number of losses, as well as physical damage and extensive economic losses to private and public property. The physical vulnerability of buildings to landslides is a term used to describe their potential for physical loss when they are affected by movements induced by unstable terrain. Therefore, monitoring plays a key role in the management of natural hazards and assumes a fundamental task to provide cost-effective solutions to mitigate or minimize physical and economic losses. In recent decades, DInSAR remote sensing techniques have proven to be powerful investigative tools due to their high spatial and multi-temporal coverage, rapid data acquisition and overall reasonable costs. The main aim of this paper was to provide an integrated monitoring methodology that can be used to predict the spatial and temporal evolution of a slow landslide which affects buildings inside the campus of Azuay University. Multi-level analysis integrated with innovative monitoring techniques together with traditional and detailed methods such as geophysical surveys, is a valid strategy for continuous risk update. This represents the first step to prevent and mitigate the risk of natural disasters such as landslides which affects the city of Cuenca, a UNESCO World Heritage Site. Cuenca is in continuous expansion, and, at the same time, affected by many landslides. The latter represent a major problem for the population and existing structures. This work provides a preliminary stage of control and monitoring to decrease the vulnerability of the city.

CHAPTER 5

The Use DInSAR Technique for the Study of Land Subsidence Associated with Illegal Mining Activities in Zaruma - Ecuador, a Cultural Heritage Cite

Zaruma, a well-known mining district in the province of El Oro in Ecuador, suffers from subsidence phenomena related to illegal underground mining. Mining in this area goes back to the pre-Hispanic time; recorded history shows the first settlements of the Cañari culture and thru the Inca culture, and passing from the Spanish, American, and Canadian presence in the area up to modern times. Mining in this district has been in a constant transition from legal to illegal mining, technical and non-technical mining, prevailing activities in the present are illegal and non-technical over what is declared as the nonexploitation area under the city of Zaruma. This brings a series of problems among this land subsidence affecting the city cited as a cultural heritage cite; subsidence and collapses have accrued sporadically in the past, but in recent years (since 2017) this phenomenon has become a relatively consistent manner. In fact, December 15th, 2021, is the most recent sinkhole event resulting in the evacuation of over 300 people and the banning of over ten city blocks. For this reason, it is essential to find a quick and economical technique that can generate information about the spatial and temporal development of uncontrolled underground activities to improve risk management. In this work, the Differential Interferometry Synthetic Aperture Radar (DInSAR) technique, implemented in the SUBSIDENCE software, has been used to study terrain deformation related to illegal artisanal mining in Ecuador (Ammirati et al., 2020). This work presents an up-to-date study of the monitoring and detection

of subsidence phenomena in the city of Zaruma, as part of a collaboration project between local and international Universities allowing to detection and monitor surface deformations using DInSAR techniques as a tool applied to monitoring mining-related subsidence phenomena.

Keywords: DInSAR, risk management, ground subsidence, mining subsidence, illegal mining, Zaruma subsidence.

5.1 Introduction

It is known that underground mining activities can negatively affect subsidence and sinkhole phenomena (Marcus, 1997, Carrión-Mero et al., 2021). Particular attention must be paid when such activities are developed near urban areas and primarily when such activities are conducted without any regulation (Oliva-González et al., 2017). This is the case of the city of Zaruma in Ecuador, located in the southeast of the Province of El Oro, characterized by one of the most crucial Ecuadorian gold deposits (Ammirati et al., 2020, Marcus, 1997, Carrión-Mero et al., 2021, Oliva-González et al., 2017), where in December 2021, some buildings collapsed due to the formation of a sinkhole.

The social component has been a fundamental part of the mining history of Zaruma. It is currently a controversial issue since 65% of the economically active population depends directly or indirectly on this industry. The first mining company, the Great Zaruma Gold Mining, was formed in 1880, which was awarded the exploitation in several zones of Zaruma district, bringing significant changes to the mining environment and considerably increasing the open and later abandoned galleries. Later, the South American Development Company (SADCO) acquired the most considerable concessions in the area of Zaruma and later acquired many other veins. In 1923 it averaged 800 workers and 200 employees, who worked 300 days a year, extracting a combination of gold and silver ratio of 92.6%; the company brought with it a mining boom for Zaruma. In 1939 a concentration plant was set up, taking a huge step forward in terms of mineral transformation. The Mining Regulation and Control Agency (ARCOM) currently registers 92 mining concessions between Zaruma and Portovelo, with around 65 km of galleries (Oliva-González et al., 2017). The current mining situation in Zaruma is, in a sense, the key to the current problem of subsidence, resulting from many small-scale mining actors and artisanal miners, as well as the intervention of illegal miners who arrived in the region and began mining the galleries that had previously been abandoned.

It is worth pointing out that mining activity was developed without considering the consequences that this activity could generate. The

conditions of exploitation and benefit were not the best, and many tunnels and galleries were carried out in a very antitechnical way; in turn, the population of Zaruma continued to grow. Therefore, a study of the subsoil's geotechnical asset and the possible effects of such tunnels on the built environment is of fundamental importance. In recent years, monitoring techniques have been developed to investigate surface deformation with sub-centimeter accuracy in order to prevent the occurrence of catastrophic phenomena such as sinkholes in urban environments (Rispoli et al., 2020). Among the different techniques, Differential SAR Interferometry (DInSAR) (Franceschetti et al., 1992) has proven to be among the most effective for monitoring surface deformations in urban environments (Del Soldato et al., 2019, Miano et al., 2021, Mele et al., 2022, Ponzo et al., 2021, Talledo et al., 2022), therefore useful in the context of procedures for sinkhole susceptibility assessment (Parise, 2015). In this work, analyses for the evaluation of the effects of subsidence on buildings induced by the presence of the tunnels were firstly carried out, and then processed, using the DInSAR technique, images from the SENTINEL-1 constellation for the period 2018-2021 that allowed to verify the deformation trend before the collapse that occurred in December 2021.

5.2 Study area and geological setting

Pre-Mesozoic metamorphic rocks characterize the region's geology, encompassing the Amotape -Tahuin (Ta) massif in the south and the Chaucha metamorphic and volcanic rocks in the north (Pilatasig et al., 2005), all overlaid by younger volcanism. The most relevant feature structurally is a tremendous regional fault of Portovelo that separates the Cretacic volcanics of the Celica formation from the Tahuin metamorphic and constitutes the limit of the mineralization in the Zaruma - Portovelo mining district. The Zaruma Urcu Rhyolite (RZU) is another representative lithology in the area consisting of dyke stocks and rhyolitic intrusions (Van Thournout et al., 1996). The basement of the Zaruma area, referred to as the El Oro metamorphic complexes overlaid by calc-alkaline materials of the Saraguro formation (FM Sa)

of subaerial depositional characteristics, is well known to southern Ecuador (Figure 5.1b). The Saraguro formation comprises a variety of lithology's andesite's, andesitic basalt lavas, highly weathered andesitic tuffs, dacitic tuffs, and ignimbrites (Litherland et al., 1994, Pratt et al., 1997). Predominant volcanic rocks in the area are characterized by high weathering and intense surficial reworking, ranging from poor to inferior quality. These characteristics notably increase terrain instability. The Zaruma gold deposits are considered epithermal origin, genetically associated with calc-alkaline Eocene to late Miocene igneous complexes in central and southern Ecuador (Billingsley, 1926, Van Thournout et al., 1996); these features all run under de city area and are the main target for legal and illegal mining activities.

In order to implement a geological-geotechnical model, the boreholes realized in the investigated area have been considered (Figure 5.1a). A geotechnical profile along some of the boreholes mentioned above has also been drawn (Figure 5.2). This profile has been used to evaluate the settlements induced at ground level by the presence of the tunnels.

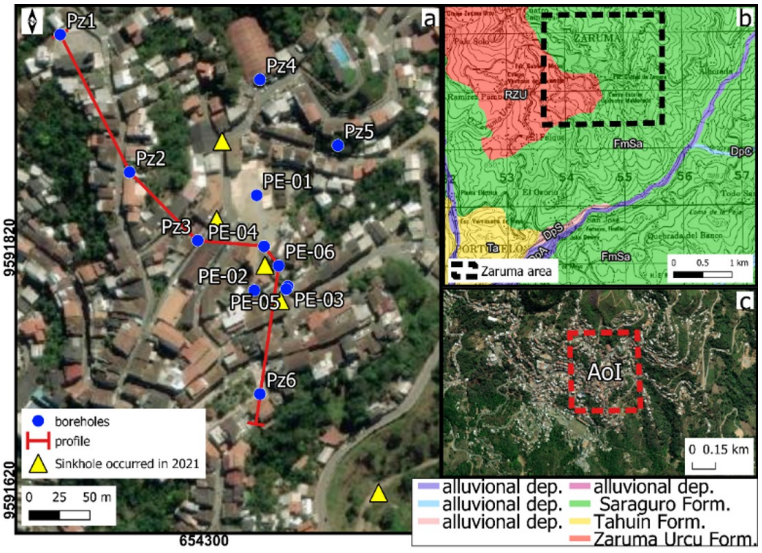

Figure 5.1: Study area: a) Location of boreholes, sinkholes reported (see Section 5.4.2) and profile of cross section AA' (Figure 5.2). b) Geological sketch map. c) Location of the area of interest.

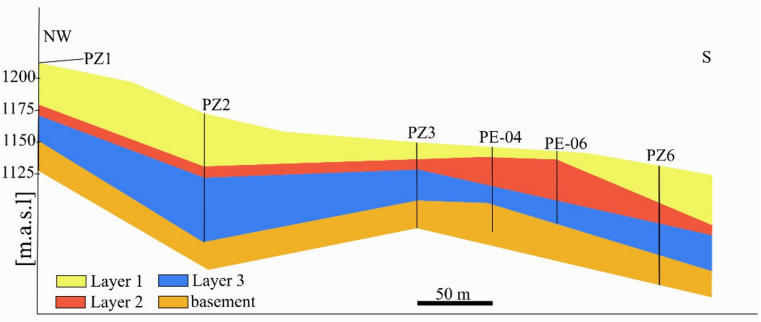

Figure 5.2: Section along some of the boreholes shown in Figure 5.1).

5.3 Data Set and Methods

5.3.1 Sentinel Data

In this work, Sentinel-1A and B ascending mode images, obtained via the Sentinel Scientific Data Hub, were acquired in the time span from January 2018 to December 2021 (Table 5.1). In detail, 113 C-band strip maps in ascending mode images, characterized by a ground resolution of 20 x 4 m were processed by the SUBSIDENCE software, which implemented Coherent Pixels Technique - Temporal Phase Coherence (CPT-TPC) approach (Mora et al., 2003, Iglesias et al., 2015) and developed at Remote Sensing Laboratory (RSLab) of the Universitat Politecnica de Catalunya of Barcelona has been used.

Table 5.1: Synthetic aperture radar (SAR) data stacks analyzed in this study.

Mission	Acquisition time	Product	Images	Pass	Polarization
Sentinel-1	January 2018 December 2021	Single look complex (SLC)	113	Ascending	VV

5.3.2 Geotechnical Analysis

An integrated approach based on geotechnical modeling and DInSAR was used to purpose the aims. The first is a general geotechnical finite element analysis obtained using PLAXIS B.V. (Delft, Netherlands), widely used to analyze various complex geotechnical projects. It can be used to solve the solidification analysis of problems involving super-porous pressure growth and dissipation, as well as the plastic analysis of foundations, excavations, supports, loading, etc. Using a convenient graphical user interface, the application quickly creates a geometry model and finite element mesh based on a representative vertical cross-section of the problem. A plane strain or an axisymmetric model may be used to simulate 2D real-world situations. There are four subroutines in the user interface (Input, Calculations, Output, and Curves). The input program defines the problem geometry, creates a finite element mesh, and specifies the calculation phases. The first step for numerical modeling is to create the model geometry. The model's geometry is created according to the thickness of the layers, dimensions, and tunnel depth. A geological profile (stratigraphy) is a rock material with different thicknesses and three layers (Table 5.2).

Table 5.2: Physical-Mechanical parameters for each Geological layer (1: Saprolite, 2: weathered rock, 3: medium weathered rock (Moreno Morejón, 2019)).

Material	**Specific weight** (MN/m^3)	**Module of Young** (Mpa)	**Coefficient of Poisson**	**Angle of friction** (°)	**Cohesion** (Mpa)
Layer 1	0.027	0.617	0.11	5.50	0.04851
Layer 2	0.027	303.17	0.11	2.40	0.09500
Layer 3	0.027	480.35	0.11	36.98	0.19100

A borehole is used to define rock layers in Plaxis software. By defining a borehole, rock layers of different thicknesses are created. The tunnel has also been excavated at different depths with different dimensions. The geotechnical characteristics of the materials follow the Mohr-Coulomb model and require five parameters, including Module of Young, Poisson's ratio (ν), the angle of internal friction (φ), cohesion

(c), and dilatancy angle (Ψ), which is less than other models, so, Mohr-Coulombs model was chosen in this work. These parameters are summarized in Table 5.3.

Table 5.3: Geotechnical parameters (Moreno Morejón, 2019).

Parameter	**Layer 1**	**Layer 2**	**Layer 3**
γ_d (kN/m^3)	27	27	27
γ_{sat} (kN/m^3)	27	27	27
E (kN/m^2)	617	303170	480350
ν(-)	0.11	0.11	0.11
c (kN/m^2)	48.51	95	191
φ (°)	5.5	2.4	36.98
ψ (°)	0	0	0

The Output is a post-processor that displays the results of calculations in a twodimensional view or cross-section, as well as plots graphs (curves) of output quantities of selected geometry points.

5.3.3 DInSAR Analysis

DInSAR approach is a highly effective tool for detecting, with sub-centimetric accuracy (Wasowski y Bovenga, 2014), deformation phenomena of the Earth's surface, based on the use of time series of radar images (Del Soldato et al., 2019), acquired by sensors installed on satellite platforms that travel along semi-polar orbits defined ascending and descending. The interferometric approach is based on the observation that radar targets, namely Permanent Scatterers, maintain the same "electromagnetic signature" in all images, as the acquisition geometry and weather conditions vary, thus preserving information over time. PS are typically parts of buildings, metallic structures, rocks, or elements already present on the ground, for which the electromagnetic characteristics do not vary appreciably over time.

Interferometric analyses work on radar images that are arrays of pixels, each associated with a resolution cell. An image contains

amplitude and phase information. The amplitude identifies the portion of the electromagnetic field incident on all objects belonging to the ground resolution cell and backscattered toward the sensor (Line of Sight). The phase is given by the contribution of multiple terms, summarized in the following equation (Eq. 5.1):

$$\varphi = \psi + \frac{4\pi}{\lambda} r + \alpha + n \tag{5.1}$$

where ψ is the phase term due to the reflectivity of the target, α is a contribution related to the atmosphere, r is the distance sensor - target and n is a noise of the acquisition system, related to the curvature of the earth, the signal-to-noise ratio (SNR) and instrumental noise. The $\frac{4\pi}{\lambda}$ factor is referred to as the propagator term (Blanco, 2009).

Therefore, the phase values of radar images contain information on the double sensor-target path taken by the signal and, therefore, constitute the essential information for all interferometric techniques. By comparing a stack of images on the same area, where specific targets (PS) will be identified, it will be possible to obtain maps of mean displacement rates and the time series of the deformations measured along the LoS.

5.4 Results

5.4.1 Geotechnical Results

Since the numerical modeling, the tunnel has also been excavated at different depths, varying between 50 and 80 m, with different dimensions, between 6 and 20 m. Different boreholes are used to define rock layers in Plaxis software. By defining boreholes (Litherland et al., 1994), rock layers of different thicknesses are created. Figure 5.3 shows the geometry modeled in Plaxis software for 0 + 100, 0 + 120, 0 + 140, 0 + 150 m.

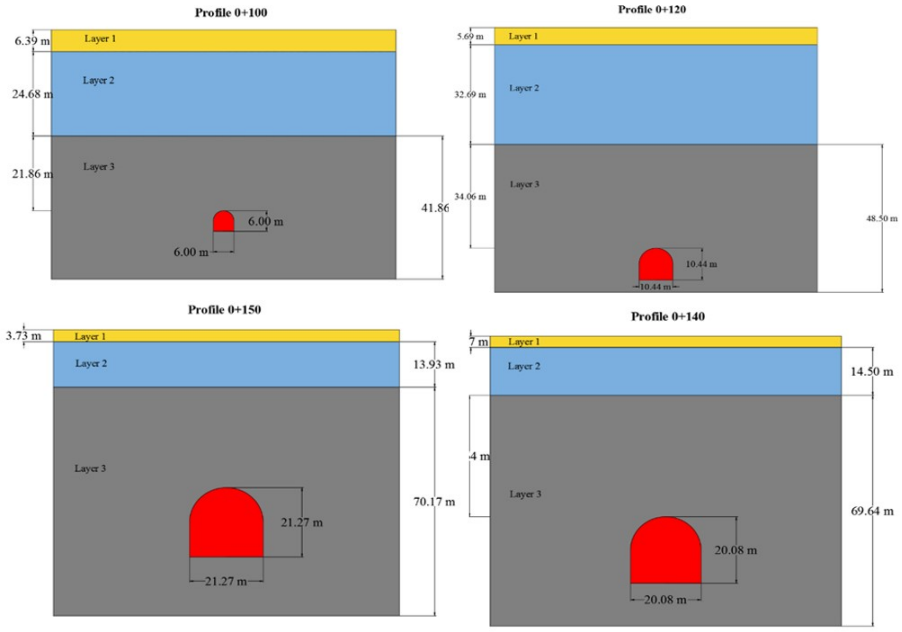

Figure 5.3: Geometry modeling for 0 + 100, 0 + 120, 0 + 140, 0 + 150 m.

The cross section is reported in Figure 5.1. A material model with the Mohr-Columbus criterion has been used to model the behavior of rock layers. After creating the stratigraphy in Figure 5.3, the geotechnical parameters of the materials are assigned to each layer.

After creating the initial effective stresses in the second phase, the tunnel is excavated. In this phase, the cluster inside the tunnel is deactivated. After defining these two phases, calculations are performed, and the outputs can be checked. Figure 5.4 shows the deformations caused by tunnel excavation in meters of 0 + 100, 0 + 120, 0 + 140, 0 + 150 respectively. Also, Figure 5.4 shows the amount of deformation of the ground surface due to tunnel excavation. Higher deformation values are recorded in correspondence of 0 + 140 and 0 + 150 sections, with values of about 70-80 mm, while lower values are registered in 0 + 100 and 0 + 120 sections, with values variable between 5 and 20 mm (Figure 5.5).

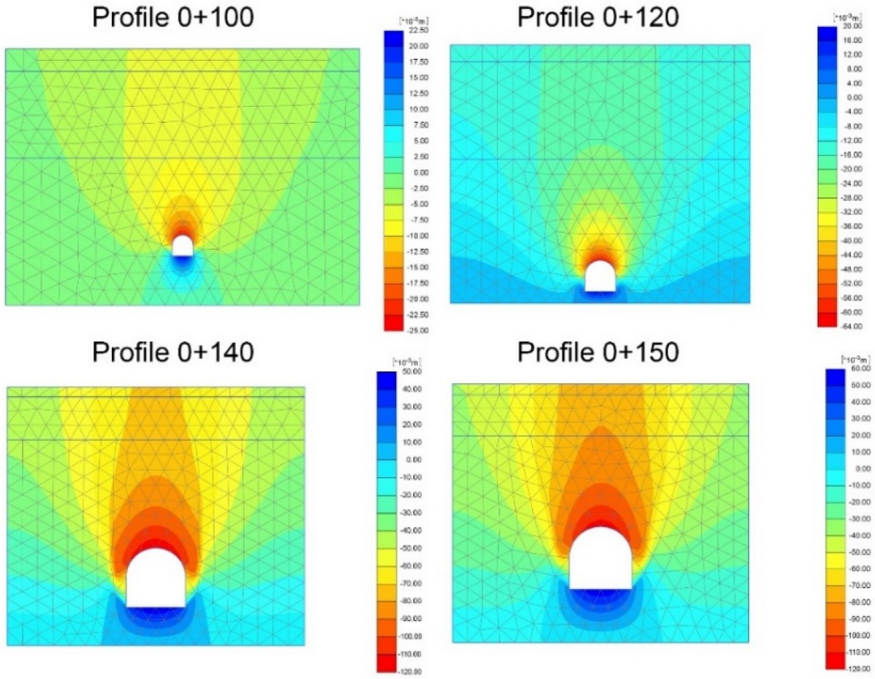

Figure 5.4: Plaxis results.

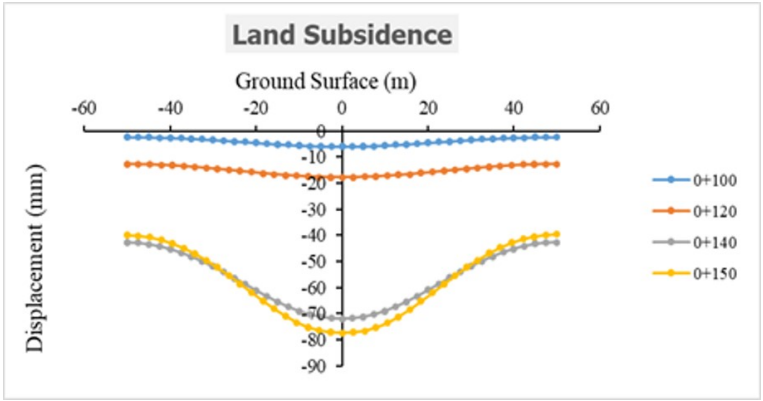

Figure 5.5: Settlements profiles 0 + 100, 0 + 120, 0 + 140, 0 + 150 m sections.

5.4.2 Interferometric Results

CPT-TPC has been used to obtain ground displacements from satellite radar images. In detail, all images have been co-registered starting from the ascending dataset. Using spatial and temporal baseline thresholds of 100 m and 100 days, respectively, it was possible to identify 947 interferograms. Moreover, CPT-TSC allows to select points in the investigated area, characterized by a phase quality higher than a threshold value set by the operator according to the error in the displacement estimation considered acceptable (in this case less than 1.5 mm), which in turn is a function of the expected mean displacement rate. In this case, a phase quality value equal to 0.7 has been set to obtain an acceptable displacement error lower than 1.5 mm, and select an adequate number of points.

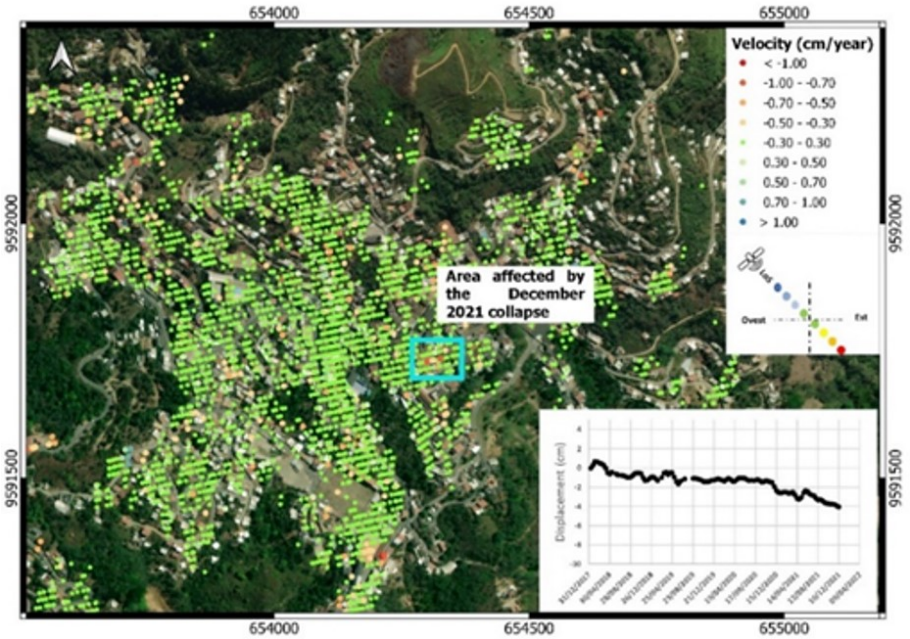

Figure 5.6: Mean displacement rate map obtained through the SENTINEL-1 images processing and the time series of displacement of a point located in correspondence of the area affected by the December 2021 collapse.

In Figure 5.6, map of the primary displacement rates recorded over

the analysed time interval is shown. In the blue square, it is possible to observe how in the area affected by the collapse of 15 December 2021, the identified PSs showed significant deformation rates, higher than 0.5 cm/year. Even more significant element is the time series of these points, which shows an acceleration starting from June 2021, thus six months before the collapse. In addition, it is emphasized that the analyses were conducted until December 10, 2021, while the collapse occurred on December 15, 2021, highlighting the suitability of this technique in terms of forecasting. In order to verify interferometric results field survey has been carried out following Sellers et al. (2021b), using MARLI (Mobile application for regional landslide inventories) application.

It is essential to point out that other sectors have shown significant displacement rates. Therefore, it will be necessary to carry out studies to avoid phenomena such as those that occurred in December 2021.

5.5 Conclusions

As known, the city of Zaruma in Ecuador is among the most sinkhole hazard sites in the world (Marcillo-Delgado et al., 2021). This dangerousness is related to a dense network of legal and illegal tunnels, many of them unknown, increasing the municipal territory's fragility. In fact, several phenomena have been recorded in recent years, particularly in 2016 with the collapse of the Inmaculada School and in 2021 with the collapse of 4 buildings.

On the one hand, we know that the excavations done anonymously are illegal and lack any concrete supports, which may explain why the results of radar processing are more precise than those of Plexis software. On the other hand, we worked in a time series when we processed radar images, which gives us a more accurate determination of displacements in the area since Plexis software examines the pre-and post-drilling displacements.

Therefore, with this study, it was possible to highlight the need to implement a continuous monitoring system, for example, in order to

utilize remote sensing techniques, to prevent phenomena such as those that occurred in 2016 and 2021 by identifying those areas of the city that need a more comprehensive knowledge of the subsoil that is probably affected by excavation activities to date still unknown.

CHAPTER 6

The role of risk management and governance.

6.1 Background

The Sendai Framework for Disaster Risk Reduction 2015 - 2030), it is the successor instrument to the *Hyogo Framework for Action: Increasing the resilience of nations and communities to disasters* and was adopted at the third United Nations World Conference held in Sendai, Japan, on the 18 of March, 2015. It is considered the product of a series of consultations among interested parties for Disaster Risk Reduction. The Sendai Framework can be considered the first milestone that leads to a paradigm shift since prevention and risk management are prioritized instead of crisis management, with the main purpose of avoiding loss of life and the economic effects of material losses. Thus, the Framework urges countries, before 2030, to deploy **national and local strategies** where their main objectives are 1) to improve the resilience of communities, 2) to increase scientific knowledge and early warning, and 3) to increase the preparedness of the population before disasters. Thus, **prevention and governance are the main pillars on which efforts to deal with natural disasters must be based**.

The Framework sets seven global targets for disaster risk management:

- **Reduce the mortality rate** per 100,000 inhabitants due to disasters.
- **Reduce the number of people affected** per 100,000 inhabitants due to disasters.
- **Reduce damage to vital infrastructure and disruption to basic services**, increasing the resilience of health and educational facilities.
- **Increase the number of countries that have disaster risk reduction strategies** at the national and local levels by 2020.
- **Improve international cooperation** for developing countries.
- **Increase the availability of early warning systems** on multiple hazards and increase the information on disaster risk transmitted to the population.

Ecuador has been associated with the Sendai Framework since 2015, since then it has been focused on adopting measures on the three dimensions of disaster risk (exposure to threats, vulnerability and capacity, and characteristics of threats) in order to prevent the occurrence of new risks, reduce existing risks and increase resilience. In this context, the Constitution of the Republic of Ecuador determines that the National Decentralized Risk Management System will be made up of the Risk Management Units, with the attribution of *coordinating actions and strategies that allow the mainstreaming of risk management between the public and private sector.* In this way, support is provided to the Municipal and Metropolitan Decentralized Autonomous Governments (GAD) to materialize the incorporation of risk management in their municipal and territorial development processes. For this, they developed the instrument that allows the articulation and coordination between the instances and actors that will make up the Cantonal Disaster Risk Management System and facilitate the execution of actions to generate knowledge of risk and reduce possible human and economic losses.

These facts are institutionalized in article 140 of the Organic Code of Territorial Organization, Autonomy and Decentralization

(COOTAD), which establishes: *Municipal GADs will obligatorily adopt technical standards for the prevention and management of risks in their territories with the purpose to protect people, communities and nature, in their territorial ordering processes.* For its part, Article 11 of the Organic Law on Territorial Planning, Land Use and Management (LOOTUGS) determines that the Municipal and Metropolitan GADs must *classify all cantonal land, as well as define the use and soil management and the identification of natural and anthropogenic risks.*

In parallel, the National Service for Risk and Emergency Management (SNGRE) establishes five *guidelines for the Governance of Disaster Risk Management in the Municipal and Metropolitan GAD* that seek to mainstream disaster risk management in the different processes and services provided by the GAD. These guidelines are part of compliance with the national policies established in the National Development Plan and in global guidelines such as the Sustainable Development Goals (SDGs), the Paris Agreement as well as the Sendai Framework for Disaster Risk Reduction. Additionally, it converges with the objectives of the World Campaign for Resilient Cities of the United Nations Office for Disaster Risk Reduction (UNRRD).

The SNGRE guidelines are:

- Guideline 1: Form the **cantonal risk management system** - SCGR.
- Guideline 2: **Regulate disaster risk management in the Municipal GAD**.
- Guideline 3: Form the **risk management unit** and strengthen its articulation with other municipal agencies.
- Guideline 4: Execute **strategic disaster risk management actions** as a transversal axis in the different processes and services provided by local governments.
- Guideline 5: **Progressive increase in strategic actions for disaster risk management** in the territory.

Specifically, the contributions derived from this doctoral thesis are mainly focused on guideline 4. In the said guideline, 19 strategic actions were established (Figure 6.1), which contemplate the stages of analysis, reduction, preparation, response, and recovery to disaster risk, all aimed at developing resilience.

The first five actions contemplated in said scheme (evaluation of 1) threats, 2) the exposure of the elements in the territory, 3) the vulnerability of the elements in the territory, 4) zoning the risks to disasters, and 5) monitoring the risks present in the territory) are considered essential and critical to understanding the risk of disasters in the territory. However, it is impossible to start such a cycle if the location of the threats is unknown. In this sense, when evaluating the risk governance process in Ecuador and the available information, particularly from the province of Azuay and the canton of Cuenca, it was possible to verify the existence of severe cadences concerning risk management, in general and the risk of landslides (mass movements), in particular. These phenomena are frequent in the Cuenca canton and have come to create problems for the population and cause the destruction of infrastructures.

Figure 6.1: Acciones estratégicas de la Gestión del Riesgos de Desastres incluidas en el lineamiento 4. Source: https://www.gestionderiesgos.gob.ec/wp-content/uploads/downloads/2021/12/RESOLUCION-SNGRE-155-2021.pdf.

An event that marked the region was the slide from Mount Tamuga that occurred on the left bank of the Paute River in the southern Andes (Figure 6.2). This event, which occurred at the end of 1993, is known as the Josefina disaster and evidenced both the vulnerability of the infrastructures and the population. The balance: more than 70 victims between dead and missing and damage to industrial facilities valued at 150 million dollars. From that event, susceptibility studies and landslide inventories were carried out in the said region, the most relevant being the Prevención-Ecuador-Cuenca-Paute pilot project (PRECUPA project). This initiative was developed within the framework of international cooperation in order to support Ecuador in strengthening its capacity to prevent natural disasters (more details in Basabe et al. (1996)). The studies carried out between 1994 - 1998 recognized the Paute basin's vulnerability to unstable terrain and the need to carry out more studies in the entire basin. Despite these results, the last update of the landslide risk map occurred in the year 2000, where some data generated from the PRECUPA project was updated. Therefore, despite what has been experienced and the evidence, the starting situation is the **lack of a detailed cantonal inventory of landslides and the absence of strategies and initiatives to develop one**.

Additionally, extreme climatic events affect the stability of natural and engineered slopes and have consequences on landslides (Gariano y Guzzetti, 2016). Several studies have raised the impact of climate change on landslides (Petley, 2010, Coe y Godt, 2012). In this scenario, an increase in the temperature of the earth's surface is estimated, which influences the intensity and frequency of rainfall, increasing the occurrence of landslides and, therefore, the risk to goods and people. Latin America will be one of the regions most affected by this chain of phenomena (Gariano y Guzzetti, 2016). Petley (2012b) showed in his study that research can play an essential role in reducing the impact of these phenomena so that countries with higher levels of research present fewer fatalities. Although there has been an increase in studies on this matter in South America in the last decade, its scientific production is still far from countries like Norway or Italy (Sepúlveda y Petley, 2015).

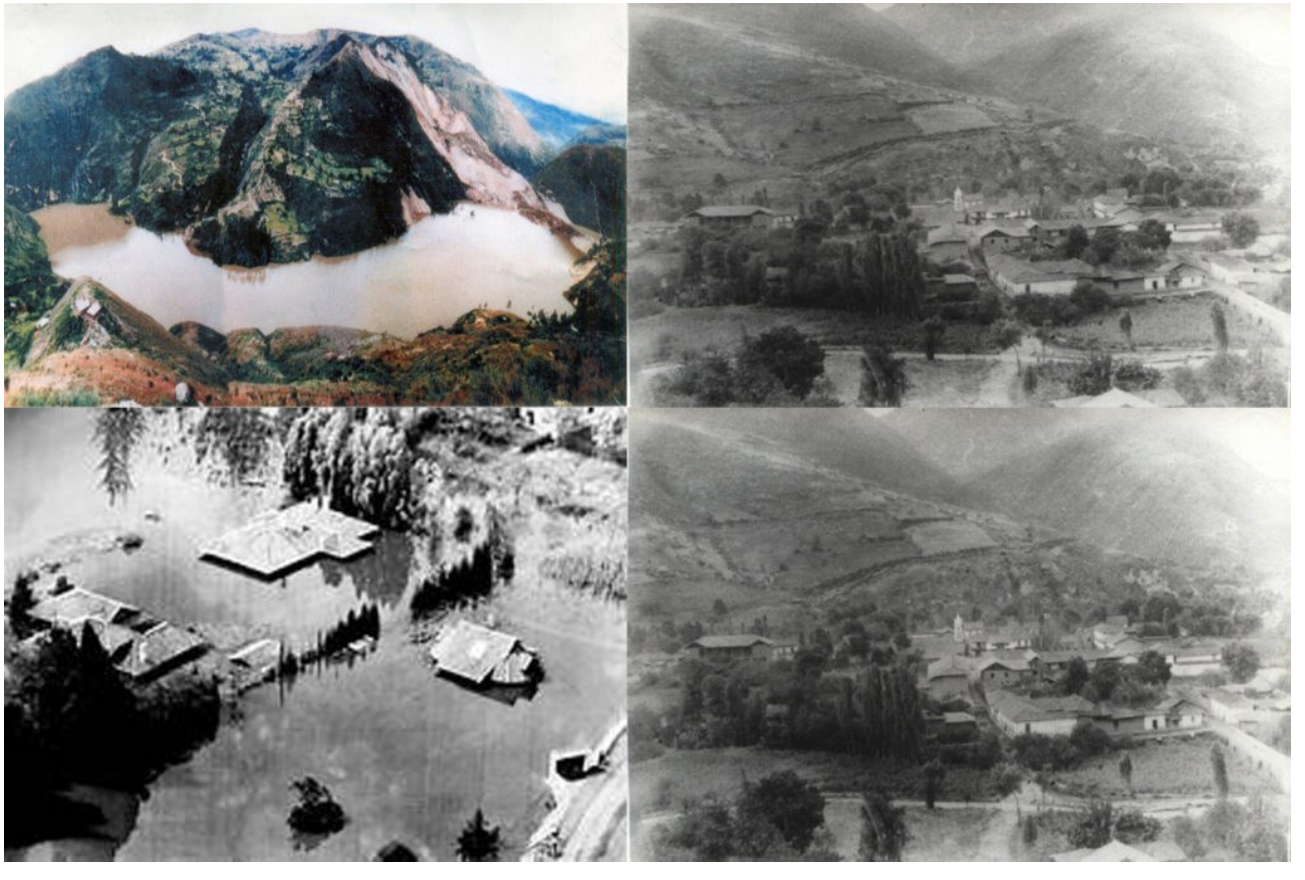

Figure 6.2: Desastre de la Josefina en imágenes. Source: https://www.gualaceo.gob.ec/gualaceo/la-josefina/.

Transversally, data from remote sensors emerge as a fundamental input for risk management and governance, specifically those related to landslides, since they allow the generation of information quickly, reliably, and multitemporally in areas that are difficult to access, aspects that are of great importance when planning the territory, even more, when it comes to the risks that affect it. The establishment of a methodology for the management and use of information from these sensors applied to risk management of mass movements represent a contribution of great importance for local authorities since they will allow the designing of mitigation measurements, to develop slope monitoring plans, and to increase both the highway user safety and the local population resilience.

In this context, the need for multi-purpose training in risk management is evident; the development of tools for the efficient capture of data and the implementation of methods and procedures for the generation of information that allow the organization of the actions that should be considered a priority to carry out an adequate and efficient management of disaster risk at the cantonal level, regional and local. Undoubtedly, the success of this chain of actions absolutely requires strengthening relations between institutions and between them and society, establishing dynamics of cooperation and dialogue.

6.2 Timeline

Taking into account the background described, this thesis was born from the imperative need to develop new methodologies applicable to risk management and governance through the use of remote sensors as the main input for locating threats. Below I will describe how real demands and events, not always foreseen, were shaping my research work until it was transformed into tools, implementations, methodologies, and information that allowed, in various ways, to contribute to risk governance in areas as close as they are far. , such as the university, the scientific, and the political-institutional. Various disaster risk management aspects have been implicitly addressed at the national,

cantonal, and local levels. A process of socialization of the findings has also been carried out through participation in congresses, symposiums, consultancies, and work meetings with competent authorities both in the area of risks and in the area of land management and sectional government.

Data recording was the first point I wanted to address with this thesis. Thus, during my stay in Spain (**Universidad de Santiago de Compostela, Campus de Lugo**, Spain) and together with my colleagues from the **Laboratorio del Territorio (LaboraTe)**, an ODK application was designed, named **MARLI** (Mobile Application for Regional Landslide Inventories in Ecuador) for the survey of landslide phenomena (Sellers et al., 2021b). This application is born from an exhaustive bibliographical review of research carried out by leading professionals such as Cees J. van Westen, Paola Reichenbach, Fausto Guzzetti, or Jordi Corominas, among many others; Resources provided by prestigious institutions such as USGS, BGS or UN, and international frameworks (Sendai, Kyoto, Hyogo).

At the same time, a group of Italian researchers from the **Federico II University of Naples (Italy)** arrives in Cuenca (Ecuador), who, through the Ecuadorian embassy in Rome (Italy), visit Ecuador to generate a proposal to collect information related to landslide risks. This proposal was socialized with public and private institutions, among which were several universities. One of them was the **Institute for Sectional Studies of Ecuador (IERSE) of the University of Azuay,** an institution to which I belong. Seeing the importance of the topic and given that the University, through the Rector's Office, had implemented a line of risk research a year before, it was possible to sign a **framework collaboration agreement** to prepare the project *Inventory map of landslides with SAR satellite interferometry, in the urban area of the city of Cuenca and the parishes of Baños, San Joaquín, Turi, Santa Ana, Pacha, Nulti, LLacao, Ricaurte, Sayausí, and Sinincay.* The general objective of this study was to automatically determine the landslide zones in the aforementioned study area by means of SAR Interferometry to finally generate a landslide hazard map. Said **information would be valid with data recorded in the field using printed sheets**.

Shortly after the signing of the framework agreement, I returned to Ecuador from my stay in Spain and was able to meet the group of researchers from the Federico II University of Naples, which was made up of PhD Diego DiMartire, PhD Massimo Ramondini and PhD Lorenzo Ammiranti. The knowledge acquired and advances made during my stay in Spain allowed me to reach meeting points with the project proposed by my colleagues, which translated into a more efficient way of executing the project. Thus, the project was restructured, and the MARLI application was adapted to the needs foreseen in the project, improving the expectations for this doctoral thesis. This event, in our view, allowed us to broaden the spectrum and vision of landslides and their application to risk governance.

Next, it was planned to carry out the physical inventory of landslides as a first step. This consisted of preparing and training a group of specialists to carry out a sweep of the study area and detect, collect and map the landslides present in the territory. Initially, this stage was planned to be carried out within a period of 10 to 12 months; however, the use of MARLI allowed the entire study area to be built in 3 months, to which were added another two months dedicated to office work, writing reporting, and map generation. In this period of time, it was possible to collect information on 710 landslides in the study area, far exceeding the best expectations of the work team. This not to mention that the **municipality risk management unit** only had data on a few landslides collected during the PRECUPA project and partially updated according to events that have occurred in recent years.

Thus, MARLI became the pillar of a fast, accurate, and standardized survey of landslides in the study area. The efficiency in data recording was due to having a device, in this case, a phone with an Android system, where the application was already developed and installed, which allowed the technicians not only a faster survey but also a more objective and standardized regardless of whether the survey is performed by a single technician or by several simultaneously. In this way, information was recorded beyond what a printed record can support (the location, photographs of the landslide, of the infrastructures and houses affected, geology, morphometry of the landslide, soil cover, presence

or not of water,... .). However, the collection of a greater amount of data was not exclusively achieved. However, it also **exponentially simplified the processing and analysis of said data**, since such data, in addition to being stored on the phone, at the moment Provided there is an Internet connection, the data is automatically saved in a database hosted on a server. This process allows data to be collected, updated, and visualized practically in real-time. Thus, we can load the registered data immediately in a web viewer, in a Geographic Information System (GIS), in an applet, or in CAD software, simply by importing the files from our server. Although all these options are available to the user, in our case, the final destination of the files is the Spatial Data Infrastructure (IDE) of the University of Azuay, a free service for managing and communicating spatial data. **This information, once processed and entered into our IDE, has served as the basis for different studies and publications**.

At this point, we have an updated landslide survey, which rigorously complies with technical and scientific aspects, with validation in the field. The development of MARLI and the recorded data were included in a scientific article. After a long wait, on September 17, 2021, this article was published in *Landslides* [1] (quality indices of both the journal and the publication were included in the Appendix B.1), becoming the first publication of this doctoral thesis and the basis of several publications, conferences and studies currently in development (thesis doctoral degree and two master's theses in risks), it also laid the foundations for an **institutional relationship with both the GAD and the Secretary of Risks**, by providing a first detailed inventory of landslides in the canton after two decades of inactivity, a critical input for territorial planning instruments (PDOT, PUGS).

In November 2021, the opportunity arose to present ourselves at the Congress of the Ecuadorian Network of Universities for Research and Postgraduate Studies (REDU) with the presentation ***Update of landslide inventory using low-cost tools in Cuenca canton*** [2],

[1] Sellers, C.A., Buján, S., Miranda, D. MARLI: a mobile application for regional landslide inventories in Ecuador. Landslides 18, 3963-3977 (2021). https://doi.org/10.1007/s10346-021-01764-9.

[2] Sellers, C., Buján, S. and Miranda, D. Landslide inventory update using low-

event in which the results of both the landslide survey project, as well as the results of MARLI and the impacts began to be publicized that were already being registered due to its development and publication.

Additionally, the results derived from this study were presented at the "V RIGTIG conference: Knowledge in action for territorial management"[3], held in March 2022, under the framework of the RIGTIG agreement (Research Network in Territory Management and Geospatial Information Technologies), a network that is made up of different public and private institutions, national and foreign universities, dedicated to the investigation of the territory and phenomena that occur in these territories. I recently participated in the first International forum: Risk and Prevention, Vulnerability and Improvement, held in Cuenca with the presentation of the communication ***SAR interferometry and low-cost tools for landslide inventories in the Cuenca canton*** footnoteSellers, C., Buján, S., Miranda, D., Di Martire, D., Calcaterra, D., Ramondini, M., Bravo, P., Pacheco, D. and Rodas, R. SAR interferometry and Low-cost tools for landslide inventories in the Cuenca canton. First International Forum: Risk and prevention - Vulnerability and improvement, made up of representatives from the University of Cuenca (Ecuador), the University of Azuay (Ecuador), and the National University of Colombia (Colombia), Oral presentation: 26 of August 2022, Cuenca - Ecuador. made in September 2022.

The collaboration with the researchers from the Federico II University of Naples was not limited to the aforementioned project but extended over time, addressing other concerns related to the detection of movement zones, comparing and validating them with the inventory carried out with MARLI, paying special attention to attention to the expansion areas of the city of Cuenca. In this case, it is relevant to mention that since the expansion zones of the city were

cost tools in Cuenca canton. VIII International Research Congress REDU 2021, oral presentation, November 15 to 18, 2021, Ambato - Ecuador.

[3]Sellers, C., Buján, S., Rodas, R. and Miranda, D. 2022. MARLI: App for updating landslide inventories in Ecuador. V Conference of the **Research Network on Land Management and Geospatial Information Technologies** (RIGTIG): Knowledge in Action for Land Management, oral presentation: March 30, 2022. Guayaquil - Ecuador.

not mapped, it was necessary to develop a procedure that would allow these zones to be determined. This was achieved through secondary information, that is, data from the electric meters installed by the **Empresa de Telecomunicaciones, Agua Potable, Alcantarillado y Saneamiento de Cuenca** (ETAPA). These meters are registered with DGPS, providing the exact location of the new facility. It also specifies the meter's capacity and the number of people it serves. Therefore, new meters are equivalent to new urban development areas, implicitly denoting the real urban expansion zones of the city. Thus, it was possible to determine the risk areas, both in the declared areas of urban expansion, as well as in the non-expansion areas and in the real areas of expansion, resulting in the most vulnerable or exposed to risk areas are precisely the areas where the real growth of the city is evident. Said zones include areas declared unsuitable for urban expansion, uncategorized zones, and to a lesser extent, "regulated" expansion zones. To these results must be added the **collaboration with ETAPA for developing useful products for both institutions**.

This research materialized in September 2021 in an oral communication presented at the international conference Geology Without Borders - 90°Congresso della Società Geologica Italiana entitled ***Multi-temporal relative landslide risk analysis for sustainable development of rapidly growing city in Latin America: the case of Cuenca, UNESCO site, Ecuador***[4], which would later evolve into a scientific article that was sent to the journal *Landslides* (quality indexes of both the journal as of the publication were included in the Appendix B.2) and which is currently under revision (minor revision)[5].

The next point that was addressed would become one of the first studies of road interconnectivity towards the city of Cuenca. Five main

[4]Di Napoli, M., Miele, P., Guerriero, L., Annibali Corona, M., Calcaterra, D., Ramondini, M., Sellers, C. and Di Martire, D. Multi-temporal relative landslide risk analysis for sustainable development of rapidly growing city in Latin America: the case of Cuenca, UNESCO site, Ecuador. 90° Congresso della Società Geologica italiana, oral presentation, September 14 to 16, 2021. Trieste - Italy.

[5]Di Napoli, M., Miele, P., Guerriero, L., Annibali Corona, M., Calcaterra, D., Ramondini, M., Sellers, C. and Di Martire, D. Multitemporal relative landslide exposure and risk analysis for the sustainable development of rapidly growing cities. Landslides (*minor revision*) (2023).

roads or corridors connect the city of Cuenca with neighboring cities and regions, all of which, at some point, suffer from landslide problems. In the winter season of 2021, the city was cut off for 15 days from the rest of the country, resulting in a shortage of food, services, and mobility in general, significantly affecting the socio-economic activities of the city. At the beginning of 2022, a macro landslide called Km49 on the Cuenca - Molleturo - Naranjal - Guayaquil road kept one of the most important connection axes, with the city of Cuenca closed for six months. Currently, work continues on the removal of materials for the stabilization of the slope, although it has been determined that the definitive solution will be the projection of an alternative layout. This case is paradoxical in the sense that evidence collected with MARLI was already available before the occurrence of this phenomenon. Thus, using the location provided with MARLI and the QPROTO plugin of Qgis, the projection wake of the total kinetic energy of the landslide was determined, resulting in modeling a significantly adjusted projection to the current reality of the macro landslide.

This **result was exposed to both the university and municipal authorities and the national risk secretary** and generated much expectation to such an extent that it was used as an input for exposing the risk in this place. In addition, within the University of Azuay, specifically in the **statistics research unit of the Faculty of Administration**, work is being done based on the vulnerability of landslides in the interconnecting road axes to the city of Cuenca to determine the social, economic and environmental impacts of the total or partial closures of these road corridors.

Two days before my trip to Naples (Italy), where I would carry out my research stay at the Federico II University of Naples in collaboration with the company Dinstar (a spinoff of the same university), postponed a year before due to the COVID pandemic, He gave another specific case of slipping. Due to a strong storm with high rainfall (> 38 mm/h) that continued for 6 hours, the average rainfall of the monthly records of previous years doubled, causing a landslide in the sector called Marianza. The landslide caused the closure of the Cuenca - Molleturo - Naranjal road, severe material losses, and livestock; unfortunately, five people died. The sector is characterized by steep slopes, intensive agricultural

activities, and very small stream protection margins, in addition to a geology dominated by weathered formations and highly fractured meta-andesites. Due to the magnitude of the event, several water intakes from the municipal drinking water company were destroyed or collapsed, causing a supply cut for almost two weeks. Considering that the city of Cuenca has around 600,000 inhabitants, the impact on this service was severe for the city and the population. **This event brought together the city's emergency committee, to which we were invited** various organizations of society, universities, the public, and private sector specialized in the area, were taking into account the previous experiences described, they invited us to carry out a detailed study of the area.

Another area currently under investigation is the Cuenca - Santa Isabel - El Empalme - Machala highway, a road of great commercial importance and access to the nearest port in the city. In addition, a hydroelectric dam, "San Francisco", was inaugurated in the area a few years ago, which is affected by a macro landslide that affects not only the infrastructure of the road but also the integrity and operation of the dam itself.

Undoubtedly, these events revealed the need to locate and quantify landslide points that can affect these interconnection pathways. For this, already during my stay in Naples, with professors D. Di Martire and S. Buján, we sought to develop a method to determine the vulnerability to landslides of the access roads to the city and the threats derived from the interruption of what we can call the feeder roads of the city. Thus, it was decided to work again with the QPROTO plugin from Qgis. Said tool, based on a Digital Elevation Model (DEM), the geology and the slope allow selecting and projecting potential rockfall by projecting the cone of affection. Finally, based on the results of this process, it was possible to automatically determine which sections of the linear infrastructures of the interconnection axes may be affected by these phenomena. This research materialized, among others, in a scientific article in December 2022 that was sent to the journal *Remote Sensing* (quality indices for both the journal and the publication were included in the Appendix B.3)

and is currently under review (submitted)[6]).

As previously mentioned, the last part of this thesis includes two specific and local applications of the use of the Differential Interferometry Synthetic Aperture Radar (DInSAR) technique, implemented in the SUBSOFT and SUBSIDENCE software, respectively, in order 1) to provide an integrated monitoring methodology that can be used to predict the spatial and temporal evolution of a slow landslide which affects buildings inside the campus of Azuay University, and 2) to study terrain deformation related to illegal artisanal mining in Ecuador. Both studies were presented at the "European Workshop on Structural Health Monitoring," which focused on monitoring studies on infrastructures, be they roads, dams, bridges, buildings,..., looking for how these affectations affect the economy, society, and people.

The first of these applications is included in the publication entitled ***Ground Deformation Monitoring of a Strategic Building Affected by Slow-Moving Landslide in Cuenca (Ecuador)***[7] (quality indices for both the book and the publication were included in the Appendix B.4), whose area of study is centered on my alma mater, the University of Azuay, which is affected by a macro sliding with a very slow speed. This scenario was presented as ideal for this study, which by means of SAR differential interferometry and establishing a fourth-order geodesic network, displacements, their direction, and their magnitude over time are monitored. This communication was presented as an oral communication at one of the most important events on landslides at an international level, the "International Symposium of Landslides", held in Colombia in February 2021[8].

[6]Sellers, C., Di Martire, D., Rodas, R., Ramondini, M., Infante, D., Miranda, D. and Buján, S. An integrated approach for rockfall susceptibility assessment-ment along linear infrastructure in Cuenca (Ecuador). Remote Sensing (submitted) (2023)

[7]Sellers, C., Rodas, R., Carrasco, N.P., De Stefano, R., Di Martire, D., Ramondini, M. (2021). Ground Deformation Monitoring of a Strategic Building Affected by Slow-Moving Landslide in Cuenca (Ecuador). In: Rizzo, P., Milazzo, A. (eds) European Workshop on Structural Health Monitoring. EWSHM 2020. Lecture Notes in Civil Engineering, vol 128. Springer, Cham. https://doi.org/10.1007/978-3-030-64908-114.

[8]Ammirati L., Rodas, R., Calcaterra D., Ramondini, M., Sellers, C., and Di Martire, D. (2021). DInSAR data for landslides mapping in UNESCO World Heritage

I recently participated as a panelist and speaker at the International Symposium Resilience in the Built Environment with the study entitled ***Slow-moving landslide monitoring using remote sensing and In-situ techniques in Cuenca-Ecuador a UNESCO Heritage site*** footnoteSellers, C., Rodas, R., Bravo, P., Delgado, O., Di Martire, D., Ramondini, M. and Calcaterra, D. Slow-moving landslide monitoring using remote sensing and In-situ techniques in Cuenca-Ecuador a UNESCO Heritage site. International Symposium on Resilience in the Built Environment, oral presentation: June 7, 2022, Cuenca - Ecuador., developed in June 2022, where the case study of the macro landslide that affects the University of Azuay was shown, presenting the results obtained by SAR interferometry and DGPS measurements updated until July 2022.

The second of the applications (chapter 5) was presented at the European Workshop on Structural Health Monitoring in Palermo, Italy, July 2022, under the title ***The Use DInSAR Technique for the Study of Land Subsidence Associated with Illegal Mining Activities in Zaruma - Ecuador, a Cultural Heritage Site***[9],[10], (quality indices for both the book and the publication were included in the Appendix B.5). In this case, a colleague from the Federico II University of Naples, Mohammad Amin Khalili, represented us as an oral presenter. We have received a lot of feedback and questions, which makes us think that the article and the presentation were well received. In this study, through the use of remote sensors (DInSAR), the subsidence phenomenon was analyzed in the Minera de Zaruma locality, in *Villa del Cerro de Oro de San Antonio de Zaruma*, also known as *Sultana del Oro*,

sites: Cuenca (Ecuador) study case. XIII International Symposium on Landslides-XIII ISL, oral presentation: February 22 to 26, 2021. Cartagena - Colombia.

[9]Sellers, C., Ammirati, L., Khalili, M.A., Buján, S., Rodas, R.A., Di Martire, D. (2023). The Use DInSAR Technique for the Study of Land Subsidence Associated with Illegal Mining Activities in Zaruma - Ecuador, a Cultural Heritage Cite. In: Rizzo, P., Milazzo, A. (eds) European Workshop on Structural Health Monitoring. EWSHM 2022. Lecture Notes in Civil Engineering, vol 270. Springer, Cham. https://doi.org/10.1007/978-3-031-07322-956.

[10]The use DInSAR technique for the study of land subsidence associated with illegal mining activities in Zaruma - Ecuador, a cultural heritage site. 10th European Workshop on Structural Health Monitoring, oral presentation: July 4 to 7, 2022, Palermo - Italy.

was founded in 1595 and is one of the oldest towns in Ecuador. This town is on the indicative list of UNESCO to be declared Cultural Heritage of Humanity. This case study is paradoxical and has great relevance due to the dichotomy between legal and illegal mining activities and the idea of protecting the cultural and architectural heritage of the city.

The idea of this study was born from a previous work that we carried out with Lorenzo Ammiranti within the framework of the agreement made between the University of Azuay and the Federico II University of Nápoles, where infrastructures and areas found in landslide areas in the city of Zaruma were detected employing SAR Interferometry. The city of Zaruma has been affected by landslides, which lead to subsidence phenomena, for decades, with these phenomena being more recurrent and having a more significant impact on the city in recent years. Such has been the impact of these phenomena that entire neighborhoods and city blocks have had to be evacuated. These phenomena are associated with different factors, including incompetent geology, legal and illegal, technical and anti-technical mining, and organic and unplanned growth of the city,... The information provided by the study allows the agency technician the possibility of planning actions to mitigate the problems associated with these events. Currently, work continues on mitigating the last event that occurred on December 15, 2021. Hence the importance of these studies to monitor and prevent this type of events.

6.3 Future work

The future is uncertain, however...

- There is currently a joint commitment between the National Secretariat of Risks, the municipality and its risk management unit, the University Federico II of Naples, the University of Santiago de Compostela, and the University of Azuay to carry out the official launch of the IDE and the landslide risk section, where all the recorded data, both those of the first campaign with

MARLI and those that followed it, will be made public. A joint effort to publish this data and make it public. The expected date is April 2023. With this, the sixth target of the Sendai Framework is being met.

- The implementation of studies on the impact of rockfall and landslides in the city's connectivity axes has been proposed as a project to determine their vulnerability to these phenomena and their economic and social implications for the city and region.

- There is a current motivation to integrate risk content in teaching and professional training to increase the technical capabilities to reduce vulnerability to mass movements, increasing the city's resilience. This through a doctoral thesis and two dissertations, also by the implementation of specialized courses in this matter. In addition, data provided within the scope of this Thesis are already being used in study cases in university subjects of University of León.

- A tool that allows obtaining automatic and systematized track sections susceptible to landslides will be implemented in a free software. With this, the third, fourth, and seventh goals of the Sendai Framework are being met.

- Within the current approach to the climate challenge, practical experiences of hazard management and risk governance are necessary to appropriately respond to climate change triggered events. The continuation of projects to generate information as accurately and temporally up to date will provide the assets for a better preparation and mitigation of this type of phenomenon, strengthening the capabilities and resilience of both the city and the population. In particular, it is intended to carry out a multivariate study associating precipitation (main trigger of landslides in this area) and the activation of landslides in the area.

- Also, the continuance to cooperate and work jointly in research and projects with international institutions and researchers such as the USC, UniNa and ULE. With this, the sixth goal of the Sendai Framework is being met.

Conclusions and Ongoing Works

Landslide mapping (or "landslide inventory making") is a mandatory step for any rational and practical investigation to zoning a territory for landslide susceptibility evaluation or determining mass movements risk. Landslide inventory (LI) prove extremely valuable for susceptibility, hazard, and risk studies, particularly over large areas; a unified methodology or standardized approach hasn't been found or is not practical, and the review of the literature shows that such products are rare.

LI maps are very effective products that should be prepared for small and large study areas, or even for entire regions or countries, to benefit society. To prepare landslide inventories, consistent and reproducible methods should be adopted, as the reliability, precision, and quality of the adopted methods influence the quality of the final inventory. The LI maps' completeness, resolution, and reliability should always be ascertained. A recognized limitation of landslide inventory maps refers to their intrinsic subjectivity and the difficulty of measuring their quality (Guzzetti et al., 2000, Malamud et al., 2004). Absolute criteria to establish the quality of landslide inventory maps have not been established.

Remote sensing techniques for landslide monitoring and prediction has gained popularity in recent years since it enables hazard identification, zonation, and mitigation. Synthetic Aperture Radar (SAR) interferometry is among the remote sensing techniques used. DInSAR is an advanced interferometric technique that uses radar sensors to estimate the phase of a given area from which the landslide activity can be

predicted. However, research concerning the use of remote sensing for landslide studies and hazard zonation is mainly carried out in developed countries.

In this thesis, we address these issues, where a standardized landslide inventory mapping methodology is developed and implemented into a mobile application for a faster more reliable survey, where the keyword is the automatization. Also, using remote sensing techniques, specifically SAR, we studied different mass movement phenomena, slow-moving landslides, rockfall, and subsidence phenomena, and the gathered data was contrasted and verified by field survey using MARLI.

Chapter one of this study describes the development of MARLI, a simple but efficient open-access platform to report landslide events using ODK system. Its design makes reporting fast, simple and cost-effective with an added benefit, and specialized knowledge is not required for its use. The results of this research, the inventory obtained, show that the surface affected by landslides has increased during the last two decades. The data obtained is loaded into an application server (Spatial Data Infrastructure) and published for the knowledge of the people. Thus, data is available to all people, technicians, and authorities, setting a baseline for other territorial studies involving risk management and land management. The development of MARLI opened the door for the realization of studies, in relation to landslides, not addressed up to now in Ecuador.

Chapter two of this study included the analysis of the Cuenca area to be zoned to identify the spatial probability of landslide initiation in areas characterized by specific materialized conditions by the environmental variables considered. In addition, the distribution of detachment is characterized by an increasing trend as time passes lower to higher susceptibility classes. This study provided information on important issues such as i) the effect of the sustained expansion of urban areas due to population growth on the relative variation in landslide risk and ii) the risk assessment method of reduced complexity only in the presence of partial data (i.e., susceptibility to slippage of land), instead of hazard and electrical supply contracts rather than population distribution). Thus, providing an innovative methodology to use alternative data,

enabling an alternative for land management and land risk management, and strengthening the toolbox and supplies needed to fortify the resilience and the capacities of mitigation of the citizens and the city itself.

In chapter three of this study we address a specific vulnerability in the region. Rock falls are considered the main danger in mountain areas worldwide, partly because of their direct consequences on the territory and the population. Mapping susceptibility to the fall of rocks is essential both for the previous assessment of the impact of the implementation of infrastructures such as to establish, a posteriori, restrictions in relation to the use of the land around these areas, with the primary objective of preventing the loss of human life and property materials. Thus, in this research, a new hybrid-based approach is used, developed on the trajectories count per grid cell produced by the QPROTO tool, to calculate the susceptibility of rock fall. This research provided a methodology and a tool to assess rockfall in linear infrastructures, and as valuable tool to local authorities since they allow them to design mitigation measurements, develop slope monitoring plans and increase highway user safety and the local population resilience. Additionally, these results also help researchers consider the effects of DEM resolution on identifying rockfall source points, the rockfall susceptibility mapping, or the identification of road sections that can be affected by rockfall or subsidence phenomena using automatic prediction tools.

Chapter four revolves around the prevention and mitigation of slope instability, which requires effective technologies to reduce the vulnerability of existing structures. Therefore, monitoring plays a key role in managing natural hazards and assumes the fundamental task of providing cost-effective solutions to mitigate or minimize physical and economic losses. Remote sensing techniques proved powerful investigative tools due to their high spatial and multi-temporal coverage, rapid data acquisition, and reasonable costs. This research provided a general methodology that can be used to predict a slow landslide's spatial and temporal evolution. In particular, this work analyses a slow-moving phenomenon that affects the University of Azuay (Cuenca - Ecuador). During this study, it was possible to obtain SAR images

from the constellation of satellites CosmoSkyMed, related to the period March 2016 to January 2018. This investigation provided an integrated monitoring methodology that can be used to predict the spatial and temporal evolution of a slow landslide affecting buildings inside Azuay University's campus. Also established a multi-level analysis integrated with innovative monitoring techniques together with traditional and detailed methods such as geophysical surveys, presenting a valid strategy for continuous risk updates. We have to mention that this collaboration and image analysis continues until this day.

In chapter five of this work, the Differential Interferometry Synthetic Aperture Radar (DInSAR) technique, implemented in the SUBSIDENCE software, has been used to study terrain deformation related to illegal artisanal mining in Ecuador. This study presents an up-to-date study of the monitoring and detection of subsidence phenomena in the city of Zaruma as part of a collaboration project between local and international Universities allowing to detect and monitor surface deformations using DInSAR techniques as a tool applied to monitoring mining-related subsidence phenomena. Here this study presents the primary displacement rates recorded over the analyzed time interval is shown. It was possible to observe how in the area affected by the collapse of 15 December 2021, the identified PSs showed significant deformation rates higher than 0.5 cm/year. An even more significant element is the time series of these points, which shows an acceleration starting from June 2021, thus six months before the collapse. In addition, it is emphasized that the analyses were conducted until December 10, 2021, while the collapse occurred on December 15, 2021, highlighting this technique's suitability in forecasting. To this matter, the DInSAR technique has proved effective in identifying areas subject to subsidence in the Zaruma town, making it possible to recognize critical zones both in areas where the presence of tunnels is known, but especially in those areas where tunnels have never been identified.

The look back at the writing of chapter six forced me to do (an overview of the legal framework in Ecuador; the vision of risk management and governance under the SENDAI protocol; a timeline of the evolution of this thesis, and the impacts that derive from the studies) allowed me not only to put into context each step followed to

complete this thesis but also each milestone achieved and the magnitude and impact that the investigations carried out have meant for the management and governance of the risk of landslides in Ecuador. Similarly, it has overwhelmingly shown the path I still have to go, and I will walk without a doubt!

This PhD thesis has achieved its main objectives, but furthermore, it has opened a broad spectrum of research topics in risk management and land management, a critical need in Ecuador due to all the natural and anthropic hazards that are latent in this territory. The tools, methodologies, and products stated in this work are valuable input for the authorities, scientists, and the population in general, to be able to face these phenomena and increase the resilience of the population, the city, and the territory in the face of reality and exposure to these dangers, especially mass movements. Additionally, the work carried out within the framework of this thesis has allowed the establishment of a network of collaboration, cooperation, and work between different local/national/international and public/private institutions related to effective management of the risks derived from the occurrence of landslides.

Ongoing Works

- At the moment, the contributions of this thesis are being used in a doctoral research at the University of Jaen, Spain, where different neural network algorithms are being analyzed for the generation of landslide susceptibility maps.
- We are in the second period of projects, where we are working on machine learning algorithms to generate landslide susceptibility maps using different methodologies and approaches.
- The second survey and update of the landslides with the MARLI application are in process, using the methodology developed in this thesis.
- A professional version of a map viewer is being developed to

manage landslide information, which will be presented to the public with the state risk secretary, the municipality, and the universities participating in the project.

References

Agliardi, F., Crosta, G.B., Frattini, P., 2009. Integrating rockfall risk assessment and countermeasure design by 3d modelling techniques. Natural Hazards and Earth System Sciences 9, 1059 – 1073. doi:https://doi.org/10.5194/nhess-9-1059-2009.

Aguirre-Ayerbe, I., Merino, M., Aye, S.L., Dissanayake, R., Shadiya, F., Lopez, C.M., 2020. An evaluation of availability and adequacy of multi-hazard early warning systems in asian countries: A baseline study. International Journal of Disaster Risk Reduction 49, 101749. doi:https://doi.org/10.1016/j.ijdrr.2020.101749.

Ahmed Khan, M.R., Brandenburger, T., 2020. ROCit: Performance assessment of binary classifier with visualization. URL: https://CRAN.R-project.org/package=ROCit.

Albano, M., Polcari, M., Bignami, C., Moro, M., Saroli, M., Stramondo, S., 2016. An innovative procedure for monitoring the change in soil seismic response by insar data: Application to the mexico city subsidence. International journal of applied earth observation and geoinformation 53, 146–158.

Alcántara-Ayala, I., Moreno, A., 2016. Landslide risk perception and communication for disaster risk management in mountain areas of developing countries: a mexican foretaste. Journal of Mountain Science 13, 2079 – 2093. doi:https://doi.org/10.1007/s11629-015-3823-0.

Alexander, D., 2012. Landslide Hazard and Risk. John Wiley & Sons Ltd. chapter Chapter 5. Vulnerability to Landslides. pp. 175 – 198. doi:https://doi.org/10.1002/9780470012659.ch5.

Allocca, V., Di Napoli, M., Coda, S., Carotenuto, F., Calcaterra, D., Di Martire, D., De Vita, P., 2021. A novel methodology

for groundwater flooding susceptibility assessment through machine learning techniques in a mixed-land use aquifer. Science of The Total Environment 790, 148067. doi:https://doi.org/10.1016/j.scitotenv.2021.148067.

AlQahtany, A.M., Abubakar, I.R., 2020. Public perception and attitudes to disaster risks in a coastal metropolis of saudi arabia. International Journal of Disaster Risk Reduction 44, 101422. doi:https://doi.org/10.1016/j.ijdrr.2019.101422.

Alvioli, M., Santangelo, M., Fiorucci, F., Cardinali, M., Marchesini, I., Reichenbach, P., Rossi, M., Guzzetti, F., Peruccacci, S., 2021. Rockfall susceptibility and network-ranked susceptibility along the italian railway. Engineering Geology 293, 106301. doi:https://doi.org/10.1016/j.enggeo.2021.106301.

Ammirati, L., Mondillo, N., Rodas, R.A., Sellers, C., Di Martire, D., 2020. Monitoring land surface deformation associated with gold artisanal mining in the zaruma city (ecuador). Remote Sensing 12. doi:10.3390/rs12132135.

Andrejev, K., Krušić, J., Đurić, U., Marjanović, M., Abolmasov, B., 2017. Relative landslide risk assessment for the city of valjevo, in: Mikoš, M., Vilímek, V., Yin, Y., Sassa, K. (Eds.), Advancing Culture of Living with Landslides, Springer International Publishing, Cham. pp. 525 – 533. doi:https://doi.org/10.1007/978-3-319-53483-1_62.

Arabameri, A., Pal, S.C., Rezaie, F., Chakrabortty, R., Saha, A., Blaschke, T., Napoli, M.D., Ghorbanzadeh, O., Ngo, P.T.T., 2022. Decision tree based ensemble machine learning approaches for landslide susceptibility mapping. Geocarto International 37, 4594–4627. doi:https://doi.org/10.1080/10106049.2021.1892210.

Arabameri, A., Pourghasemi, H.R., Yamani, M., 2017. Applying different scenarios for landslide spatial modeling using computational intelligence methods. Environmental Earth Sciences 76, 832. doi:https://doi.org/10.1007/s12665-017-7177-5.

Arabameri, A., Pradhan, B., Rezaei, K., Lee, C.W., 2019. Assessment of landslide susceptibility using statistical- and artificial intelligence-based FRâRF integrated model and multiresolution DEMs. Remote Sensing 11, 999. doi:https://www.mdpi.com/2072-4292/11/9/999.

Ardizzone, F., Cardinali, M., Galli, M., Guzzetti, F., Reichenbachv, P., 2007. Identification and mapping of recent rainfall-induced landslides using elevation data collected by airborne lidar. Natural Hazardsand Earth System Science 7, 637 – 650. doi:10.5194/nhess-7-637-2007.

Arnell, N.W., Gosling, S.N., 2016. The impacts of climate change on river flood risk at the global scale. Climatic Change 134, 387–401. doi:https://doi.org/10.1007/s10584-014-1084-5.

Basabe, P., Almeida, E., Ramón, P., Zeas, R., Alvarez, L., 1996. Avance en la prevención de desastres naturales en la cuenca del río paute, ecuador. Bulletin de l'Institut franÃ§ais d'études andines 25, 443 – 458.

Basofi, A., Fariza, A., Safitri, E.I., 2018. Landslide risk mapping in east java, indonesia, using analytic hierarchy process â natural breaks classification, in: 2018 International Seminar on Research of Information Technology and Intelligent Systems (ISRITI), IEEE. pp. 77–82. doi:10.1109/ISRITI.2018.8864367.

Bater, C.W., Coops, N.C., 2009. Evaluating error associated with lidar-derived DEM interpolation. Computers and Geosciences 35, 289 – 300. doi:https://doi.org/10.1016/j.cageo.2008.09.001.

Baum, R., Highland, L., Lyttle, P., Fee, J., Martinez, E., Wald, L., 2014. Landslide science for a safer geoenvironment. volume 1. chapter Report a Landslide: A Website to Engage the Public in Identifying Geologic Hazards. pp. 95–100. doi:10.1007/978-3-319-04999-1_8.

Beven, K.J., Kirkby, M.J., 1979. A physically based, variable contributing area model of basin hydrology / un modÃ¨le Ã base physique de zone d'appel variable de l'hydrologie du bassin versant. Hydrological Sciences Bulletin 24, 43–69. doi:https://doi.org/10.1080/02626667909491834.

Bignami, D.F., Dragoni, A., Menduni, G., 2018. Assessing and improving flood and landslide community social awareness and engagement via a web platform: The case of italy. International Journal of Disaster Risk Science 9, 530–540. doi:https://doi.org/10.1007/s13753-018-0199-0.

Billingsley, P., 1926. Geology of the zaruma gold district of ecuador. American Institute of Mining and Metallurgical Engineers 74, 255 – 275.

Blanco, P., 2009. SAR differential interferometry for deformation monitoring under a multi-frequency approach. phdthesis. Universitat Politécnica de Catalunya.

Böehner, J., Selige, T., 2006. Spatial prediction of soil attributes using terrain analysis and climate regionalisation, in: SAGA-Analyses and modelling applications, Goettinger Geographische Abhandlungen, Goettingen. pp. 13–28.

Botts, M., Percivall, G., Reed, C., Davidson, J., 2008. OGC Sensor Web Enablement: Overview and High Level Architecture. Springer Berlin Heidelberg, Berlin, Heidelberg. volume 4540. pp. 175–190. doi:10.1007/978-3-540-79996-2_10.

Brabb, E., Pampeyan, E., Bonilla, M., 1972. Landslide susceptibility in San Mateo County, California. Report 360. U.S. Geological Survey. URL: http://pubs.er.usgs.gov/publication/mf360.

Bradie, J., Leung, B., 2017. A quantitative synthesis of the importance of variables used in maxent species distribution models. Journal of Biogeography 44, 1344–1361. doi:https://doi.org/10.1111/jbi.12894.

Bragagnolo, L., da Silva, R., Grzybowski, J., 2020. Landslide susceptibility mapping with r.landslide: A free open-source gis-integrated tool based on artificial neural networks. Environmental Modelling and Software 123, 104565. doi:https://doi.org/10.1016/j.envsoft.2019.104565.

Bristow, C., 1973. Guide to the Geology of the Cuenca Basin, Southern Ecuador. Ecuadorian geological and geophysical society ed.

Bristow, C., Guevara, S., 1980. Mapa geológico de la hoja azogues (1: 100,000). Dirección General de Geología y Minas, Quito .

Brunetti, M., Guzzetti, F., Rossi, M., 2009. Probability distributions of landslide volumes. Nonlinear Processes in Geophysics 16, 179 – 188. doi:https://doi.org/10.5194/npg-16-179-2009.

Bühler, Y., Christen, M., Glover, J., Christen, M., Bartelt, P., 2016. Significance of digital elevation model resolution for numerical rockfall simulations, Lyon.

Buján, S., González-Ferreiro, E., Cordero, M., Miranda, D., 2019. PpC: a new method to reduce the density of lidar data. does its

use affect the DTM accuracy? The Photogrammetric Record 34. doi:https://doi.org/10.1111/phor.12295.

Buján, S., Guerra-Hernández, J., González-Ferreiro, E., Miranda, D., 2021. Forest road detection using LiDAR data and hybrid classification. Remote Sensing 13, 393. doi:https://doi.org/10.3390/rs13030393.

Cardinali, M., Ardizzone, F., Galli, M., Guzzetti, F., Reichenbach, P., 2000. Landslides triggered by rapid snow melting, the december 1996-january 1997 event in central italy, in: Claps, P., Siccardi, F. (Eds.), Mediterranean Storms, Proceedings Plinius Conference â99, pp. 439 – 448.

Carrara, A., 1993. Prediction and Perception of Natural Hazards. Advances in Natural and Technological Hazards Research.. Springer, Dordrecht. volume 2. chapter Uncertainty in Evaluating Landslide Hazard and Risk. pp. 101 – 109. doi:https://doi.org/10.1007/978-94-015-8190-5_12.

Carrara, A., Carratelli, E., Merenda, L., 1977. Computer-based data bank and statistical analysis of slope instability phenomena. Zeitschrift fur Geomorphologie 21, 187 – 222.

Carrión-Mero, P., Aguilar-Aguilar, M., Morante-Carballo, F., Domínguez-Cuesta, M.J., Sánchez-Padilla, C., Sánchez-Zambrano, A., Briones-Bitar, J., Blanco-Torrens, R., Córdova-Rizo, J., Berrezueta, E., 2021. Surface and underground geomechanical characterization of an area affected by instability phenomena in zaruma mining zone (ecuador). Sustainability 13. doi:10.3390/su13063272.

Castelli, M., Torsello, G., Vallero, G., 2021. Preliminary modeling of rockfall runout: Definition of the input parameters for the QGIS plugin QPROTO. Geosciences 11, 88. doi:https://doi.org/10.3390/geosciences11020088.

Cevasco, A., Pepe, G., Brandolini, P., 2014. The influences of geological and land use settings on shallow landslides triggered by an intense rainfall event in a coastal terraced environment. Bulletin of Engineering Geology and the Environment 73, 859–875. doi:https://doi.org/10.1007/s10064-013-0544-x.

Chang, M., Cui, P., Dou, X., Su, F., 2021. Quantitative risk assessment of landslides over the china-pakistan economic corridor. International

Journal of Disaster Risk Reduction 63, 102441. doi:https://doi.org/10.1016/j.ijdrr.2021.102441.

Chen, T., Zhu, L., Niu, R.q., Trinder, C.J., Peng, L., Lei, T., 2020. Mapping landslide susceptibility at the three gorges reservoir, china, using gradient boosting decision tree, random forest and information value models. Journal of Mountain Science 17, 670–685. doi:https://doi.org/10.1007/s11629-019-5839-3.

Chen, W., Peng, J., Hong, H., Shahabi, H., Pradhan, B., Liu, J., Zhu, A.X., Pei, X., Duan, Z., 2018. Landslide susceptibility modelling using GIS-based machine learning techniques for chongren county, jiangxi province, china. Science of the Total Environment 626, 1121 – 1135. doi:https://doi.org/10.1016/j.scitotenv.2018.01.124.

Chen, W., Shirzadi, A., Shahabi, H., Ahmad, B.B., Zhang, S., Hong, H., Zhang, N., 2017. A novel hybrid artificial intelligence approach based on the rotation forest ensemble and naïve bayes tree classifiers for a landslide susceptibility assessment in langao county, china. Geomatics, Natural Hazards and Risk 8, 1955 – 1977. doi:https://doi.org/10.1080/19475705.2017.1401560.

Cignetti, M., Godone, D., Bertolo, D., Paganone, M., Thuegaz, P., Giordan, D., 2021. Rockfall susceptibility along the regional road network of aosta valley region (northwestern italy). Journal of Maps 17, 54 – 64. doi:https://doi.org/10.1080/17445647.2020.1850534.

Coe, J.A., Godt, J.W., 2012. Review of approaches for assessing the impact of climate change on landslide hazards, in: Eberhardt, E., Froese, C., Turner, A.K., Leroueil, S. (Eds.), Landslides and Engineered Slopes, Protecting Society Through Improved Understanding, Taylor & Francis Group. pp. 371 – 377.

Confuorto, P., Di Martire, D., Centolanza, G., Iglesias, R., Mallorqui, J.J., Novellino, A., Plank, S., Ramondini, M., Thuro, K., Calcaterra, D., 2017. Post-failure evolution analysis of a rainfall-triggered landslide by multi-temporal interferometry sar approaches integrated with geotechnical analysis. Remote sensing of environment 188, 51–72.

Corominas, J., van Westen, C., Frattini, P., Cascini, L., Malet, J.P., Fotopoulou, S., Catani, F., Van Den Eeckhaut, M., Mavrouli, O., Agliardi, F., Pitilakis, K., Winter, M.G., Pastor, M., Ferlisi, S., Tofani, V., HervÃ¡s, J., Smith, J.T., 2014. Recommendations for

the quantitative analysis of landslide risk. Bulletin of Engineering Geology and the Environment 73, 209–263. doi:https://doi.org/10.1007/s10064-013-0538-8.

Cruden, D., Varnes, J., 1996. Landslides: investigation and mitigation. National Academy Press, Washington, DC. volume 247 of *Transportation research board. National research council.* special report Chapter 3: Landslide types and processes. pp. 36 – 75.

Dai, F., Lee, C., Ngai, Y., 2002. Landslide risk assessment and management: an overview. Engineering Geology 64, 65–87. doi:https://doi.org/10.1016/S0013-7952(01)00093-X.

De Brito, M.M., Weber, E.J., Krigger, V.S., Leitzke, F.P., 2016. Análise dos factores condicionantes de movimientos de massa no municipio de Porto Alegre a partir de registros históricos. Revista Brasileira de Cartografía 68, 1853 – 1872.

Del Soldato, M., Solari, L., Poggi, F., Raspini, F., Tomás, R., Fanti, R., Casagli, N., 2019. Landslide-induced damage probability estimation coupling insar and field survey data by fragility curves. Remote Sensing 11. doi:10.3390/rs11121486.

Di Martire, D., De Rosa, M., Pesce, V., Santangelo, M.A., Calcaterra, D., 2012. Landslide hazard and land management in high-density urban areas of campania region, italy. Natural Hazards and Earth System Sciences 12, 905–926. doi:https://doi.org/10.5194/nhess-12-905-2012.

Di Martire, D., Tessitore, S., Brancato, D., Ciminelli, M.G., Costabile, S., Costantini, M., Graziano, G.V., Minati, F., Ramondini, M., Calcaterra, D., 2016. Landslide detection integrated system (ladis) based on in-situ and satellite sar interferometry measurements. CATENA 137, 406–421. doi:https://doi.org/10.1016/j.catena.2015.10.002.

Di Napoli, M., Carotenuto, F., Cevasco, A., Confuorto, P., Di Martire, D., Firpo, M., Pepe, G., Raso, E., Calcaterra, D., 2020a. Machine learning ensemble modelling as a tool to improve landslide susceptibility mapping reliability. Landslides 17, 1897–1914. doi:https://doi.org/10.1007/s10346-020-01392-9.

Di Napoli, M., Di Martire, D., Bausilio, G., Calcaterra, D., Confuorto, P., Firpo, M., Pepe, G., Cevasco, A., 2021. Rainfall-induced shallow landslide detachment, transit and runout susceptibility mapping by

integrating machine learning techniques and gis-based approaches. Water 13. doi:https://doi.org/10.3390/w13040488.

Di Napoli, M., Marsiglia, P., Di Martire, D., Ramondini, M., Ullo, S.L., Calcaterra, D., 2020b. Landslide susceptibility assessment of wildfire burnt areas through earth-observation techniques and a machine learning-based approach. Remote Sensing 12. doi:https://doi.org/10.3390/rs12152505.

Dorren, L.K.A., Berger, F., Putters, U.S., 2006. Real-size experiments and 3-d simulation of rockfall on forested and non-forested slopes. Natural Hazards and Earth System Sciences 6, 145 – 153. doi:https://doi.org/10.5194/nhess-6-145-2006.

Dou, J., Bui, D.T., Yunus, A.P., Jia, K., Song, X., Revhaug, I., Xia, H., Zhu, Z., 2015. Optimization of causative factors for landslide susceptibility evaluation using remote sensing and GIS data in parts of niigata, japan. PLOS ONE 10, e0133262. doi:https://doi.org/10.1371/journal.pone.0133262.

de Eficiencia Energética, L., 2000. Ministerio de energía y minas del ecuador.

Elith, J., Kearney, M., Phillips, S., 2010. The art of modelling range-shifting species. Methods in Ecology and Evolution 1, 330–342. doi:https://doi.org/10.1111/j.2041-210X.2010.00036.x.

Elith, J., Phillips, S.J., Hastie, T., Dudík, M., Chee, Y.E., Yates, C.J., 2011. A statistical explanation of maxent for ecologists. Diversity and Distributions 17, 43–57. doi:https://doi.org/10.1111/j.1472-4642.2010.00725.x.

Elshahed, H., Tyson, N.d., 2020. Communicating science in the new media environment: The advancement of science literacy. Arab Media & Society 28, 1–18.

Ercanoglu, M., 2008. An overview on the landslide susceptibility assessment techniques, in: 1st WSEAS International Conference on EnvironmentalL and Gelogical Science and Engineering, Valletta, Malta.. pp. 131–134.

Fanos, A., Pradhan, B., 2018. Laser scanning systems and techniques in rockfall source identification and risk assessment: a critical review. Earth Systems and Environment 2, 163 – 182. doi:https://doi.org/10.1007/s41748-018-0046-x.

Fell, R., Corominas, J., Bonnard, C., Cascini, L., Leroi, E., Savage, W.Z., 2008. Guidelines for landslide susceptibility, hazard and risk zoning for land-use planning. Engineering Geology 102, 99–111. doi:https://doi.org/10.1016/j.enggeo.2008.03.014. landslide Susceptibility, Hazard and Risk Zoning for Land Use Planning.

Fernández Viejo, G., 1997. Estructura cortical de la cordillera cantábrica y su transición a la cuenca del duero a partir de datos de sísmica de refracción/reflexión de gran ángulo .

Ferster, C.J., Coops, N.C., Harshaw, H.W., Kozak, R.A., Meitner, M.J., 2013. An exploratory assessment of a smartphone application for public participation in forest fuels measurement in the wildland-urban interface. Forests 4, 1199 – 1219.

Fielding, A.H., Bell, J.F., 1997. A review of methods for the assessment of prediction errors in conservation presence/absence models. Environmental Conservation 24, 38â49. doi:https://doi.org/10.1017/S0376892997000088.

Fiorucci, F., Cardinali, M., Carlá, R., Rossi, M., Mondini, A., Santurri, L., Ardizzone, F., Guzzetti, F., 2011. Seasonal landslide mapping and estimation of landslide mobilization rates using aerial and satellite images. Geomorphology 129, 59 – 70. doi:10.1016/j.geomorph.2011.01.013.

Foster, C., Pennington, C., Culshaw, M., Lawrie, K., 2012. The national landslide database of Great Britain: development, evolution and applications. Environmental Earth Sciences 66, 941 – 953. doi:10.1007/s12665-011-1304-5.

Fourcade, Y., Besnard, A.G., Secondi, J., 2018. Paintings predict the distribution of species, or the challenge of selecting environmental predictors and evaluation statistics. Global Ecology and Biogeography 27, 245–256. doi:https://doi.org/10.1111/geb.12684.

Franceschetti, G., Migliaccio, M., Riccio, D., Schirinzi, G., 1992. Saras: a synthetic aperture radar (sar) raw signal simulator. IEEE Transactions on Geoscience and Remote Sensing 30, 110 – 123. doi:10.1109/36.124221.

Galli, M., Ardizzone, F., Cardinali, M., Guzzetti, F., Reichenbach, P., 2008. Comparing landslide inventory maps. Geomorphology 94, 268 – 289. doi:10.1016/j.geomorph.2006.09.023. gIS technology and models for assessing landslide hazard and risk.

García-Cortés, J.P.S.V., González, C.I.S., Villar, J.A.Á., 2008. Contextos geológicos españoles. IGME.

García-Delgado, H., Machuca, S., Medina, E., 2019. Dynamic and geomorphic characterizations of the mocoa debris flow (march 31, 2017, putumayo department, southern colombia). Landslides 16, 597–609. doi:https://doi.org/10.1007/s10346-018-01121-3.

Gariano, S.L., Guzzetti, F., 2016. Landslides in a changing climate. Earth-Science Reviews 162, 227 – 252. doi:https://doi.org/10.1016/j.earscirev.2016.08.011.

Glade, T., 2003. Landslide occurrence as a response to land use change: a review of evidence from new zealand. CATENA 51, 297–314. doi:https://doi.org/10.1016/S0341-8162(02)00170-4. geomorphic Responses to Land Use Changes.

Glade, T., Anderson, M., Crozier, M.J., 2006. Landslide Hazard and Risk. John Wiley Sons Ltd. doi:10.1002/9780470012659.

Glade, T., Crozier, M., 1996. Towards a national landslide information base for new zealand. New Zealand Geographer 52, 29 – 40. doi:https://doi.org/10.1111/j.1745-7939.1996.tb00461.x.

Goetz, J., Brenning, A., Petschko, H., Leopold, P., 2015. Evaluating machine learning and statistical prediction techniques for landslide susceptibility modeling. Computers Geosciences 81, 1–11. doi:https://doi.org/10.1016/j.cageo.2015.04.007.

Gómez, R.S., Pérez, J.G., Martín, M.D.M.L., García, C.G., 2016. Collinearity diagnostic applied in ridge estimation through the variance inflation factor. Journal of Applied Statistics 43, 1831–1849. doi:https://doi.org/10.1080/02664763.2015.1120712.

Goodchild, M.F., 2007. Citizens as sensors: the world of volunteered geography. GeoJournal 69, 211–221. doi:https://doi.org/10.1007/s10708-007-9111-y.

Grelle, G., Soriano, M., Revellino, P., Guerriero, L., Anderson, M.G., Diambra, A., Fiorillo, F., Esposito, L., Diodato, N., Guadagno, F.M., 2014. Space-time prediction of rainfall-induced shallow landslides through a combined probabilistic/deterministic approach, optimized for initial water table conditions. Bulletin of Engineering Geology and the Environment 73, 877–890. doi:https://doi.org/10.1007/s10064-013-0546-8.

Guerriero, L., Confuorto, P., Calcaterra, D., Guadagno, F.M., Revellino, P., Martire, D.D., 2019. Ps-driven inventory of town-damaging landslides in the benevento, avellino and salerno provinces, southern italy. Journal of Maps 15, 619–625. doi:https://doi.org/10.1080/17445647.2019.1651770.

Guerriero, L., Focareta, M., Fusco, G., Rabuano, R., Guadagno, F.M., Revellino, P., 2018. Flood hazard of major river segments, benevento province, southern italy. Journal of Maps 14, 597–606. doi:https://doi.org/10.1080/17445647.2018.1526718.

Guerriero, L., Ruzza, G., Calcaterra, D., Di Martire, D., Guadagno, F.M., Revellino, P., 2020a. Modelling prospective flood hazard in a changing climate, benevento province, southern italy. Water 12. doi:10.3390/w12092405.

Guerriero, L., Ruzza, G., Guadagno, F.M., Revellino, P., 2020b. Flood hazard mapping incorporating multiple probability models. Journal of Hydrology 587, 125020. doi:https://doi.org/10.1016/j.jhydrol.2020.125020.

Guillera-Arroita, G., Lahoz-Monfort, J.J., Elith, J., 2014. Maxent is not a presenceâabsence method: a comment on thibaud etÂ al. Methods in Ecology and Evolution 5, 1192–1197. doi:https://doi.org/10.1111/2041-210X.12252.

Guzzetti, F., Cardinali, M., Reichenbach, P., Carrara, A., 2000. Comparing landslide maps: A case study in the upper tiber river basin, central italy. Environmental management 25. doi:https://doi.org/10.1007/s002679910020.

Guzzetti, F., Cardinali, M., Reichenbach, P., Cipolla, F., Sebastiani, C., Galli, M., Salvati, P., 2004. Landslides triggered by the 23 november 2000 rainfall event in the imperia province, western liguria, italy. Engineering Geology 73, 229 – 245. doi:10.1016/j.enggeo.2004.01.006.

Guzzetti, F., Crosta, G., Detti, R., Agliardi, F., 2002. STONE: a computer program for the three-dimensional simulation of rock-falls. Computers & Geosciences 28, 1079 – 1093. doi:https://doi.org/10.1016/S0098-3004(02)00025-0.

Guzzetti, F., Mondini, A.C., Cardinali, M., Fiorucci, F., Santangelo, M., Chang, K.T., 2012. Landslide inventory maps: New tools for an

old problem. Earth-Science Reviews 112, 42 – 66. doi:10.1016/j.earscirev.2012.02.001.

Guzzetti, F., Reichenbach, P., Ardizzone, F., Cardinali, M., Galli, M., 2006. Estimating the quality of landslide susceptibility models. Geomorphology 81, 166–184. doi:https://doi.org/10.1016/j.geomorph.2006.04.007.

Hair, J.F., Black, W.C., Babin, B.J., 2010. Multivariate Data Analysis: A Global Perspective. Global Edition.

Hanley, J.A., McNeil, B.J., 1982. The meaning and use of the area under a receiver operating characteristic (roc) curve. Radiology 143, 29–36. doi:https://doi.org/10.1148/radiology.143.1.7063747. pMID: 7063747.

Hanssen, R.F., 2001. Radar interferometry: data interpretation and error analysis. volume 2. Springer Science & Business Media.

Hearn, G.J., Hart, A.B., 2019. Landslide susceptibility mapping: a practitionerâs view. Bulletin of Engineering Geology and the Environment 78, 5811 – 5826. doi:https://doi.org/10.1007/s10064-019-01506-1.

Heerdegen, R.G., Beran, M.A., 1982. Quantifying source areas through land surface curvature and shape. Journal of Hydrology 57, 359–373. doi:https://doi.org/10.1016/0022-1694(82)90155-X.

Hijmans, R.J., 2012. Cross-validation of species distribution models: removing spatial sorting bias and calibration with a null model. Ecology 93, 679–688. doi:https://doi.org/10.1890/11-0826.1.

Hijmans, R.J., 2022. raster: Geographic data analysis and modeling. URL: https://CRAN.R-project.org/package=raster.

Huat, B.B.K., Ali, F.H.J., Low, T.H., 2006. Water infiltration characteristics of unsaturated soil slope and its effect on suction and stability. Geotechnical Geological Engineering 24, 1293–1306. doi:https://doi.org/10.1007/s10706-005-1881-8.

Hungerbühler, D., Steinmann, M., Winkler, W., Seward, D., Egüez, A., Dawn E. Peterson, Urs Helg, Cliff Hammer, 2002. Neogene stratigraphy and andean geodynamics of southern ecuador. Earth-Science Reviews 57, 75 – 124. doi:https://doi.org/10.1016/S0012-8252(01)00071-X.

Hungerbühler, D., Steinmann, M., Winkler, W., Seward, D., Egüez, A., Peterson, D.E., Helg, U., Hammer, C., 2002. Neogene stratigraphy and andean geodynamics of southern ecuador. Earth-Science Reviews 57, 75–124.

Iglesias, R., Mallorqui, J.J., Monells, D., López-Martínez, C., Fabregas, X., Aguasca, A., Gili, J.A., Corominas, J., 2015. Psi deformation map retrieval by means of temporal sublook coherence on reduced sets of sar images. Remote Sensing 7, 530 – 563. doi:10.3390/rs70100530.

Infante, D., Di Martire, D., Calcaterra, D., Miele, P., Scotto di Santolo, A., Ramondini, M., 2019. Integrated procedure for monitoring and assessment of linear infrastructures safety (i-pro monalisa) affected by slope instability. Applied Sciences 9, 5535.

Jaboyedoff, M., Labiouse, V., 2011. Technical note: Preliminary estimation of rockfall runout zones. Natural Hazards and Earth System Sciences 11, 819 – 828. doi:https://doi.org/10.5194/nhess-11-819-2011.

Jäger, D., Kreuzer, T., Wilde, M., Bemm, S., Terhorst, B., 2018. A spatial database for landslides in northern bavaria: A methodological approach. Geomorphology 306, 283 – 291. doi:http://dx.doi.org/10.1016/j.geomorph.2015.10.008.

Jamalullail, S.N.R., Sahari, S., Shah, A.A., Batmanathan, N., 2021. Preliminary analysis of landslide hazard in brunei darussalam, se asia. Environmental Earth Sciences 80, 512. doi:https://doi.org/10.1007/s12665-021-09815-z.

James, G., Hastie, T., Witten, D., Tibshirani, R., . An Introduction to Statistical Learning with Applications in R. First ed., Springer New York Heidelberg Dordrecht London. URL: https://hastie.su.domains/ISLR2/ISLRv2_website.pdf, doi:10.1007/978-1-4614-7138-7.

Jenks, G.F., 1967. The data model concept in statistical mapping, in: International Yearbook of Cartography, pp. 186 – 190.

Joy, J., Kanga, S., Singh, S.K., 2019. Kerala flood 2018: Flood mapping by participatory GIS approach, Meloor Panchayat. International Journal on Emerging Technologies 10, 197 – 205.

Juliev, M., Mergili, M., Mondal, I., Nurtaev, B., AlimPulatov, Hübl, J., 2019. Comparative analysis of statistical methods for landslide

susceptibility mapping in the bostanlik district, uzbekistan. Science of the Total Environment 653, 801 – 814. doi:https://doi.org/10.1016/j.scitotenv.2018.10.431.

Karsli, F., Atasoy, M., Yalcin, A., Reis, S., Demir, O., Gokceoglu, C., 2009. Effects of land-use changes on landslides in a landslide-prone area (ardesen, rize, ne turkey). Environmental Monitoring and Assessment 156, 241 – 255.

Kirschbaum, D., Stanley, T., 2018. Satellite-based assessment of rainfall-triggered landslide hazard for situational awareness. Earth's Future 6, 505–523. doi:10.1002/2017EF000715.

Kirschbaum, D., Stanley, T., Zhou, Y., 2015. Spatial and temporal analysis of a global landslide catalog. Geomorphology 249, 4 – 15. doi:10.1016/j.geomorph.2015.03.016.

Kirschbaum, D.B., Adler, R., Hong, Y., Hill, S., Lerner-Lam, A., 2010. A global landslide catalog for hazard applications: method, results, and limitations. Natural Hazards 52, 561–575. doi:10.1007/s11069-009-9401-4.

Klimeš, J., Müllerová, H., Woitsch, J., Bíl, M., Křížová, B., 2020. Century-long history of rural community landslide risk reduction. International Journal of Disaster Risk Reduction 51, 101756. doi:https://doi.org/10.1016/j.ijdrr.2020.101756.

Klimeš, J., Rios Escobar, V., 2010. A landslide susceptibility assessment in urban areas based on existing data: an example from the iguanÃ¡ valley, medellÃn city, colombia. Natural Hazards and Earth System Sciences 10, 2067–2079. doi:https://doi.org/10.5194/nhess-10-2067-2010.

Knox, J.C., 1993. Large increases in flood magnitude in response to modest changes in climate. Nature 361, 430–432. doi:https://doi.org/10.1038/361430a0.

Kocaman, S., Gokceoglu, C., 2019. A citsci app for landslide data collection. Landslides 16, 611–615. doi:https://doi.org/10.1007/s10346-018-1101-2.

Kornejady, A., Ownegh, M., Bahremand, A., 2017. Landslide susceptibility assessment using maximum entropy model with two different data sampling methods. CATENA 152, 144 – 162. doi:https://doi.org/10.1016/j.catena.2017.01.010.

Latini, M., Köbben, B., 2005. A web application for landslide inventory using data-driven svg, in: P., v., S., Z., M., F.E. (Eds.), Geo-information for Disaster Management, Springer, Berlin, Heidelberg. pp. 1041 – 1054. doi:10.1007/3-540-27468-5_73.

Leine, R.I., Capobianco, G., Bartelt, P., Christen, M., Caviezel, A., 2021. Stability of rigid body motion through an extended intermediate axis theorem: application to rockfall simulation. Multibody System Dynamics 52, 431 – 455. doi:https://doi.org/10.1007/s11044-021-09792-y.

Li, Z., Nadim, F., Huang, H., Uzielli, M., Lacasse, S., 2010. Quantitative vulnerability estimation for scenario-based landslide hazards. Landslides 7, 125–134. doi:https://doi.org/10.1007/s10346-009-0190-3.

Liang, W.T., Lee, J.C., Chen, K.H., Hsiao, N.C., 2017. Citizen earthquake science in taiwan: from science to hazard mitigation. Journal of Disaster Research 12, 1174 – 1181. doi:10.20965/JDR.2017.P1174.

Litherland, M., Aspden, J., Jemielita, R. (Eds.), 1994. The metamorphic belts of Ecuador. Number 11 in Overseas Memoir Institute of Geological Sciences, British Geological Survey.

Liu, W., Wang, S., Zhou, Y., Wang, L., 2014. An android intelligent mobile terminal application: field data survey system for forest fires. Natural Hazards 73, 1483 – 1497. doi:10.1007/s11069-014-1147-y.

Lombardo, L., Fubelli, G., Amato, G., Bonasera, M., 2016. Presence-only approach to assess landslide triggering-thickness susceptibility: a test for the mili catchment (north-eastern sicily, italy). Natural Hazards 84, 565–588. doi:https://doi.org/10.1007/s11069-016-2443-5.

Lombardo, L., Mai, P.M., 2018. Presenting logistic regression-based landslide susceptibility results. Engineering Geology 244, 14 – 24. doi:https://doi.org/10.1016/j.enggeo.2018.07.019.

Lombardo, L., Opitz, T., Ardizzone, F., Guzzetti, F., Huser, R., 2020. Space-time landslide predictive modelling. Earth-Science Reviews 209, 103318. doi:https://doi.org/10.1016/j.earscirev.2020.103318.

Losasso, L., Jaboyedoff, M., Sdao, F., 2017. Potential rock fall source areas identification and rock fall propagation in the province of potenza territory using an empirically distributed approach.

Landslides 14, 1593 – 1602. doi:https://doi.org/10.1007/s10346-017-0807-x.

Loye, A., Jaboyedoff, M., Pedrazzini, A., 2009. Identification of potential rockfall source areas at a regional scale using a DEM-based geomorphometric analysis. Natural Hazards and Earth System Sciences 9, 1643 – 1653. doi:https://doi.org/10.5194/nhess-9-1643-2009.

de Luiz Rosito Listo, F., Carvalho Vieira, B., 2012. Mapping of risk and susceptibility of shallow-landslide in the city of são paulo, brazil. Geomorphology 169-170, 30–44. doi:https://doi.org/10.1016/j.geomorph.2012.01.010.

Lupiano, V., Rago, V., Terranova, O.G., Iovine, G., 2019. Landslide inventory and main geomorphological features affecting slope stability in the picentino river basin (campania, southern italy). Journal of Maps 15, 131 – 141. doi:10.1080/17445647.2018.1563836.

Malamud, B.D., Turcotte, D.L., Guzzetti, F., Reichenbach, P., 2004. Landslide inventories and their statistical properties. Earth Surface Processes and Landforms 29, 687 – 711. doi:https://doi.org/10.1002/esp.1064.

Mantovani, F., Gracia, F.J., de Cosmo, P.D., Suma, A., 2010. A new approach to landslide geomorphological mapping using the open source software in the olvera area (cadiz, spain). Landslides 7, 69 – 74. doi:10.1007/s10346-009-0181-4.

Marcillo-Delgado, J.C., Álvarez-García, A., García-Carrilloa, A., 2021. Analysis of risk and disaster reduction strategies in South American countries. International Journal of Disaster Risk Reduction 61, 102363. doi:10.1016/j.ijdrr.2021.102363.

Marcus, J.J. (Ed.), 1997. Mining Environmental Handbook: Effects of Mining on the Environment and American Environmental Controls on Mining. Imperial College Press, London. doi:10.1142/p022.

Mavrouli, O., Fotopoulou, S., Pitilakis, K., Zuccaro, G., Corominas, J., Santo, A., Cacace, F., De Gregorio, D., Di Crescenzo, G., Foerster, E., Ulrich, T., 2014. Vulnerability assessment for reinforced concrete buildings exposed to landslides. Bulletin of Engineering Geology and the Environment 73, 265–289. doi:https://doi.org/10.1007/s10064-014-0573-0.

Meena, S.R., Nachappa, T.G., 2019. Impact of spatial resolution of digital elevation model on landslide susceptibility mapping: A case study in kullu valley, himalayas. Geosciences 9, 360. doi:https://doi.org/10.3390/geosciences9080360.

Mele, A., Miano, A., Di Martire, D., Infante, D., Ramondini, M., Prota, A., 2022. Potential of remote sensing data to support the seismic safety assessment of reinforced concrete buildings affected by slow-moving landslides. Archives of Civil and Mechanical Engineering 22. doi:10.1007/s43452-022-00407-7.

Merow, C., Smith, M.J., Silander Jr, J.A., 2013. A practical guide to maxent for modeling species' distributions: what it does, and why inputs and settings matter. Ecography 36, 1058–1069. doi:https://doi.org/10.1111/j.1600-0587.2013.07872.x.

Metternicht, G., Hurni, L., Gogu, R., 2005. Remote sensing of landslides: An analysis of the potential contribution to geo-spatial systems for hazard assessment in mountainous environments. Remote Sensing of Environment 98, 284 – 303. doi:https://doi.org/10.1016/j.rse.2005.08.004.

Miano, A., Mele, A., Calcaterra, D., Martire, D.D., Infante, D., Prota, A., Ramondini, M., 2021. The use of satellite data to support the structural health monitoring in areas affected by slow-moving landslides: a potential application to reinforced concrete buildings. Structural Health Monitoring 20, 3265 – 3287. doi:https://doi.org/10.1177/1475921720983232.

Miele, P., Di Napoli, M., Guerriero, L., Ramondini, M., Sellers, C., Corona, M.A., Di Martire, D., 2021. Landslide awareness system (LAwS) to increase the resilience and safety of transport infrastructure: The case study of pan-american highway (cuencaâecuador). Remote Sensing 13, 1564. doi:https://doi.org/10.3390/rs13081564.

Mondini, A., Guzzetti, F., Reichenbach, P., Rossi, M., Cardinali, M., Ardizzone, F., 2011. Semi-automatic recognition and mapping of rainfall induced shallow landslides using optical satellite images. Remote Sensing of Environment 115, 1743 – 1757. doi:10.1016/j.rse.2011.03.006.

Montealegre, A.L., Lamelas, M.T., Riva, J.D.L., 2015. A comparison of open-source LiDAR filtering algorithms in a mediterranean forest environment. IEEE Journal of Selected Topics in Applied Earth

Observations and Remote Sensing 8, 4072–4085. doi:https://doi.org/10.1109/JSTARS.2015.2436974.

Moore, I.D., Grayson, R.B., Ladson, A.R., 1991. Digital terrain modelling: A review of hydrological, geomorphological, and biological applications. Hydrological Processes 5, 3 – 30. doi:https://doi.org/10.1002/hyp.3360050103.

Moos, C., Fehlmann, M., Trappmann, D., Stoffel, M., Dorren, L., 2018. Integrating the mitigating effect of forests into quantitative rockfall risk analysis â two case studies in switzerland. International Journal of Disaster Risk Reduction 32, 55 – 74. doi:http://dx.doi.org/10.1016/j.ijdrr.2017.09.036.

Mora, O., Mallorqui, J., Broquetas, A., 2003. Linear and nonlinear terrain deformation maps from a reduced set of interferometric sar images. IEEE Transactions on Geoscience and Remote Sensing 41, 2243 – 2253. doi:10.1109/TGRS.2003.814657.

Moreno Morejón, E.A., 2019. Aplicación de modelos teóricos para estimar la subsidencia minera que afecta el área de la Unidad Educativa âLa Inmaculada Fe y Alegríaâ, cantón Zaruma. mathesis. Universidad Central del Ecuador. URL: http://www.dspace.uce.edu.ec/bitstream/25000/18033/1/T-UCE-0012-FIG-084.pdf.

Muñoz-Sotomayor, V., Tubío-Sánchez, J.M., Morales-Ramos, V., 2018. Ragioni ed esiti di una ricerca sul territorio e sul progetto rurale contemporaneo. Prisma. chapter Mercados de suelo informal en las fronteras urbano-rurales. El caso de Loja. pp. 199 – 212.

Musakwa, W., van Niekerk, A., 2015. Earth observation for sustainable urban planning in developing countries: Needs, trends, and future directions. Journal of Planning Literature 30, 149–160. doi:https://doi.org/10.1177/0885412214557.

Muscarella, R., Galante, P.J., Soley-Guardia, M., Boria, R.A., Kass, J.M., Uriarte, M., Anderson, R.P., 2014. Enmeval: An r package for conducting spatially independent evaluations and estimating optimal model complexity for maxent ecological niche models. Methods in Ecology and Evolution 5, 1198–1205. doi:https://doi.org/10.1111/2041-210X.12261.

Naimi, B., Hamm, N.A.S., Groen, T.A., Skidmore, A.K., Toxopeus, A.G., 2014. Where is positional uncertainty a problem for species

distribution modelling? Ecography 37, 191–203. doi:https://doi.org/10.1111/j.1600-0587.2013.00205.x.

Niethammer, U., James, M., Rothmund, S., Travelletti, J., Joswig, M., 2012. Uav-based remote sensing of the super-sauze landslide: Evaluation and results. Engineering Geology 128, 2 – 11. doi:https://doi.org/10.1016/j.enggeo.2011.03.012.

Noblet, C., Lavenu, A., Schneider, F., 1988. Étude géodynamique d'un bassin intramontagneux tertiaire sur décrochements dans les andes du sud de l'équateur: l'exemple du bassin de cuenca. Géodynamique 3, 117–138.

Novellino, A., Cesarano, M., Cappelletti, P., Di Martire, D., Di Napoli, M., Ramondini, M., Sowter, A., Calcaterra, D., 2021. Slow-moving landslide risk assessment combining machine learning and insar techniques. CATENA 203, 105317. doi:https://doi.org/10.1016/j.catena.2021.105317.

O'Hare, G., Rivas, S., 2005. The landslide hazard and human vulnerability in la paz city, bolivia. The Geographical Journal 171, 239–258. URL: http://www.jstor.org/stable/3451554.

Ohlmacher, G.C., 2007. Plan curvature and landslide probability in regions dominated by earth flows and earth slides. Engineering Geology 91, 117–134. doi:https://doi.org/10.1016/j.enggeo.2007.01.005.

Oke, O.A., Thompson, K.A., 2015. Distribution models for mountain plant species: The value of elevation. Ecological Modelling 301, 72–77. doi:https://doi.org/10.1016/j.ecolmodel.2015.01.019.

Oliva-González, A.O., Pozo, A.F.R., Gallardo-Amaya, R.J., 2017. Terrain instability in areas of mining activity: case zaruma city, ecuador. Revista Redes de Ingeniería 8, 69 – 81. doi:10.14483/2248762X.12116.

Olyazadeh, R., Sudmeier-Rieux, K., Jaboyedoff, M., Derron, M.H., Devkota, S., 2016. An offline–online web-gis android application for fast data acquisition of landslide hazard and risk. Natural Hazards and Earth System Sciences 17, 549–561. doi:10.5194/nhess-17-549-2017.

Orhan, O., Bilgilioglu, S.S., Kaya, Z., Ozcan, A.K., Bilgilioglu, H., 2022. Assessing and mapping landslide susceptibility using different

machine learning methods. Geocarto International 37, 2795 – 2820. doi:https://doi.org/10.1080/10106049.2020.1837258.

Palazzolo, N., Peres, D.J., Bordoni, M., Meisina, C., Creaco, E., Cancelliere, A., 2021. Improving spatial landslide prediction with 3d slope stability analysis and genetic algorithm optimization: Application to the oltrepó pavese. Water 13, 801. doi:https://doi.org/10.3390/w13060801.

Parise, M., 2001. Landslide mapping techniques and their use in the assessment of the landslide hazard. Physics and Chemistry of the Earth, Part C: Solar, Terrestrial Planetary Science 26, 697 – 703. doi:https://doi.org/10.1016/S1464-1917(01)00069-1.

Parise, M., 2015. A procedure for evaluating the susceptibility to natural and anthropogenic sinkholes. Georisk: Assessment and Management of Risk for Engineered Systems and Geohazards 9, 272 – 285. doi:https://doi.org/10.1080/17499518.2015.1045002.

Park, D.W., Lee, S.R., Vasu, N.N., Kang, S.H., Park, J.Y., 2016. Coupled model for simulation of landslides and debris flows at local scale. Natural Hazards 81, 1653–1682. doi:https://doi.org/10.1007/s11069-016-2150-2.

Park, D.W., Nikhil, N.V., Lee, S.R., 2013. Landslide and debris flow susceptibility zonation using trigrs for the 2011 seoul landslide event. Natural Hazards and Earth System Sciences 13, 2833–2849. doi:https://doi.org/10.5194/nhess-13-2833-2013.

Peterson, A.T., Soberón, J., Pearson, R.G., Anderson, R.P., Martínez-Meyer, E., Nakamura, M., Araújo, M.B., 2011. Ecological Niches and Geographic Distributions MPB-49). Monographs in Population Biology, Princeton University Press. URL: http://www.jstor.org/stable/j.ctt7stnh.

Petley, D., 2010. On the impact of climate change and population growth on the occurrence of fatal landslides in south, east and se asia. Quarterly Journal of Engineering Geology and Hydrogeology 43, 487 – 496. doi:10.1144/1470-9236/09-001.

Petley, D., 2012a. Global patterns of loss of life from landslides. Geology 40, 927–930. doi:https://doi.org/10.1130/G33217.1. _eprint: https://pubs.geoscienceworld.org/gsa/geology/article-pdf/40/10/927/3542823/927.pdf.

Petley, D., 2012b. Landslides and engineered slopes: protecting society through improved understanding, in: Eberhardt, E., Froese, C., Turner, A.K., Leroueil, S. (Eds.), Landslides and engineered slopes: protecting society through improved understanding, Taylor and Francis Group.

Pham, B.T., Bui, D.T., Prakash, I., Dholakia, M., 2017. Hybrid integration of multilayer perceptron neural networks and machine learning ensembles for landslide susceptibility assessment at himalayan area (india) using GIS. CATENA 149, 52 – 63. doi:https://doi.org/10.1016/j.catena.2016.09.007.

Pham, B.T., Pradhan, B., Bui, D.T., Prakash, I., Dholakia, M., 2016. A comparative study of different machine learning methods for landslide susceptibility assessment: A case study of uttarakhand area (india). Environmental Modelling & Software 84, 240 – 250.

Phillips, S., 2017. A brief tutorial on maxent. Lessons in Conservation 3, 108–135. URL: https://www.amnh.org/content/download/141371/2285439/file/LinC3_SpeciesDistModeling_Ex.pdf.

Phillips, S.J., Dudík, M., 2008. Modeling of species distributions with maxent: new extensions and a comprehensive evaluation. Ecography 31, 161–175. doi:https://doi.org/10.1111/j.0906-7590.2008.5203.x.

Pilatasig, L., Gordon, D., Palacios, O., Sánchez, J., 2005. Proyecto multinacional Andino: nGeociencias para las comunidades Andinas. Ecuador - Perú - Canadá. Technical Report. DINAGE and INGEMMET.

Plaza, G., Zevallos, O., Cadier, É., 2011. La josefina landslide dam and its catastrophic breaching in the andean region of ecuador, in: Evans, S., R.L., H., A., S., Scarascia-Mugnozza, G. (Eds.), Natural and Artificial Rockslide Dams, Springer, Berlin. pp. 389–406. doi:https://doi.org/10.1007/978-3-642-04764-0_14.

Ponzo, F.C., Iacovino, C., Ditommaso, R., Auletta, G., Soldovieri, F., Bonano, M., Cuomo, V., 2021. Civil Structural Health Monitoring. Springer International Publishing. volume 156 of *Lecture Notes in Civil Engineering*. chapter An advanced approach to the long term SHM of structures and transport infrastructures. pp. 373 – 388. doi:10.1007/978-3-030-74258-4_25.

Pourghasemi, H.R., Gayen, A., Park, S., Lee, C.W., Lee, S., 2018. Assessment of landslide-prone areas and their zonation using logistic regression, LogitBoost, and NaÃ¯veBayes machine-learning algorithms. Sustainability 10, 3697. doi:https://doi.org/10.3390/su10103697.

Pourghasemi, H.R., Mohammady, M., Pradhan, B., 2012. Landslide susceptibility mapping using index of entropy and conditional probability models in GIS: Safarood basin, iran. CATENA 97, 71–84. doi:https://doi.org/10.1016/j.catena.2012.05.005.

Pourghasemi, H.R., Rahmati, O., 2018. Prediction of the landslide susceptibility: Which algorithm, which precision? CATENA 162, 177 – 192. doi:https://doi.org/10.1016/j.catena.2017.11.022.

Pratt, W., Figueroa, J., Flores, B., 1997. Mapa geológico de la cordillera occidental 3Âº-4Âº s. escala: 1:200.000.

Qiu, H., Zhu, Y., Zhou, W., Sun, H., He, J., Liu, Z., 2022. Influence of DEM resolution on landslide simulation performance based on the scoops3d model. Geomatics, Natural Hazards and Risk 13, 1663 – 1681. doi:https://doi.org/10.1080/19475705.2022.2097451.

R Core Team, 2021. R: A Language and Environment for Statistical Computing. Version: 4.1.2 (2021-11-01). URL: https://www.R-project.org/.

R Development Core Team, 2010. R: A Language and Environment for Statistical Computing.

Rahman, T., 2012. Landslide risk reduction of the informal foothill settlements of Chittagong city through strategic design measure. mathesis. BRAC University. URL: http://hdl.handle.net/10361/3405.

Raja, A., Tridane, A., Gaffar, A., Lindquist, T., Pribadi, K., 2014. Android and ODK base d data collection framework to aid in epidemiological analysis. Journal of Public Health Informatics 5, 228. doi:10.5210/ojphi.v5i3.4996.

Raso, E., Mandarino, A., Pepe, G., Calcaterra, D., Cevasco, A., Confuorto, P., Napoli, M.D., Firpo, M., 2021. Geomorphology of cinque terre national park (italy). Journal of Maps 17, 171–184. doi:https://doi.org/10.1080/17445647.2020.1837270.

Reichenbach, P., Rossi, M., Malamud, B.D., Mihir, M., Guzzetti, F., 2018. A review of statistically-based landslide susceptibility models. Earth-Science Reviews 180, 60 – 91. doi:https://doi.org/10.1016/j.earscirev.2018.03.001.

Reu, J.D., Bourgeois, J., Bats, M., Zwertvaegher, A., Gelorini, V., Smedt, P.D., Chu, W., Antrop, M., Maeyer, P.D., Finke, P., Meirvenne, M.V., Verniers, J., CrombÃ©, P., 2013. Application of the topographic position index to heterogeneous landscapes. Geomorphology 186, 39 – 49. doi:https://doi.org/10.1016/j.geomorph.2012.12.015.

Rispoli, C., Martire, D.D., Calcaterra, D., Cappelletti, P., Graziano, S.F., Guerriero, L., 2020. Sinkholes threatening places of worship in the historic center of naples. Journal of Cultural Heritage 46, 313 – 319. doi:10.1016/j.culher.2020.09.009.

Rivera Torres, G., Serrano Fernández de Córdova, E.R., 2019. Asentamientos informales en Cuenca: el otro lado de la moneda. Revista Planeo .

Roberts, D.R., Bahn, V., Ciuti, S., Boyce, M.S., Elith, J., Guillera-Arroita, G., Hauenstein, S., Lahoz-Monfort, J.J., Schröder, B., Thuiller, W., Warton, D.I., Wintle, B.A., Hartig, F., Dormann, C.F., 2017. Cross-validation strategies for data with temporal, spatial, hierarchical, or phylogenetic structure. Ecography 40, 913–929. doi:https://doi.org/10.1111/ecog.02881.

Rojas, C., Pino, J., Jaque, E., 2013. Strategic environmental assessment in latin america: A methodological proposal for urban planning in the metropolitan area of concepción (chile). Land Use Policy 30, 519–527. doi:https://doi.org/10.1016/j.landusepol.2012.04.018.

Rosser, B., Dellow, S., Haubrock, S., Glassey, P., 2017. New zealandâs national landslide database. Landslides 14, 1949 – 1959. doi:10.1007/s10346-017-0843-6.

Rossi, M., Sarro, R., Reichenbach, P., Mateos, R.M., 2021. Probabilistic identification of rockfall source areas at regional scale in el hierro (canary islands, spain). Geomorphology 381, 107661. doi:https://doi.org/10.1016/j.geomorph.2021.107661.

Saleem, N., Huq, M.E., Twumasi, N.Y.D., Javed, A., Sajjad, A., 2019. Parameters derived from and/or used with digital elevation models (dems) for landslide susceptibility mapping and landslide risk

assessment: A review. International Journal of Geo-Information 8, 545. doi:10.3390/ijgi8120545.

Sarma, C.P., Dey, A., Krishna, A.M., 2020. Influence of digital elevation models on the simulation of rainfall-induced landslides in the hillslopes of guwahati, india. Engineering Geology 268, 105523. doi:https://doi.org/10.1016/j.enggeo.2020.105523.

Sassa, K., 2015. Isdr-icl sendai partnerships 2015–2025 for global promotion of understanding and reducing landslide disaster risk. Landslides 12, 631–640. doi:10.1007/s10346-015-0586-1.

Sassa, K., 2019. Journal landslides, the international consortium on landslides, and the kyoto landslide commitment 2020. Landslides 16, 1623–1628. doi:10.1007/s10346-019-01242-3.

Scaioni, M., Longoni, L., Melillo, V., Papini, M., 2014. Remote sensing for landslide investigations: An overview of recent achievements and perspectives. Remote Sensing 6, 9600 – 9652. doi:https://doi.org/10.3390/rs6109600.

Schlögel, R., Marchesini, I., Alvioli, M., Reichenbach, P., Rossi, M., Malet, J.P., 2018. Optimizing landslide susceptibility zonation: Effects of DEM spatial resolution and slope unit delineation on logistic regression models. Geomorphology 301, 10 – 20. doi:https://doi.org/10.1016/j.geomorph.2017.10.018.

Segoni, S., Pappafico, G., Luti, T., Catani, F., 2020. Landslide susceptibility assessment in complex geological settings: sensitivity to geological information and insights on its parameterization. Landslides 17, 2443–2453. doi:https://doi.org/10.1007/s10346-019-01340-2.

Sellers, C., Rodas, R., Carrasco, N.P., De Stefano, R., Di Martire, D., Ramondini, M., 2021a. Ground deformation monitoring of a strategic building affected by slow-moving landslide in cuenca (ecuador), in: Rizzo, P., Milazzo, A. (Eds.), European Workshop on Structural Health Monitoring, Springer International Publishing, Cham. pp. 149–158. doi:https://doi.org/10.1007/978-3-030-64908-1_14.

Sellers, C.A., Buján, S., Miranda, D., 2021b. MARLI: a mobile application for regional landslide inventories in ecuador. Landslides 18, 3963 – 3977. doi:https://doi.org/10.1007/s10346-021-01764-9.

Sepúlveda, S.A., Petley, D.N., 2015. Regional trends and controlling factors of fatal landslides in latin america and the caribbean. Natural

Hazards and Earth System Sciences 15, 1821 – 1833. doi:10.5194/nhess-15-1821-2015.

Smith, D.D., Wischmeier, W.H., 1957. Factors affecting sheet and rill erosion. Eos, Transactions American Geophysical Union 38, 889 – 896. doi:https://doi.org/10.1029/TR038i006p00889.

Steinmann, M., 1997. The cuenca basin of southern ecuador: tectono-sedimentary history and the tertiary andean evolution. doi:https://doi.org/10.3929/ethz-a-001843356.

Suárez, M.H., Coronel, C.E.I., Cueto, O.G., Bravo, E.L., Iznaga, Á.S., 2008. Propiedades mecánicas de un rhodic ferralsol requeridas para la simulación de la interacción suelo implemento de labranza mediante el método de elementos finitos: Parte i. Revista Ciencias Técnicas Agropecuarias 17, 31–38.

Sultana, N., Tan, S., 2021. Landslide mitigation strategies in southeast bangladesh: Lessons learned from the institutional responses. International Journal of Disaster Risk Reduction 62, 102402. doi:https://doi.org/10.1016/j.ijdrr.2021.102402.

Swets, J.A., 1988. Measuring the accuracy of diagnostic systems. Science 240, 1285–1293. doi:https://doi.org/10.1126/science.3287615.

Talledo, D.A., Miano, A., Bonano, M., Di Carlo, F., Lanari, R., Manunta, M., Meda, A., Mele, A., Prota, A., Saetta, A., Stella, A., 2022. Satellite radar interferometry: Potential and limitations for structural assessment and monitoring. Journal of Building Engineering 46, 103756. doi:10.1016/j.jobe.2021.103756.

Tanyaş, H., Lombardo, L., 2020. Completeness index for earthquake-induced landslide inventories. Engineering Geology 264, 105331. doi:10.1016/j.enggeo.2019.105331.

Tanyaş, H., van Westen, C.J., Allstadt, K.E., Jessee, M.A.N., Gorum, T., Jibson, R.W., Godt, J.W., Sato, H.P., Schmitt, R.G., Marc, O., Hovius, N., 2017. Presentation and analysis of a worldwide database of earthquake-induced landslide inventories. Journal of Geophysical Research: Earth Surface 122, 1991 – 2015. doi:10.1002/2017JF004236.

Tao, Z., Zhang, H., Zhu, C., Hao, Z., Zhang, X., Hu, X., 2019. Design and operation of app-based intelligent landslide monitoring system: the case of three gorges reservoir region. Geomatics, Natural Hazards

and Risk 10, 1209 – 1226. doi:https://doi.org/10.1080/19475705.2019.1568312.

Therneau, T., Atkinson, B., 2019. rpart: Recursive partitioning and regression trees. r package version 4.1-15. URL: https://CRAN.R-project.org/package=rpart. r package version 4.1-15.

Tien Bui, D., Tuan, T.A., Klempe, H., Pradhan, B., Revhaug, I., 2016. Spatial prediction models for shallow landslide hazards: a comparative assessment of the efficacy of support vector machines, artificial neural networks, kernel logistic regression, and logistic model tree. Landslides 13, 361 – 378. doi:https://doi.org/10.1007/s10346-015-0557-6.

Torsello, G., Vallero, G., Milan, L., Barbero, M., Castelli, M., 2022. A quick QGIS-based procedure to preliminarily define time-independent rockfall risk: The case study of sorba valley, italy. Geosciences 12. doi:https://doi.org/10.3390/geosciences12080305.

Tyoda, Z., 2013. Landslide susceptibility mapping: remote sensing and GIS approach. URL: http://hdl.handle.net/10019.1/79856.

Žabota, B., Repe, B., Kobal, M., 2019. Influence of digital elevation model resolution on rockfall modelling. Geomorphology 328, 183 – 195. doi:https://doi.org/10.1016/j.geomorph.2018.12.029.

Van Den Eeckhaut, M., Hervás, J., 2012. State of the art of national landslide databases in europe and their potential for assessing landslide susceptibility, hazard and risk. Geomorphology 139 - 140, 545 – 558. doi:10.1016/j.geomorph.2011.12.006.

Van Thournout, F., Salemink, J., Valenzuela, G., Merlyn, M., Boven, A., Muchez, P., 1996. Portovelo: a volcanic-hosted epithermal vein-system in ecuador, south america. Mineralium Deposita 31, 269 – 276.

Van Westen, C., 2004. Geo-information tools for landslide risk assessment: an overview of recent developments. Landslides: evaluation and stabilization 1, 39 – 56. Publisher: Balkema London, AA.

van Westen, C.J., Rengers, N., Soeters, R., 2003. Use of geomorphological information in indirect landslide susceptibility assessment. Natural Hazards 30, 399–419. doi:https://doi.org/10.1023/B:NHAZ.0000007097.42735.9e.

Varnes, D., 1978. Landslide Analysis and Control, National Academy of Sciences. Transportation Research Board Special Report, Washington D.C.. volume 176. chapter Slope movements: types and processes. pp. 11 – 33.

Varnes, D.J., 1984. Landslide hazard zonation : a review of principles and practice. 3, Natural Hazards. URL: http://worldcat.org/isbn/9231018957.

Venkatasrinivasa Murthy, M., 2017. Field GIS: Towards mobile computing to support pre-disaster spatial analysis in the fiels. Marter thesis. Faculty of Geo-Information Science and Earth Observation, University os Twente. Enschede, The Netherlands.

Vulović, N., Kitanović, O., Stanković, R., Vorkapić, D., Vulović, A., 2017. BEWARE multi-device web GIS application for landslides, in: Mikoš, M., Arbanas, Ž., Yin, Y., Sassa, K. (Eds.), Advancing Culture of Living with Landslides, Springer International Publishing, Cham. pp. 423–430. doi:10.1007/978-3-319-53487-9.

Wang, H.B., Wu, S.R., Shi, J.S., Li, B., 2013. Qualitative hazard and risk assessment of landslides: a practical framework for a case study in china. Natural Hazards 69, 1281–1294. doi:https://doi.org/10.1007/s11069-011-0008-1.

Warren, D.L., Seifert, S.N., 2011. Ecological niche modeling in maxent: the importance of model complexity and the performance of model selection criteria. Ecological Applications 21, 335–342. doi:https://doi.org/10.1890/10-1171.1.

Wasowski, J., Bovenga, F., 2014. Investigating landslides and unstable slopes with satellite multi temporal interferometry: Current issues and future perspectives. Engineering Geology 174, 103 – 138. doi:10.1016/j.enggeo.2014.03.003.

Wenger, S.J., Olden, J.D., 2012. Assessing transferability of ecological models: an underappreciated aspect of statistical validation. Methods in Ecology and Evolution 3, 260–267. doi:https://doi.org/10.1111/j.2041-210X.2011.00170.x.

van Westen, C.J., Castellanos, E., Kuriakose, S.L., 2008. Spatial data for landslide susceptibility, hazard, and vulnerability assessment: An overview. Engineering Geology 102, 112 – 131. doi:https://doi.org/10.1016/j.enggeo.2008.03.010. landslide Susceptibility, Hazard and Risk Zoning for Land Use Planning.

Wieczorek, G., Mandrone, G., DeCola, L., 1997. The influence of hillslope shape on debris-flow initiation, in: Chen, C.I. (Ed.), Debris-Flow Hazards Mitigation: Mechanics, Prediction and Assessment, ASCE. pp. 21–31.

Wubalem, A., 2022. The impact of DEM resolution on landslide susceptibility modeling. Arabian Journal of Geosciences 15, 967.

Xu, C., Xu, X., Dai, F., Wu, Z., He, H., Shi, F., Wu, X., Xu, S., 2013. Application of an incomplete landslide inventory, logistic regression model and its validation for landslide susceptibility mapping related to the may 12, 2008 wenchuan earthquake of china. Natural hazards 68, 883–900.

Zevenbergen, L.W., Thorne, C.R., 1987. Quantitative analysis of land surface topography. Earth Surface Processes and Landforms 12, 47–56. doi:https://doi.org/10.1002/esp.3290120107.

Zhang, T.y., Mao, Z.a., Wang, T., 2020. Gis-based evaluation of landslide susceptibility using a novel hybrid computational intelligence model on different mapping units. Journal of Mountain Science 17, 2929–2941. doi:https://doi.org/10.1007/s11629-020-6393-8.

Zhao, P., Masoumi, Z., Kalantari, M., Aflaki, M., Mansourian, A., 2022. A GIS-based landslide susceptibility mapping and variable importance analysis using artificial intelligent training-based methods. Remote Sensing 14, 211. doi:https://doi.org/10.3390/rs14010211.

Zhou, C., Yin, K., Cao, Y., Ahmed, B., Li, Y., Catani, F., Pourghasemi, H.R., 2018. Landslide susceptibility modeling applying machine learning methods: A case study from longju in the three gorges reservoir area, china. Computers and Geosciences 112, 23 – 37. doi:https://doi.org/10.1016/j.cageo.2017.11.019.

Zieher, T., Formanek, T., Bremer, M., Meissl, G., Rutzinger, M., 2012. Digital terrain model resolution and its influence on estimating the extent of rockfall areas. Transactions in GIS 16, 691 – 699. doi:https://doi.org/10.1111/j.1467-9671.2012.01334.x.

Zorn, M., 2018. Natural disasters and less developed countries, in: Nature, tourism and ethnicity as drivers of marginalization. Springer, pp. 59–78.

List of Figures

List of Tables

Appendices

APPENDIX A

Appendices of Chapter 2. Multitemporal relative landslide exposure and risk analysis

A.1 Factors used for susceptibility analysis.

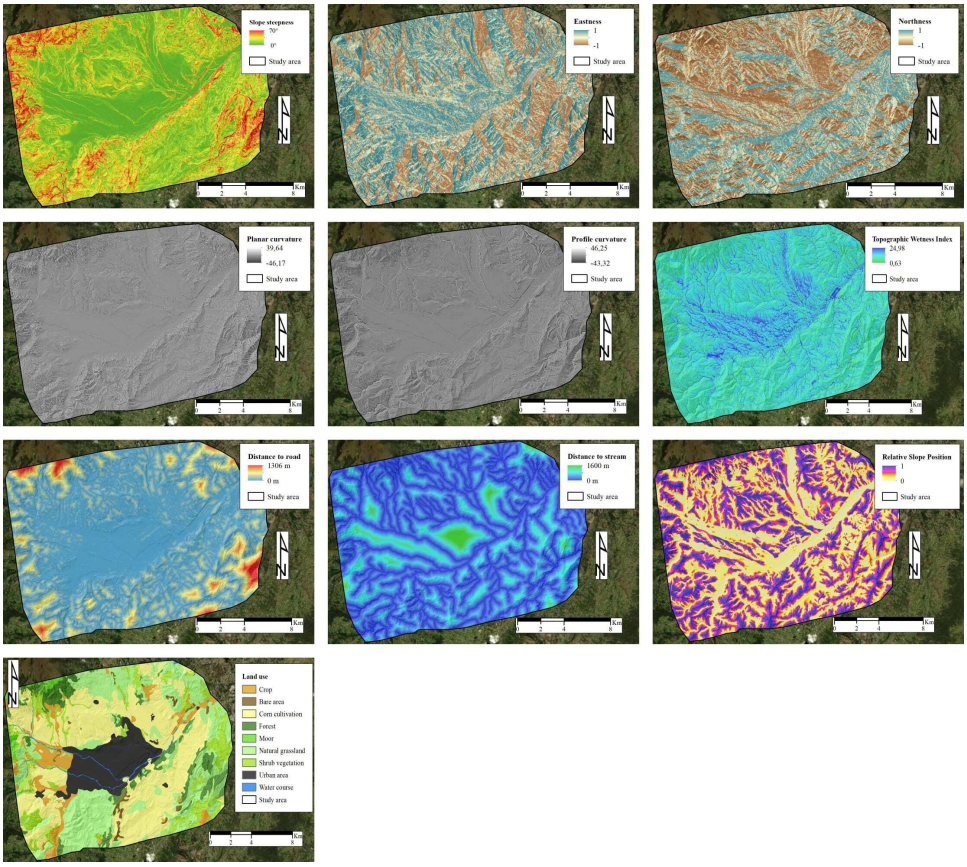

Figure A.1: Predisposing factors used for susceptibility analysis.

A.2 The conducted analysis to estimate the rate electricity supply contracts.

Table A.1: Detailed table with all the conducted analysis to estimate the rate electricity supply contracts.

	Susc	Electricity supply contracts rates							Electricity supply contracts rates to 100			Susc area	Susc area
		10 Nr	10 - 18 %	18 Nr	10 - 19 %	19 Nr	10 - 20 %	20 Nr	10 - 18 %	10 - 19 %	10 - 20 %	%	kmq
SIDCAY	*S1*	113	42%	161	42%	161	49%	168	24%	21%	22%	23%	1.41
	S2	200	32%	264	40%	279	41%	282	32%	34%	32%	33%	2.03
	S3	139	28%	178	34%	186	40%	195	19%	21%	22%	22%	1.34
	S4	74	39%	103	42%	105	47%	109	14%	14%	14%	14%	0.85
	S5	44	50%	66	55%	68	59%	70	11%	10%	10%	9%	0.53
		570	192%	772	212%	799	236%	824	100%	100%	100%	100%	6.16

	Susc	Electricity supply contracts rates							Electricity supply contracts rates to 100			Susc area	Susc area
		10 Nr	10 - 18 %	18 Nr	10 - 19 %	19 Nr	10 - 20 %	20 Nr	10 - 18 %	10 - 19 %	10 - 20 %	%	kmq
SINCAY	*S1*	276	51%	416	60%	442	66%	457	11%	11%	10%	19%	4.54
	S2	842	44%	1216	53%	1288	57%	1323	29%	28%	27%	30%	7.13
	S3	710	50%	1063	60%	1136	66%	1181	27%	27%	27%	25%	5.90
	S4	564	47%	829	60%	901	70%	957	20%	21%	22%	17%	4.03
	S5	282	59%	449	72%	484	80%	509	13%	13%	13%	8%	1.90
		2674	251%	3973	304%	4251	339%	4427	100%	100%	100%	100%	23.50

	Susc	Electricity supply contracts rates							Electricity supply contracts rates to 100			Susc area	Susc area
		10 Nr	10 - 18 %	18 Nr	10 - 19 %	19 Nr	10 - 20 %	20 Nr	10 - 18 %	10 - 19 %	10 - 20 %	%	kmq
SANTANA	*S1*	68	31%	89	37%	93	43%	97	11%	12%	12%	33%	3.22
	S2	85	41%	120	48%	126	58%	134	19%	20%	20%	25%	2.42
	S3	87	39%	121	44%	125	49%	130	18%	18%	18%	16%	1.58
	S4	113	35%	152	38%	156	42%	161	21%	21%	20%	13%	1.25
	S5	152	36%	207	41%	214	47%	224	30%	30%	30%	14%	1.37
		505	182%	689	208%	714	240%	746	100%	100%	100%	100%	9.84

continued on next page

Table A.1 – Detailed table with all the conducted analysis to estimate the rate electricity supply contracts. (continued).

	Susc	Electricity supply contracts rates							Electricity supply contracts rates to 100			Susc area	Susc area
		10 Nr	10 - 18 %	18 Nr	10 - 19 %	19 Nr	10 - 20 %	20 Nr	10 - 18 %	10 - 19 %	10 - 20 %	%	kmq
SAYAUSI	S1	44	227%	144	270%	163	282%	168	14%	14%	14%	42%	8.62
	S2	149	142%	361	166%	397	177%	412	30%	30%	30%	26%	5.33
	S3	146	136%	344	156%	374	170%	394	28%	28%	28%	18%	3.72
	S4	89	149%	222	173%	243	180%	249	19%	19%	18%	10%	2.06
	S5	22	295%	87	345%	98	373%	104	9%	9%	9%	5%	0.95
		450	950%	1158	1112%	1275	1181%	1327	100%	100%	100%	100%	20.68

	Susc	Electricity supply contracts rates							Electricity supply contracts rates to 100			Susc area	Susc area
		10 Nr	10 - 18 %	18 Nr	10 - 19 %	19 Nr	10 - 20 %	20 Nr	10 - 18 %	10 - 19 %	10 - 20 %	%	kmq
VALLE	S1	615	27%	779	41%	869	44%	884	8%	11%	11%	19%	5.54
	S2	1228	34%	1641	41%	1729	44%	1772	21%	21%	21%	26%	7.90
	S3	1372	38%	1898	46%	1997	48%	2032	27%	26%	26%	25%	7.35
	S4	1514	36%	2061	41%	2139	45%	2196	28%	26%	27%	20%	5.95
	S5	808	39%	1122	45%	1172	48%	1198	16%	15%	15%	11%	3.15
		5537	174%	7501	214%	7906	229%	8082	100%	100%	100%	100%	29.89

	Susc	Electricity supply contracts rates							Electricity supply contracts rates to 100			Susc area	Susc area
		10 Nr	10 - 18 %	18 Nr	10 - 19 %	19 Nr	10 - 20 %	20 Nr	10 - 18 %	10 - 19 %	10 - 20 %	%	kmq
ZHIMAD	S1		33%		33%		33%		16%	15%	15%		0.23
	S2		77%		77%		85%		40%	38%	41%		0.33
	S3		67%		67%		67%		24%	23%	22%		0.22
	S4		250%		250%		250%		20%	19%	19%		0.14
	S5		0%		100%		100%		0%	4%	4%		0.09
			427%		527%		535%		100%	100%	100%		1.00

continued on next page

Table A.1 – Detailed table with all the conducted analysis to estimate the rate electricity supply contracts. (continued).

	Susc	Electricity supply contracts rates							Electricity supply contracts rates to 100			Susc area	Susc area
		10 Nr	10 - 18 %	18 Nr	10 - 19 %	19 Nr	10 - 20 %	20 Nr	10 - 18 %	10 - 19 %	10 - 20 %	%	kmq
TARQUI	*S1*	16	50%	24	50%	24	50%	24	17%	16%	15%	14%	0.32
	S2	39	15%	45	18%	46	18%	46	13%	14%	13%	26%	0.58
	S3	21	48%	31	52%	32	57%	33	21%	22%	23%	24%	0.53
	S4	13	62%	21	69%	22	69%	22	17%	18%	17%	17%	0.38
	S5	23	65%	38	65%	38	70%	39	32%	30%	31%	18%	0.40
		112	240%	159	255%	162	264%	164	100%	100%	100%	100%	2.21

	Susc	Electricity supply contracts rates							Electricity supply contracts rates to 100			Susc area	Susc area
		10 Nr	10 - 18 %	18 Nr	10 - 19 %	19 Nr	10 - 20 %	20 Nr	10 - 18 %	10 - 19 %	10 - 20 %	%	kmq
TURI	*S1*	63	79%	113	116%	136	124%	141	5%	6%	6%	7%	1.70
	S2	228	58%	360	75%	400	80%	410	14%	14%	13%	19%	4.56
	S3	382	47%	563	62%	619	64%	627	20%	19%	18%	23%	5.60
	S4	596	45%	865	60%	952	64%	978	30%	28%	28%	25%	6.12
	S5	485	58%	764	90%	920	96%	953	31%	34%	35%	25%	6.13
		1754	287%	2665	403%	3027	428%	3109	100%	100%	100%	100%	24.11

	Susc	Electricity supply contracts rates							Electricity supply contracts rates to 100			Susc area	Susc area
		10 Nr	10 - 18 %	18 Nr	10 - 19 %	19 Nr	10 - 20 %	20 Nr	10 - 18 %	10 - 19 %	10 - 20 %	%	kmq
CHIQUAUINT	*S1*	210	31%	275	36%	285	46%	306	36%	35%	38%	32%	1.43
	S2	257	23%	317	27%	326	31%	336	34%	33%	31%	35%	1.56
	S3	141	28%	180	35%	190	39%	196	22%	23%	21%	23%	1.03
	S4	36	31%	47	42%	51	53%	55	6%	7%	7%	8%	0.36
	S5	5	80%	9	80%	9	140%	12	2%	2%	3%	3%	0.14
		649	193%	828	219%	861	308%	905	100%	100%	100%	100%	4.52

continued on next page

Table A.1 – Detailed table with all the conducted analysis to estimate the rate electricity supply contracts. (continued).

	Susc	Electricity supply contracts rates							Electricity supply contracts rates to 100			Susc area	Susc area
		10 Nr	10 - 18 %	18 Nr	10 - 19 %	19 Nr	10 - 20 %	20 Nr	10 - 18 %	10 - 19 %	10 - 20 %	%	kmq
LLACCAO	*S1*	157	32%	207	51%	237	55%	243	15%	18%	18%	23%	2.89
	S2	304	32%	400	48%	449	51%	460	29%	33%	33%	33%	4.12
	S3	276	29%	357	37%	377	41%	390	25%	23%	24%	21%	2.68
	S4	217	31%	285	36%	296	40%	303	21%	18%	18%	15%	1.94
	S5	90	36%	122	40%	126	42%	128	10%	8%	8%	8%	1.01
		1044	160%	1371	212%	1485	229%	1524	100%	100%	100%	100%	12.64

	Susc	Electricity supply contracts rates							Electricity supply contracts rates to 100			Susc area	Susc area
		10 Nr	10 - 18 %	18 Nr	10 - 19 %	19 Nr	10 - 20 %	20 Nr	10 - 18 %	10 - 19 %	10 - 20 %	%	kmq
BANOS	*S1*	151	69%	255	96%	296	99%	301	7%	8%	8%	17%	3.99
	S2	309	96%	607	117%	669	128%	705	21%	20%	20%	27%	6.45
	S3	325	111%	686	146%	799	164%	857	26%	26%	27%	25%	6.05
	S4	351	117%	760	145%	859	158%	906	29%	28%	28%	19%	4.64
	S5	184	130%	423	165%	488	184%	523	17%	17%	17%	12%	2.77
		1320	523%	2731	668%	3111	734%	3292	100%	100%	100%	100%	23.90

	Susc	Electricity supply contracts rates							Electricity supply contracts rates to 100			Susc area	Susc area
		10 Nr	10 - 18 %	18 Nr	10 - 19 %	19 Nr	10 - 20 %	20 Nr	10 - 18 %	10 - 19 %	10 - 20 %	%	kmq
RICAURTE	*S1*	1956	40%	2731	46%	2848	51%	2959	47%	47%	48%	37%	5.10
	S2	939	44%	1348	50%	1410	56%	1467	25%	25%	25%	26%	3.65
	S3	495	46%	723	52%	754	57%	775	14%	14%	13%	18%	2.50
	S4	294	60%	470	67%	491	69%	497	11%	10%	10%	12%	1.64
	S5	115	59%	183	73%	199	76%	202	4%	4%	4%	7%	0.90
		3799	248%	5455	288%	5702	309%	5900	100%	100%	100%	100%	13.79

continued on next page

Table A.1 – Detailed table with all the conducted analysis to estimate the rate electricity supply contracts. (continued).

	Susc	Electricity supply contracts rates							Electricity supply contracts rates to 100			Susc area %	Susc area kmq
		10 Nr	10 - 18 %	18 Nr	10 - 19 %	19 Nr	10 - 20 %	20 Nr	10 - 18 %	10 - 19 %	10 - 20 %		
SANJAOAQUIN	*S1*	215	69%	484	96%	622	99%	642	7%	8%	8%	36%	4.54
	S2	151	96%	355	117%	414	128%	427	21%	20%	20%	31%	3.85
	S3	51	111%	120	146%	143	164%	147	26%	26%	27%	19%	2.34
	S4	34	117%	69	145%	81	158%	84	29%	28%	28%	9%	1.13
	S5	11	130%	26	165%	30	184%	31	17%	17%	17%	5%	0.61
		462	523%	1054	668%	1290	734%	1331	100%	100%	100%	100%	12.47

	Susc	Electricity supply contracts rates							Electricity supply contracts rates to 100			Susc area %	Susc area kmq
		10 Nr	10 - 18 %	18 Nr	10 - 19 %	19 Nr	10 - 20 %	20 Nr	10 - 18 %	10 - 19 %	10 - 20 %		
NULTI	*S1*	17	100%	34	141%	41	165%	45	5%	6%	6%	36%	4.54
	S2	82	44%	118	54%	126	57%	129	11%	10%	10%	31%	3.85
	S3	172	41%	243	52%	262	54%	265	21%	21%	20%	19%	2.34
	S4	267	39%	371	50%	400	53%	409	31%	31%	31%	9%	1.13
	S5	155	70%	264	90%	295	93%	299	32%	32%	32%	5%	0.61
		693	294%	1030	387%	1124	422%	1147	100%	100%	100%	100%	12.47

	Susc	Electricity supply contracts rates							Electricity supply contracts rates to 100			Susc area %	Susc area kmq
		10 Nr	10 - 18 %	18 Nr	10 - 19 %	19 Nr	10 - 20 %	20 Nr	10 - 18 %	10 - 19 %	10 - 20 %		
PACCHA	*S1*	128	35%	173	46%	187	47%	188	7%	7%	7%	15%	3.69
	S2	336	28%	430	34%	449	36%	458	15%	14%	14%	21%	5.30
	S3	450	31%	591	41%	636	43%	644	23%	23%	23%	23%	5.62
	S4	589	34%	790	44%	846	47%	866	33%	32%	32%	22%	5.48
	S5	387	34%	518	48%	574	52%	587	21%	23%	23%	19%	4.66
		1890	162%	2502	213%	2692	225%	2743	100%	100%	100%	100%	24.75

continued on next page

Table A.1 – Detailed table with all the conducted analysis to estimate the rate electricity supply contracts. (continued).

CUENCA	Susc	Electricity supply contracts rates							Electricity supply contracts rates to 100			Susc area %	Susc area kmq
		10 Nr	10 - 18 %	18 Nr	10 - 19 %	19 Nr	10 - 20 %	20 Nr	10 - 18 %	10 - 19 %	10 - 20 %		
	S1	33360	23%	41089	26%	42144	28%	42713	53%	52%	52%	55%	40.92
	S2	5726	55%	8865	63%	9346	67%	9534	21%	22%	21%	18%	13.26
	S3	2308	79%	4121	91%	4398	96%	4518	12%	12%	12%	12%	8.55
	S4	1725	81%	3123	94%	3351	99%	3427	10%	10%	10%	10%	7.06
	S5	782	77%	1388	91%	1491	95%	1528	4%	4%	4%	6%	4.24
		43901	315%	58586	365%	60730	384%	61720	100%	100%	100%	100%	74.03

A.3 Models obtained through ENMEval R package

Table A.2: The models obtained through ENMEval R package by setting different values of regularization multiplier and considering different feature classes.

settings	features	rm	train.AUC	avg.test.AUC	var.test.AUC	avg.diff.AUC	var.diff.AUC	avg.test.orMTP	var.test.orMTP	avg.test.or10pct	var.test.or10pct	AIC_c	ΔAIC_c	w.AIC	parameters
1	L_0.5 L	0.5	0.79	0.67	0.02	0.14	0.03	0.02	0.00	0.27	0.05	13512.89	107.60	$3.40e^{-24}$	31
2	LQ_0.5 LQ	0.5	0.80	0.71	0.01	0.11	0.02	0.02	0.00	0.25	0.03	13443.09	37.80	$4.88e^{-09}$	38
3	H_0.5 H	0.5	0.84	0.73	0.01	0.12	0.02	0.02	0.00	0.29	0.03	13834.69	429.40	$4.50e^{-94}$	197
4	LQH_0.5 LQH	0.5	0.84	0.73	0.01	0.12	0.02	0.02	0.00	0.29	0.03	13848.54	443.25	$4.43e^{-97}$	199
5	LQHP_0.5 LQHP	0.5	0.84	0.72	0.01	0.13	0.02	0.03	0.00	0.29	0.03	13739.80	334.51	$1.81e^{-73}$	182
6	LQHPT_0.5 LQHPT	0.5	0.87	0.74	0.01	0.14	0.01	0.01	0.00	0.34	0.04	14321.18	915.90	$1.03e^{-199}$	156
7	L_1 L	1	0.78	0.68	0.02	0.13	0.03	0.02	0.00	0.25	0.04	13513.60	108.32	$2.38e^{-24}$	29
8	LQ_1 LQ	1	0.80	0.71	0.01	0.11	0.02	0.02	0.00	0.24	0.02	13452.82	47.53	$3.76e^{-11}$	37
9	H_1 H	1	0.83	0.73	0.01	0.11	0.02	0.02	0.00	0.26	0.03	13599.35	194.07	$5.70e^{-43}$	143
10	LQH_1 LQH	1	0.83	0.73	0.01	0.11	0.02	0.02	0.00	0.26	0.03	13662.58	257.29	$1.06e^{-56}$	158
11	LQHP_1 LQHP	1	0.83	0.73	0.01	0.12	0.02	0.02	0.00	0.27	0.03	13632.16	226.87	$4.30e^{-50}$	155
12	LQHPT_1 LQHPT	1	0.85	0.73	0.01	0.14	0.02	0.02	0.00	0.32	0.04	13463.35	58.07	$1.94e^{-13}$	144
13	L_1.5 L	1.5	0.78	0.69	0.02	0.12	0.03	0.02	0.00	0.24	0.04	13510.03	104.75	$1.42e^{-23}$	26
14	LQ_1.5 LQ	1.5	0.80	0.71	0.01	0.10	0.02	0.02	0.00	0.23	0.02	13450.69	45.41	$1.09e^{-10}$	30
15	H_1.5 H	1.5	0.82	0.74	0.01	0.10	0.02	0.03	0.00	0.24	0.03	13567.08	161.80	$5.80e^{-36}$	128
16	LQH_1.5 LQH	1.5	0.82	0.74	0.01	0.10	0.02	0.03	0.00	0.24	0.03	13552.06	146.77	$1.06e^{-32}$	124
17	LQHP_1.5 LQHP	1.5	0.83	0.73	0.01	0.11	0.02	0.03	0.00	0.25	0.03	13511.98	106.69	$5.36e^{-24}$	117
18	LQHPT_1.5 LQHPT	1.5	0.84	0.74	0.01	0.12	0.01	0.02	0.00	0.28	0.03	13436.97	31.68	$1.04e^{-07}$	113

continued on next page

Table A.2 – The models obtained through ENMEval R package by setting different values of regularization multiplier and considering different feature classes (continued).

settings	features	rm	train.AUC	avg.test.AUC	var.test.AUC	avg.diff.AUC	var.diff.AUC	avg.test.orMTP	var.test.orMTP	avg.test.or10pct	var.test.or10pct	AIC_c	ΔAIC_c	w.AIC	parameters
19	L_2 L	2	0.78	0.69	0.02	0.11	0.03	0.02	0.00	0.24	0.03	13509.62	104.33	$1.74e^{-23}$	24
20	LQ_2 LQ	2	0.79	0.71	0.01	0.10	0.02	0.02	0.00	0.22	0.02	13460.94	55.66	$6.47e^{-13}$	28
21	H_2 H	2	0.82	0.74	0.01	0.09	0.02	0.03	0.00	0.23	0.03	13499.71	94.42	$2.47e^{-21}$	102
22	LQH_2 LQH	2	0.82	0.74	0.01	0.10	0.02	0.03	0.00	0.24	0.03	13506.60	101.32	$7.88e^{-23}$	103
23	LQHP_2 LQHP	2	0.82	0.73	0.01	0.10	0.02	0.03	0.00	0.24	0.03	13513.16	107.87	$2.98e^{-24}$	108
24	LQHPT_2 LQHPT	2	0.83	0.74	0.01	0.11	0.01	0.03	0.00	0.25	0.03	13412.34	7.06	0.02	91
25	L_2.5 L	2.5	0.78	0.70	0.02	0.11	0.02	0.02	0.00	0.21	0.02	13514.14	108.86	$1.82e^{-24}$	24
26	LQ_2.5 LQ	2.5	0.79	0.72	0.02	0.09	0.02	0.02	0.00	0.22	0.02	13473.23	67.94	$1.39e^{-15}$	26
27	H_2.5 H	2.5	0.82	0.74	0.01	0.09	0.02	0.02	0.00	0.22	0.02	13535.71	130.43	$3.76e^{-29}$	106
28	LQH_2.5 LQH	2.5	0.82	0.74	0.01	0.09	0.02	0.03	0.00	0.21	0.02	13460.28	55.00	$9.01e^{-13}$	81
29	LQHP_2.5 LQHP	2.5	0.82	0.74	0.01	0.10	0.02	0.03	0.00	0.24	0.03	13452.33	47.04	$4.82e^{-11}$	81
30	LQHPT_2.5 LQHPT	2.5	0.83	0.74	0.01	0.10	0.02	0.03	0.00	0.22	0.02	13408.27	2.98	0.18	79
31	L_3 L	3	0.78	0.71	0.02	0.10	0.02	0.02	0.00	0.20	0.02	13519.34	114.06	$1.35e^{-25}$	24
32	LQ_3 LQ	3	0.79	0.72	0.02	0.09	0.02	0.02	0.00	0.21	0.02	13479.47	74.18	$6.15e^{-17}$	25
33	H_3 H	3	0.82	0.75	0.01	0.08	0.02	0.02	0.00	0.21	0.02	13575.30	170.01	$9.54e^{-38}$	112
34	LQH_3 LQH	3	0.81	0.74	0.01	0.08	0.02	0.03	0.00	0.20	0.02	13493.85	88.56	$4.64e^{-20}$	85
35	LQHP_3 LQHP	3	0.82	0.74	0.01	0.09	0.02	0.03	0.00	0.20	0.02	13507.25	101.96	$5.71e^{-23}$	91
36	LQHPT_3 LQHPT	3	0.82	0.75	0.01	0.09	0.02	0.03	0.00	0.21	0.02	13421.81	16.52	0.00	74
37	L_3.5 L	3.5	0.78	0.71	0.02	0.09	0.02	0.02	0.00	0.20	0.02	13523.49	118.20	$1.70e^{-26}$	23

continued on next page

Table A.2 – The models obtained through ENMEval R package by setting different values of regularization multiplier and considering different feature classes (continued).

settings	features	rm	train.AUC	avg.test.AUC	var.test.AUC	avg.diff.AUC	var.diff.AUC	avg.test.orMTP	var.test.orMTP	avg.test.or10pct	var.test.or10pct	AIC_c	ΔAIC_c	w.AIC	parameters
38	LQ_3.5 LQ	3.5	0.79	0.72	0.02	0.09	0.02	0.02	0.00	0.20	0.01	13489.17	83.89	$4.80e^{-19}$	25
39	H_3.5 H	3.5	0.82	0.75	0.01	0.08	0.02	0.02	0.00	0.21	0.02	13488.95	83.66	$5.38e^{-19}$	80
40	LQH_3.5 LQH	3.5	0.81	0.75	0.01	0.08	0.02	0.03	0.00	0.19	0.02	13500.46	95.17	$1.70e^{-21}$	82
41	LQHP_3.5 LQHP	3.5	0.81	0.74	0.01	0.08	0.02	0.03	0.00	0.19	0.02	13491.77	86.48	$1.31e^{-19}$	79
42	LQHPT_3.5 LQHPT	3.5	0.82	0.75	0.01	0.08	0.02	0.03	0.00	0.21	0.02	13405.29	0.00	0.79	60
43	L_4 L	4	0.78	0.71	0.02	0.09	0.02	0.02	0.00	0.19	0.02	13527.41	122.12	$2.39e^{-27}$	22
44	LQ_4 LQ	4	0.79	0.73	0.02	0.08	0.02	0.02	0.00	0.19	0.02	13496.44	91.16	$1.27e^{-20}$	24
45	H_4 H	4	0.81	0.75	0.01	0.08	0.02	0.02	0.00	0.21	0.02	13514.49	109.20	$1.53e^{-24}$	83
46	LQH_4 LQH	4	0.81	0.75	0.01	0.08	0.02	0.03	0.00	0.19	0.02	13470.73	65.45	$4.85e^{-15}$	65
47	LQHP_4 LQHP	4	0.81	0.74	0.01	0.08	0.02	0.02	0.00	0.19	0.02	13486.04	80.75	$2.30e^{-18}$	71
48	LQHPT_4 LQHPT	4	0.82	0.75	0.01	0.08	0.02	0.03	0.00	0.19	0.02	13414.09	8.81	0.01	57
49	L_4.5 L	4.5	0.78	0.72	0.02	0.08	0.02	0.02	0.00	0.19	0.01	13533.59	128.31	$1.09e^{-28}$	22
50	LQ_4.5 LQ	4.5	0.79	0.73	0.02	0.08	0.02	0.02	0.00	0.18	0.01	13503.78	98.50	$3.23e^{-22}$	23
51	H_4.5 H	4.5	0.81	0.75	0.01	0.07	0.02	0.02	0.00	0.20	0.02	13495.85	90.57	$1.70e^{-20}$	72
52	LQH_4.5 LQH	4.5	0.81	0.75	0.01	0.07	0.02	0.02	0.00	0.18	0.01	13471.70	66.42	$2.99e^{-15}$	60
53	LQHP_4.5 LQHP	4.5	0.81	0.75	0.01	0.08	0.02	0.02	0.00	0.18	0.01	13496.82	91.53	$1.05e^{-20}$	70
54	LQHPT_4.5 LQHPT	4.5	0.82	0.75	0.01	0.07	0.02	0.02	0.00	0.18	0.01	13422.30	17.01	0.00	54
55	L_5 L	5	0.78	0.72	0.02	0.08	0.02	0.02	0.00	0.17	0.02	13540.33	135.05	$3.74e^{-30}$	22
56	LQ_5 LQ	5	0.78	0.73	0.02	0.08	0.02	0.02	0.00	0.17	0.01	13514.61	109.32	$1.44e^{-24}$	23

continued on next page

Table A.2 – The models obtained through ENMEval R package by setting different values of regularization multiplier and considering different feature classes (continued).

settings	features	rm	train.AUC	avg.test.AUC	var.test.AUC	avg.diff.AUC	var.diff.AUC	avg.test.orMTP	var.test.orMTP	avg.test.or10pct	var.test.or10pct	AIC_c	ΔAIC_c	w.AIC	parameters
57	H_5 H	5	0.81	0.75	0.01	0.07	0.02	0.02	0.00	0.19	0.02	13514.43	109.14	$1.58e^{-24}$	74
58	LQH_5 LQH	5	0.81	0.75	0.01	0.07	0.02	0.02	0.00	0.17	0.01	13463.52	58.24	$1.78e^{-13}$	52
59	LQHP_5 LQHP	5	0.81	0.75	0.01	0.07	0.02	0.02	0.00	0.17	0.01	13472.34	67.05	$2.17e^{-15}$	56
60	LQHPT_5 LQHPT	5	0.81	0.75	0.01	0.07	0.02	0.02	0.00	0.18	0.01	13439.62	34.33	$2.77e^{-08}$	54
61	L_5.5 L	5.5	0.78	0.73	0.02	0.08	0.02	0.02	0.00	0.16	0.01	13542.83	137.54	$1.07e^{-30}$	20
62	LQ_5.5 LQ	5.5	0.78	0.73	0.02	0.08	0.02	0.02	0.00	0.17	0.01	13524.26	118.97	$1.16e^{-26}$	22
63	H_5.5 H	5.5	0.81	0.75	0.01	0.07	0.02	0.02	0.00	0.18	0.02	13527.31	122.03	2.51^{-27}	74
64	LQH_5.5 LQH	5.5	0.81	0.75	0.01	0.07	0.02	0.02	0.00	0.16	0.01	13481.65	76.36	$2.07e^{-17}$	54
65	LQHP_5.5 LQHP	5.5	0.81	0.75	0.01	0.07	0.02	0.02	0.00	0.17	0.01	13478.35	73.06	$1.08e^{-16}$	53
66	LQHPT_5.5 LQHPT	5.5	0.81	0.75	0.01	0.07	0.02	0.02	0.00	0.17	0.01	13439.24	33.95	$3.35e^{-08}$	47
67	L_6 L	6	0.78	0.73	0.02	0.08	0.02	0.02	0.00	0.16	0.01	13547.28	141.99	$1.16e^{-31}$	19
68	LQ_6 LQ	6	0.78	0.73	0.02	0.07	0.02	0.02	0.00	0.16	0.02	13533.82	128.53	$9.70e^{-29}$	21
69	H_6 H	6	0.81	0.75	0.01	0.07	0.01	0.02	0.00	0.18	0.02	13529.80	124.52	$7.22e^{-28}$	70
70	LQH_6 LQH	6	0.80	0.75	0.01	0.07	0.01	0.02	0.00	0.16	0.01	13493.28	87.99	$6.17e^{-20}$	53
71	LQHP_6 LQHP	6	0.80	0.75	0.01	0.07	0.02	0.02	0.00	0.17	0.01	13494.86	89.58	$2.79e^{-20}$	54
72	LQHPT_6 LQHPT	6	0.81	0.75	0.01	0.07	0.02	0.02	0.00	0.17	0.01	13433.94	28.65	$4.74e^{-07}$	37
73	L_6.5 L	6.5	0.77	0.73	0.02	0.07	0.02	0.02	0.00	0.16	0.01	13551.77	146.49	$1.23e^{-32}$	18
74	LQ_6.5 LQ	6.5	0.78	0.73	0.02	0.07	0.02	0.02	0.00	0.15	0.01	13543.10	137.82	$9.35e^{-31}$	20
75	H_6.5 H	6.5	0.81	0.75	0.01	0.07	0.01	0.02	0.00	0.17	0.02	13531.61	126.32	$2.93e^{-28}$	65

continued on next page

Table A.2 – The models obtained through ENMEval R package by setting different values of regularization multiplier and considering different feature classes (continued).

settings	features	rm	train.AUC	avg.test.AUC	var.test.AUC	avg.diff.AUC	var.diff.AUC	avg.test.orMTP	var.test.orMTP	avg.test.or10pct	var.test.or10pct	AIC_c	ΔAIC_c	w.AIC	parameters
76	LQH_6.5 LQH	6.5	0.80	0.75	0.01	0.07	0.01	0.02	0.00	0.15	0.01	13503.99	98.71	$2.90e^{-22}$	52
77	LQHP_6.5 LQHP	6.5	0.80	0.75	0.01	0.07	0.01	0.02	0.00	0.17	0.01	13498.12	92.83	$5.49e^{-21}$	50
78	LQHPT_6.5 LQHPT	6.5	0.81	0.75	0.01	0.07	0.01	0.02	0.00	0.16	0.01	13461.80	56.51	$4.22e^{-13}$	42
79	L_7 L	7	0.77	0.73	0.02	0.07	0.02	0.02	0.00	0.15	0.01	13558.85	153.56	$3.56e^{-34}$	18
80	LQ_7 LQ	7	0.78	0.74	0.02	0.07	0.02	0.02	0.00	0.14	0.01	13557.06	151.78	$8.70e^{-34}$	20
81	H_7 H	7	0.80	0.75	0.01	0.07	0.01	0.02	0.00	0.16	0.01	13542.70	137.41	$1.14e^{-30}$	63
82	LQH_7 LQH	7	0.80	0.76	0.02	0.07	0.01	0.02	0.00	0.15	0.01	13482.56	77.27	$1.31e^{-17}$	39
83	LQHP_7 LQHP	7	0.80	0.75	0.01	0.07	0.01	0.02	0.00	0.17	0.01	13508.72	103.43	$2.74e^{-23}$	50
84	LQHPT_7 LQHPT	7	0.80	0.75	0.01	0.07	0.01	0.02	0.00	0.17	0.01	13476.71	71.43	$2.44e^{-16}$	42
85	L_7.5 L	7.5	0.77	0.74	0.02	0.07	0.02	0.02	0.00	0.15	0.01	13564.21	158.92	$2.44e^{-35}$	17
86	LQ_7.5 LQ	7.5	0.77	0.74	0.02	0.07	0.01	0.02	0.00	0.14	0.01	13563.48	158.20	$3.51e^{-35}$	18
87	H_7.5 H	7.5	0.80	0.75	0.01	0.06	0.01	0.02	0.00	0.15	0.01	13554.46	149.18	$3.19e^{-33}$	63
88	LQH_7.5 LQH	7.5	0.80	0.76	0.02	0.07	0.01	0.02	0.00	0.15	0.01	13501.12	95.83	$1.22e^{-21}$	42
89	LQHP_7.5 LQHP	7.5	0.80	0.75	0.01	0.07	0.01	0.02	0.00	0.16	0.01	13498.35	93.07	$4.88e^{-21}$	41
90	LQHPT_7.5 LQHPT	7.5	0.80	0.75	0.01	0.07	0.01	0.02	0.00	0.16	0.01	13502.70	97.41	$5.55e^{-22}$	46
91	L_8 L	8	0.77	0.74	0.02	0.07	0.01	0.02	0.00	0.14	0.01	13569.45	164.17	$1.78e^{-36}$	16
92	LQ_8 LQ	8	0.77	0.74	0.02	0.07	0.01	0.02	0.00	0.14	0.01	13570.32	165.03	$1.15e^{-36}$	17
93	H_8 H	8	0.80	0.76	0.01	0.06	0.01	0.02	0.00	0.15	0.01	13545.81	140.52	$2.42e^{-31}$	55
94	LQH_8 LQH	8	0.80	0.76	0.02	0.07	0.01	0.02	0.00	0.15	0.01	13512.33	107.05	$4.49e^{-24}$	42

continued on next page

Table A.2 – The models obtained through ENMEval R package by setting different values of regularization multiplier and considering different feature classes (continued).

settings	features	rm	train.AUC	avg.test.AUC	var.test.AUC	avg.diff.AUC	var.diff.AUC	avg.test.orMTP	var.test.orMTP	avg.test.or10pct	var.test.or10pct	AIC_c	ΔAIC_c	w.AIC	parameters
95	LQHP_8 LQHP	8	0.80	0.76	0.02	0.07	0.01	0.02	0.00	0.16	0.01	13515.00	109.72	$1.18e^{-24}$	43
96	LQHPT_8 LQHPT	8	0.80	0.76	0.02	0.07	0.01	0.02	0.00	0.16	0.01	13520.92	115.64	$6.12e^{-26}$	46
97	L_8.5 L	8.5	0.77	0.74	0.02	0.07	0.01	0.02	0.00	0.13	0.01	13576.89	171.60	$4.31e^{-38}$	16
98	LQ_8.5 LQ	8.5	0.77	0.74	0.02	0.07	0.01	0.02	0.00	0.13	0.01	13576.89	171.60	$4.31e^{-38}$	16
99	H_8.5 H	8.5	0.80	0.76	0.01	0.06	0.01	0.02	0.00	0.15	0.01	13549.60	144.31	$3.63e^{-32}$	52
100	LQH_8.5 LQH	8.5	0.80	0.76	0.02	0.06	0.01	0.02	0.00	0.14	0.01	13524.89	119.61	$8.42e^{-27}$	42
101	LQHP_8.5 LQHP	8.5	0.80	0.76	0.02	0.06	0.01	0.02	0.00	0.15	0.01	13526.39	121.11	$3.97e^{-27}$	42
102	LQHPT_8.5 LQHPT	8.5	0.80	0.76	0.02	0.06	0.01	0.02	0.00	0.15	0.01	13553.82	148.53	$4.40e^{-33}$	53
103	L_9 L	9	0.77	0.74	0.02	0.07	0.01	0.02	0.00	0.13	0.01	13582.23	176.95	$2.97e^{-39}$	15
104	LQ_9 LQ	9	0.77	0.74	0.02	0.07	0.01	0.02	0.00	0.13	0.01	13582.25	176.97	$2.95e^{-39}$	15
105	H_9 H	9	0.80	0.76	0.01	0.06	0.01	0.02	0.00	0.15	0.01	13580.81	175.53	$6.05e^{-39}$	59
106	LQH_9 LQH	9	0.79	0.76	0.02	0.06	0.01	0.02	0.00	0.14	0.02	13535.06	129.77	$5.22e^{-29}$	41
107	LQHP_9 LQHP	9	0.79	0.76	0.02	0.06	0.01	0.02	0.00	0.14	0.01	13545.68	140.39	$2.58e^{-31}$	44
108	LQHPT_9 LQHPT	9	0.79	0.76	0.02	0.06	0.01	0.02	0.00	0.14	0.01	13545.52	140.24	$2.79e^{-31}$	44
109	L_9.5 L	9.5	0.76	0.74	0.02	0.06	0.01	0.02	0.00	0.13	0.01	13589.84	184.56	$6.63e^{-41}$	15
110	LQ_9.5 LQ	9.5	0.76	0.74	0.02	0.06	0.01	0.02	0.00	0.13	0.01	13589.87	184.58	$6.54e^{-41}$	15
111	H_9.5 H	9.5	0.80	0.76	0.01	0.06	0.01	0.02	0.00	0.15	0.01	13570.27	164.98	$1.18e^{-36}$	50
112	LQH_9.5 LQH	9.5	0.79	0.76	0.02	0.06	0.01	0.02	0.00	0.14	0.01	13530.70	125.41	$4.61e^{-28}$	34
113	LQHP_9.5 LQHP	9.5	0.79	0.76	0.02	0.06	0.01	0.02	0.00	0.15	0.01	13526.90	121.62	$3.08e^{-27}$	31

continued on next page

Table A.2 – The models obtained through ENMEval R package by setting different values of regularization multiplier and considering different feature classes (continued).

settings	features	rm	train.AUC	avg.test.AUC	var.test.AUC	avg.diff.AUC	var.diff.AUC	avg.test.orMTP	var.test.orMTP	avg.test.or10pct	var.test.or10pct	AIC_c	ΔAIC_c	w.AIC	parameters
114	LQHPT_9.5	LQHPT	9.5	0.79	0.76	0.02	0.06	0.01	0.02	0.00	0.15	0.01	13545.50	140.21	$2.82e^{-31}$	39
115	L_10	L	10	0.76	0.74	0.02	0.06	0.01	0.02	0.00	0.13	0.01	13595.37	190.08	$4.18e^{-42}$	14
116	LQ_10	LQ	10	0.76	0.74	0.02	0.06	0.01	0.02	0.00	0.12	0.01	13595.37	190.08	$4.18e^{-42}$	14
117	H_10	H	10	0.80	0.76	0.01	0.06	0.01	0.02	0.00	0.14	0.01	13583.16	177.87	$1.87e^{-39}$	50
118	LQH_10	LQH	10	0.79	0.76	0.02	0.06	0.01	0.02	0.00	0.14	0.01	13542.60	137.31	$1.20e^{-30}$	34
119	LQHP_10	LQHP	10	0.79	0.76	0.02	0.06	0.01	0.02	0.00	0.15	0.01	13562.23	156.94	$6.58e^{-35}$	41
120	LQHPT_10	LQHPT	10	0.79	0.76	0.02	0.06	0.01	0.02	0.00	0.15	0.01	13550.58	145.30	$2.22e^{-32}$	36

A.4 Exposure map representing the density of energy supply contracts in 2020.

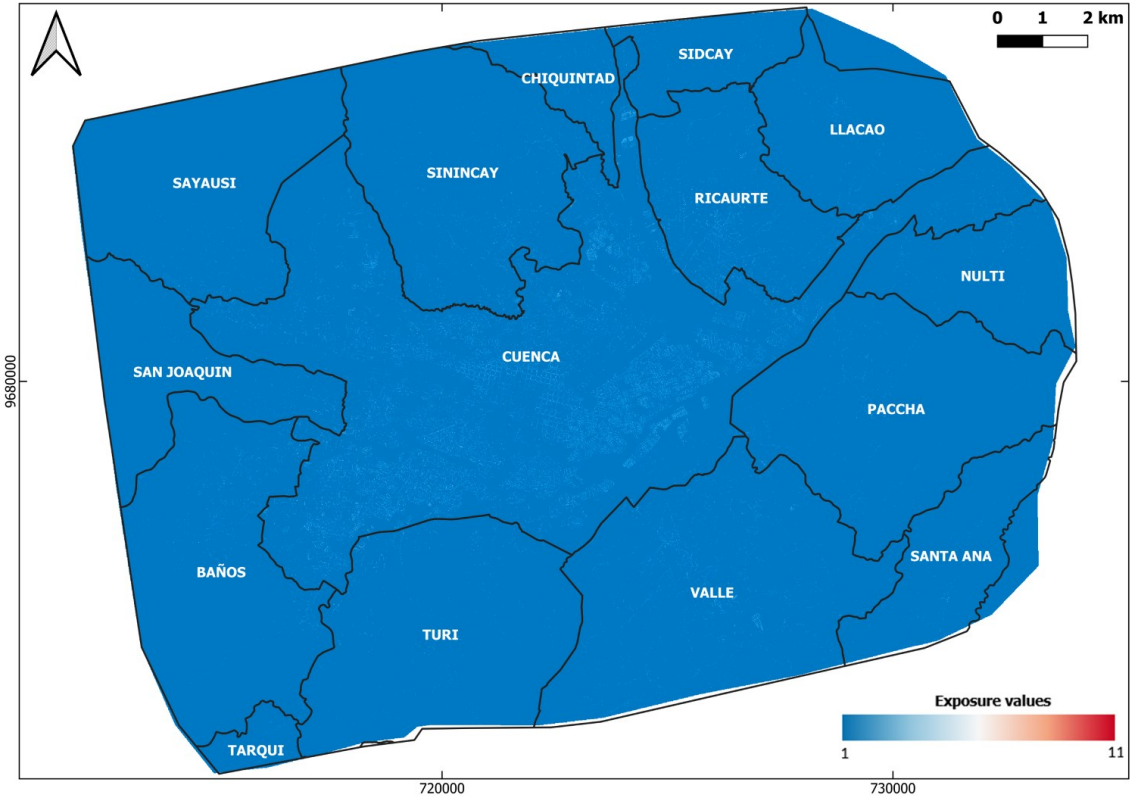

Figure A.2: Exposure map (cell size $10x10m$) representing the density of energy supply contracts in 2020 on the whole study area. This thematic map has been used in the final relative risk map creation (Figure 2.10 in the main text).

APPENDIX B

Publications associated with this thesis. Quality Indices.

B.1 Publications associated with Chapter 1.

The contents of Chapter 1 were included in:

Sellers, C.A.[1], Buján, S.[2], Miranda, D.[2], 2021. MARLI: a mobile application for regional landslide inventories in ecuador. Landslides 18(12), 3963 - 3977. doi: https://doi.org/10.1007/s10346-021-01764-9.

1	IERSE, University of Azuay, Av. 24 de Mayo 7-77 y Hernan Malo, 01.01.981, Cuenca, Ecuador.
2	GI-1934 TB-Biodiversity - LaboraTe, Department of Agroforestry Engineering and IBADER, University of Santiago de Compostela, C/ Benigno Ledo s/n, 27001, Lugo, Spain.

Author's Contribution.

The author of this thesis contributed to conceive the presented the idea, developed the theory and designed the forms for MARLI. The author developed the application, and performed all computations, verified de analytics and resulting data, discussed the results and contributed to the final manuscript. The author read and approved the final manuscript. The author participated in the correction of errors in the peer review process.

Access to the original article.

https://doi.org/10.1007/s10346-021-01764-9

Quality Indices of the Journal.

The aim of the journal *Landslides* (ISSN 1612-510X, https://www.springer.com/journal/10346) is to be the common platform for the publication of integrated research on landslide processes, hazards, risk analysis, mitigation, and the protection of our cultural heritage and the environment. *Landslides* is indexed in Journal Citation Reports, Scopus,...

Table B.1: Chapter 1. Journal Citation Reports (2021).

Subject Area	**Impact Factor**	**5-years Impact Factor**	**Quantile**	**Ranking**
Geosciences Multidisciplinary	6.153	6.864	Q1	19/202
Engineering, Geological	6.153	6.864	Q1	4/41

Table B.2: Chapter 1. Scopus - SCImago (2021).

Subject Area	**Cite Score**	**SJR**	**SNIP**	**H-Index**	**Ranking**
Geotechnical Engineering and Engineering Geology	10.6	1.918	2.582	89	6/203 (97th)

Table B.3: Chapter 1. Citations.

WOS	**SCOPUS**	**Google Scholar**	**ResearchGate**
4	4	5	4

Journal Authorization.

License Number: 5445361443319

License date: Dec 10, 2022

Licensed Content Publisher: Springer Nature

Licensed Content Publication: Landslides

Licensed Content Title: MARLI: a mobile application for regional landslide inventories in Ecuador

Licensed Content Author: Chester Andrew Sellers et al

Licensed Content Date: Sep 17, 2021

Type of Use: Thesis/Dissertation

Link to licence:
https://drive.google.com/file/d/1aIvXWxxa7Qe-kCl3qkaGyMW_F9bWoSUa/view?usp=share_link.

B.2 Publications associated with Chapter 2.

The contents of Chapter 2 were included in:

Di Napoli, M. [1], Miele, P.[2], Guerriero, L.[2], Annibali Corona, M.[2], Calcaterra, D.[2], Ramondini, M.[3], Sellers, C.[4] and Di Martire, D.[2], 2023. Multitemporal relative landslide exposure and risk analysis for the sustainable development of rapidly growing cities. Landslides (LASL-D-21-00573 - minor revision).

1	Department of Earth, Environmental and Life Sciences, University of Genoa, Genoa, 16132, Italy.
2	Department of Earth, Environment and Resources Sciences, Federico II University of Naples, Naples, 80126, Italy.
3	Department of Civil, Architectural and Environmental Engineering, Federico II University of Naples, Naples, 80125, Italy.
4	IERSE, University of Azuay, Av. 24 de Mayo 7-77 y Hernan Malo, 01.01.981, Cuenca, Ecuador.

Author's Contribution.

The author of this thesis contributed to conceive the presented the idea and developed the theory. The author performed the computations, verified de analytics and resulting data, discussed the results and contributed to the final manuscript. The author read and approved the final manuscript. The author participated in the correction of errors in the peer review process.

Access to the original article.

Not yet published.

Quality Indices of the Journal.

The aim of the journal *Landslides* (ISSN 1612-510X, https://www.springer.com/journal/10346) is to be the common platform for the publication of integrated research on landslide processes, hazards, risk analysis, mitigation, and the protection of our cultural heritage and the environment. *Landslides* is indexed in Journal Citation Reports, Scopus,...

Table B.4: Chapter 2. Journal Citation Reports (2021).

Subject Area	**Impact Factor**	**5-years Impact Factor**	**Quantile**	**Ranking**
Geosciences Multidisciplinary	6.153	6.864	Q1	19/202
Engineering, Geological	6.153	6.864	Q1	4/41

Table B.5: Chapter 2. Scopus - SCImago (2021).

Subject Area	**Cite Score**	**SJR**	**SNIP**	**H-Index**	**Ranking**
Geotechnical Engineering and Engineering Geology	10.6	1.918	2.582	89	6/203 (97th)

Table B.6: Chapter 2. Citations.

WOS	**SCOPUS**	**Google Scholar**	**ResearchGate**
-	-	-	-

Journal Authorization.

License Number:

License date:

Licensed Content Publisher:

Licensed Content Publication:

Licensed Content Title:

Licensed Content Author:

Licensed Content Date:

Type of Use:

Link to licence: not yet published.

B.3 Publications associated with Chapter 3.

The contents of Chapter 3 were included in:

Sellers, C.[1], Di Martire, D.[2], Rodas, R.[1], Ramondini, M.[3],Infante, D. [1], Miranda, D.[5] and Buján, S.[6], 2023. An integrated approach for rockfall susceptibility assess-ment along linear infrastructure in Cuenca (Ecuador). Remote Sensing (submitted).

1	IERSE, University of Azuay, Av. 24 de Mayo 7-77 y Hernan Malo, 01.01.981, Cuenca, Ecuador.
2	Department of Earth, Environment and Resources Sciences, Federico II University of Naples, Naples, 80126, Italy.
3	Department of Civil, Architectural and Environmental Engineering, Federico II University of Naples, Naples, 80125, Italy.
4	SINTEMA Engineering s.r.l., Via Toledo, 156 - 80134 Napoli, Italy.
5	GI-1934 TB-Biodiversidad - LaboraTe, Departamento de Ingeniería Agroforestal e IBADER, Universidad de Santiago de Compostela, C/ Benigno Ledo s/n, 27001, Lugo, Spain.
6	Departamento de Tecnología Minera, Topografía y de Estructuras, Universidad de León, Av. de Astorga s/n, 24401, Ponferrada, Spain.

Author's Contribution.

The author of this thesis contributed to conceive the presented the idea and developed the theory. The author performed the computations, verified de analytics and resulting data, discussed the results and contributed to the final manuscript. The author read and approved the final manuscript. The author participated in the correction of errors in the peer review process.

Access to the original article.

Not yet published.

Quality Indices of the Journal.

Remote Sensing (ISSN 2072-4292, https://www.mdpi.com/journal/remotesensing) is a peer-reviewed, open access journal about the science and application of remote sensing technology, and is published semimonthly online by MDPI. *Remote Sensing* is indexed in Journal Citation Reports, Scopus,...

Table B.7: Chapter 3. Journal Citation Reports (2021).

Subject Area	**Impact Factor**	**5-years Impact Factor**	**Quantile**	**Ranking**
Image Science & Photographic Technology	5.349	5.786	Q1	6/28
Geosciences, Multidisciplinary	5.349	5.786	Q1	30/202
Remote Sensing	5.349	5.786	Q2	11/34
Environmental Sciences	5.349	5.786	Q2	83/279

Table B.8: Chapter 3. Scopus - SCImago (2021).

Subject Area	**Cite Score**	**SJR**	**SNIP**	**H-Index**	**Ranking**
General Earth and Planetary Sciences	7.4	1.283	1.546	144	17/191 (91th)

Table B.9: Chapter 3. Citations.

WOS	**SCOPUS**	**Google Scholar**	**ResearchGate**
-	-	-	-

Journal Authorization.

License Number:

License date:

Licensed Content Publisher:

Licensed Content Publication:

Licensed Content Title:

Licensed Content Author:

Licensed Content Date:

Type of Use:

Link to licence: not yet published.

B.4 Publications associated with Chapter 4.

The contents of Chapter 4 were included in:

Sellers, C.[1], Rodas, R.[1], Carrasco, N. P.[2], De Stefano, R.[3],Di Martire, D.[3] and Ramondini, M.[3], 2021. Ground Deformation Monitoring of a Strategic Building Affected by Slow-Moving Landslide in Cuenca (Ecuador). In European Workshop on Structural Health Monitoring: Springer, Cham, pp. 149 - 158. doi:https://doi.org/10.1007/978-3-030-64908-1_14.

1	IERSE, University of Azuay, Av. 24 de Mayo 7-77 y Hernan Malo, 01.01.981, Cuenca, Ecuador.
2	University of Castilla-La Mancha, Toledo, Spain.
3	Federico II University of Naples, Naples, 80126, Italy.

Author's Contribution.

The author of this thesis conceived the presented the idea, developed the theory and designed the methodology. The author developed the study, and performed all computations, verified de analytics and resulting data, discussed the results and contributed to the final manuscript. The author read and approved the final manuscript. The author participated in the correction of errors in the peer review process.

Access to the original article.

https://doi.org/10.1007/978-3-030-64908-1_14.

Quality Indices of the Journal.

Lecture Notes in Civil Engineering (ISSN 2366-2557, https://www.springer.com/series/15087) (LNCE) publishes the latest developments in Civil Engineering-quickly, informally and in top quality. Though original research reported in proceedings and post-proceedings represents the core of LNCE, edited volumes of exceptionally high quality and interest may also be considered for publication. Volumes published in LNCE embrace all aspects and subfields of, as well as new challenges in, Civil Engineering. *Lecture Notes in Civil Engineering* is indexed in EI Compendex, INSPEC, Norwegian Register for Scientific Journals and Series, SCImago, SCOPUS and zbMATH.

Table B.10: Chapter 4. Scopus - SCImago (2021).

Subject Area	**Cite Score**	**SJR**	**SNIP**	**H-Index**	**Ranking**
Civil and Structural Engineering	0.5	0.133	0.176	13	296/326 (9th)

Table B.11: Chapter 4. Citations.

WOS	**SCOPUS**	**Google Scholar**	**ResearchGate**
-	2	1	1

Journal Authorization.

License Number: 5445380553817

License date: Dec 10, 2022

Licensed Content Publisher: Springer Nature

Licensed Content Publication: Springer eBook

Licensed Content Title: Ground Deformation Monitoring of a Strategic Building Affected by Slow-Moving Landslide in Cuenca (Ecuador)

Licensed Content Author: Chester Andrew Sellers et al

Licensed Content Date: Jan 1, 2021

Type of Use: Thesis/Dissertation

Link to licence:
https://drive.google.com/file/d/1ddciNQxdkCnBGWrYOchBwpxzknSuZ5kr/view?usp=share_link.

B.5 Publications associated with Chapter 5.

The contents of Chapter 5 were included in:

Sellers, C.[1], Ammirati, L.[2], Khalili, M. A.[2], Buján, S.[3,4], Rodas, R.[1], and Di Martire, D.[2], 2023. The Use DInSAR Technique for the Study of Land Subsidence Associated with Illegal Mining Activities in ZarumaâEcuador, a Cultural Heritage Cite. In European Workshop on Structural Health Monitoring: Springer, Cham, pp. 553 - 562. doi:https://doi.org/10.1007/978-3-031-07322-9_56.

1	IERSE, University of Azuay, Av. 24 de Mayo 7-77 y Hernan Malo, 01.01.981, Cuenca, Ecuador.
2	Department of Earth Sciences, Environment, and Resources, University of Naples, Federico II, 80126, Naples, Italy.
3	GI-1934 TB-Biodiversidad - LaboraTe, Departamento de Ingeniería Agroforestal e IBADER, Universidad de Santiago de Compostela, C/ Benigno Ledo s/n, 27001, Lugo, Spain.
4	Departamento de Tecnología Minera, Topografía y de Estructuras Universidad de León, Av. de Astorga s/n, 24401, Ponferrada, Spain.

Author's Contribution.

The author of this thesis conceived the presented the idea, developed the theory and designed the methodology. The author developed the study, and performed all computations, verified de analytics and resulting data, discussed the results and contributed to the final manuscript. The author read and approved the final manuscript. The author participated in the correction of errors in the peer review process.

Access to the original article.

https://doi.org/10.1007/978-3-031-07322-9_56.

Quality Indices of the Journal.

Lecture Notes in Civil Engineering (ISSN 2366-2557, https://www.springer.com/series/15087) (LNCE) publishes the latest developments in Civil Engineering-quickly, informally and in top quality. Though original research reported in proceedings and post-proceedings represents the core of LNCE, edited volumes of exceptionally high quality and interest may also be considered for publication. Volumes published in LNCE embrace all aspects and subfields of, as well as new challenges in, Civil Engineering. *Lecture Notes in Civil Engineering* is indexed in EI Compendex, INSPEC, Norwegian Register for Scientific Journals and Series, SCImago, SCOPUS and zbMATH.

Table B.12: Chapter 5. Scopus - SCImago (2021).

Subject Area	**Cite Score**	**SJR**	**SNIP**	**H-Index**	**Ranking**
Civil and Structural Engineering	0.5	0.133	0.176	13	296/326 (9th)

Table B.13: Chapter 5. Citations.

WOS	**SCOPUS**	**Google Scholar**	**ResearchGate**
-	-	-	-

Journal Authorization.

License Number: 5445380850542

License date: Dec 10, 2022

Licensed Content Publisher: Springer Nature

Licensed Content Publication: Springer eBook

Licensed Content Title: The Use DInSAR Technique for the Study of Land Subsidence Associated with Illegal Mining Activities in Zaruma â Ecuador, a Cultural Heritage Cite.

Licensed Content Author: Chester Andrew Sellers et al

Licensed Content Date: Jan 1, 2023

Type of Use: Thesis/Dissertation

Link to licence:
https://drive.google.com/file/d/1NgTlKarBrVy7o7t0IY2w4wFNmv4ERWF9/view?usp=share_link.

The main objective of this doctoral thesis is to analyze the use of remote sensors, the information that can be obtained to determine how these sensors and methodologies can be used to generate and update geospatial information for risk management and governance. To acquire this objective, after an extensive review, it is intended to develop from a purely practical and applied point of view, which are materialized in different case studies. And, applied to projects that are immersed in risk management focused on mass movements in Ecuador. This thesis is conformed of six chapters addressing mass movements from different perspectives objectives and, study areas.